12-11-2015 12:00 AM

Development of a Novel Humanized Single Chain Antibody-Streptococcal Superantigen-Derived Immunotherapy Targeting the 5T4 Oncofetal Antigen

Kelcey G. Patterson
The University of Western Ontario

Supervisor
Dr. John McCormick
The University of Western Ontario

Graduate Program in Microbiology and Immunology
A thesis submitted in partial fulfillment of the requirements for the degree in Doctor of Philosophy

DEVELOPMENT OF A NOVEL HUMANIZED SINGLE CHAIN ANTIBODY-STREPTOCOCCAL SUPERANTIGEN-DERIVED IMMUNOTHERAPY TARGETING THE 5T4 ONCOFETAL ANTIGEN

(Thesis format: Monograph)

by

Kelcey Grace Patterson

Graduate Program in Microbiology and Immunology

A thesis submitted in partial fulfillment
of the requirements for the degree of
Doctor of Philosophy

The School of Graduate and Postdoctoral Studies
The University of Western Ontario
London, Ontario, Canada

ABSTRACT

Superantigens (SAgs) are microbial toxins that cross-link T cell receptors with major histocompatibility complex (MHC) class II (MHC II) molecules leading to the activation of large numbers of T cells. Herein, the development and preclinical testing of a novel tumour-targeted SAg (TTS) therapeutic built using the streptococcal pyrogenic exotoxin C (SpeC) SAg and targeting cancer cells expressing the 5T4 tumour-associated antigen (TAA) was described. To inhibit potentially harmful widespread immune cell activation, a SpeC mutation within the high-affinity MHC II binding interface was generated ($SpeC_{D203A}$) that demonstrated a pronounced reduction in mitogenic activity, yet this mutant could still induce immune cell-mediated cancer cell death *in vitro*. To target $5T4^{+}$ cancer cells, a humanized single-chain variable fragment (scFv) antibody to recognize 5T4 (scFv5T4) was engineered. Specific targeting of scFv5T4 was verified. $SpeC_{D203A}$ fused to scFv5T4 maintained the ability to activate and induce immune cell-mediated cytotoxicity of colon cancer cells. Using a xenograft model of established human colon cancer, it was demonstrated that the SpeC-based TTS was able to control the growth and spread of large tumours *in vivo*. This required both TAA targeting by scFv5T4 and functional SAg activity. These studies lay the foundation for the development of streptococcal SAgs as 'next-generation' TTSs for cancer immunotherapy.

KEYWORDS

colorectal cancer, superantigen, single-chain variable fragment antibody, tumour-associated antigen, cancer immunotherapy, xenogeneic mouse model

ACKNOWLEDGMENTS

Firstly, I would like to express my sincere gratitude and appreciation to my advisor Dr. John McCormick for the continued support throughout my studies, and for his constant guidance, insight, motivation, and compassion. I would like to thank him for encouraging my research throughout this journey and allowing me to truly grow as a scientist, both individually and as a collaborator. The positive research environment and opportunties has truly been inspirational and I attribute his tremendous mentorship for the reason of my continued passion for research. I truly appreciate all that has come with my time within his lab; countless skills that will undoubtably carry through to my future endeavors.

I would like to acknowledge the sources of funding for the research provided during my tenure, including Dr. McCormick's support from Canadian Institues of Health Resarch (CIHR), as well as the direct support I have received from Western Graduate Research Scholarship (WGRS), Schulich Graduate Scholarship, and Schulich Scholarship for Medical Research from Western University.

In addition to my advisor, I would like to thank my thesis advisory committee members Drs. Mansour Haeryfar and Fred Dick, for their enouragments, insightful comments, and discussions, which continually provided opportunities to widen my research from various perspectives. I would like to acknowledge Dr. Haeryfar further for the seemingly endless use of his lab equipment, reagents, and scientific techniques, providing tools and opportunities in my research that would otherwise not have been achievable.

I would like to take this opportunity to give a sincere acknowlegemnt to the faculty and supportive staff members within the Department of Microbiology and Immunology for their continued support for not only myself, but for all students, and for providing a network of truly talented researchers that are welcoming, helpful, and whom generate an environment of endless opportunities and facilities to foster great science.

I thank Dr. David Hess and his team, for use of his reagents, lab space, and assistance in conducting related research. I am also grateful to Delfina Siroen for all of her support,

especially for assistance with *in vivo* work and in the world of histological techniques. I would like to acknowledge the previous hard work and contributions made by Jennifer Dixon and Peter Bastedo in order to move this research forward.

I sincerely thank my fellow lab members not only for all of the stimulating discussions, scientific or otherwise, and the continuous assistance and support, but importantly, for the many, many laughs over the years, the friendships, and of course, fond memories.

Lastly, I would like the express my gratitude to all of my friends and family, in particular my parents, brother, and sister, who have wholeheartedly given support not only through this journey, but throughout every endeavor and undoubtably any future ones. And of course, a huge thank you to Brent, my fellow labmate, best friend, and significant other, to whom, throughout our entire experience, I am greatly indebted. I truly cannot express in words how much his unconditional support has been, and will remain, appreciated.

TABLE OF CONTENTS

LIST OF TABLES

LIST OF FIGURES

LIST OF APPENDICES

LIST OF ABBREVIATIONS

°C	degrees Celsius
Ω	Ohms
× g	times gravity
5-FU	5-fluorouracil
7-AAD	7-aminoactinomycin D
µF	microfarad
µg	microgram
µl	microliter
µm	micrometer
ABS	antigen binding site
ACT	adoptive cell therapy
ADC	antibody-drug conjugate
ADCC	antibody-dependent cell-mediated cytotoxicity
AFP	alpha-fetoprotein
APC	allophycocyanin
APCs	antigen presenting cells
BCA	bicinchoninic acid
BCG	Bacillus Calmette-Guérin
BiTE	bispecific T cell engaging antibody
bp	base pair
BSA	bovine serum albumin
CAR	chimeric antigen receptor
CCL	chemokine (C-C motif) ligand
CD(n)	cluster of differentiation (n)
CDC	complement-dependent cytotoxicity
cDMEM	complete DMEM
cDNA	complementary DNA
CDR	complementarity determining region
CEA	carcinoembryonic antigen
CFSE	carboxyfluorescein succinimidyl ester
C_H	heavy chain, constant domain
CIMP	CpG island methylator phenotype
C_L	light chain, constant domain
cm	centimeter
cMEM	complete MEM
ConA	concanavalin A
CPM	counts per minute
CRC	colorectal cancer
cRPMI	complete RPMI-1640

CT	cancer-testis antigen
CTL	cytotoxic T lymphocyte
CTLA-4	cytotoxic T-lymphocyte-associated protein 4
DAPI	4’,6-diamidino-2-phenylindole
DC	dendritic cell
DFS	disease-free survival
DLT	dose-limiting toxicity
DMEM	Dulbecco’s modified Eagle’s medium
DMSO	dimethyl sulfoxide
DNA	deoxyribonucleic acid
dNTP	deoxyribonucleotide triphosphate
EC_{50}	half maximal effective concentration
EDTA	ethylenediaminetetraacetic acid
egc	enterotoxin gene cluster
EGF	epidermal growth factor
EGFP	enhanced green fluorescent protein
EGFR	epidermal growth factor receptor
EK	enterokinase
EMT	epithelial-mesenchymal transition
EpCAM	epithelial cell adhesion molecule
ES	embryonic stem cell
FA	folinic acid
Fab	antigen-binding fragment
FACS	fluorescence-activated cell sorting
FAP	familial adenomatous polyposis
FBS	fetal bovine serum
Fc	fragment crystallizable region (constant domain of antibody)
FcγR	Fc-gamma receptor
FDA	Food and Drug Administration
FITC	fluorescein isothiocyanate
FOLFOX	5-FU plus FA with oxaliplatin
FOLRIRI	5-FU plus FA with irinotecan
FoxP3	forkhead box P3
FR	framework region
Fv	variable fragment (antibody)
g	gram
GFP	green fluorescent protein
GM-CSF	granulocyte macrophage colony-stimulating factor
GST	glutathione S-transferase
H&E	hematoxylin and eosin

h	hour
HAMA	human anti-mouse antibody
HEPES	4-(2-hydroxyethyl)-1-piperazineethanesulfonic acid
HER2	human epidermal growth factor receptor 2
HLA	human leukocyte antigen
HNPCC	hereditary nonpolyposis colorectal cancer
hpf	high-power field
HPLC	high performance liquid chromatography
HPV	human papillomavirus
HV	hypervariable region
IDO	immunomodulatory molecules indoleamine-2,3-dioxygenase
IFN	interferon
Ig	immunuoglobulin
IgG	immunoglobulin G
IHC	immunohistochemistry
IL-(*n*)	interleukin-(*n*)
ip	intraperitoneal injection
IPTG	isopropyl-D-thiogalactopyranoside
iv	intravenous injection
IRDye	infrared dye
JAM	just another method
K_d	dissociation constant
kDa	kilodalton
kg	kilogram
kV	kilovolts
LAG-3	lymphocyte-activation gene 3
LB	Luria-Bertani broth
LRR	leucine rich-repeat
Mϕ	macrophage
mAb	monoclonal antibody
MAP	MUTYH-associated polyposis
mCRC	metastatic CRC
MCS	multiple cloning site
MDSC	myeloid-derived suppressor cell
MEF	mouse embryonic fibroblast
MEM	Minimum Essential Media
MET	metastasis
min	minute
MIP	macrophage inflammatory protein
MHC	major histocompatability complex

mL	milliliter
mm	millimeter
mM	millimolar
mRFP1	monomeric red fluorescent protein 1
MMR	mismatch repair genes
ms	millisecond
MSI	microsatellite instability
MTD	maximum tolerated dose
MVA	modified vaccinia virus Ankara
MW	molecular weight marker
ng	nanogram
NK	natural killer
NKT	natural killer T cell
nM	nanomolar
NSCLC	non-small-cell lung carcinoma
NSG	NOD scid gamma (NOD.Cg-*Prkdc*^{scid}/*Il2rg*^{tm1Wjl}/SzJ)
OB	oligonucleotide/oligosaccharide-binding
OD	optical density
O/N	overnight
OS	overall survival
PBMC	peripheral blood mononuclear cell
PBS	phosphate buffered saline
PBST	phosphate buffered saline with tween-20
PCR	polymerase chain reaction
PD-1	programmed cell death protein 1
PD-L1/2	programmed death-ligand 1/2
PDB	Protein Data Bank
PE	phyocerythrin
PFS	progression-free survival
PHA	phytohaemagglutinin
pMHC	peptide-major histocombatability complex
PMN	polymorphonuclear cell
psi	pound per square inch
PVDF	polyvinylidene difluoride
RCC	renal cell carcinoma
RPMI-1640	Roswell Park Memorial Institute medium
RT	room temperature
SADCC	SAg-mediated antibody-dependent cell cytotoxicity
SAg	superantigen
scFv	single-chain variable fragment (antibody)

SCID	severe combined immunodeficient
SDCC	SAg-dependent cellular cytotoxicity
SDS-PAGE	sodium dodecyl sulfate polyacrylamide gel electrophoresis
SE	staphylococcal enterotoxin
SEA	staphylococcal enterotoxin A
sec	second
SEl	SE-like
SEM	standard error of mean
Spe	streptococcal pyrogenic exotoxin
SpeC	streptococcal pyrogenic exotoxin C
STBM	syncytiotrophoblast microvillous plasma membrane
TAA	tumour associated antigen
TAM	tumour-associated macrophages
TBS	tris-buffered saline
TBST	tris-buffered saline with tween-20
TCR	T cell receptor
TdT	terminal deoxynucleotidyl transferase
TEV	tobacco etch virus
TGF	transforming growth factor
Thr	thrombin
TIC	tumour-initiating cells
TIL	tumour-infiltrating lymphocyte
TIM-3	T cell immunoglobulin mucin-3
TNM	Tumour-Node-Metastasis
TNF	tumour necrosis factor
Treg	regulatory T cell
TRITC	tetramethylrhodamine
TrxA	thioredoxin
TPC	tumour progenitor cells
TPBG	trophoblast glycoprotein
TSS	toxic shock syndrome
TTS	tumour-targeted superantigen
TUNEL	terminal deoxynucleotidyl transferase dUTP nick end labeling
U	unit
V	volt
Vα	variable alpha chain
Vβ	variable beta chain
V_H	heavy chain, variable domain
V_L	light chain, variable domain
VEGF	vascular endothelial growth factor

vWF	von Willebrand factor
WHO	World Health Organization
WT	wild type
XELOX	capecitabine plus oxaliplatin

CHAPTER 1: INTRODUCTION

1.1 General overview of cancer

Cancer is a leading cause of both disease and death worldwide, with a recent incidence rate of approximately 14.1 million new cases and 8.2 million deaths annually (1). A generic term for a large group of diseases, cancer is "the rapid creation of abnormal cells that grow beyond their usual boundaries," as described by the World Health Organization (WHO) (2). Initially affecting any part of the body, cancers can further spread and invade tissues and organs, with these metastases generating the bulk of death from cancer (2). According to the WHO, the multistage transition of normal cells to malignant tumours results from a combination of fundamental factors including an individual's genetics, ageing processes, and external agents comprising of physical (*e.g.* ultraviolet, radiation), chemical (*e.g.* tobacco), or biological (*e.g.* infection) carcinogens (2). As such, the most common causes of cancer death worldwide, in descending order, are those of lung, breast, colorectal, prostate, stomach, and liver cancer (1), coordinating with the associated key risk factors of tobacco use, alcohol use, unhealthy diet, and physical inactivity (2). Additionally, in many developing countries, chronic infections are major risk factors. By modifying or avoiding these major factors, it has been estimated that more than 30% of cancer deaths could be prevented (2). Although strides in preventative screening and early diagnosis are aiding in the overall outcome of this disease, it is still expected that the number of new cases will rise approximately 70% over the next 20 years, nearing 22 million new cases annually (2).

Specifically within Canada, cancer is responsible for nearly 30% of all deaths (3). According to statistics from the Canadian Cancer Society for 2015, approximately 196 900 new cases of cancer will develop and 78 000 patients will die of this disease; numbers that are ever increasing with each year (3). As a result, almost half of all Canadians will be expected to develop this disease within their lifetime, and consequently one quarter are predicted to die of cancer. Related to worldwide estimations, it is expected that new cases will dramatically rise (79%) in Canada over the next 15 years, largely due to the ever-increasing aging population (3). Indeed, despite that this devastating disease can occur at any age, the vast majority (89%) of individuals who currently develop cancer are over the age of 50 (3). The importance of continued research

and development of additional heath resources for managing this disease is highlighted from this staggering predicted increase in incidence rate. Cancers of the lung, breast, colorectal, and prostate, similar to other developed, westernized countries, are responsible for more than half of new cancer cases (51%) annually and although all cancers are of importance, may warrant particular focus due to their sheer prevalence. Current efforts, despite ongoing challenges, have made significant progress in the fight against cancer. Today, with the continuous knowledge growing in cancer biology, the risk factors, surveillance, and treatments, many improvements have been made; most notably resulting in the steady decline of the cancer mortality rate since its peak in 1988 within Canada (3).

1.2 Colorectal cancer

Colorectal cancer (CRC) represents a major health concern worldwide, being accountable for more than 600 000 deaths per year (4). Despite advances in screening and treatment, CRC remains the third most common cancer in men, 10% of the total, and the second in women, 9.4% of the total, worldwide (1). Similar to the rest of the Western world, CRC is one of the four major contributors to new cancer diagnoses in Canada, accounting for more than half of all cancers and is the second and third most common cause of cancer-related death for males and females, respectively (3). The overall 5-year survival rate is 65% (5), but varies extensively depending on the stage of CRC progression at diagnosis (**Table 1**).

Although the risk factors of developing CRC can have a hereditary component, it is more common that environmental factors are influential in its high incidence rate. These risk factors are outlined in **Table 2**. As an example, epidemiological studies have demonstrated that individuals who have immigrated to the Western world from a once CRC low-incidence country, eventually developed CRC at a similar rate to those native-born (6, 7). Moreover, evidence during the past decade suggests that the Western influence globally, in particular with diet, has caused incidence rates of CRC in these once low-rate countries to rise dramatically (6-8). Such preventable influences include elevated consumption of dairy, meat, eggs, and oil or fat, which remain preeminent in

Table 1. TNM classification of CRC malignant tumours

Stages are based on the UICC and AJCC groups with associated 5-year survival rate percentage. Modified from Meyerhardt *et al*. 2005, Sobin LH *et al*. 2011, and O'Connell *et al*. 2004 (9-11).

Stage	TNM classification	Dukes' classification	5-year survival (%)
0	Tis, N0, M0		
I	T1, N0, M0 T2, N0, M0	A B1	>90
IIA **IIB** **IIC**	T3, N0, M0 T4a, N0, M0 T4b, N0, M0	B2	70-85
IIIA **IIIB** **IIIC**	T1-2, N1, M0 **or** T1, N2a, M0 T3-4a, N1, M0 **or** T2-3, N2a, M0 **or** T1-2, N2b, M0 T4a, N2a, M0 **or** T3-4a, N2b, M0 **or** T4b, N1-2, M0	C1 C2 C2	40-55
IVA **IVB**	T(any), N(any), M1a T(any), N(any), M1b	D	<10
TX	Cannot be assessed		
Tis	Carcinoma *in situ*		
T1	Invades submucosa		
T2	Invades muscularis propria (muscle layer)		
T3	Penetrates muscularis propria and invades subserosa		
T4	Direct invasion of other organs or structures, or perforates membrane lining 4a - perforates visercal peritoneum 4b - directly invades other organs or structures		
NX	Regional lymph nodes cannot be assessed		
N0	No metastases		
N1	Metastases in 1-3 nodes 1a – metastasis in 1 regional lymph node 1b – metastasis in 2-3 regional lymph nodes 1c – satellites in the lymph drainage areas of the subserosa or the surrounding tissue without regional lymph node metastasis		
N2	Metastases in 4 or more nodes 2a – metastasis in 4-6 regional lymph nodes 2b – metastasis in 7 or more regional lymph nodes		
MX	Presence or absence cannot be determined		
M0	None detected		
M1	Detected 1a – metastasis confined to 1 organ or non-regional lymph node(s) 1b – metastasis in more than 1 organ or the peritoneum		

Table 2. Risk factors for the development of CRC

	Risk factor associated with increased incidence[a]
Unpreventable/hereditary	Age 50^{+} years
	Previous CRC or polyps
	Family history of CRC
	Inflammatory bowel disease: ulcerative colitis, Crohn's disease
Preventable	High-fat diet
	Diet low in fruits and vegetables
	Physical inactivity
	Obesity
	Tobacco use
	Alcohol use

[a] Modified from Benson, 2007 (6)

high-fat diets of many countries today, lacking in a regular intake of fruit and vegetables (6). Furthermore, increased risk is also associated with lifestyle; inactivity, obesity, tobacco, and alcohol use of the most common factors (6, 12, 13). Indeed, location and socioeconomic status continue to be the main correlations with the incidence rate of CRC globally.

This carcinoma, unlike many other malignancies, may be potentially curable if early stage tumours are able to be removed. As such, it has been predicted that the implementation of screening programs aimed at early detection are imperative to reducing overall incidence and associated mortality of CRC (14). However, CRC is difficult to diagnose with few symptoms until the onset of stage III or IV, based on the Tumour-Node-Metastasis (TNM) classification (**Table 1**). At the time of diagnosis, approximately 20% of patients will present with inoperable CRC, and 20-25% with pre-existing metastatic disease (5, 15). Although tumour resection is performed when possible (10, 15), high mortality rates remain associated with CRC. Of those patients receiving surgical intervention, 40-50% will relapse or die from metastatic disease, the majority due to complications of liver metastases (6, 10, 15).

1.2.1 CRC development and carcinogenesis

The first CRC carcinogenesis model was described by Fearon and Vogelstein in 1990 (16) and since, the multi-stage progression of CRC and contributing influences has had significant progress in understanding its molecular pathogenesis, as well as remaining challenges, which have been the focus of many comprehensive studies and reviews (16-21). Foremost, CRCs develop gradually as a multifaceted result of epithelial cells transforming into adenocarcinomas through a sequential accumulation of genetic and epigenetic changes across multiple molecular pathways. As such, CRCs are known to be genetically diverse; each tumour has a unique combination of genetic alterations, and only a few mutations are common to CRCs (22). The pathological progression begins as a benign adenomatous polyp from a microscopic mucosal lesion, that further spreads and localizes within the submucosa and muscularis propria (muscle layer) (23). Further progression advances into high-dysplasia adenoma, potentially disseminating into

regional lymph nodes and surrounding tissues. Without intervention, non-regional lymph nodes and/or other organs may be invaded, advancing into late stage CRC of invasive metastatic disease (23).

The majority of CRC occurrences are sporadic, nonhereditary, and have complex, heterogeneous etiological factors for carcinogenesis (24). To date, at least three molecular pathways for sporadic CRC have been described. The most common subgroup, termed chromosomal instability pathway, is characteristic for accumulations of point mutations in specific oncogenes and tumour suppressor genes (*e.g APC*, *BRAF*, *KRAS*, *TP53*) causing numerical and structural chromosomal irregularities (25). This pathway is mainly associated with 1) a mutation and/or loss of *APC*, functionally interrupting the suppression of the Wnt-signaling pathway, 2) mutation of the *KRAS* oncogene, consequently constitutively activating downstream signaling (RAS-RAF-MEK-ERK pathway) and 3) either mutation or chromosomal loss that contains *TP53*, encoding p53, an important tumour suppressor gene (26). Second, the microsatellite instability (MSI) pathway leads to genetic hypermutability as an outcome of misregulation of DNA mismatch repair genes (MMR) (27). In this pathway, single point or frameshift mutations occur in areas of the genome containing microsatellites, short repeat nucleotide sequences that can be inserted or deleted, from a defective mechanism (27). Although a hallmark trait of Lynch syndrome, also often called hereditary nonpolyposis colorectal cancer (HNPCC), this genetic irregularity occurs in ~13% of sporadic CRC (27, 28). Lastly, known as the CpG island methylator phenotype (CIMP) pathway, the expression of key tumour suppression genes (*e.g. MLH1,* a MMR gene) is epigenetically silenced and inactivated with hypermethylation of genetic promoter regions (29). Although there is not one universally recognized panel of CIMP markers, CRC carcinogenesis has associations with two separate genetic mutations, *KRAS* and *BRAF* (downstream of *KRAS* signaling) (30). Notably, these pathways are not mutually exclusive in the development of sporadic CRC, with this disease frequently presenting features from all three pathways (24).

A lesser proportion of CRC cases are of known hereditary decent (~20-30%) (31); ~5% of cases are associated with highly penetrant inherited mutations with well-characterized clinical presentations (32). Currently, the etiologies of the remaining 15%–25% of

inherited CRCs are not completely understood or clarified. Conditions characterized are HNPCC, commonly known as Lynch syndrome described briefly above, familial adenomatous polyposis (FAP), attenuated FAP, and MUTYH-associated polyposis (MAP). Lynch syndrome is caused by genomic instability from an autosomal dominant inherited germline mutation in MMR genes, eventually leading to MSI (28, 31). Although the term nonpolyposis is used for this disease, the CRC frequently develops from polyps that, once formed, tend to become rapidly malignant, affecting sufferers at an early age (mean 45 years) (28, 31). Similarly, in patients with FAP, untreated CRC develops at an early age (mean 39 years), arising from autosomal dominant germline mutations in the *APC* gene, leading to constitutively activate Wnt signaling (31, 32). Consequentially, a characteristic feature of FAP includes the cellular over-growth and development of hundreds to thousands of colonic adenomas, beginning in early adolescence, and inevitable CRC progression in untreated individuals (32). Also presenting with autosomal dominant mutations in *APC*, attenuated FAP is a less-severe form of the disease, characterized on average of thirty colonic adenomatous polyps and a later age of polyp and CRC development (32). Lastly, MAP, an autosomal recessive form of FAP and mimics presence of adenomatous polyps increasing the risk of CRC at an early age, but is caused by bi-allelic mutations in *MUTYH* (also referred to as *MYH*). Characterized as part of the base-excision repair pathway, a mechanism for DNA corrections from spontaneous and environmentally induced genotoxic or miscoding base lesions, the *MUTYH* product, a DNA glycosylase, is specifically involved in defending against oxidative DNA damage (32, 33).

1.2.2 Standard treatments for CRC

Current treatment strategies for CRC include surgical intervention when possible (34-36), chemotherapy (37-39), anti-angiogenic therapies (40-43), and epidermal growth factor receptor (EGFR) inhibitors (44, 45). To date, surgical procedures remain the basis of curative treatment for CRC, however, disease management is typically a multimodal approach of conventional chemotherapy and local radiation therapies; the combination of surgery followed with chemotherapy being most widely accepted (46). Some patients with metastases confined to liver and/or lung can be cured of initially unresectable

disease using such approaches with intensive chemotherapy and secondary resection (15), however targeted therapies have largely impacted the treatment of metastatic disease (mCRC). In particular, anti-angiogenic drugs have had an advantageous role in treatment of mCRC where they are becoming components of standard-of-care therapy, as with their incorporation into combination chemotherapy regimens, there is improvement in patient survival outcomes (41, 47-50). mCRCs unfortunately have a tendency to develop resistance to the currently available anti-angiogenic therapies, and further, conventional approaches are highly limited due to toxicity and lack of tumour specificity, ultimately maintaining a poor prognosis of metastatic disease (51) and CRC in general. The predictive and prognostic biomarkers for biological therapies of mCRC are summarized in **Table 3**.

Specifically, the standard first-line drug treatments are fluoropyrimidine-based regimes classically comprised of 5-fluorouracil (5-FU) plus folinic acid (FA, also known as leucovorin, LV) in combination with irinotecan (FOLRIRI) or oxaliplatin (FOLFOX) (46, 52). Regimes may also include cytotoxic drugs capecitabine or raltitrexed, (37, 53), with the combination of capecitabine and oxaliplatin (XELOX) as a common adjuvant chemotherapy (15). As described above, patients with advanced CRC may also have treatments including monoclonal antibody (mAb) targeted anti-angiogenic agents [(anti-vascular endothelial growth factor (VEGF)], such as bevacizumab (Avastin) (41, 54, 55) or anti-EGFR antagonists cetuximab (Erbitux) or panitumumab (Vectibix) for indicated *KRAS* wild-type mCRCs (44, 45, 52, 56, 57). Unfortunately, a predictive marker of EGFR-inhibitor therapy is the presence of active mutations in *KRAS* or *BRAF* (V600E), in that those CRC sufferers do not respond to their therapeutic effect (58, 59). Novel antiangiogenic drugs, such as regorafenib (a novel multikinase inhibitor) and aflibercept (Zaltrap; a recombinant protein inhibitor of VEGF), have also been recently licensed by Health Canada in 2013 and 2014, respectively. Approved for the treatment of patients with mCRC, regorafenib is reserved for those who have been previously treated with fluoropyrimidine-based chemotherapy, oxaliplatin, irinotecan, an anti-VEGF therapy, and anti-EGFR therapy (60). The use of aflibercept is approved for use in combination with

Table 3. Predictive and prognostic biomarkers for biological therapy in mCRC

Biomarker	Prevalence	Available evidence	Predictive and prognostic value
KRAS mutations	40%	Conclusive	Negative predictive biomarker for anti-EGFR mAbs
		Insufficient	Predicts poor prognosis, but not an independent prognostic factor
BRAF mutations	10%	Substantial	Prognostic marker for poor outcome
		Insufficient	Potential predictive marker for resistance to anti-EGFR mAbs
NRAS mutations	3%-5%	Insufficient[a]	Potential predictive marker for resistance to anti-EGFR mAbs
PIK3CA mutations	15%-20%	Insufficient[a]	Potential predictive marker for resistance to cetuximab (exon 20 mutations) Potential prognostic marker for poor outcome
PTEN (loss of expression)	20%-40%	Insufficient[a]	Potential predictive marker for resistance to cetuximab Associated with activation of the PIK3CA pathway and adverse disease outcome
P53 mutations	1%-5%	Insufficient[a]	An independent predictive factor for cetuximab benefit Not prognostic
Epiregulin, amphiregulin (high expression)	50%-60%	Insufficient[a]	Associated with resistance to anti-EGFR antibody therapy and adverse clinical outcome
VEGF-D	40%-75%	Insufficient[a]	Potential predictive marker for response to bevacizumab
VEGF-A	nd	Insufficient[a]	Not predictive of response to bevacizumab

Modified from Luo and Xu, 2014 (61)

[a] Insufficient: The current clinical evidence cannot definitively demonstrate that the biomarker has predictive or prognostic value in mCRC. nd, not determined.

FOLFIRI, for patients with mCRC that are resistant to or progressed following an oxaliplatin-containing regimen (42, 60). The potential treatment combinations have been recently compiled in an extensive review by Schmoll *et al*., highlighting the benefits of an overall personalized patient approach when defining treatment regimens (15).

Due to its prevalence and preventative nature, CRC has been a focus in the field of oncology; though much progression hindered by the broad range of its stages at diagnosis, complexity of progression, heterogeneity, and diversity among patients. Optimal treatment choice for an individual highly depends on the disease extent and localization, overall tumour biology, and ultimately, considerations for sustaining quality of life while enabling long-term survival (15). Toxicity and lack of tumour specificity are the most important limits of conventional approaches. Evidence from the widening range of available tailored regimens, or those in development, advocates that the use of personalized medicine techniques will remain fundamental in how CRC, and cancer in general, will be treated in the future (15).

1.3 Cancer immunology: immunosurveillance and immunoediting

The concept that arising nascent malignant cells are recognized and eliminated as a function of the immune system has been a dynamic debate in tumour immunology since its original proposal in 1909 by Ehrlich (62), later formally designated as the theory of cancer immunosurveillance by Burnet and Thomas (63, 64). However, in the mid-20th century, this concept remained controversial with lack of sufficient evidence in some tumour-bearing models (65). Over the past two decades, this concept has seen a resurgence of interest and with extensive work and advancements in the experimental field of tumour immunology, there is now a much broader understanding of the interactions between the immune system and tumour cells. As such during this integral time, according to a recent review by Mittal *et al.* (2014) (66), the long-lasting dispute of the immune system effects on tumour development has diminished with clear evidence that intact immunity can, in fact, have three contradictory complex functions: facilitating cellular transformation, prevention or control of tumour development, and influence on the immunogenicity of tumours (66). With recognition that immunosurveillance

represents only one part of a broader process, this concept was refined to accurately capture the dynamic process, termed ‘cancer immunoediting’ (67, 68). This theory includes the dual role of the immune system in the active elimination of tumour cells but also highlights its importance in tumour-shaping and promoting tumour outgrowth.

Overall, the immunogenicity of developing tumour cells can be shaped by the immune system. This occurs most notably by adaptive immunity (particularly T cells), but recent evidence suggests that innate immunity, such as natural killer (NK) cells and M1 macrophages, to some degree, also contribute to this editing process (69). A fundamental principle in this process of immunological destruction or sculpting of a developing cancer is the T-cell recognition of tumour antigens (70). Indeed, T cell-dependent immunoselection has been demonstrated as one crucial mechanism of cancer immunoediting, allowing the outgrowth of less immunogenic tumour cells that lack strong antigens, as a result of either reduced expression or presentation on major histocompatibility complex (MHC) class I (MHC I) (70-72). Additionally, the evidence for immunoediting is not only restricted to tumour-bearing animals, but has also been clinically observed in human patients receiving targeted vaccine immunotherapy (73, 74).

With the complex progression from immune surveillance to immune escape, cancer immunoediting comprises of three proposed sequential phases: elimination, equilibrium, and escape (67, 68, 75, 76). As a hallmark of the original immunesurveillance concept, the elimination phase is a process in which innate and adaptive immunity cohesively detect and destroy developing tumour cells, prior to clinical appearance. In the equilibrium phase, some tumour cell variants may not be entirely eliminated and the immune system maintains the tumour in a state of ‘functional dormancy’ in which the balance between anti-tumour (*e.g.* interferon [IFN]-γ, interleukin [IL]-12) and tumour promoting cytokines (*e.g.* IL-10, IL-23) in the tumour microenvironment and the adaptive immunity controls the growth of clinically undetectable, occult tumour cells. Due to constant immune pressure however, some tumour cells may undergo genetic and epigenetic changes (immunoselection), and begin evolving mechanisms that resist immune recognition such as antigen loss or expression deficiency, or induce immunosuppression, such as upregulation of programmed death-ligand 1 (PD-L1).

During the final step, the escape phase, progressive growth of edited tumour cells presents as clinical disease after the immune system fails to restrict the tumour cell population. Tumours may escape by a variety of complementary mechanisms of immunosuppression and tolerance, often exhibited simultaneously. This can include reduced immune recognition (*e.g.* loss of MHC I or tumour antigen expression), increased resistance or survival (*e.g.* upregulation of anti-apoptotic molecules), or establishment of a complex immunosuppressive microenvironment (*e.g.* VEGF, transforming growth factor [TGF]-β expression, induction of immunomodulatory molecules indoleamine-2,3-dioxygenase [IDO], PD-L1, T cell immunoglobulin mucin-3 [TIM-3]). Importantly, escape from immune control is now recognized to be one of the 'hallmarks of cancer' (77). Extensive work has been undertaken to elucidate the mechanisms involved in cancer immunoediting and reviewed in great detail (66, 71, 76, 78).

CRCs are collectively known to be able to manipulate and evade the immune system with increasing evidence that immune cells have an important role in tumour development and metastasis. Efforts to evaluate these mechanisms are continually ongoing [reviewed in (79-82)], some of which will be highlighted. CRC, among other solid tumours, contain a diverse subset of leukocytes, including both myeloid- and lymphoid lineages. Notably, immunogenicity of CRC tissues was demonstrated with increased activation, cytotoxic activity, and functional reactivity of tumour-infiltrating T lymphocytes (TILs) correlated with the presence of systemic functional tumour antigen-reactive T cells (83). However, the proportion of the activated tumour-associated T lymphocytes decreased significantly with higher tumour stage and was inversely correlated with the overall stage of the tumour (83). In another study, while adjacent normal mucosa contained normal levels of NK cells, impaired migration of these cells was apparent during tumour development. These cells were largely scarce within CRC tumours, despite high local tumour chemokine levels that was also independent of human leukocyte antigen (HLA) class I expression (84). While the role in CRC remains controversial, tumour-associated macrophages (TAMs) play an overall role in CRC progression. TAMs can both promote immunoselection by further inducing an inflammatory response (M1) or in response to immunosuppressive cytokines, generate a tumour-promoting TAM (M2). These TAMs

can secrete a variety of growth factors including epidermal growth factors (EGF), TGF-β, VEGF, and proteolytic enzymes such as matrix metalloproteinases that can degrade collagen of basement membranes, supporting the movement and metastasis of tumour cells (79).

Immune escape of CRC has also been closely associated with the establishment of a microenvironment that actively suppresses anti-tumour immunity. A prominent increase of myeloid-derived suppressor cells (MDSC) (characterized as $Lin^{-/low}HLA\text{-}DR^{-}CD11b^{+}CD33^{+}$) was identified both in tumour tissue and systemically when compared to a healthy population and correlated with tumour stage and metastasis. With further analysis *ex vivo*, these cells were able to inhibit the proliferative function of autologous T cells (85). Regulatory T cells (Tregs) have a complex role in CRC that may be dependent on the tumour type and stage; however, Tregs are in general associated with interference of anti-tumour immune responses, but their presence seem to correlate with a favourable prognosis (80, 81, 86). Although it is clear that an enhanced number of the tumour infiltrating T cells, among the other T cell subsets, express $FoxP3^{+}$ (87), a hallmark marker of Tregs, the contributory role remains unsettled and paradoxical within CRCs (86, 88). In addition to immune cell suppression within the microenvironment, CRC evasion has also been associated with the pro-tumour inflammatory responses, in particular IL-17, shown to increase inflammation and promote carcinogenesis in some tumours (89), as well as increased IL-6 expression has correlated with advanced stages of CRC and decreased survival (90). Observed within the tumour microenvironment of tumour-bearing mouse models of liver metastasis, high expression of IL-10, TGF-β, and TGF-α were associated with enhanced tumour growth (79, 82). Lastly, CRC tumour cells can actively suppress the immune response by downregulation or reduced expression of MHC I (91), and upregulation of PD-L1 (92).

Overall, based on the current knowledge and ever widening field of cancer immunology, in consensus, an important obstacle to overcome when treating cancers is tumour immunosuppression and tolerance (93).

1.4 Immunotherapy for the treatment of cancer

Cancer immunotherapy collectively refers to a number of intended strategies to harness and manipulate immune-mediated mechanisms to specifically target cancer for stabilization or eradication (94). The concept of immunotherapy, although increasingly prominent over the past two decades, has been well documented for over a century. In 1881, a young surgeon in New York, Dr. William Coley, initiated efforts to reproduce the observed spontaneous remissions of sarcomas in patients whom had developed erysipelas, an acute bacterial infection commonly associated with group A *Streptococcus*, by administering intratumoural injections of live or heat-inactivated *Streptococcus pyogenes* and subsequently, mixed with *Serratia marcescens*, later known as 'Coley's Toxin' (95). Coley speculated that the infection localized around the tumour site would induce a direct cytotoxic reaction and as a secondary event, lead to regression, and even cure, of a malignant disease (95). The first streptococcal culture injection treatment encouragingly resulted in the extensive necrosis of an inoperable tumour and a disease-free outcome for eight years (96, 97). However, subsequent clinical responses remained variable from patient to patient, attributed primarily to disease heterogeneity and infection severity among patients, Coley also importantly noted that injections in a remote anatomic site could result in impressive tumour responses. From this, he concluded that even a systemic response to an infection, though mechanistically unclear, resulted in tumour destruction (95).

Following forty-years of treating a variety of malignant diseases, successes were sporadic, difficult to reproduce (98), and were controversial among clinicians. One notable exception however is the further application of this theory in intravesical injection of Bacillus Calmette-Guérin (BCG), prepared from *Mycobacterium bovis*, for treatment of superficial bladder cancer after surgical resection, which has shown to prolong patient survival and remains an acceptable treatment today (94, 99). During this period of time however, oncologists, excluding the BGC application, continued to rely heavily on surgery, and increasingly, on effective new emerging methods, such as radiation therapy and eventually chemotherapy. Due to the risks associated with administering infectious agents to already weakened cancer patients, Coley's strategy was never fully embraced

and became generally disregarded until the middle of 20th century; a present irony given the trauma associated with the treatments that were becoming common practice (94). Cancer immunotherapy applications began to re-emerge as *in vivo* chemical inducible tumour models were developed, allowing for readily accessible testing of various cancer treatments (99).

Today, dramatic advances in the field of cancer immunotherapy have been made, with several broad therapeutic strategies now recognized. These approaches comprise of cancer vaccines, adoptive T lymphocyte transfer, immunomodulatory/immune check point blockade, and antibody-based therapies. In the subsequent sections, each treatment avenue will be introduced, with emphasis on antibody-based therapies, in addition to summaries of potential avenues directed specifically for CRC. It is recognized that the great breadth of knowledge that has developed within this field to date is beyond the scope of the purposes for this discussion, but have been comprehensively reviewed elsewhere (94, 99-102).

To broaden the response of cancer and to treat resistance, the combinational use of chemotherapeutic drugs has traditionally been the foundation for treatment. A significant advantage of immune-based therapies is that they can be combined rationally with these conventional treatments for optimal therapeutic effect, as well as with other emerging immunotherapies (94). For reference throughout subsequent sections, the standard clinical trial outcome and phase definitions have been included with **Appendix 3** and **Appendix 4.**

1.4.1 Vaccine therapy

Cancer vaccines aim to actively prime and stimulate the immune system against tumour cells for a specific and directed anti-tumour response. The vaccines can be designed for the prevention of tumour formation (prophylactic) or, as in the majority of those in study, the therapeutic format, for the inhibition of growing tumours and directed immune responses; both forms having the intent to generate prolonged protection (94). Antigen-based vaccines are generated through short peptides (~20-mer), with a suitable dendritic cell (DC) activating adjuvant, full length proteins with a broader epitope range, or

through viral vectors encoding tumour antigens (94). Cellular-based vaccines use either whole tumour cells or lysates (autologous or allogeneic), which contain a wide range of antigens for targeting including mutated proteins. Lastly, DC-based vaccines, where DCs are isolated from the patient, loaded with antigens *ex vivo*, activated, and then re-infused into the patient are also being explored as potential approaches, though remain in early development (94).

Despite the promising success of prophylactic vaccines used for cancers of viral origin (*e.g.* human papillomavirus [HPV]), to date, therapeutic vaccines have been less successful (94, 103). One limitation is that vaccine effectiveness relies largely on the induction and regulation of T cells, DCs, and other cell-mediated immune responses such as Treg suppression (104). Indeed, although a large number of T cells are present that are capable of recognizing tumour antigens (in preclinical models), this has been insufficient to mediate tumour regression (105-107) suggesting that T cells, in order to mediate anti-tumour effects, must be in the correct state of activation and differentiation (105). Cancer vaccines are usually administered with adjuvants, such as BCG, to enhance the immune response, and are often combined with cytokines such as granulocyte macrophage colony-stimulating factor (GM-CSF) (108, 109). Recently, co-administration of IL-2 with a short peptide derived from glycoprotein 100 (gp100), a melanocyte antigen, augmented tumour responses and progression-free survival (PFS) was prolonged (110). Ongoing advancements to understand the basic immune responses of therapeutic cancer vaccines have suggested that effective strategies may require the integration of immunomodulators through checkpoint blockade (*e.g.* cytotoxic T-lymphocyte-associated protein 4 [CTLA-4], programmed cell death protein 1 [PD-1]) to interfere with immune regulatory control to maximize the vaccine effectiveness (94, 111).

Vaccination trials for CRC have largely been tumour cell–based vaccines, consisting of irradiated autologous tumour cells (112). From meta-analyses, there was evidence of significant improvement in disease-free survival (DFS), however none in overall survival (OS). Encouragingly, in subsets of patients with resected liver metastases, there has been a significant advantage in OS and metastases-free survival (113). To date, carcinoembryonic antigen (CEA) has been the most common peptide-based vaccine in

CRC trials, however, despite supporting preclinical evidence, the results and tumour response of the studies have not remained consistent (112, 114). Alternative targeted antigens remain ongoing in clinical trials however, for further evaluation of cancer vaccines in the treatment of CRC (**Table 4)**.

1.4.2 Adoptive cell therapy

In the treatment of cancer, adoptive cell therapy (ACT) is the transfer of lymphocytes bearing tumouricidal properties to the patient for directed anti-cancer effects (115, 116). A variety of cellular therapies have been incorporated into cancer treatment, including the infusion of polyclonal or antigen-specific T cells, NK cells, DC, and macrophages (Mϕ). Most recognized for transfer are the naturally occurring TILs, isolated from resected tumours of the patient, expanded in culture (with exogenous IL-2) and subsequently re-infused into the patient for therapeutic effect (115). Contradictory to other forms of immunotherapy, ACT does not rely on the *in vivo* mediation of T cell activation for tumour regression but allows for the *ex vivo* selection and expansion of high-avidity, autologous effector T cells. Importantly, developing the T cells as such also breaks tolerance to the tumour antigen, removes *in vivo* inhibitory or suppressive signals, and enables the manipulation of the recipient host (*e.g.* lymphodepletion), generating a favorable environment for effective cell transfer and engraftment (94, 115). Although limited to the identification of T cells that target tumour antigens exclusively, with this treatment approach, patients with melanoma have had marked clinical responses, experiencing tumour regressions that were durable and complete (115, 117).

Initially beneficial to patients with reactive T cells from resectable tumours, advances in genetic engineering technology of T cells has expanded ACT opportunities to patients with unresectable, solid tumours (116). Expression of specific conventional TCRs or recombinant chimeric antigen receptors (CARs) (118) in ‘normal’ T cells isolated from peripheral blood enable directed T cell effects to cognate targets. As recombinant receptors that provide both antigen-binding and T-cell-activating functions, CARs allow the immediate activation of the T cell upon recognition of the intact surface protein (118). With the use of these approaches, ACT has demonstrated discernible regressions in a

Table 4. Select representation of immunotherapy trials for the treatment of CRC currently under investigation

Treatment under clinical trial	NCT number	Phase	Study endpoints	Primary completion
Vaccines				
Study of Imprime PGG® in Combination with Cetuximab in Subjects with Recurrent or Progressive KRAS Wild Type CRC	NCT01309126	III	OS; PFS, CR, PR, OR, QoL, PK	April 2016
Gene and Vaccine Therapy in Treating Patients with Advanced Malignancies: Vaccine that targets NY-ESO-1	NCT01697527	II	Safety/Efficacy; clinical response	October 2018
Immunotherapy with CEA(6D) VRP Vaccine (AVX701) in Patients with Stage III CRC	NCT01890213	I	Safety; Number of AE	November 2015
Vaccine Therapy in Treating Patients with Metastatic Solid Tumours: Biological Agent HER2 Vaccine	NCT01376505	I	Safety/Efficacy; immune response	January 2016
Adoptive cell therapy				
Immunotherapy using Tumour Infiltrating Lymphocytes for Patients with Metastatic Cancer	NCT01174121	II	Safety/Efficacy	December 2018
CAR T Cell Receptor Immunotherapy Targeting VEGFR2 for Patients With Metastatic Cancer	NCT01218867	I/II	Safety/Efficacy; ORR	October 2018
T Cell Receptor Immunotherapy Targeting MAGE-A3 for Patients With Metastatic Cancer (HLA-DP0401+)	NCT02111850	I/II	Safety/Efficacy; safe dose	December 2016
Anti-Tumour Effects of Escalating Doses of Adoptively Infused *Ex Vivo* Expanded Autologous Natural Killer (NK) Cells Against Metastatic Cancers	NCT00720785	I	Safety; MTD, escalating dose	January 2018
Immunomodulatory molecules and immune checkpoint therapy				
Continuous Infusion of rhIL-15 for Adults With Advanced Cancer	NCT01572493	I	Safety; MTD, DLT	April 2016
Trial of NHS-IL12 in Patients With Metastatic Solid Tumours	NCT01417546	I	Safety; MTD, DLT	January 2016

Nivolumab and Nivolumab plus Ipilimumab in Recurrent and mCRC[†]	NCT02060188	I/II	Efficacy study; ORR	December 2016
A Phase I Study of MPDL3280A (anti-PD-L1) in Patients with Locally Advanced or Metastatic Solid Tumours	NCT01375842	I	Safety; DLT	April 2014 (104)
Study of Pembrolizumab (MK-3475; anti-PD-1) in Patients with Microsatellite Unstable (MSI) Tumours	NCT01876511	II	Efficacy study; PFS, ORR	June 2017
A Study of MPDL3280A Administered in Combination with Bevacizumab and/or with Chemotherapy in Participants with Locally Advanced or Metastatic Solid Tumours	NCT01633970	I	Safety; number of AE, DLT/MTD	February 2016
Anti-PD-L1, MEDI4736, in Combination with Tremelimumab in Subjects with Advanced Solid Tumours	NCT01975831	I	Safety; number of AE	December 2016
A Study of CDX-1127 (Varlilumab) in Patients with Select Solid Tumour Types	NCT01460134	I	Safety; number of AE	September 2015
Monoclonal Antibodies				
Combination Study of Urelumab (anti-4-1BB/CD137) and Cetuximab in Patients with Advanced/mCRC	NCT02110082	I	Safety; number of AE	January 2017
Comparing the Efficacy and Safety of RO5520985 (bispecific anti-ANG-2/anti-VEGF-A) and FOLFOX with Bevacizumab and FOLFOX in Patients with Untreated mCRC	NCT02141295	II	Efficacy; PFS, ORR	May 2017
Ensituximab (NPC-1C), a Monoclonal Antibody Against a MUC5AC-related antigen to Treat CRC	NCT01040000	II	Safety/Efficacy; ORR, OS	January 2018
A Trial of Trametinib and Panitumumab in RAS/RAF Wild Type Advanced CRC[†]	NCT02399943	II	Efficacy; % patients with CR, PR, or stable disease	June 2018

Information gathered from the Cancer Research Institute as of 2015 (http://www.cancerresearch.org/); [†]Canadian locations
Study endpoint abbreviations: AE, adverse events; CR, complete response; DLT, dose limiting toxicity; MTD, maximum tolerated dose; OR, objective response; ORR, objective response rate; OS, overall survival; PFS, progression free survival; PK, pharmacokinetic; PR, partial response; QoL, quality of life.

variety of cancer indications, including melanoma, leukemia, lymphoma, and cervical cancer (115, 119-123). To date, issues remain surrounding the selection of safe targets and the scarcity of such targets, toxicity, and manufacturing complexity. Additionally, in clinical assessment, the lack of durable responses in some patients indicates that to properly direct and activate T cells within the tumour microenvironment, further interventions may be required to have lasting treatment effects (94).

While ACT has predominantly been applied to the treatment of haematological malignancies to date (124), this therapy may be beneficial for epithelial solid cancers with advancements in identification of suitable targets. Indeed, ACT clinical trials for the treatment of CRC are currently ongoing, with focus on metastatic disease (**Table 4**).

1.4.3 Immunomodulatory molecule and immune checkpoint therapy

Within anti-cancer therapies, immunomodulatory molecules can function to indirectly increase the activity of effector lymphocytes, or directly by reducing tumour growth (109). Clinical evaluations have foremost focused on systemic administration or direct tumour injection of immunostimulatory cytokines IFN-α and IL-2 (109). Independent administration of IFN-α and IL-2 has demonstrated increased survival responses in a subset of advanced melanoma and renal cell cancers (109, 125-127). Associated with low response rates in general, these treatments can also have a considerable risk of high-dose toxicity and systemic inflammation due to lack of specificity (94, 125). To date, even though IFN-α and IL-2 have been supportive therapies in particular for these cancers, as well as haematological malignancies, the mechanism and why the therapeutic effect is limited to select patients is not fully understood. With focus on T cell activation, the use of antibodies targeting known receptors (*e.g.* 4-1BB, CD27, OX40, GITR) has progressed as the next generation of immunomodulators undergoing clinical evaluations (**Table 4**) (94).

In advanced CRC patients, modest immune responses have been demonstrated with the combination of IL-2 and GM-CSF (128). Recent evaluations in mCRC patients has further indicated that chemotherapy (FOLFOX) in combination with IL-2 and GM-CSF,

has a marked improvement in overall response rate and progression free survival compared to chemotherapy alone, with a trend towards improved overall survival (129).

Cancer immunotherapy has significantly progressed over the last decade with the development of immune checkpoint antagonists. Inherently, the immune system regulates induced responses by feedback inhibitory loops to minimize tissue damage, suppress autoimmunity, and maintain proper immune homeostatsis. Importantly, these mechanisms control T cell responses influencing communication between T cells and antigen presenting cells (APCs) through inhibitory receptors on the lymphocytes and respective ligands, two of which are currently clinically active for blockade, CTLA-4 and PD-1 (101). Though these checkpoint receptors act through different mechanisms (130), both are expressed on activated effector T cells, and upon cognate ligand binding, reduce effector functions. In addition, CTLA-4 and PD-1 (among other checkpoint receptors, such as lymphocyte-activation gene [LAG-3] and TIM-3) are highly expressed on Tregs but contrary to effector cells, ligand binding enhances Treg proliferation and function, promoting the suppression and attenuation of effector cells (101, 131). Predominately, antibody-based therapies have been used for directed blockade at these immune checkpoints.

Extensively studied for the role in T cell responses, CTLA-4, as a key negative regulator of CD28-dependent responses, functions by binding members of the co-stimulatory B7 family of accessory molecules on APCs required for T cell activation, and thereby inhibits further activation and expansion (132). Ipilimumab, a mAb to CTLA-4, as well as effectively blocking the negative regulation of this receptor, also down-regulates the immune suppressive function of Tregs, facilitating anti-tumour effects of T cells and limiting Treg activity in tumours (131, 133-135). In a pivotal phase III trial, administration of ipilumumab provided a significant improvement in overall survival (136) for advanced metastatic melanoma, granting its clinical approval by the Food and Drug Administration (FDA) in 2011 and by Health Canada in 2012, and is arguably one of the most important developments for cancer immunotherapy to date. In a long-term follow-up, ipilimumab has shown a durable complete response, and potentially curative tumour regression in a subset of treated melanoma patients (133, 137). Blockade of

CTLA-4 has since been undergoing further evaluation in numerous clinical settings, including mCRC (NCT02060188) (138).

Another approach receiving some clinical validation is targeting immunosuppression at the tumour site in addition to immune cells (94). PD-1 is expressed predominantly on T cells (including Tregs) after induction, but can also be expressed on B cells, monocytes, natural killer T (NKT) cells, and some DCs (139, 140). Upon binding with its ligands PD-L1 or PD-L2, which are expressed by potential target cells and can also be upregulated in a variety of cancers (141, 142), the T cells are rendered unresponsive (140). Duly summarized in Ohaegbulam *et al*. (143), several mAbs to PD-1 or PD-L1 have been clinically studied in Phase I trials and continue to be evaluated further either as a monotherapy or in combination. Of these trials, this strategy for immunomodulatory therapy has been well tolerated with impressive response rates and durability in melanoma, non-small-cell lung carcinoma (NSCLC), and renal cell carcinoma (RCC) (143). Currently, a PD-1 blocker (Nivolumab) is in clinical trials involving mCRC (NCT02060188) and similarly, studies are also proceeding using an anti-PD-L1 blocker in refractory mCRC as a single agent (NCT01375842; NCT01876511) with early responsive results (144) or in a multimodal approach with chemotherapy and bevacizumab (NCT01633970) or tremelimumab (anti-CTLA-4; NCT01975831) (**Table 4**).

1.4.4 Antibody-based therapy

Over the past two decades, antibody-based therapy for cancer has become well recognized and for patients with haematological malignancies and solid tumours, one of the most successful treatment strategies (145). Soon after the discovery of antibodies in the late nineteenth century, Paul Ehrlich described a ‘magic bullet concept,’ where drugs directly proceed to their intended structural targets (146). Targeted medicine, in his proposed theory, should efficaciously defend against invading pathogens (including cancerous cells) but remain harmless to healthy tissues (146). With clinical controversy however, this approach received little value until the ability to generate mAbs with advancements in hybridoma technology was described in 1975 by César Milstein and

Georges Köhler (147). In light of these developments, the search for cancer-specific antigens was initiated with efforts focused on identifying suitable surface structures, a challenge that still persists today (145). This family of molecules, termed tumour-associated antigens, will be described further in **Section 1.5**.

In this form of immunotherapy, antibodies can function through respective responses such as mediating alterations in antigen or receptor function (agonist or antagonist functions; *e.g.* anti-angiogenic effect), modulating the immune response or environment, or directing conjugated drugs or radiolabelled compounds that specifically target TAAs (148, 149). In addition, unconjugated mAb therapies may have immunological cytotoxic effects through opsonizing tumour cells and complement-dependent cytotoxicity (CDC), triggering apoptosis, or by removal through antibody-dependent cell-mediated cytotoxicity (ADCC) (150). All of these approaches have been successfully applied within the clinic, a proportion of those for the treatment of haematological malignancies (*e.g.* targeting CD20, CD30) including both as unconjugated mAbs and for the delivery of cytotoxic drugs or radioisotopes (145). For patients with solid tumours, the most successful mAb therapies to date have been targeting the ErbB family of receptors (including EGFR, human epidermal growth factor receptor [HER]2/neu) and VEGF, demonstrating improved tumour responses and survival (145). Immune regulation by antibodies has also has remarkable success within the clinic as described in Section 1.4.3. As of early 2015 there were 31 antibody treatments (or derivatives) that were approved by Health Canada for clinical use as monotherapy or in combination, 12 of which are designated for the treatment of various specified cancers (**Table 5**).

In the development of antibody-based therapies, preclinical and clinical evaluations have revealed the importance of target antigen selection but have also highlighted the major considerations related to therapeutic mAbs, including 1) affinity and avidity, 2) the choice of antibody construct, and 3) the desired therapeutic approach (*e.g.* signaling abrogation, immune effector function). As such, antibodies have interdependent properties that can be used for molecular alteration to improve the clinical potential. Key elements may include antibody immunogenicity, size, effector function, and overall pharmacokinetics (145, 151).

Table 5. Antibody therapies approved by Health Canada for medical use in the treatment of cancer

Name	Target	Source	Approval for indication[a]	Proposed mechanism
Alemtuzumab; Campath	CD52	humanized from rat, IgG1 mAb	Second-line therapy for CLL	targets CD52 on the surface of mature lymphocytes for elimination
Bevacizumab; Avastin	VEGF-A	humanized from mouse, IgG1 mAb	mCRC; unresectable, metastatic or recurrent NSCLC; glioblastoma after relapse or disease progression	angiogenesis inhibitor
Brentuximab vedotin; Adcetris	CD30	chimeric (mouse/human), IgG1 mAb	Relapsed or refractory HL and sALCL	antibody-drug conjugate
Catumaxomab; Removab	EpCAM and CD3	rat/mouse hybrid mAb; trifunctional	management of malignant ascites with EpCAM-positive carcinomas where standard therapy is not available or feasible	elicits immune reaction by binding $EpCAM^+$ cells to $CD3^+$ cells and Mϕ, DC or NK cells (Fc receptor)
Cetuximab; Erbitux	EGFR	chimeric (mouse/human), IgG1 mAb	EGFR-expressing metastatic CRC when used in combination with irinotecan in patients with non-mutated KRAS	competitive antagonist to EGFR; inhibits growth signals
Ipilimumab; Yervoy	CTLA-4	human, IgG1 mAb	unresectable or metastatic melanoma in patients who have failed or do not tolerate other systemic therapy	prevents inhibitory mechanism to allow T lymphocytes to function
Obinutuzumab; Gazyva	CD20	humanized from mouse, IgG1 mAb	CLL in combination with chemotherapy	targets B cells (CD20) for elimination
Panitumumab; Vectibix	EGFR	human, IgG2 mAb	refractory EGFR-expressing metastatic CRC in patients with non-mutated KRAS	competitive antagonist to EGFR; inhibits growth signals

Pertuzumab; Perjeta	HER2/neu; dimerization domain	humanized from mouse, IgG1 mAb	HER2-positive metastatic breast cancer; in combination with trastuzumab and docetaxel	inhibits dimerization of HER2 receptor preventing growth
Rituximab; Rituxan	CD20	chimeric (mouse/human), IgG1 mAb	B-cell non-HL, resistant to chemotherapy regimens	targets B cells (CD20) for elimination
Trastuzumab; Herceptin	HER2/neu; subdomain IV	humanized from mouse, IgG1 mAb	HER2-positive metastatic breast cancer	interferes with the HER2/neu receptor preventing growth
Trastuzumab emtansine; Kadcyla	HER2/neu; subdomain IV	humanized from mouse, IgG1 mAb	HER2-positive metastatic breast cancer	antibody-drug conjugate

Information gathered from Health Canada Drug Product Database (www.hc-sc.gc.ca) as of May 2015.

[a]Cancer abbreviations: CLL, chronic lymphocytic leukemia; CRC, colorectal cancer; HL, Hodgkin's lymphoma; NSCLC, non-small cell lung cancer; sALCL, systemic anaplastic large cell lymphoma

Traditionally, murine mAbs were developed for therapeutic use and were first to be tested clinically; however, these mAbs are restricted by several factors (152-154). These mAbs are highly immunogenic, have a short-half life in humans, and as a result, are also inefficient at eliciting human effector functions (153). In particular, a major limiting factor due to the murine structure of the mAb, is the induction of human anti-mouse antibody (HAMA) response. After a first dose, administration can generate a strong response in up to 50% of patients, and >80% with repeated doses (153, 155, 156). Such responses can cause rapid clearance or direct neutralization of the administered mAb, compromise therapeutic efficacy and prevent further dosing or induction of systemic toxicity stemming from a requirement of high doses for effective treatment. In severe cases, typically associated with repeated intravenous administration, 'serum sickness' from immune complex formation can led to an anaphylactic response (155). The current success of therapeutic mAbs can be attributed to the development of chimeric and humanized mAbs by recombinant technology, and later fully human mAbs (**Figure 1**). Using these mAb strategies demonstrates reduced immunogenicity, a longer half-life, and can promote human effector functions (157-160) and are now the preferred technologies for developing antibodies as therapeutics. Chimeric antibodies are engineered by joining the antigen-binding variable domain (Fv) of a murine mAb to the constant domains of a human antibody (161, 162). Humanized antibodies are generated by grafting the antigen-binding complementarity determining region (CDRs) from a mouse mAb within a human mAb (163, 164). To create a high-affinity humanized mAb however, the transfer of one or more additional residues from the framework regions (FRs) of the parental mouse mAb is generally required (165). High-affinity fully human antibodies are customarily derived from phage display libraries (166-168) or by hybridoma technology using transgenic mice that express human immunuoglobulin (Ig) genes (169-172).

In addition to overcoming immunogeneticity and systemic clearance, to gain exposure to the intended target antigen, the mAb must also overcome capillary extravasation, movement from the capillaries into the tumour tissue (173) and high interstitial pressure gradients, in particular for solid tumours (174, 175). As such, distribution of mAbs within the tumour is commonly heterogenous, even perivascular, after intravenous

Figure 1. Humanization of therapeutic antibodies for reduced immunogenicity

Schematic illustration of antibodies developed from murine origin to human to reduce immunogenicity that is applied for use in therapies. Antibodies used include fully murine mAb, chimeric mAb, where the only the variable region is murine (65% human), humanized mAb, where only the CDR loops are murine (>90% human), and fully human mAb. A generic suffix designates the form of antibody as listed. Fc indicates fragment crystallizable region (constant domain); Fab, antigen-binding fragment; ABS, antigen binding site; C_H, heavy chain, constant domain; C_L, light chain, constant domain; V_H, heavy chain, variable domain; V_L, light chain, variable domain. Figure modified from Foltz *et al.* (176).

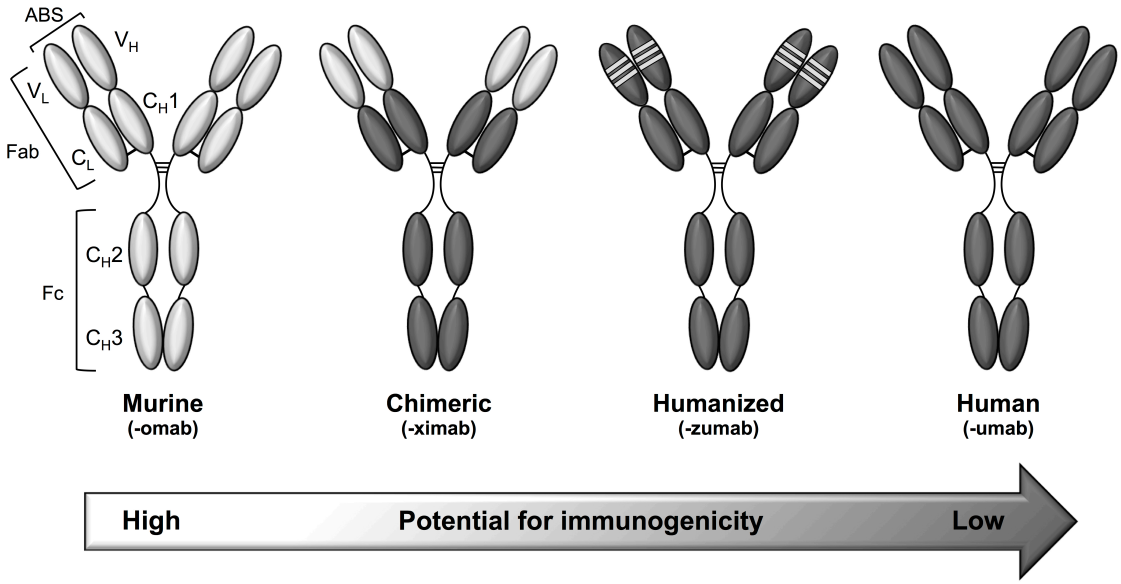
ABS
V_H
V_L
C_H1
Fab
C_L
C_H2
Fc
C_H3
Murine
(-omab)
Chimeric
(-ximab)
Humanized
(-zumab)
Human
(-umab)
High
Potential for immunogenicity
Low

administration (177). While this distribution can arise from heterogeneous antigen expression and vasculature, as well as tumour necrosis, it is also in part due to mAb size and antigen-binding affinity, proposed in the 'binding-site barrier' model where there is an inverse relationship between affinity and penetration (177, 178). This poor penetration can decrease overall efficacy and partial exposure to the intended therapeutic, increasing the risk of acquiring resistance (177). The molecular architecture of antibodies can be modified however to generate formats that varies in both size and valency (the number of antigen binding sites) (151). The growing range of alternative antibody formats can span a range of molecular weight, valency, and include multiple distinct antigen-binding specificities (**Figure 2**). The antibody building block that is most frequently used as a base in the design of non-natural formats is the single-chain variable fragment (scFv). The scFv comprises of the variable domains from the heavy and light chain (V_H and V_L) joined by a peptide linker of ~15 amino acid residues (151). Although eliminated more rapidly through renal clearance, smaller antibody fragments, like scFv, extravasate more efficiently than IgG, and diffuse more readily within tumours (151), characteristics that may be suited in particular for clinical imaging. Antibody fragments also offer the potential to avoid fragment crystallizable region (Fc)-dependent effector functions, reducing the severity of a HAMA response and can show a range of pharmacokinetic properties (151). While a reduction in distribution is characteristic of a full mAb, this form is commonly favoured for its long half-life, clearly demonstrating that each format can have opposing factors limiting success and that the design consideration can be dependent on a number of factors, including desired biological potency, the targeted tumour, and overall clinical application (179).

Similar to the choice of antibody fragment size, the effector function of the antibody can also be considered for alternation based on the target antigen, therapeutic strategy, and clinical setting (179). While increasing effector functions such as ADCC and CDC may increase therapeutic efficacy for some interventions, in others, prevention may be desired to reduce unnecessary side effects or toxicity. By mutational analysis and computational design methods, the interactions between IgG molecules and various Fc-gamma receptors (FcγR) for activation (*e.g.* FcγRI, FcγRIIa, FcγRIIIa and FcγRIIIb) and inhibition

Figure 2. Recombinant antibody formats for targeted therapy

A selection of possible recombinant antibody formats represented as a schematic illustration and relative approximate size (kDa). Depicted are **A)** full mAb (IgG), **B)** building blocks for antigen-binding reformatting, **C)** possible reformatted antibodies to alter size and include multivalent platforms, and **D)** multi-specific antibody options for targeting multiple antigens. Fc indicates fragment crystallizable region (constant domain); Fab, antigen-binding fragment; ABS, antigen binding site; C_H, heavy chain, constant domain; C_L, light chain, constant domain; V_H, heavy chain, variable domain; V_L, light chain, variable domain.

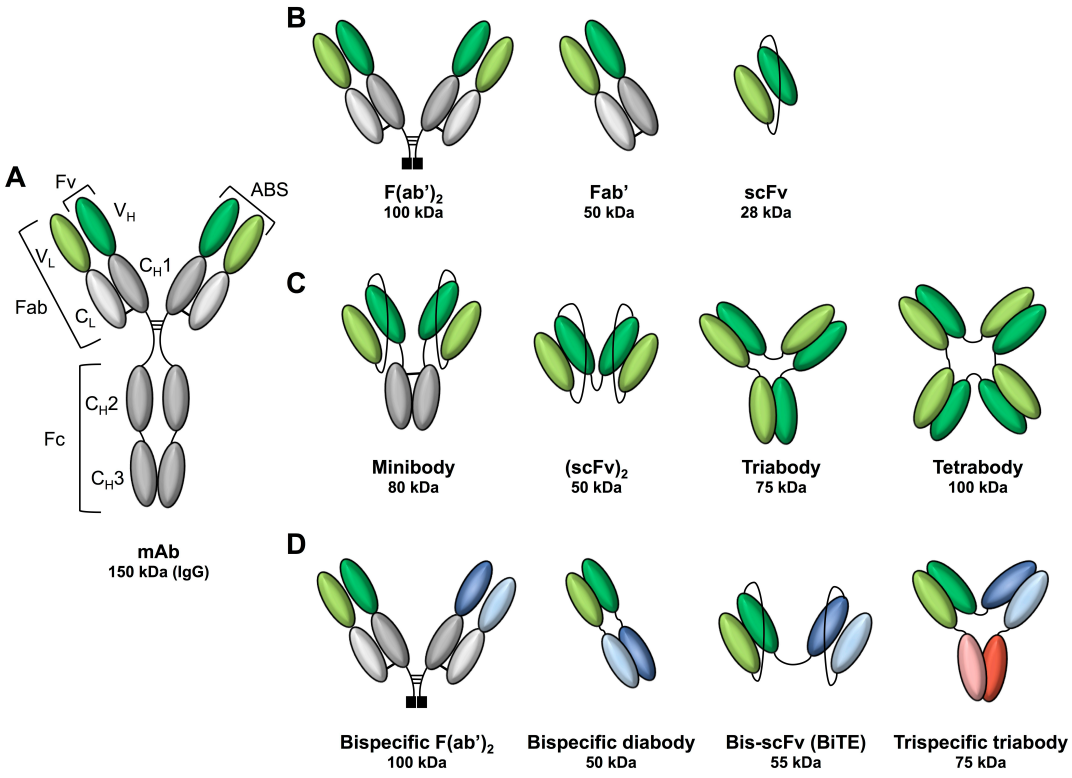
A
Fv
V_H
ABS
V_L
C_H1
Fab
C_L
C_H2
Fc
C_H3
mAb
150 kDa (IgG)
B
F(ab')2
100 kDa
Fab'
50 kDa
scFv
28 kDa
C
Minibody
80 kDa
(scFv)2
50 kDa
Triabody
75 kDa
Tetrabody
100 kDa
D
Bispecific F(ab')2
100 kDa
Bispecific diabody
50 kDa
Bis-scFv (BiTE)
55 kDa
Trispecific triabody
75 kDa

(FcγRIIb) has enabled the engineering of the Fc region to modulate effector functions (180). Relatedly, the regulation of serum IgG concentration has been investigated to increase (or decrease) the terminal half-life of IgG through tailoring of the interaction with FcRn, a receptor known to protect IgG from degradation (181). Lastly, the majority of currently developed unconjugated mAbs are based on human IgG, nearly all containing the IgG1 isotype. With the intent to increase mAb diversity and to develop mAbs that are often inefficient at supporting effector function, the use of classes IgG2 and IgG4 have been of interest, based on the distinct structural and functional properties (151, 182).

Stemmed from the wide range of antibody formats, the repertoire of antibody-based therapeutics is continually being expanded and presented with novel functions by conjugations and genetic fusions, including enzymes, toxins, drugs, and radioisotopes (183). A notable contribution has been bispecific antibodies, designed to bind two different epitopes, invariably on two different antigens. Most widely used for delivering immune effector cells to tumours, the single chain bispecific T cell engaging antibody (BiTE) concept allows for a convenient approach that engages both the activation of the effector cells, most commonly the T cell receptor (TCR) (anti-CD3) and an antigen on the tumour cell surface, redirecting and localizing cytotoxic lymphocytes at the tumour site (94, 184).

Even with optimal development strategies, antibody-based therapies are still limited by irregular bidistribution of the targeted antigen or receptor, accompanied by target heterogeneity, presence or development of mutations, or downregulation of expression (145). The persisting major clinical challenge is to determine therapeutic efficacy of the antibody or conjugate as a safe agent while ultimately minimizing toxicity of normal cells.

Clinically, the most successful biologic therapies, and the only approved for mCRC to date, have been with the use of mAbs (114). As mentioned in the standard treatments of CRC (**Section 1.2.2**), bevacizumab, alfilbercept, cetuximab, and panitumumab have all been approved for medical use in mCRC, and demonstrate overall clinical benefit.

Bevacizumab, a humanized antagonist mAb directed against VEGF, blocks angiogenesis and also plays a role in immune modulation through the Fc region. Similarly, aflibercept is a recombinant protein made of human VEGF receptors 1 and 2 fused to the human Fc portion, to sequester circulating VEGF and prevent activation of receptors. Cetuximab is a human/mouse chimeric antibody directed at extracellular EGFR, blocking activation of receptor-associated kinases that result in inhibition of cell growth, apoptosis, and has been shown to increase the effects of chemotherapy (185, 186). Lastly, as an additional mAb to EGFR, panitumumab is a recombinant human mAb and has similar anti-tumour effects compared to cetuximab. Of important note however, EGFR-specific Abs are restricted to only patients that have wild-type *KRAS*, as those with mutations do not exhibit improved responses, disease control, or survival (58, 187). Currently there are many investigational mAbs in clinical trials, those that are expected to generate an anti-tumour response by ADCC, augment T cell responses or further inhibit angiogenesis (**Table 4**)

1.5 Tumour-associated antigens

Traditionally, the development of an immunotherapy begins with the identification of a suitable cancer target, collectively known as tumour-associated antigens (TAAs) (188). TAAs are molecules that are selectively expressed and/or accumulated by tumours as a result of genomic instability that can generate genetic mutations, translocations, or misregulation as the tumour develops. As targets, ideally the TAA is displayed homogeneously on the surface of the tumour cells, but minimally expressed in normal tissues and serum (189)**.** Although TAAs are heterologous in nature, several non-viral families are now characterized by their expression pattern as unique, overexpressed/accumulated, cancer-testis (CT), and differentiation antigens (190, 191).

Unique antigens, also referred to as neo-antigens, arise from chromosomal aberrations such as mutations, splicing and/or translocation in normal genes but are often characteristic for an individual tumour (*e.g.* mutated *KRAS*, *BRAF*) (190). Antigens that are overexpressed or accumulated by a tumour are often also widely expressed by normal tissues, but at a comparatively lower level (*e.g.* epithelial cell adhesion molecule

[EpCAM], Her2/neu). CT antigens are characterized by epigenetic alterations that induce expression of otherwise silenced genes, of which, only cancer cells and adult reproductive tissues primarily testis and occasionally placenta characteristically express (*e.g.* MAGE family, NY-ESO-1). Lastly, differentiation antigens are commonly shared between tumours and have restricted expression on normal tissues, typically of the same lineage. This family includes oncofetal antigens, where normal expression is generally limited during fetal development but is upregulated in adult tumour cells (*e.g.* alpha-fetoprotein [AFP], 5T4) (190, 191). TAAs encoded by tumourigenic transforming viruses (*e.g.* HPV E6/E7) can also be characterized by abnormal protein expression, termed oncoviral antigens (190, 191). Although the families of TAAs are characterized, it should be noted that these categories are not mutually exclusive and tumour antigens may fall across categories (191).

In general, methods for TAAs identification include detection by screening expression cDNA libraries from human solid tumours with sera of the autologous patients (*e.g.* SEREX) (192), screening of trophoblasts and cancer cells for shared antigenic characteristics, though not currently frequently used (193, 194), and most common, reverse immunology aiming to identify TAAs that are defined by T cell specific recognition (195). A selection of TAAs recognized by T cells derived from CRC patients is summarized in **Table 6**. This group of TAA molecules is ever expanding and is commonly evaluated for use in diagnosis, to follow treatment of tumours, or as a target for developing immunotherapeutics.

1.5.1 5T4 oncofetal antigen

The 5T4 oncofetal antigen, also designated as trophoblast glycoprotein (TPBG), is a cell surface glycoprotein normally found on trophoblasts, the outermost interfacing cell type within the placenta between the fetus and mother, but has restricted expression on normal adult tissues (196). The protein was originally identified by Hole and Stern when searching for shared surface molecules of human trophoblasts and cancer cells, that,

Table 6. TAAs recognized by T cells derived from CRC patients

Antigen[1]	Expression pattern	T cell source	HLA restriction	Recognized epitope[a]
TGFβRII mutation	MSI^+ tumours	TIL and PBMC of patients	DR	$SLVRLSSCVPVALMSAMTTSSSQ_{128-150}$
SART3	Several tumours	TIL	A2	$WLHDEISMA_{152-160}$, $LLQAEAPRL_{302-310}$, $RLAEYQAYI_{309-317}$
		PBMC of patients	A24	$VYDYNCHVDL_{109-118}$, $AYIDFEMKI_{315-323}$
Cyclophilin B	Ubiquitous	TIL	A2	$KLKHYGPGWV_{129-138}$, $VLEGMEVV_{172-179}$
$p56^{lck}$	Lymphocytes and normal colorectal tissue, several epithelial tumours	PBMC of metastatic patient	A2	$KLVERLGAA_{246-254}$, $DVWSFGILL_{422-430}$
			A24	$HYTNASDGL_{208-216}$, $TFDYLRSVL_{486-494}$, $DYLRSVLEDF_{488-497}$
CEA	Epithelial differentiation antigen, over-expressed in several epithelial tumours	PBMC of vaccinated patient	A2	$YLSGANLNL_{571-579}$
Ep-CAM	Epithelial differentiation antigen	PBMC of metastatic patients	A2	$GLKAGVIAV_{263-271}$
Her2/neu	Epithelial differentiation antigen, over-expressed in several epithelial tumours	PBMC of metastatic patients	A2	$IISAVVGIL_{654-662}$
p53	Ubiquitious; mutated and over-expressed in several tumours	PBMC of metastatic patients	Class II	----
KRAS mutations	Several tumours	PBMC of vaccinated patient	B44	$MTEYKLVVVGAG\underline{\mathbf{D}}VGKSALTIQLIQ_{1-25}$[b]
		PBMC of patient	A2	$KLVVVGA\underline{\mathbf{D}}GV_{5-14}$[c]

Modified from Dalerba *et al.*2003 and Vigneron et al. 2013 (198, 199)

[1] A complete database of T-cell defined tumour antigens can be accessed through http://cancerimmunity.org/peptide/

[a] Numbers indicate amino acid positions within the protein

[b] This peptide encompasses the glycine (G) to aspartic acid (D) mutation in position 13 of the KRAS protein and contains an undefined HLA-B44-restricted epitope; the mutated amino acid is underlined and typed in bold

[c] This peptide encompasses the glycine (G) to aspartic acid (D) mutation in position 12 of the KRAS protein; the mutated amino acid is underlined and typed in bold

would reflect functional similarities concerned with growth, invasion, and immunosurveillance that allow for fetal or tumour survival within its host (194). As such, human 5T4 was first defined by mouse mAbs, raised from purified glycoproteins from human syncytiotrophoblast microvillous plasma membranes (STBM), the outer epithelial layer covering the villi of the placenta. Comparative tissue screening established that the 5T4-targeting mAb detected antigen expression by different tumour cells but only low levels in normal tissue epithelia (194, 196). Subsequently, 5T4 has been identified on an array of carcinomas including cervix (197), colorectal (198-200), gastric (201, 202), lung (203, 204), oral (205), ovarian (206), prostate (207), and renal carcinomas (208). Further, as this protein remains membrane-bound and is not cleaved, there is no evidence of circulating 5T4 antigen (209).

Moreover, 5T4 has been specifically associated with metastasis in CRC (199), and there is evidence of poorer clinical outcome for CRC, gastric, and ovarian cancer with a direct relationship between the expression of 5T4 and the stage of carcinoma (198, 201, 206). Acquired from Eisen *et al*. (209), the reactivity for 5T4 antigen revealed from collected immunohistochemical studies of patient samples demonstrated the high prevalence and distribution of this TAA across multiple cancers and stages (**Table 7**).

Despite the potential therapeutic value of 5T4, the function and molecular mechanisms of this protein remain poorly understood. However, over the past two decades, biochemical and genomic studies have provided insight that this 72 kDa (420 amino acid) single-pass transmembrane-bound protein is heavily *N*-glycosylated (7 putative sites) and is a member of the family of proteins containing leucine rich-repeats (LRR) (210-213). Recent structural analysis of the extracellular domain of 5T4 confirmed that this transmembrane protein is constructed of a multiple LRR motif and associated flanking regions, clustered in two domains separated by a short, rigid, hydrophilic core (211). The LRR motif is known to contribute directly to protein-protein interactions and is associated with a functionally diverse group of molecules (210, 214). The cytoplasmic region has been reported to interact through a PDZ-binding motif (Ser-Asp-Val), commonly involved in mediating protein-protein interactions, with the PDZ domain of

Table 7. 5T4 expression of various tumour types and stages

Cancer	Type/Stage	Reactivity[a]	Summary
Breast	Mixed	56/63	85-95% of patients express 5T4
Cervix	Mixed	5/5	85-90% of patients express 5T4
	I	22/25	
	II	22/26	
	III	9/10	
	IV	5/6	
CRC[b]	Mixed	11/22	40-50% of patients express 5T4 with > 70% in stage D.
	A	2/8	
	B	7/34	
	C	13/21	
	D	7/9	
NSCLC	Mixed	259/261	99% of patients express 5T4
Ovarian	Mixed	4/7	> 70% of patients express the 5T4 antigen with 90–95% 5T4 positive for stage IV patients
	I	2/10	
	II	4/57	
	III	21/29	
	IV	24/26	
Pancreatic	Mixed	23/23	100% of patients express 5T4
Prostate	Mixed	26/26	100% of patients express 5T4
Renal	Clear cell	215/222	> 95% of patients express 5T4
	Papillary	18/18	
	Mixed	36/37	

[a]Reactivity of patient cancer biopsies for 5T4 expression. Extrapolated from Eisen *et al*. 2014 (209)

[b]CRC represented in Dukes' classification system.

TIP-2/GIPC, a cytoplasmic interacting protein associated with the cytoskeleton (215, 216). To date, further mechanisms of downstream signal transduction for 5T4 remain unknown. From studies focused on elucidating its role, 5T4 expression was involved with early embryonic stem (ES) cell differentiation (mouse and human) and increased cellular motility (217, 218). It has also been associated with the process of epithelial-mesenchymal transition (EMT) in ES cells (219, 220), an important process during development but also designated as a key process involved in the metastatic spread of epithelial tumours (221, 222). Overexpression of 5T4 glycoprotein showed influences on cellular morphological changes, including disruption of cell-cell contacts, reduction in adherence, and actin cytoskeletal organization (223-226).

5T4 has further been shown to modulate CXCR4 function by regulation of surface expression in differentiating ES cells, mouse embryonic fibroblasts (MEFs) and cancer cells (204, 223, 227). This facilitates an increased biological response to CXCL12-mediated chemotaxis, signaling important for cell mobilization (204, 223, 227). Both CXCR4 and CXCL12 chemokines have been associated with embryogenesis as well as with tumourigenesis in many cancers with upregulated CXCR4 expressing tumours preferentially spreading to tissues that highly express CXCL12, such as the lung, liver, lymph nodes and bone marrow (228-230). Lastly, 5T4 has been found to inhibit the Wnt/β-catenin signaling pathway (231), a key pathway involved in embryonic development and also a major target in anticancer therapeutics (232, 233). The Wnt family of proteins is known to regulate fundamental developmental mechanisms directing cellular proliferation, cell fate determination, and tissue homeostasis (234). By acting as a feedback inhibitor of canonical Wnt signaling, 5T4 activates non-canonical, misregulated signaling, often associated with disease progression prominently found in cancers (231, 235)

Comparable to ‘normal’ cancerous tissues, similar 5T4 expression and function has been found in tumour progenitor cells (TPCs; also known as tumour-initiating cells [TICs], or cancer stem cells) of NSCLC. Specifically, 5T4 was associated with the undifferentiated state and the EMT of the TPCs (203, 236). From this, the therapeutic value of 5T4 is

enhanced by the ability to target the aggressive and tumourigenic populations within the tumour (TPCs) (189).

There have been extensive studies elucidating the role of 5T4 in development, and recently TPCs, and though taken together, the functional biology of 5T4 is consistent with a role in movement of cells, as summarized in a recent comprehensive review by Stern *et al*. (189), the specific function of 5T4 remains unknown. Nonetheless, 5T4 has been considered an ideal candidate for cancer diagnostics and/or as a target for cancer immunotherapy, with widespread tumour expression and a link to a tumour progenitor cell phenotype (237). These characteristics have driven the development of 5T4-based therapeutics and indeed, there are currently three 5T4-targeting agents evaluated with clinical development.

Firstly, efforts to generate a vaccine using a modified vaccinia virus Ankara (MVA) encoding human 5T4 (designated TroVax) has induced an anti-tumour immune response with 5T4 epitopes recognized by T cells in preclinical cancer models (238, 239). A succession of Phase I or II clinical trials in CRC, prostate, and RCC (including in combination with chemotherapy or cytokine treatments) has established this vaccine in safety, tolerability and vaccine immunogenicity, as well as for optimal dose and route of vaccination [reviewed in (237)]. This vaccine is presently in on-going evaluations for ovarian carcinoma in Phase II clinical trials (NCT01556841). A number of targeted based therapies have also become active in development, some of which have compelling representatives to support clinical advancement. These include guiding chemotherapies as antibody-drug conjugates (ADC) (240, 241), and activation of immune effectors as tumour-targeted immunotoxins (209, 242). The 5T4-targeted ADC (A1-mcmMMAF; PF-06263507) had potent targeted anti-tumour responses in preclinical models, including primates, with limited non-specific exposure and low toxicity that was well tolerated (241). Recently terminated from Phase I clinical trials (NCT01891669), an early report noted that trial completion was not due to any safety concerns, but as a result of the program sponsor's prioritization. Secondly, a 5T4-targeted immunotoxin (ABR-21760; Naptumomab estafenatox) has demonstrated preclinical therapeutic efficacy, and has completed Phase II/III clinical trials (NCT00420888) with early reports suggesting an

overall good safety profile and a clinical benefit in a subset of patients (209, 242). Thirdly, and most recent, with the sequence resolution of the mAb defining 5T4 (243), a pre-clinical research program has been initiated for evaluation of re-targeting effectors using engineered CAR T-cell therapy (244, 245) with promising *in vitro* cytotoxicity directed specifically at 5T4 expressing tumour cells (246).

1.6 Bacterial superantigens

Bacterial superantigens (SAgs) are a unique class of microbial toxin that are known to be potent activators of T lymphocytes (247-251). The term SAg was introduced to emphasize the novel immune stimulatory properties and remarkable T cell expansion of these toxins (247, 252). Since their designation, this 'family' of toxins has expanded extensively over the last decade, heavily revealed by bacterial genome sequencing efforts (253). These toxins are primarily produced by *Staphylococcus aureus* and *Streptococcus pyogenes* (group A *Streptococcus*), and with more than 30 distinct SAgs currently known, are also the best characterized. Although SAgs are similar in function, a general feature of these low-molecular weight proteins (ranging from 22-29 kDa) (248) is that those that are genetically distinct are also antigenically distinct (253). The biological activity of these proteins is unusually stable, being resistant to heat (despite boiling for one hour), desiccation, and in general, proteolysis and acids (such as stomach acids) (254).

Clinically, SAgs from both *S. aureus* and *S. pyogenes* have been associated with toxic shock syndrome (TSS), a toxin-mediated acute life-threatening illness. Albeit in different forms, this syndrome is a result of an elicited 'cytokine storm' (248, 255, 256). As noted above, these toxins are not limited to *S. aureus* and *S. pyogenes* and in fact recently, as highlighted in Spaulding *et al.,* an increasing number of reports describe staphylococci strains of animal origin as well as other beta-hemolytic streptococci, namely groups B, C, and G as producers of SAgs (254, 257). SAgs have also been reported to occur in some viruses and other microorganisms, including *Mycoplasma arthritidis, Yersinia enterocolitica, Yersinia pseudotuberculosis, Plasmodium falciparum, Clostridium perfringens, Candida albicans,* and *Toxoplasma gondii* (254).

1.6.1 Staphylococcal superantigens

S. aureus are bacteria that can appear as part of the human normal microbiota, but has the ability to become a capable pathogen, causing a wide range of host infections including skin and soft tissue, as well as severe invasive infections (258). SAgs produced by *S. aureus* include the staphylococcal enterotoxin (SEs), toxic shock syndrome toxin-1 (TSST-1), and related SE-like proteins (SEl) (259). Presently classified by their SAg function, SEs were formerly defined by their enterotoxin properties in the pathogenesis of staphylococcal food poisoning (249, 260). Although SAgs from *S. aureus* and *S. pyogenes* share similar structure and immune-stimulating properties, this activity is thought to be independent of the ability to activate T cells (261) and a property not associated with streptococcal SAgs (262). Currently this group of SAgs includes ten SE serotypes: A to E, G to I, R, and T (259). Although both homologous and structurally similar to SEs, SEl group of SAgs, of those evaluated, lack the emetic properties of the bona fide SEs (259). This group of SAgs presently includes serotypes J to Q, S, U, V, and X (259, 263).

A subgroup of genetically linked SEs and SEls, most commonly including SEG, SEI, SEl-M, SEl-N, and SEl-O and two pseudotoxins compromise an operon designated as the staphylococcal 'enterotoxin gene cluster' (*egc*) (263). Compared to classic SEs, human serum levels of neutralizing antibodies against the *egc* SEs have been shown to be lower, despite their broad distribution and prevalence (264).

1.6.2 Streptococcal superantigens

S. pyogenes (group A *Streptococcus*) is a prominent bacterial pathogen that can cause a diverse range of clinical manifestations, from common bacterial pharyngitis to severe complications related to invasive infections (265). To date, eleven genetically distinct SAgs are known to be produced by *S. pyogenes*. Commonly referred to as erythrogenic toxins, these virulence factors currently include streptococcal pyrogenic exotoxin (Spe) serotypes A, C, and G to M, as well as streptococcal mitogenic exotoxin Z (SmeZ), and streptococcal superantigen (SSA) (257). Historically defined as scarlet fever toxins, streptococcal SAgs are also associated in the pathogenesis of this illness (266). Widely

recognized in clinical implications, the contribution of SAgs for bacterial welfare is largely unknown; however recent work highlights that the biological function of streptococcal SAgs may promote the initial establishment of infection in humans, as evaluated in an acute infection of the upper respiratory tract of mice expressing human MHC II molecules. Further, SAgs may exist in redundancy to avoid host anti-SAg humoral immune responses and overcome polymorphisms of host MHC II (267).

1.6.3 Superantigen structure and mechanism of action

SAg structures and host cell interactions have been extensively reported from numerous structural and mutational analyses extensively reviewed by Fraser and Proft (268). Though SAg molecules generally share low amino acid sequence homology, the overall protein structure is conserved among protein family members, consisting of two major protein domains: an N-terminal oligonucleotide/oligosaccharide-binding (OB) domain, and a C-terminal β-grasp motif connected through a central α-helix (269). With similar structures, SAgs also share potent immnuomodulatory properties, remarkably detected with picogram (10^{-12} g) quantities (248).

SAg-mediated activation of T cells mechanistically differs from conventional T cell activation as a processed peptide presented in the context of MHC (pMHC) on APCs (**Figure 3A**), as well as from non-specific T cell mitogens (*e.g.* phytohaemagglutinin [PHA], concanavalin A [ConA]). Instead, SAgs function by engaging lateral surfaces of pMHC as unprocessed proteins (270-273), while simultaneously engaging germline-encoded regions within the variable region of the TCR β-chain (Vβ) (**Figure 3B**) (274-278). MHC II molecules possess two independent binding sites for bacterial SAgs: a low-affinity site on the conserved α-chain and a zinc-dependent, high-affinity site on the polymorphic β-chain (279, 280). SAg-mediated crosslinking of these adaptive immune receptors generates a ‘wedge’ that allows for the large-scale activation of T cells that is independent of the peptide antigen presented within MHC II. As there are ~50 functional Vβ genes in humans (281, 282), and because different SAgs can often target multiple Vβs, though preferential Vβ binding is displayed (280, 283), these toxins stimulate a very large percentage of exposed T cells and the subsequent release of pro-inflammatory cytokines,

Figure 3. Structural overview of a representative SAg-mediated T cell activation complex

Cartoon representations of **A)** conventional T cell activation in complex with pMHC II (284) and **B)** representative Group IV SAg (SpeC) in complex with TCR and pMHC II cross-linked by SpeC through zinc-mediated, high affinity binding site and a low affinity binding site (272, 285, 286). The ternary model of TCR-SpeC-$(MHC)_2$ was produced as previously described (277). In brief, the cartoon was generated by superimposing the co-crystal structures of SpeC-TCR (PDB code 1KTK) (285), high affinity binding site SpeC-MHC II (PDB code 1HQR) (272) and low affinity binding site as predicted from SEC-MHC II (PDB code 1JWM) (287). Colours are as follows: MHCII-α-chains, *red*; MHCII-β-chains, *green*; antigenic peptides, *black*; zinc atom, *magenta*; TCR Vα chain, *yellow*; TCR Vβ chain, *grey*; SpeC SAg, *blue*.

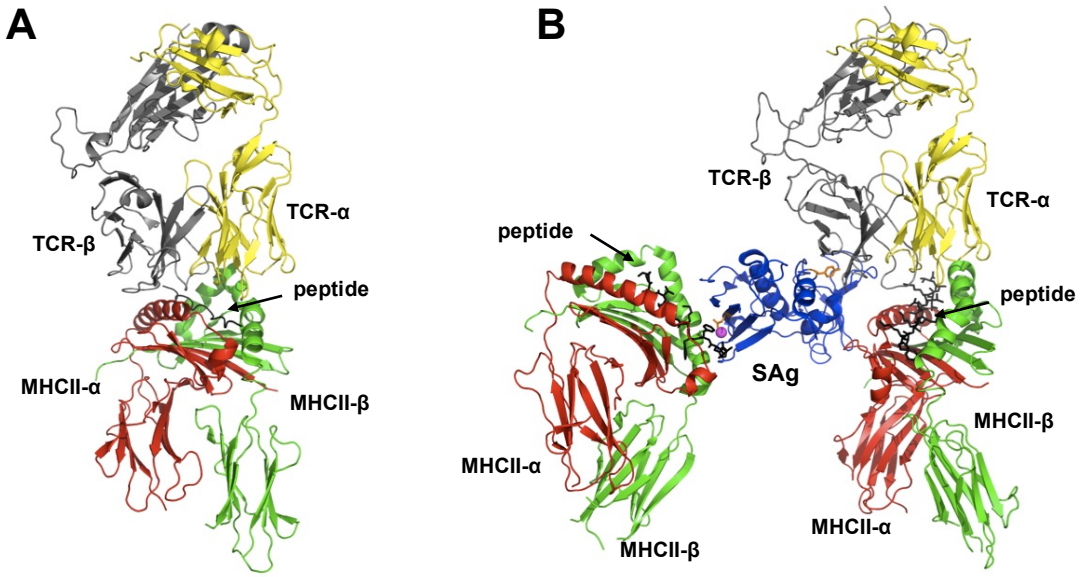
A
TCR-α
TCR-β
peptide
MHCII-α
MHCII-β
B
TCR-β
TCR-α
peptide
peptide
SAg
MHCII-α
MHCII-β
MHCII-α
MHCII-β

often referred to as a 'cytokine storm' (*e.g.* IL-2, IFN-γ, and tumour necrosis factor [TNF]-α) (248). This leads to the polyclonal expansion of particular Vβ subsets of T cells or T cell subsets, a process known as Vβ skewing. Typically, in conventional T cell activation, antigens stimulate ~0.01% of naïve T cells through specific interactions as processed peptides displayed in the context of MHC II on APCs. In contrast, the aforementioned mechanism demonstrated by SAgs can stimulate >20% of all exposed T cells (248). Although SAgs do not engage MHC I molecules, these toxins do activate both $CD4^+$ and $CD8^+$ T cells (288)**,** as well as in specific cases, unconventional T cell subsets such as invariant NKT cells (289) and γδ T cells (290). Collectively, this activation will further lead to bystander activation of accessory cells such as NK cells (291), and the recruitment of monocytes, Mϕ, neutrophils, and DCs (248, 251, 280). Reports have also demonstrated that stimulation from evaluated SAgs can result in a dose-dependent TCR Vβ-specific expansion of activation-induced $CD25^+$ $FoxP3^+$ cells, indicative of a Treg phenotype. Though these cells express IL-10, their suppressive function remained highly cell-cell contact dependent (292, 293).

Although SAg toxins have long been recognized to induce Vβ-specific T cell anergy, a state of unresponsiveness to stimulation and/or deletion following activation (294-296), evidence suggests that the fate of the T cell population may be influenced by both SAg concentration and duration of exposure, and that with addition of IL-2, the anergic cells may be indeed rescued (297).

1.6.4 Superantigen classification

A phylogenetic classification scheme of the SAg exotoxins has recently been updated where SAgs from staphylococci and streptococci are placed into five evolutionary groups based on amino acid alignments (253). Within this classification, the Group I SAgs contain only one member, the evolutionary distinct TSST-1. This group contains only one MHC II binding site in the OB-fold; a low-affinity site that interacts with the α-chain of MHC II molecules (271). Lacking the proposed emetic cystine loop of SEs, this SAg indeed does not induce emesis (262), though is considered the major cause of the menstrual form of TSS (298, 299).

The Group II SAgs contain both staphylococcal and streptococcal SAgs with members commonly linked with both non-menstrual-associated cases of staphylococcal TSS [SEB; (300)] and streptococcal TSS [SpeA; (256)]. Similar to Group I, Group II SAgs contain only one low-affinity α-chain MHC II binding site as highlighted in Spaulding *et al*. (254).

The Group III SAgs are only populated by staphylococcal SAgs and although the Group II SE SAgs are often implicated as well, this Group generally contains those most commonly associated with staphylococcal food poisoning (*e.g.* SEA, SEE) (301). Unique to the Group II and III SAgs is a "cystine-loop structure" that is thought to be important for emetic activity (302), though its presence does not assure emesis, demonstrated by a lack of this activity by SpeA (262). Group III SAgs contain a low-affinity α-chain MHC II binding site as in previous groups, but also contain a second, zinc-mediated high-affinity MHC II β-chain binding site within the SAg β-grasp domain (248, 303).

The Group IV SAgs are restricted to only streptococcal members, and are characterized as having the high-affinity binding sites for MHC II molecules, as in Group III but lack the designated cystine loop and therefore are known for lack of emesis (248). Although the low-affinity MHC II α-chain interaction has not been characterized structurally, considerable evidence has indicated its presence (286, 304).

The Group V SAgs, with the exception of SpeI (and related orthologues) contain mostly staphylococcal SAgs, and are the most recent to be described and highlighted in Spaulding *et al*. (254). Further, this Group includes only SEl toxins, other than SEI. Members of Group V are predicted to contain both the high- (305) and low-affinity MHC II binding sites and lack the emetic cysteine loop (254). Interestingly, SEI is the only SAg outside of the Group II and III SAgs reported to have emetic activity, albeit comparably weak (306). Lastly, Group V SAgs are characterized by a unique, relatively conserved ~15 amino acid extension referred to as the α3–β8 loop (307). The evolutionary SAg Groups are summarized in **Table 8**, highlighting key structural features discussed.

Regardless of the subtle or dramatic differences within the SAg-mediated T cell activation complexes, each member within the SAg family of toxins, despite its group

Table 8. Structural features of known staphylococcal and group A streptococcal SAgs

Group	SAgs[a]	MHC II interactions	Cystine loop[b]
I	TSST-1	low-affinity site α-chain	No
II	SEB, SEC, SEG, SER, SEl-U, SpeA, SpeH, SSA,	low-affinity site α-chain	Yes
III	SEA, SED, SEE, SEH, SEl-J, SEl-N, SEl-O, SEl-P, SEl-S	low-affinity site α-chain, high-affinity site β-chain	Yes
IV	SpeC, SpeG, SpeJ, SpeK, SpeL, SpeM, SmeZ	low-affinity site α-chain, high-affinity site β-chain	No
V	SEI, SEl-K, SEl-L, SEl-M, SEl-Q, SEl-V, SpeI	low-affinity site α-chain, high-affinity site β-chain	No

Modified from Spaulding *et al.* 2013 (254) based on current phylogenetic classification scheme (253). [a] SAgs SET and SEl-X are currently not aligned amongst established evolutionally groups. [b] Presence of cystine loop, although related, is not fully predictive of emetic activity.

classification, is able to efficiently activate large numbers of T cells. Notably, the one common structural feature of all characterized SAgs, with the exception of the Vα-specific SEH, is the engagement of the Vβ CDR2 loop, which appears to be the critical determinant for Vβ-specificity (277).

1.6.5 Superantigens and cancer therapy

There have been significant efforts to design SAg-based immunotoxins, collectively known as tumour-targeted superantigens (TTSs), in order to artificially 'force' T cells to recognize TAAs in a non-MHC-restricted manner. TTSs are recombinant fusion proteins that consist of an anti-tumour antibody moiety genetically fused to a SAg (308, 309). The intent of TTSs is to treat tumours through localization and activation of the patient's immune system at the tumour site, with particular aims to augment a cytotoxic T lymphocyte (CTL) response. Presented in **Figure 4** are the highlights from TTS preclinical and clinical developmental.

1.6.5.1 Developmental concept of 'first-generation' TTSs

The concept of using SAgs as a targeting moiety for human CTLs was initially developed based on early studies by Dohlsten *et al*. and Hedlund *et al*. (310, 311). In these studies, MHC II^+ tumour cells function as a receptor for members of SE SAgs, wherein at pM concentrations, this complex specifically lead to subsequent triggering and lysis by CTLs; a mechanism coined SAg-dependent cellular cytotoxicity (SDCC) (310-313). As MHC II^+ tumour cells are of minority in malignant disease and systemic T-cell activation would be expected, the general application of this treatment was limited (308).

From this concept, tumour-specific SAgs emerged, originally created by coupling wild-type SEA SAg to tumour-reactive mAbs (C215 or C242) to 'coat' the tumour cells with TTS (mAb::SEA) (308, 314). C215 (IgG2a) and C242 (IgG1) are mouse mAbs obtained after immunization with human colon carcinoma cell line (Colo205) and are known to recognize tumour-related epitopes associated with human colon and pancreatic carcinomas, respectively (315-317). In this pioneering work, the TTSs presented as cytotoxic mediators, selectively targeting SEA-responsive CTLs, *in vitro* and *in vivo*, for

Figure 4. Developmental timeline of TTSs in preclinical and clinical evaluation.
Schematic illustration of the developmental timeline of TTSs over nearly three decades. Highlights for preclinical and clinical arms of evaluation are represented by year of publication, TTS involved, and if applicable, key facts of model or phase trial. All combinational TTS preclinical work was completed in a murine C215-B16 tumour model. References are listed within **Appendix 5**.

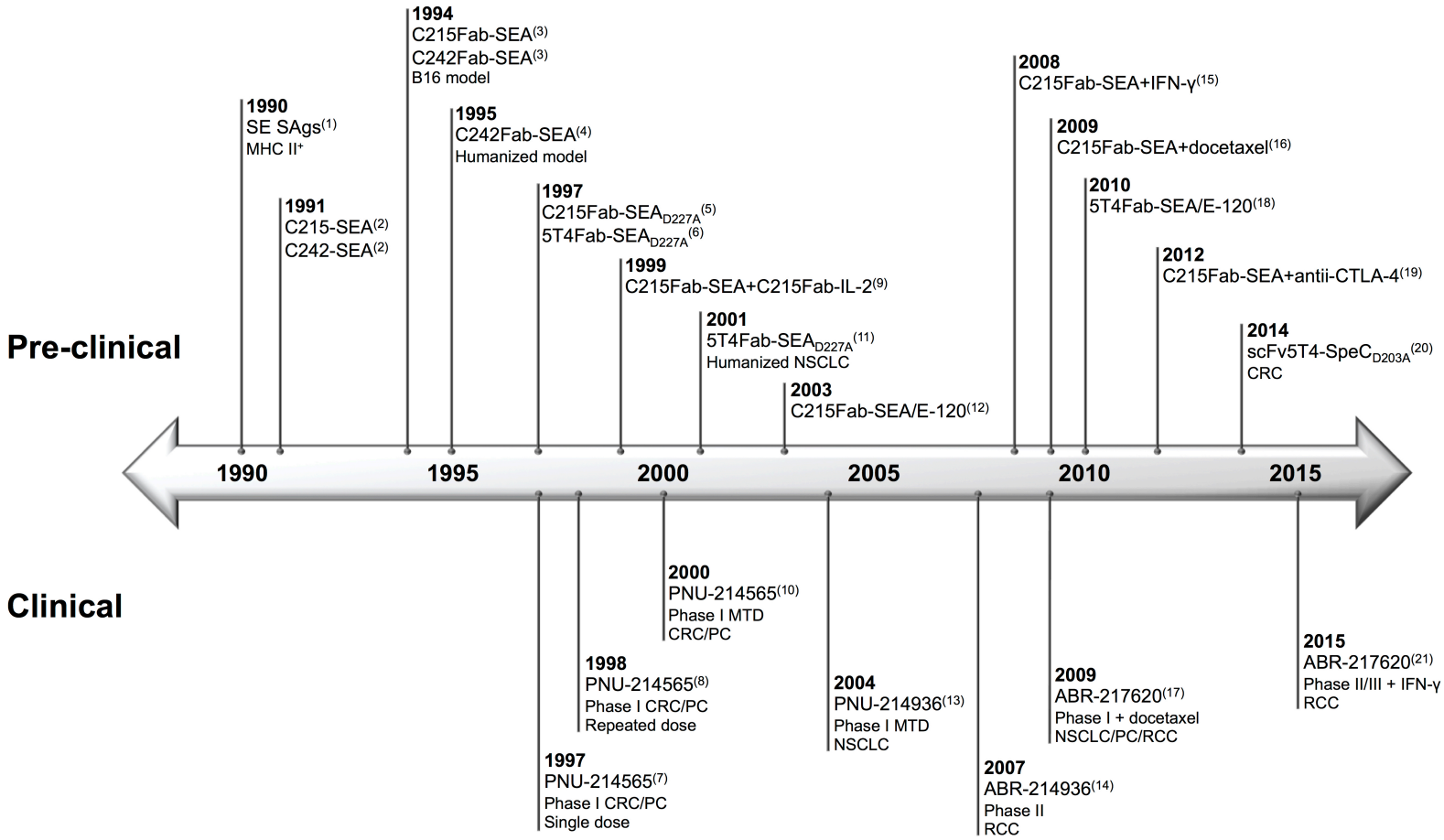
Pre-clinical
1990
SE SAgs(1)
MHC II+
1991
C215-SEA(2)
C242-SEA(2)
1994
C215Fab-SEA(3)
C242Fab-SEA(3)
B16 model
1995
C242Fab-SEA(4)
Humanized model
1997
C215Fab-SEAD227A(5)
5T4Fab-SEAD227A(6)
1999
C215Fab-SEA+C215Fab-IL-2(9)
2001
5T4Fab-SEAD227A(11)
Humanized NSCLC
2003
C215Fab-SEA/E-120(12)
2008
C215Fab-SEA+IFN-γ(15)
2009
C215Fab-SEA+docetaxel(16)
2010
5T4Fab-SEA/E-120(18)
2012
C215Fab-SEA+antii-CTLA-4(19)
2014
scFv5T4-SpeCD203A(20)
CRC
1990
1995
2000
2005
2010
2015
Clinical
2000
PNU-214565(10)
Phase I MTD
CRC/PC
1998
PNU-214565(8)
Phase I CRC/PC
Repeated dose
1997
PNU-214565(7)
Phase I CRC/PC
Single dose
2004
PNU-214936(13)
Phase I MTD
NSCLC
2007
ABR-214936(14)
Phase II
RCC
2009
ABR-217620(17)
Phase I + docetaxel
NSCLC/PC/RCC
2015
ABR-217620(21)
Phase II/III + IFN-γ
RCC

localization against tumour cells in a MHC II independent manner. Progression of the TTS concept lead to the assembly of genetic fusions containing wild-type SEA SAg and the antigen-binding fragment (Fab) region of the tumour-reactive mAbs, producing a recombinant protein (Fab::SEA) (309). These TTSs maintained efficient tumour targeting and T cell stimulatory properties but resulted in an overall reduction of MHC II binding (compared to native SEA) (309). Designated as SAg-mediated antibody-dependent cell cytotoxicity (SADCC), the Fab-SEA demonstrated a substantial reduction in tumour burden and improved the rate of mortality in a C215-expressing B16 syngeneic melanoma metastasis model (309, 318-322). Most notable, four daily injections of Fab-SEA resulted in 90–95% reduction in the number of metastases (321). The potential to render the immune system in a hyporesponsive state was noted with this regime (321); however, the inability to eradicate residual tumours was recovered with two repeated cycles of TTS amongst a resting period, successfully eliciting a secondary anti-tumour response and significantly prolonging survival (322). Furthermore, in a humanized severe combined immunodeficient (SCID) mouse model, reconstituted with human PBMCs and disseminated human Colo205, C242Fab-SEA treatment resulted in strong inhibition of tumour growth, reduction in overall burden, and full resolution of carcinoma in a proportion of animals (318, 319).

1.6.5.2 'First generation' TTSs in clinical trials

In Phase I clinical trials for the treatment of advanced CRC and pancreatic cancer, safety was established in single dose infusion (323, 324) and escalating repeated dose regimens (325) of the Fab moiety of mAbC242 fused to SEA (PNU-214565; nacolomab tafenatox). Although transient and manageable, toxicities occurred among patients; of these adverse events, fever and hypotension were the most common and correlated with a high induction of circulating IL-2 and TNF-α (324). Rapid systemic immune activation and associated toxicities presumed to be a result of TTS interaction with MHC II containing tissues, followed by engagement of appropriate Vβ subsets of T cells (323-325). To avoid severe systemic toxicity, the treatment could only be given in very low amounts, limiting the initial dose range (0.01 ng kg^{-1}-4 ng kg^{-1}) and ultimately, illustrated the considerable biological activity of the TTS (323, 324).

In an accompanying repeated-dose trial, the TTS treatment was safely administered in the program (one cycle of 4 consecutive daily infusions), and though not cumulative, parallel toxicities among patients remained (325). Once more, toxicity preceded with systemic cytokine induction and adverse events further correlated with transient losses in lymphocyte subsets (323, 325). In addition to cytokine induction, the required dose for half maximal effective concentration (EC_{50}) correlated highly with the ratio of baseline circulating anti-SEA antibodies (pre-existing) and necessitated unanticipated individualized dosing (325). Laboratory and clinical findings showed no detectable HAMA responses to TTS infusions and despite the ability to bind to normal colon tissue, the TTS demonstrated no obvious organ-related side effects (324, 325).

1.6.5.3 Development of 'second-generation' TTSs

The first generation Fab::SEA TTSs, through the SAg moiety, still retained a considerable affinity for MHC II molecules (326), resulting in systemic T cell activation and cytokine toxicity from accumulation in MHC II positive tissues (324, 326, 327), a reported source of dose limiting toxicities (DLTs). To circumvent this response and allow for successive administration regimes, 'second generation' TTSs were introduced with a mutated version of SEA. Resembling other class III (SE) and IV (Spe) SAgs (253), SEA has two distinct MHC II binding sites (328, 329); one of which is low affinity and the other contains residues that co-ordinate a Zn^{2+} ion to form a high affinity binding site to the β-chain of MHC II (328, 330). Designed with a substitution at a key amino acid involved at this interface, Asp^{227} (328, 330), the altered SEA maintained T cell stimulatory properties and cytokine release in the presence of MHC II, albeit at a much reduced activity (>100-fold compared to wild type SEA) (328, 331). Administered at high doses *in vivo*, the tailored TTS (Fab::SEA_{D227A}) eliminated systemic immune activation and toxicity but maintained a strong T cell-dependent antitumour response in both a C215-B16 model of mice transgenic for TCR Vβ3 (332), a preferential Vβ binding for SEA (332, 333), as well as in an anti-CD19 humanized mouse model carrying B lymphoma cells (Daudi) (334). Overall, the Fab tumour specificity replaced the initially required MHC II reactivity properties of the SAg, allowing targeting and activation of cytotoxic T cells (326, 334).

Later studies utilized a recombinant fusion of the modified SEA (Asp^{227}) with a mouse Fab to target the oncofetal antigen, 5T4 (335, 336). While maintaining a reduced binding for MHC II through the modified SEA, this 5T4-targeting moiety had a high affinity for this tumour-restricted antigen (nM; mean K_d of 10^{-9} M) (335). This TTS resulted in ~95% reduction of tumour mass in a NSCLC model (335).

1.6.5.4 'Second generation' TTSs in clinical trials

Using the treatment anatumomab mafenatox (5T4Fab::SEA_{D227A}; PNU/ABR-214936) in a Phase I clinical trial, safety and maximum tolerated dose (MTD) was established in NSCLC patients as the primary objective (337). The treatment, received as single infusions on four consecutive days, had minor tumour responses in assessable patients (66/78), defined as greater than 25% tumour regression (12% [8/66] of patients) (337). Among certain patients, DLTs were reported and fever, hypotension, and nausea remained common adverse events overall (337). The MTD ranged from 103 ng kg^{-1} to 601 ng kg^{-1}, a relatively low dose, although a marked improvement from the TTS predecessor (337). Encouragingly from Phase II studies in RCC patients, a prolonged survival was observed compared to expected survival rates, and in particular, patients receiving the highest dose of treatment within this study lived almost double the amount of time than expected (338). The largest proportion of patients (27/43) showed stable disease and one patient (1/43) showed a partial response (PR). Notably, a large increase in patient IL-2 serum levels observed on the second day of treatment correlated postitively with overall prognosis and importantly, a significantly longer survival time. From this, circulating IL-2 levels may provide a useful pharmacodynamic marker for clinical effect of this TTS (338).

Although with promising clinical trial results, many patients had pre-existing antibodies to SEA which required individualized dose-escalation TTS treatment regimens to overcome neutralizing effects of these antibodies (337). Consequently, patients with high anti-SEA antibody values were not recommended for treatment with anatumomab mafenatox in subsequent studies (337). This response remained within Phase II as an increase in titers following the first cycle were reported in a majority of patients, but this

was not further boosted by further exposure (338). Further, the murine Fab led to elevations in HAMA levels following multiple cycles of treatment (337, 338). Together, these effects lead to the requirement of relatively high doses for a measurable anti-cancer treatment.

1.6.5.5 Development of 'third-generation' TTSs

In parallel the initial clinical evaluation of anatumomab mafenatox, a 'third-generation' TTS was developed to advance the concept. The main intention was to reduce the overall immunogenicity demonstrated by the SAg moiety in predecessors and reduce the neutralizing effects of preformed antibodies in patients. Previously reported, SEA specifically had pre-existing anti-SEA antibodies in a proportion of patients (337). Additionally, as TTS treatment is most effective when given in repeated cycles (321, 322), high titers of antibodies against SEA can be developed (339).

In order to reduce antigenicity, the succeeding generation of this TTS therapeutic, naptumomab estafenatox (ABR-217620; ANYARA) was established. This TTS, like the predecessor, consists of the murine anti-5T4 Fab, but is linked to the chimeric SAg moiety, SEA/E-120, engineered in a multi-step process by Erlandsson *et al.*, resulting in a TTS with a distinct pharmacological prolife (339). In addition to reduced MHC class II binding (Asp^{227}), SEA/E-120 has structural modifications to reduce immunogenicity and decrease binding by human antibodies (339). Designed with the premise that individuals in general are reported to have lower pre-existing antibodies to SEE compared to SEA, and that SEE demonstrated low anti-tumour properties, the chimeric SAg demonstrated that ~85% of the antibodies binding the previous SEA no longer affected SEA/E-120 in preclinical studies (339). Further, this TTS formulation demonstrated a higher efficiency compared to its predecessors of inducing T cell-mediated cytotoxicity of tumour cells *in vitro*, a superior binding affinity for the target antigen 5T4, and a dramatic reduction in tumour mass with repeated administrated in a humanized murine model (intraperitoneal [ip]) of human lung metastases (Calu-1) (242).

Later studies reported that multimeric naptumomab estafenatox selectively binds to, activates, and expands T cells expressing Vβ7-9, including $CD4^+$ and $CD8^+$ subsets and

directs CTL cytotoxicity to 5T4-expressing cells despite the diminished MHC II binding and structural epitope alterations (340). Based on the succession of TTS generations and balancing the binding relationships of the TTS, it is currently hypothesized that for an optimal formulation to maximize anti-tumour effects, the immunotoxin ideally has a high affinity for the tumour antigen, low affinity for the TCR, and very low affinity for MHC II proteins; a formulation exhibited by the current TTS, naptumomab estafenatox (209).

1.6.5.6 'Third generation' TTSs in clinical trials

The latest TTS, naptumomab estafenatox, has undergone two prospective Phase I clinical trials as a monotherapy in patients with advanced NSCLC, pancreatic cancer, and RCC, and as a combination therapy [based on (341)] with docetaxel, a cytostatic chemotherapeutic drug, in patients with NSCLC (342). With the primary aim to establish the MTD, the secondary objectives were to evaluate safety profile, immunological response, pharmacokinetic parameters, and effects on disease. Within the monotherapy evaluation, naptumomab estafenatox was administered daily (0.5 μg kg^{-1} – 27.4 μg kg^{-1}) for five consecutive days, based on large animal safety/toxicology (*Macaca fascicularis*) studies [unpublished data reported in (342)] and previous clinical evaluations (anatumomab mafenatox), acknowledging the designed insensitivity to preformed anti-SAg antibodies, with select patients receiving a second or third treatment cycle. Within the combination arm, TTS doses were obtained from the monotherapy information, and docetaxel was administered as a fixed standard dose (75 mg m^{-2}) (342).

In both arms of evaluation, naptumomab estafenatox was well tolerated, with manageable treatment-related adverse events of fever, nausea, hypotension, and rigors, all pronounced during the first treatment cycle (342). Recorded DLTs associated with this TTS consisted of fever, hypotension, liver toxicity, and acute vascular leak syndrome; all patients whom had received >20 μg kg^{-1} dose but unlike its predecessors, independent of preformed patient anti-SAg antibodies (342, 343). An immediate (3 hour) dose-dependent increase in systemic immune activation of IL-2, IFN-γ, and IL-10 plasma levels was observed with some evidence of anti-tumour activity. This included stabilization of disease in 36% (14/39) and 38% (5/13) of patients receiving monotherapy (NSCLC and RCC) and

combination therapy (NSCLC), respectively, and partial responses in 15% (2/13) of patients within the combination arm (342). Among these patients, the SAg reactive population of T cells were selectively expanded after TTS infusions, and returned to normal levels one month post-treatment, with enhancement of tumour infiltration of T cells after treatment in tumour biopsied NSCLC patients (343). Anti-SAg antibodies were increased in approximately 50% of patients after one cycle, and although low, levels of HAMA were detected but were reported not to effect the overall pharmacokinetics of naptumomab estafenatox (mean plasma concentration half-life of ~1 h over all cycles), presumed due to exceedingly small doses compared to non-conjugated mAb-based therapies (343). Based on the IL-2 level post-administration of the TTS, unlike previous trials, sufficient drug access could be monitored and dosing for patients adjusted within this evaluation (343). Overall, naptumomab estafenatox was concluded to be safe for administration to patients with advanced malignant disease and pharmacological proof-of-principle obtained for the TTS concept (342, 343).

Based on preclinical models with TTSs and IFN-α (344), a randomized Phase II/III trial in patients with advanced RCC was conducted with naptumomab estafenatox, comparing the TTS (15 μg kg^{-1} given 3 cycles of 4 daily intravenous [iv] infusions; MTD for RCC in Phase I trials) plus interferon-α (9×10^6 U given subcutaneous 3× weekly), to interferon-α alone (same dosing). Although well-tolerated and comparable to Phase I trials, early information revealed that the study did not reach the primary endpoint of OS; however, an unexpected majority of patients had high levels of pre-formed anti-SEA/E-120 antibodies, which may have contributed to suboptimal therapy (209, 345, 346). Notably, a subgroup analysis of those patients with normal anti-SEA/E-120 neutralizing antibodies and low basal IL-6, a current biomarker for immune status of the tumour microenvironment (347), demonstrated that the combinational therapy with IFN-γ may improve and did demonstrate treatment advantages in both OS and PFS (346, 348). Furthermore, preliminary assessment of the immunological responses revealed patients with pronounced IL-2 induction and T cell expansion after treatment correlated with longer OS (348). After three days of initial treatment, the total T cell population, including TTS-specific T cells, was reduced in the peripheral blood of assessed patients. However, the expansion level of TTS-specific $CD8^+$ and predominately $CD4^+$ T cells was

significantly higher eight days after the first treatment cycle (4 days post-last TTS infusion) (348). Preliminary reports noted a large proportion of the expanded TTS-specific $CD4^+$ T cells displayed a memory phenotype (CD45RO) and were also detected in $FoxP3^-$ and not $FoxP3^+$ cells, suggesting that the TTS expanded T effectors cells rather than Tregs. This response was preceded with an increase of serum levels of IL-6, IL-10, and TNF-α, particularly after the first treatment cycle (4 days post-last TTS infusion) (348). Although this form of therapy may need to be patient specific (209, 346), the human data for TTS remains promising, and studies have clearly demonstrated the potential of TTSs for cancer immunotherapy. Presently, future development strategies are aimed at starting a Phase II/III with a novel combination of naptumomab estafenatox with a tyrosine kinase inhibitor (209).

1.6.5.7 Directed-cytotoxic mechanisms of preclinical TTSs

Although specific mechanisms of TTS-induced anticancer immunotherapy have not been fully elucidated, it can be speculated that the therapeutic efficacy is attributed collectively from several combination of mechanisms: 1) activation and direct lysis by T cells of TAA-expressing tumour cells, 2) suppression of tumour cell growth by secretion of cytokines and 3) recruitment of immune cells and cytokine secretion that eliminates TAA-negative tumour cell variants (**Figure 5**) (209, 349, 350).

SAgs are able to induce cytotoxicity by direct activation of CTLs (310) and induction of activated T cell cytokine release, primarily IL-2, TNF-α, and IFN-γ with subsequent activation of accessory cells such as NK cells (349, 351, 352). Consistently, initial preclinical studies report that therapeutic effects of TTS were largely associated with immune infiltration, inflammation, and activation localized to the tumour (318, 320, 322, 350, 353, 354). Predominantly present were $CD4^+$ and $CD8^+$ T cells, as well as a large fraction of Mϕ (354). The overall response resulted in a strong T cell-dependent direct cell-mediated cytotoxicity through apoptosis (312, 332) and a release of pro-inflammatory cytokines, predominantly TNF-α and IFN-γ (312, 313, 353, 354). Specifically reported, in a single-cell based study with SEA, the cytokines IL-2, IL-4, IL-5, IL-10, IL-12, TNF-α, IFN-γ, GM-CSF, and TGF-β were foremost produced; the

Figure 5. TTS proposed mechanism of action

TTS proposed mechanisms leading to anti-tumour effects represented as schematic illustrations. Images were modified from Eisen *et al.* (209), targeting the TAA 5T4 and based on **A)** preclinical investigations with TTSs and **B**) immunological responses observed from early analysis of clinical treatment cycles of naptumomab estafenatox (348).

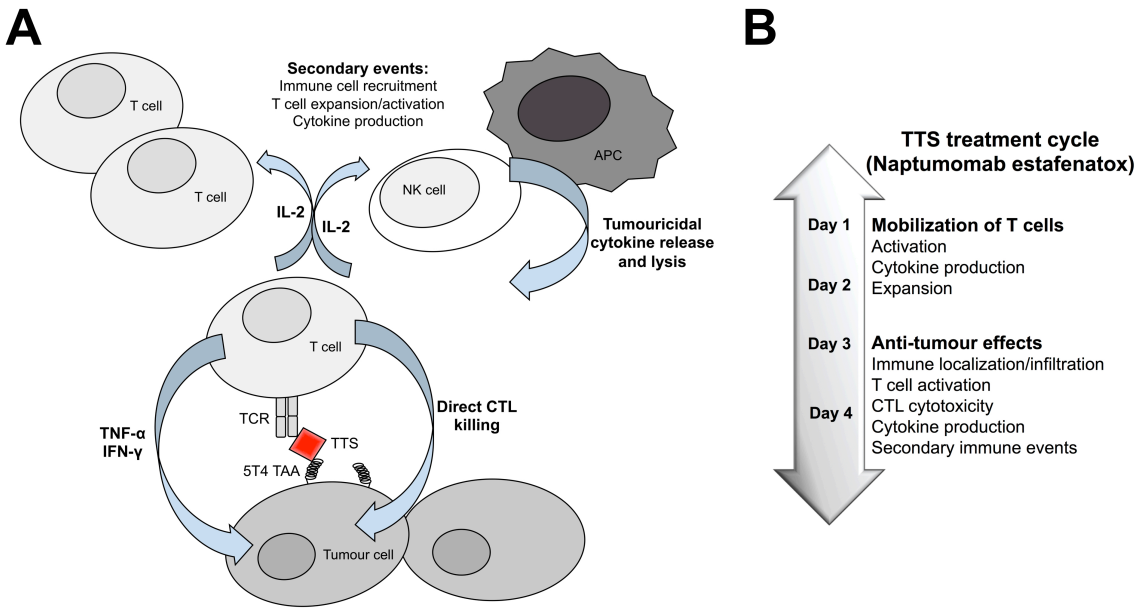
A
Secondary events:
Immune cell recruitment
T cell expansion/activation
Cytokine production
T cell
T cell
APC
NK cell
IL-2
IL-2
Tumouricidal
cytokine release
and lysis
T cell
TCR
TTS
5T4 TAA
Direct CTL
killing
TNF-α
IFN-γ
Tumour cell
B
TTS treatment cycle
(Naptumomab estafenatox)
Day 1
Mobilization of T cells
Activation
Cytokine production
Day 2
Expansion
Day 3
Anti-tumour effects
Immune localization/infiltration
T cell activation
Day 4
CTL cytotoxicity
Cytokine production
Secondary immune events

majority of the TNF-α, IL-2, IL-12, and IFN-γ were made by the infiltrating human leukocytes, while the tumour cells were induced to produce IL-4, IL-10, and TNF-α (353), ultimately leading to SAg-mediated cytotoxicity. Derived primarily from CTLs, perforin-mediated lysis largely contributed to the eradication of local TAA positive cells (354, 355) and concomitantly, CD95 Fas receptor expression occurred to induce programmed cell death in the tumour cells (353).

A synergistic effect of these cytokines resulted in growth inhibition of cells (tumour suppressive), including those lacking the targeted TAA, and overall increased inflammation in the tumour area (314, 350, 353, 355, 356). IFN-γ production through $CD4^+$ T cells was classified an important mediator for the overall cytostatic response, and was found to exert both direct and indirect anti-tumour effects (354). From knock-out *in vivo* studies, recruitment of cytotoxic cells and Mϕ depended on this cytokine to mediate strong tumouricial effects (354) and effective therapy was influenced by the overall release of IFN-γ (354, 355). Preclinical work implied that both $CD4^+$, as well as $CD8^+$ T cells were necessary to collaborate for optimal anti-tumour effects of TTS (354). Repeated injections augmented these effects (320, 321, 350) with a strong SEA_{D227A}-induced production of IL-2, INF-γ, TNF-α, and IL-6 (326) and also resulted in more pronounced primary synthesis of macrophage inflammatory protein (MIP)-1α (CCL3) and MIP-1β (CCL4) at the local tumour site for immune cell recruitment (354). SAg-reactive T cells simultaneously produced high levels of IL-2 inducing expansion and sustained T cell proliferation, with accumulation within the tumour area (354). These secondary events were important for anti-tumour effects against sub-populations of cancer cells not expressing the targeted TAA (335, 354).

Mechanistically, SAgs have the potential to induce T cell anergy and deletion, predominately after a period of strong T cell activation (295); however experimental studies *in vivo* with repeated exposure of TTSs have demonstrated that the T cell effector functions were recovered after eight weeks (321, 322). Further, the potential induction of dose-dependent T cell unresponsiveness may be resolved with combination of IL-2 (357, 358) and remains, among other immune modulators, an area of study for potential combinational therapies.

Recently, clinical applications of repeated cycles of TTSs have described immunological responses, proposing a sequence of events that may lead to therapeutic efficacy (209, 348). Initial mobilization of T cells occurs immediately after administration, signified by T cell activation and increase in cytokine production (*e.g.* IL-2, TNF-α, IFN-γ) and expansion (Days 1-2). Throughout the treatment cycle on Days 3-4, full localization of the TTS occurs, encouraging further T cell infiltration, activation, cytokine production, and immune elimination (*e.g.* CTLs) of the targeted tumour cells with the elicited secondary events destroying TAA-negative bystander cells (**Figure 5B**) (209, 348).

1.6.5.8 Combinational therapies of TTSs

Clinically, TTSs have the compelling ability to also be used in combinational therapies. Early preclinical studies exhibited sustained T cell activation ($CD4^+$ and $CD8^+$) and an increase in IFN-γ and TNF-α production when the first generation TTS (C215Fab-SEA) was co-administered with a tumour targeted IL-2 fusion protein (357, 359). Improved therapeutic efficacy and long-term survival of the combination treatment correlated with tumour infiltration and prolonged immune response compared to either treatment alone in an established murine C215-B16 melanoma model (357, 359).

Later studies demonstrated a synergistic anti-tumour response in the C215-B16 model when the TTS C215Fab-SEA was administered in a combined treatment with IFN-α (344). This response was accompanied with heightened $CD8^+$ T cell infiltration into the tumour area, enhanced induction of perforin-dependent cytotoxicity, and prolonged survival time (344). Further, when combined in a multi-cycle regimen with the cytostatic drug docetaxel, a member of the widely used conventional cancer chemotherapies, pretreatment did not interfere with T cell responses but enhanced cytotoxicity and the overall tumour therapy was significantly improved (341). When compared to monotherapies, prolonged long-term survival was synergistic and administration of docetaxel reduced the development of anti-SEA response after repeated TTS treatment (341). This preclinical work was subsequently applied to an ongoing Phase I clinical trial with naptumomab estafenatox as a combination evaluation with docetaxel with encouraging synergistic effects (342).

Immunotherapeutic modalities, such as TTS, may expand tumour antigen-specific Tregs as well as T effector cells, inducing immune suppression and diminishing expansion of effector cells (360). Increased levels of Tregs ($Foxp3^+$) were reported in recent Phase II/III clinical trials after treatment cycles with naptumomab estasfenatox but interestingly were not within the TTS-specific $CD4^+$ subpopulations (348). Preclinical models of this TTS in conjunction with blockade of CTLA-4, a key negative regulator of immune responses, induced a favorable shift in the ratio between T effector and Tregs infiltrating the tumour and significantly prolonged the overall CTL response and sustained augmented responses in repeated TTS cycles (361). Monotherapy of an antagonistic CTLA-4 mAb was ineffective against tumours but enhanced anti-tumour effects in tumour-bearing animals and improved overall long-term survival (361).

1.6.6 Streptococcal pyrogenic exotoxin C and immune mediator interactions

Streptococcal pyrogenic exotoxin C (SpeC) is a 24 kDa, 235 amino acid protein (362) produced by *S. pyogenes* that was first characterized in 1977 by Schlievert *et al.* (363). Clinically, SpeC has been generally associated with streptococcal TSS, a toxin-mediated acute life-threatening illness, which results from a 'cytokine storm' elicited by the polyclonal T-cell expansion properties of SAgs (248). SpeC has also been implicated in other toxin-mediation ailments, such as scarlet fever, but a strict association is not always detected (364).

Since its initial description, this Group IV SAg has been well-studied in terms of both structure (272, 285, 365) and functional engagement of host receptors (277, 286, 366-368). As distinct SAgs typically display unique Vβ T cell activation profiles (283), it was determined that SpeC preferentially binds and activates human $V\beta2^+$ T cells, although it is also capable of binding to Vβ3, 4, 12, and 15 T cell subsets (283, 366). Indeed, a co-crystal structure of SpeC bound to human Vβ2.1 chain identified extensive binding interactions of SpeC with CDR1, CDR2, hypervariable region 4 (HV4), FR3, and CDR3 of the TCR (285), and further work has elucidated its important interactions in a functional-map analysis specifically with CDR2 (277). Extensive work with SpeC has revealed that the TCR and pMHC II are cross-linked by SpeC through a zinc-mediated,

high-affinity binding site, 'docking' the SAg within the complex, and a predicted low-affinity binding site, two distinct interfaces interacting with MHC II molecules (272, 286, 369). The high-affinity interaction is between the C-terminal domain of SpeC and the β-chain of MHC II (272), while the low affinity interaction occurs between the N-terminal domain of SpeC and the α-chain of MHC II (286) (**Figure 6**).

Comprehensive mutational analysis has generated 'functional' maps that have designated critical amino acid residues of SpeC involved at each binding interface (286, 367, 368, 370). Such analysis has allowed for the development of a non-mitogenic and non-lethal SpeC molecule, that when used as a vaccine, was able to protect against a rabbit model of TSS (367). Indeed, the single Asp^{203} to Ala mutation in SpeC, a critical amino acid in the zinc-mediated, high affinity MHC II interaction, has also been demonstrated to dramatically reduce toxicity in a lethal model of TSS (369). A representative structural overview of the SpeC-mediated T cell activation complex, along with highlighted critical residue mutations, Tyr^{15} (368) and Asp^{203} (272, 286, 369) is presented in **Figure 6B.** This knowledge may also allow for SpeC to be engineered as a prototype SAg for future use in immunotherapy treatments of human disease, such as those directed at cancer.

1.7 Rationale and Hypothesis

In recent years it is clearly evident that giant strides have been made in the development of cancer immunotherapeutics and that it will be vital for research to continue to provide alternative treatments for such a worldwide devastating disease. In the work to be described, it was sought to expand the repertoire of TTSs to include the first streptococcal SAg, using SpeC as the prototype. Bacterial genomic sequencing efforts over the last decade have now revealed an extensive 'family' of SAg exotoxins in both *S. aureus* and *S. pyogenes*. A general feature of these toxins is that genetically distinct SAgs are also antigenically distinct, and furthermore, distinct SAgs also typically display unique Vβ activation profiles (283). Thus, *S. aureus* and *S. pyogenes* have provided an abundance of T cell mitogens that could potentially be engineered as TTSs for cancer therapy. Prior to this work, TTSs had been built exclusively using members of the SE class of SAg, and SEs are also agents of staphylococcal food-borne illness, an activity

Figure 6. Structural overview of the SpeC-mediated T cell activation complex and important residues involved at binding interfaces

Cartoon representations of **A)** SpeC in complex with TCR and pMHC II cross-linked by SpeC through zinc-mediated, high affinity binding site and a low affinity binding site (272, 285, 286). **B)** Close up view showing two important SpeC residues involved in the interaction at the TCR interface (Y15) and the high-affinity binding MHC II binding interface (D203). The ternary model of TCR-SpeC-$(MHC)_2$ was produced as previously described (277). In brief, the cartoon was generated by superimposing SpeC-TCR (PDB code 1KTK) (285), high affinity binding site SpeC-MHC II (PDB code 1HQR) (272) and low affinity site as predicted from SEC-MHC II (PDB code 1JWM) (287). Colours are as follows: MHCα-chains, *red*; MHCβ-chains, *green*; antigenic peptides, *black*; zinc atom, *magenta*; TCR Vα chain, *yellow*; TCR Vβ chain, *grey*; SpeC, *blue* with important interface residues highlighted in *orange*.

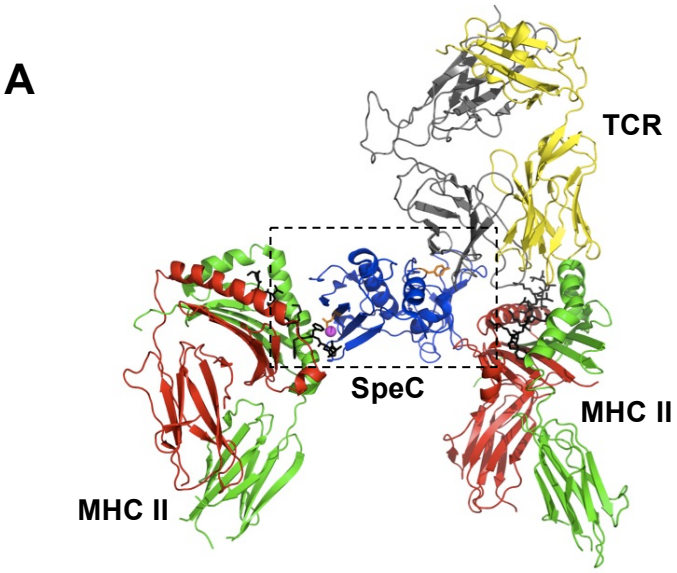
A
TCR
SpeC
MHC II
MHC II

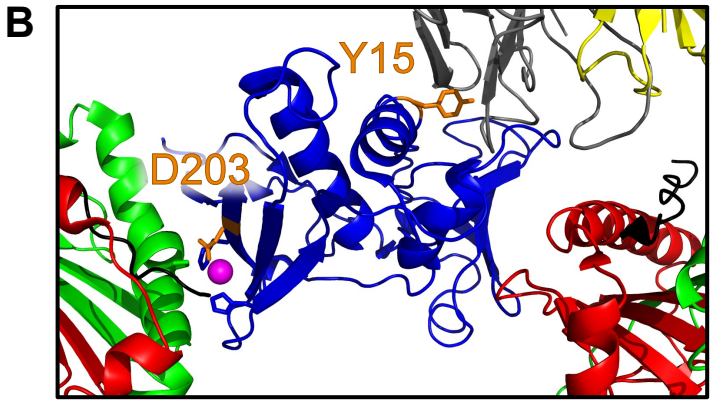
B
Y15
D203

that is thought to be independent of the ability to activate T cells (261). Although manageable, some of the side effects seen in TTS Phase I and Phase II clinical trials included nausea, vomiting, and diarrhea (323, 338, 342), and may have been related to the emetic properties of SEA (371). A potential advantage of engineering a streptococcal SAg as a TTS is that these toxins naturally lack bona fide emetic activity (262), which may result in fewer side effects. Also, SpeC is very well studied in terms of both structure (272, 285, 365) and function for host receptor engagement (277, 286, 366-368), providing a platform for tailoring activity. Herein, it is hypothesized that SpeC mutagenized within the zinc-dependent, high-affinity MHC II binding domain ($SpeC_{D203A}$) will have reduced superantigenicity while retaining tumouricidal properties and a $SpeC_{D203A}$-based TTS fusion protein using an engineered scFv that specifically targets human 5T4 (scFv5T4) can be generated (scFv5T4::$SpeC_{D203A}$). Finally, it is speculated that in a humanized mouse model of colon cancer, the scFv5T4::$SpeC_{D203A}$ TTS will control the growth potential of an established colon cancer tumour, and that this anti-tumour activity requires both specific targeting by the scFv5T4 moiety, as well as SAg function.

This dissertation is based, in part, on the publication “Control of established colon cancer xenografts using a novel humanized single chain antibody-streptococcal superantigen fusion targeting the 5T4 oncofetal antigen” Patterson KG, Dixon Pittaro JL, Bastedo PS, Hess DA, Haeryfar SMM, McCormick JK (2014) PLoS ONE 9(4): e95200) and has been reformatted to departmental guidelines.

CHAPTER 2: METHODS AND MATERIALS

2.1 Ethics statements

Experiments using primary human lymphocytes were reviewed and approved by Western University's Research Ethics Board (REB) for Health Sciences Research Involving Human Subjects (**Appendix 1**). Informed written consent was obtained from all blood donors were performed under REB 09911E. All animal experiments were performed by Animal Use Protocol (AUP) Number: 2012-026 in accordance with the Canadian Council on Animal Care Guide to the Care and Use of Experimental Animals, and was approved by the Animal Use Subcommittee at Western University (London, ON, Canada) (**Appendix 2**)

2.2 Cell culture growth conditions

2.2.1 Bacterial cell growth conditions

E. coli strains were grown aerobically at 37°C or room temperature (RT) in Difco™ Luria-Bertani (LB) broth with shaking (BD Biosciences, Franklin Lakes, NJ, USA) or on LB with 1.5% Difo™ Agar (BD Biosciences, Franklin Lakes, NJ, USA), and if required, the following antibiotics to maintain target plasmids or endogenous mutations: kanamycin (50 μg mL^{-1} for BL21 [DE3] and 15 μg mL^{-1} for Origami B [DE3]), chloramphenicol (10 μg mL^{-1}), ampicillin (100-200 μg mL^{-1}), and/or tetracycline (12.5 μg mL^{-1}) (all from Sigma-Aldrich, St. Louis, MO, USA). For storage, bacterial strains were frozen in LB with 20% glycerol and maintained at -80°C. All bacterial strains used within this study are listed in **Table 9.**

2.2.2 Tissue culture media, growth conditions, and propagation

All tissue culture basal media (Gibco®, Life Technologies Inc, Carlsbad, CA, USA) was supplemented with 10% heat-inactivated fetal bovine serum (FBS; Sigma-Aldrich, St. Louis, MO, USA) and the following supplements, all supplied from Gibco®: 10 mM N-2-hydroxyethylpiperazine-N-2-ethane sulfonic acid (HEPES), 2 mM L-Glutamine, 1 mM sodium pyruvate, 100 μM non-essential amino acids, 100 μg mL^{-1} streptomycin, and 100 U mL^{-1} penicillin (Gibco®, Life Technologies Inc, Carlsbad, CA, USA) all filtered through 0.2 μm PES filter (Nalgene™, Thermo Scientific, Waltham, MA, USA).

Table 9. Bacterial strains used within this study

Cell	Description	Purpose	Source
DH5α	F^{-} Φ80lacZΔM15 Δ(*l*acZYA^{-}argF) *U169 recA1 endA1 hsdR17* (*rK*$^{-}$, *mK*$^{+}$) phoA supE44 λ– thi-1 gyrA96 relA1	Cloning	Invitrogen
XL1 Blue	*recA1 endA1 gyrA96 thi-1 hsdR17 supE44 relA1 lac* [F′ *proAB lacI*^{q}*ZΔM15 Tn10* (*Tet*^{R})]	Cloning	Stratagene
SCS110	*rpsL* (Str^{r}) *thr leu endA thi-1 lacY galK galT ara tonA tsx dam dcm supE44* Δ(*lac-proAB*) [F′ *traD36 proAB lacI*^{q}*ZΔM15*]	Cloning	Stratagene
BL21 (DE3)	F^{-} *ompT hsdS*$_{B}$(*r*$_{B}^{-}$, *m*$_{B}^{-}$) *gal dcm* (DE3)	Protein expression	Novagen
Origami B (DE3)	F^{-} *ompT hsdS*$_{B}$(*r*$_{B}^{-}$, *m*$_{B}^{-}$) *gal dcm lacY1 aphC* (DE3) *gor522*::Tn*10 trxB* (Kan^{R}, Tet^{R})	Protein expression	Novagen
BL21 (DE3) pBirAcm	BL21 (DE3) containing pBirAcm	Protein biotinylation	This study
Origami B (DE3) pBirAcm	Origami B (DE3) containing pBirAcm	Protein biotinylation	This study

All cells used within this study and respective complete supplemented medias for each cell line are listed in **Table 10**.

To prepare cultures from cryopreservation, cells were thawed quickly within a 37°C water bath and diluted 1:10 in pre-warmed media with no antibiotics. Cells were pelleted by centrifugation at 330 × *g* (Allegra 6, Beckman Coulter, Brea, CA, USA) for 5 min at RT, and the supernatant removed. The pellet was gently washed 3× following the same centrifugation, and after the final wash, the cells were seeded onto a 25 cm^2 or 75 cm^2 tissue culture flask, dependent on cellular concentration of adherent cells. All tissue culture cells were maintained at 37°C with 5% CO_2 in FBS supplemented complete media. At 70-80% confluence, the cells were harvested for subculturing by removal of the media, and gently rinsing the cells with 1× phosphate buffered saline (PBS) (Gibco®, Life Technologies Inc, Carlsbad, CA, USA). The cells were incubated with cold 0.05% Trypsin-0.53 mM ethylenediaminetetraacetic acid (EDTA) (Gibco®, Life Technologies Inc, Carlsbad, CA, USA) for 5 min at 37°C with 5% CO_2 and gently rocked to detach the cells. Pre-warmed complete culture media with FBS was added immediately to the flask (1:1) to neutralize the trypsin and collect detached cells. The cells were collected by centrifugation at 330 × *g*, for 5 min at RT and resuspended in completed media with FBS and reseeded based on subculture ratio (**Table 10**).

For cryopreservation, cell cultures with no exposure to antibiotics, were harvested as above and prior to reseeding, an aliquot stained with trypan blue exclusion dye (1:1) (Gibco®, Life Technologies Inc, Carlsbad, CA, USA) was counted using a haemocytometer. Cells were pelleted as above and resuspended in cold FBS with 10% dimethyl sulfoxide (DMSO). Cells were quickly transferred to cryopreservation vials and placed at -20°C for 2-3 h (or until frozen) and subsequently stored at -80°C for overnight (O/N) or until relocated to liquid nitrogen vapor cryotank for long-term storage.

The HT-29 cells tested negative for murine pathogens and *Mycoplasma* spp. using Infectious Microbe PCR Amplification Test III (IMPACT III) profiling prior to use in animal models (IDEXX BioResearch Laboratories, Westbrook, ME, USA).

Table 10. Cell lines and primary cells used within the study

Cell	Description	Medium	Subculture ratio	Source	ATCC No.
HEK293	*Homo sapiens* (human); **Organ:** embryonic kidney	cMEM + 10% FBS	1:10	J. Madrenas, McGill University, Montreal, QC	CRL-1573
HT-29	*Homo sapiens* (human); **Organ:** colon; **Disease**: colorectal adenocarcinoma	cDMEM + 10% FBS	1:5	J. Koropatnick, Western University, London, ON	HTB-38
WiDr	*Homo sapiens* (human); **Organ:** colon; **Disease**: colorectal adenocarcinoma	cDMEM + 10% FBS	1:5	J. Madrenas, McGill University, Montreal, QC	CCL-218
PBMCs	*Homo sapiens* (human); **Source:** whole blood	cRPMI-1640 + 10% FBS	N/A	Various donors	N/A

Human peripheral blood mononuclear cells (PBMCs) were prepared from the whole blood of healthy donors and isolated by density centrifugation over Ficoll-Paque Plus (GE Healthcare Life Sciences, Piscataway, NJ, USA). In brief, heparinized whole blood was diluted 1:1 with RPMI-1640 (Gibco®, Life Technologies Inc, Carlsbad, CA, USA), layered on top of Ficoll-Paque Plus, and components separated by centrifugation at 910 × *g* (Allegra 6, Beckman Coulter, Brea, CA, USA) for 1 h, with no applied brake for deceleration. The buffy coat layer containing the PBMCs was collected and washed 2× 20 min with RPMI-1640 by centrifugation at 510 × *g*. PBMCs were diluted in cRPMI-1640 with 10% heat-inactivated FBS for experimental use and an aliquot stained with trypan blue exclusion dye (Gibco®, Life Technologies Inc, Carlsbad, CA, USA) was used to quantify cell concentration with a haemocytometer. Reagents and media used for isolation were pre-warmed prior to use. PBMCs were cultured within a tissue culture flask and maintained at 37°C with 5% CO_2.

2.3 Plasmid isolation

Plasmid DNA was isolated and purified from 1-2 mL of pelleted *E. coli* in stationary phase (O/N aerobic growth at 37°C) with QIAprep Spin Miniprep Kit (Qiagen, Venlo, Limburg, Netherlands) as per manufacturer's protocol. Plasmid DNA was eluted in 10 mM Tris·Cl, pH 8.5 and stored at -20°C. For preparation and concentration of plasmids for transfection, 6-10 mL of pelleted *E. coli* in stationary phase was processed for purification over a single column and eluted in 20-30 µl 10 mM Tris·Cl, pH 8.5. All plasmids generated within this study are listed in **Table 11**.

2.4 DNA visualization and quantification

DNA was visualized on 0.8%, 1%, or 1.2% UltraPure™ Agarose (Invitrogen, Life Technologies Inc, Carlsbad, CA, USA) in 1×TAE dependent on desired resolution. Electrophoresis was performed for 1 h at 100 V (Bio-Rad Laboratories Inc, Hercules, CA, USA) of DNA samples, containing loading dye, followed by staining with ethidium bromide (EtBr) solution for visualization under ultraviolet light (Gel Doc™, Bio-Rad Laboratories Inc, Hercules, CA, USA). For size determination, experimental DNA was compared to 1 Kb Plus DNA Ladder (Invitrogen, Life Technologies Inc, Carlsbad, CA,

Table 11. Plasmid DNA constructs used within this study

Plasmid name	Relevant characteristics[a]	Source
pCMV6-XL5	Mammalian expression vector; engineered from pCMV6-XL5::5t4 by removal of 5t4 with *Not*I sites; Ap^r	This study
pCMV6-XL5::*egfp*	*egfp* from pEGFP-N1 inserted into *Sac*I and *Xba*I sites of pCMV6-XL5::5t4 replacing 5t4 gene; Ap^r	This study
pCMV6-XL5::*5t4*	*5t4*, human trophoblast glycoprotein (TPBG), transcript variant 1 inserted into *Eco*RI and *Sal*I sites of pCMV6-XL5; Ap^r	Origene Technologies
pEGFP-N1	Mammalian expression vector with N-terminal *egfp* tag; Km^r	Clontech Technologies
pEGFP-N1::*5t4*	*5t4* from pCMV6-XL5::*5t4* inserted into *Eco*RI and *Bam*HI sites of pEGFP-N1; Km^r	Dixon (372)
pET-41a(+)::TEV	Protein expression vector with modified protease cleavage site; Km^r	Rahman *et al*. (368)
pET-32a(+)	Protein expression vector; N-terminal TrxA and His_6 tags; Ap^r	Novagen
pET-32a(+)::TEV	Protein expression vector with modified protease cleavage site; Ap^r	This study
pBirAcm	pACYC184 with inducible biotin ligase; Cm^r	Avidity
pET-41a(+)::TEV::*speC*$_{WT}$	*speC* inserted into *Nco*I and *Bam*HI of pET-41a; Km^r	Dixon (372)
pET-41a(+)::TEV::*speC*$_{WT}$::biotin	*speC* inserted into *Nco*I and *Bam*HI of pET-41a with a C-terminal biotin tag; Km^r	C Herfst (unpublished)
pET-41a(+)::TEV::*speC*$_{Y15A}$	*speC*$_{Y15A}$ inserted into *Nco*I and *Bam*HI of pET-41a; Km^r	Rahman *et al*. (368)
pET-41a(+)::TEV::*speC*$_{D203A}$	*speC*$_{D203A}$ inserted into *Nco*I and *Bam*HI of pET-41a; Km^r	Kasper *et al*. (286)
pET-41a(+)::TEV::*speC*$_{D203A}$::biotin	*speC*$_{D203A}$ inserted into *Nco*I and *Bam*HI of pET-41a with a C-terminal biotin tag; Km^r	This study
pET-41a(+)::TEV::*speC*$_{Y15A/D203A}$	*speC*$_{Y15A/D203A}$ inserted into *Nco*I and *Bam*HI of pET-41a; Km^r	This study
pET-41a(+)::TEV::*speC*$_{Y15A/D203A}$::biotin	*speC*$_{Y15A/D203A}$ inserted into *Nco*I and *Bam*HI of pET-41a with a C-terminal biotin tag; Km^r	This study
pET-28a(+)::*scFv5T4*	*scFv5T4* inserted into *Bam*HI and *Eco*RI sites of pET-28a; Km^r	Dixon (372)
pET-28a(+)::*scFv5T4*::*speC*$_{D203A}$	*scFv5T4* translationally fused with *speC*$_{D203A}$ with an engineered GGP-*Eco*RI linker; inserted into *Bam*HI and *Hin*dIII sites of pET-28a; Km^r	Bastedo (373)

pET-28a(+)::*scFv5T4*::*speC*$_{Y15A/D203A}$	*scFv5T4* translationally fused with *speC*$_{Y15A/D203A}$ with an engineered GGP-*Eco*RI linker; inserted into *Bam*HI and *Hin*dIII sites of pET-28a; Km^r	Bastedo (373)
pBluescript II SK(+)	Standard cloning vector; MCS within *lacZ* for colorimetric screening of insertions; Ap^r	Stratagene
pBluescript::*scFv5T4*::*speC*$_{D203A}$::TEV::biotin	*scFv5T4*::*speC*$_{D203A}$::TEV::biotin inserted into *Eco*RV site; Ap^r	This study
pBluescript::*scFv5T4*::*speC*$_{Y15A/D203A}$::TEV::biotin	*scFv5T4*::*speC*$_{Y15A/D203A}$::TEV::biotin inserted into *Eco*RV site; Ap^r	This study
pET-28a(+)::*scFv5T4*::*speC*$_{D203A}$::TEV::biotin	s*cFv5T4* translationally fused with *speC*$_{D203A}$ with an engineered GGP-*Eco*RI linker; inserted into *Nco*I and *Hin*dIII sites of pET-28a; C-terminal biotin tag; Km^r	This study
pET-28a(+)::*scFv5T4*::*speC*$_{Y15A/D203A}$::TEV::biotin	*scFv5T4* translationally fused with *speC*$_{Y15A/D203A}$ with an engineered GGP-*Eco*RI linker; inserted into *Nco*I and *Hin*dIII sites of pET-28a; C-terminal biotin tag; Km^r	This study
pUC57::*scFv5T4*::TEV::biotin	Murine codon optimized *scFv5T4* sequence with *Nco*I and *Hin*dIII sites; C-terminal biotin tag; Ap^r	GenScript Corp
pET-28a(+)::*scFv5T4*::TEV::biotin	Murine s*cFv5T4* inserted into *Nco*I and *Eco*RI sites of pET-28a; C-terminal biotin tag; Km^r	This study
pET-28a(+)::*scFv5T4*::*speC*$_{D203A}$::TEV::biotin	Murine s*cFv5T4* translationally fused with *speC*$_{D203A}$ with an engineered GGP-*Eco*RI linker; inserted into *Nco*I and *Hin*dIII sites of pET-28a; C-terminal biotin tag; Km^r	This study
pET-28a(+)::*scFv5T4*::*speC*$_{Y15A/D203A}$::TEV::biotin	Murine *scFv5T4* translationally fused with *speC*$_{Y15A/D203A}$ with an engineered GGP-*Eco*RI linker; inserted into *Nco*I and *Hin*dIII sites of pET-28a; C-terminal biotin tag; Km^r	This study
pET-32a(+)::*scFv5T4*::TEV::biotin	Murine *scFv5T4* inserted into *Nco*I and *Eco*RI sites of pET-32a; C-terminal biotin tag; Ap^r	This study
pET-32a(+)::*scFv5T4*::*speC*$_{D203A}$::TEV::biotin	Murine *scFv5T4* translationally fused with *speC*$_{D203A}$ with an engineered GGP-*Eco*RI linker; inserted into *Nco*I and *Hin*dIII sites of pET-32a; C-terminal biotin tag; Ap^r	This study
pET-32a(+)::*scFv5T4*::*speC*$_{Y15A/D203A}$::TEV::biotin	Murine *scFv5T4* translationally fused with *speC*$_{Y15A/D203A}$ with an engineered GGP-*Eco*RI linker; inserted into *Nco*I and *Hin*dIII sites of pET-32a; C-terminal biotin tag; Ap^r	This study
pUC57::*scFv5T4*^{H}::TEV::biotin	Humanized, codon optimized *scFv5T4* sequence with *Nco*I and *Hin*dIII sites; C-terminal biotin tag; Ap^r	GenScript Corp
pMSP3535::mRFP1	mRFP1 inserted into *Bam*HI and *Spe*I sites of pMSP3535 shuttle vector; Erm^r	McCormick (unpublished)
pET-32a(+)::*scFv5T4*^{H}::mRFP1	Humanized *scFv5T4* from pUC57::*scFv5T4*::biotin inserted into *Nco*I and *Hin*dIII sites of pET-32a; mRFP1 from pMSP3535::mRFP1 inserted into *Eco*RI and *Hin*dIII sites replacing biotin tag and fused to scFv5T4 with GGP linker; Ap^r	This study

pET-32a(+)::*scFv5T4*^{H}:: TEV::biotin	Humanized *scFv5T4* from pUC57::*scFv5T4*::biotin inserted into *Nco*I and *Hin*dIII sites of pET-32a; C-terminal biotin tag; Ap^{r}	This study
pET-32a(+)::*scFv5T4*^{H}:: *speC*$_{D203A}$::TEV::biotin	Humanized *scFv5T4* from pUC57::*scFv5T4*::biotin inserted into *Nco*I and *Hin*dIII sites of pET-32a; translationally fused with *speC*$_{D203A}$ with an engineered GGP-*Eco*RI linker; C-terminal biotin tag; Ap^{r}	This study
pET-32a(+)::*scFv5T4*^{H}:: *speC*$_{Y15A/D203A}$::TEV::biotin	Humanized *scFv5T4* from pUC57::*scFv5T4*::biotin inserted into *Nco*I and *Hin*dIII sites of pET-32a; translationally fused with *speC*$_{Y15A/D203A}$ with an engineered gly-gly-pro (GGP)/*Eco*RI linker; C-terminal biotin tag; Ap^{r}	This study
pET-32a(+)::TEV:: *scFv5T4*^{H}::EK::biotin	Humanized *scFv5T4* from pUC57::*scFv5T4*::biotin inserted into *Nco*I and *Hin*dIII sites of pET-32a; C-terminal EK protease site modified site Ap^{r}	This study
pET-32a(+)::TEV:: *scFv5T4*^{H}::*speC*$_{D203A}$:: EK::biotin	Humanized *scFv5T4* from pUC57::*scFv5T4*::biotin inserted into *Nco*I and *Hin*dIII sites of pET-32a; translationally fused with *speC*$_{D203A}$ with an engineered GGP-*Eco*RI linker; C-terminal biotin tag with modified EK protease cleavage site; Ap^{r}	This study
pET-32a(+)::TEV:: *scFv5T4*^{H}::*speC*$_{Y15A/D203A}$::EK ::biotin	Humanized *scFv5T4* from pUC57::*scFv5T4*::biotin inserted into *Nco*I and *Hin*dIII sites of pET-32a; translationally fused with *speC*$_{Y15A/D203A}$ with an engineered GGP-*Eco*RI linker; C-terminal biotin tag with modified EK protease cleavage site; Ap^{r}	This study

[a] Abbreviations: Ap^{r}, ampicillin resistance; Cm^{r}, chloramphenicol; Erm^{r}, erythromycin resistance; Km^{r}, kanamycin resistance; GGP, gly-gly-pro; scFv5T4^{H}, humanized scFv5T4

USA). Buffer and reagent composition is in **Table 12**. All DNA was quantified, using a NanoDrop 1000 Spectrophotometer (Thermo Fisher Scientific Inc, Waltham, MA USA).

2.5 DNA gel extraction

To isolate and purify DNA fragments by gel extraction, digested DNA was separated by gel electrophoresis on 0.6% agarose UltraPure™ Agarose (Invitrogen, Life Technologies Inc, Carlsbad, CA, USA) in 1×TAE for 1 h at 100 V (Bio-Rad Laboratories Inc, Hercules, CA, USA) and stained with EtBr solution. Desired fragments were excised under ultraviolet light and purified using QIAquick Gel Extraction Kit (Qiagen, Venlo, Limburg, Netherlands) as per manufacturer's protocol and eluted in 10 mM Tris·Cl, pH 8.5.

2.6 Ethanol precipitation

Concentration of plasmid DNA for transfection purposes was performed by adding 1/10 volume of cold (4°C) 3 M sodium acetate to the DNA sample followed by 2× volume of cold (-20°C) 95% EtOH. The DNA was incubated at -20°C for 25 min and pelleted by centrifugation at 21 000 × *g* for 10 min at 4°C. The pellet was washed by inversion with 0.75 mL cold (-20°C) 70% EtOH and centrifugation repeated for 5 min. EtOH was decanted and remaining evaporated for ~25 min prior to pellet resuspension in a low volume (10-15 µl) of 10 mM Tris·Cl, pH 8.5.

2.7 Primer generation

Primers were designed using the software Primer3Plus Version: 2.3.6 (374) and synthesized by Sigma Life Sciences (St. Louis, MO, USA). Primers were rehydrated as master stocks as 100 µM and diluted 1:10 for working stocks, both in sterile Milli-Q water (Millipore, Bedford, MA, USA). Primers used within the study listed in **Table 13**.

2.8 Polymerase chain reaction

Polymerase chain reaction (PCR) products were amplified (Peltier Thermocycler PTC-200, MJ Research, Waltham, MA, USA) with reactions containing 0.3 mM deoxyribonucleotide triphosphates (dNTPs; Roche Diagnostics, Basel, Switzerland),

Table 12. Buffer composition and reagents used within the study

Reagent	Composition	Application
Coomassie Blue staining solution	45% (v/v) methanol, 10% (v/v) glacial acetic acid, 0.1% (w/v) Coomassie Brilliant Blue R-250	Protein visualization
Destain solution	45% (v/v) methanol, 10% (v/v) glacial acetic acid	Protein visualization
DNA loading dye (6×)	40% (v/v) glycerol, 0.25% (w/v) bromophenol blue	DNA visualization
FACS Buffer	2% FBS, 0.01% sodium azide in 1×PBS	FACS
HEPES Buffer (1×)	150 mM NaCl, 10 mM 4-(2-hydroxyethyl)-1-piperazineethanesulfonic acid (HEPES), pH 7.4	Protein purification
Laemmeli buffer (4×)	240 mM Tris pH 6.8, 8% (w/v) SDS, 40% (v/v) glycerol, 0.01% (w/v) bromophenol blue, 1% (v/v) β-mercaptoethanol	Protein visualization
PBS (1×)	137 mM NaCl, 10 mM Na_2HPO_4, 2.7 mM KCl, 1.8 mM KH_2PO_4, pH 7.4	Various
PBST (1×)	137 mM NaCl, 10 mM Na_2HPO_4, 2.7 mM KCl, 1.8 mM KH_2PO_4, 0.1% (v/v) Tween-20	Various
PFU Buffer (1×)	20 mM Tris-HCl (pH 8.8), 10 mM $(NH_4)_2SO_4$, 10 mM KCl, 0.1% (v/v) Triton X-100, 0.1 mg mL^{-1} BSA, 2 mM $MgSO_4$	Molecular cloning: PCR
Polyacrylamide resolving gel (12%)	12% (v/v) acrylamide/bisacrylamide (37.5:1) aqueous solution, 0.25% (v/v) 1.5 M Tris-HCl pH 8.8, 0.1% (w/v) SDS, 0.1% (w/v) APS, 0.15% (v/v) TEMED	Protein visualization
Polyacrylamide stacking gel (5%)	1.3% SDS, 25% v/v 0.5 M Tris-HCl pH 6.8, 5% v/v acrylamide/bisacrylamide (37.5:1) aqueous solution, 0.1% (w/v) APS, 0.2% (v/v) TEMED	Protein visualization
PSI broth	2% (w/v) tryptone, 0.5% (w/v) yeast extract, 0.5% (w/v) $MgSO_4$, pH 7.6	Chemical competent cells
TAE (1×)	40 mM Tris-acetate, 1 mM EDTA, pH 8.0	DNA visualization
TBS	50 mM Tris-HCl pH 7.6, 150 mM NaCl	Histology
TBST (1×)	50 mM Tris-HCl pH 7.6, 150 mM NaCl, 2.5% Tween-20	Histology
TfbI solution	100 mM $RbCl_2$, 50 mM $MnCl_2 \cdot 4H_2O$, 30 mM CH_3COOK, 10 mM $CaCl_2$, 15% (v/v) glycerol, pH 5.8	Chemical competent cells

TfbII solution	75 mM $CaCl_2$, 10 mM $C_7H_{15}NO_4S$ (MOPS), 10 mM $RbCl_2$, 15% (v/v) glycerol, pH 6.5	Chemical competent cells
Tris-Glycine Running buffer (1×)	192 mM glycine, 25 mM Tris, 0.1% (w/v) SDS, pH 8.3-8.6	Protein visualization
Western Blot Transfer Buffer	20% methanol, 48 mM Tris base, 39 mM glycine, 0.037% (w/v) SDS	Protein visualization

Table 13. Primer oligonucleotides used for molecular cloning procedures and sequencing

Primer name	Sequence (5' - 3')[a]	Restriction enzyme site
T7 promoter	TAA TAC GAC TCA CTA TAG GG	n/a
T7 terminator	GCT AGT TAT TGC TCA GCG G	n/a
M13/pUC Forward	CGC CAG GGT TTT CCC AGT CAC GAC	n/a
M13/pUC Reverse	TCA CAC AGG AAA CAG CTA TGA C	n/a
SpeC For NcoI	GCG CCC ATG GGA GGA GGG CCG GAC TCT AAG AAA GAC ATT TCG	*Nco*I
SpeC D203A Rev BamHI	GCG CGG ATC CTT ATT TTT CAA GAT AAA TAG CGA AAT G	*Bam*HI
scFv5T4 For BspHI	CCC TCA TGA TAG AGG TCC AGC TTC AGC AGT C	*Bsp*HI
SpeC D203A Rev HindIII Biotin	CCC AAG CTT TTA TTC GTG CCA TTC GAT TTT CTG AGC CCT CGA AGA TGT CGT TCA GAC GCG CAC CAC TTT TGG AAA TAC AAG TTT TCT TTT TCA AAG ATA AAT AGC GAA ATG	*Hin*dIII
mRFP1-GGP For EcoRI	CCC GAA TTC GGA GGC CCG ATG GCC TCC TCC GAG G	*Eco*RI
mRFP1 Rev HindIII	CCC AAG CTT TTA GGC GCC GGT GGA GT	*Hin*dIII
scFv5T4 TEV For	CGC AGA TCT GGA AAA CTT GTA TTT CCA AAG TGC CAT GGA AGT GCA GCT GGT	*Bgl*II
scFv5T4 EK Biotin Rev	CGC AAG CTT TTA TTC GTG CCA TTC GAT TTT CTG AGC CTC GAA GAT GTC GTT CAG ACC GCC ACC CTT GTC GTC GTC GTC GAA TTC TTT GAT TTC CAG TTT CG	*Hin*dIII
SpeC D203A EK Biotin Rev	CGC AAG CTT TTA TTC GTG CCA TTC GAT TTT CTG AGC CTC GAA GAT GTC GTT CAG ACC GCC ACC CTT GTC GTC GTC GTC TTT TTC AAG ATA AAT AGC GAA ATG A	*Hin*dIII

[a] Underlined nucleotides represent restriction enzyme recognition site

5 mM $MgSO_4$, 1 µM oligonucleotide primers, 1×PFU buffer, 1 µl template DNA and 1:100 *Pfu* polymerase (generated internally, unpublished). Oligonucleotides (Sigma Genosys, St. Louis, MO, USA) are listed in **Table 13.** Amplification was performed with the following standard conditions: initial denature at 95°C for 5 min followed by repeated cycles (36×) of denaturing at 95°C for 1 min, annealing with primer-specific temperature for 30 sec [as designed with Primer3.0 Plus software (374)], and extension at 74°C at 1 kb min^{-1}, with final extension at 74°C for 5 min and maintained at 4°C until further processing. PCR products were purified with QIAquick PCR Purification kit (Qiagen, Venlo, Limburg, Netherlands) as per manufacturer's protocol and eluted in 10 mM Tris·Cl, pH 8.5.

2.9 Sequencing

All plasmid DNA inserts were sequenced at the DNA Sequencing Facility at Robarts Research Institute (Western University, London, ON, Canada) using standard T7 promoter and T7 terminator primers, or specifically designed primers, all listed in **Table 13**. DNA concentrations and primers were prepared as per requirements of the DNA Sequencing Facility.

2.10 Molecular cloning

2.10.1 Restriction digestions

Restriction enzyme digestion of DNA was performed as per manufacturer's specifications (New England BioLabs Inc, Ipswich, MA, USA or Roche Diagnostics, Basel, Switzerland). In brief, for the specific restriction enzymes used within this study, a digestion reaction containing target DNA, 1 U enzyme μg^{-1} DNA, 1× enzyme-specific buffer and if required, 1× bovine serum albumin (BSA) (New England BioLabs Inc, Ipswich, MA, USA), was incubated for 1-2 h in a 37°C water bath. Double digestion completion was compared to single digestion controls by visualization on a 1% agarose gel as above and subsequently purified with QIAquick PCR Purification kit (Qiagen, Venlo, Limburg, Netherlands) as per manufacturer's protocol with final elution in 10 mM Tris·Cl, pH 8.5.

2.10.2 DNA ligations

Ligations of DNA were performed for 1 h in a water bath at 16°C with reactions containing 40 U T4 DNA Ligase (New England BioLabs Inc, Ipswich, MA, USA), 1× T4 Ligase Buffer (New England BioLabs Inc, Ipswich, MA, USA), and appropriate concentrations of digested vector and insert. A standard reaction had ~100 ng total vector DNA and ~1 μg total insert DNA, calculated from a molar ratio of either 1:1 or 3:1 (insert:vector), based on the size variation of the insert compared to the vector. Blunt-end ligations used a molar ratio of 5:1 (insert:vector).

2.10.3 Competent cell preparation

2.10.3.1 Chemical competent *E. coli* preparation (rubidium chloride; RbCl)

E. coli strains were inoculated 1:100 from stationary phase (O/N growth at 37°C) into PSI broth and grown aerobically at 37°C to optical density $(OD)_{600}$ = 0.5. Cells were incubated on ice for 15 min prior to centrifugation at 2400 × *g* for 5 min at 4°C (Beckman Avanti® J-25 High Speed Centrifuge, Beckman Coulter, Brea, CA, USA). Cell pellets were gently resuspended and incubated for 15 min on ice in 0.4× original volume of TfbI solution. After repeated centrifugation, cells were resuspended in 0.04× original volume of TfbII solution and incubated 15 min on ice prior to aliquoting and immediate -80°C storage. Buffer and reagent composition are listed in **Table 12**.

2.10.3.2 Chemical competent *E. coli* preparation (calcium chloride; $CaCl_2$)

E. coli strains were inoculated 1:100 from stationary phase (O/N growth at 37°C) into LB broth and grown aerobically at 37°C to OD_{600} = 0.5. Cells were incubated on ice for 10 min prior to centrifugation at 4000 × *g* for 5 min at 4°C (Beckman Avanti® J-25 High Speed Centrifuge, Beckman Coulter, Brea, CA, USA). Cell pellets were gently resuspended in 10 mL of cold 0.1 M $CaCl_2$ and incubated for 20 min on ice. After repeated centrifugation, cells were gently resuspended in 5 mL cold 0.1 M $CaCl_2$ with 15% (v/v) glycerol and aliquoted for immediate use or -80°C storage.

2.10.3.3 Electrocompetent *E. coli* preparation

Electrocompetent cells were prepared with *E. coli* from stationary phase (O/N growth at 37°C) by subculturing 1:500 into LB media (5 mL) with appropriate antibiotics and grown for 3 h at 37°C, with shaking. The cells were pelleted by centrifugation at 2100 × *g* for 5 min at 4°C and pellet resuspended in 5 mL ice cold 10% glycerol. Centrifugation was repeated and the pellet was resuspended in 1 mL ice cold 10% glycerol followed by a final centrifugation and resuspension in 0.2 mL ice cold 10% glycerol. Cells were aliquoted into 0.1 mL fractions and immediately used for transformation or placed at -80°C for storage.

2.10.4 Transformation and transfection

2.10.4.1 Chemical competent *E. coli* transformation

To transform chemical competent *E. coli*, the ligation reaction (~10 µL) was added to the cell aliquot once thawed on ice, and incubated for 30 min remaining on ice. The cells were incubated at 42°C for 45 sec ($RbCl_2$-competent cells) or 2 min ($CaCl_2$-competent cells) for heat shock and subsequently placed on ice for 2 min. LB culture media (0.9 mL) was added to the cells prior to incubation for 1 h at 37°C with shaking. The transformation was cultured by spread plating (200 µL per plate) on LB Agar with appropriate antibiotics and grown O/N (18-24 h) at 37°C.

2.10.4.2 Electroporation of *E. coli*

Plasmid DNA (1 µL) was added to electrocompetent *E. coli*, prepared as described, and incubated on ice for 3 min. Samples were loaded into 0.2 cm electroporation cuvettes (VWR, Radnor, PA, USA) and pulsed at 200 Ω, 25 µF, 2.5 kV for 5 ms (Gene Pulser Xcell™ System, Bio-Rad Laboratories Inc, Hercules, CA, USA). The cells were immediately resuspended in 1 mL of LB culture media and incubated for 1 h at 37°C with shaking. The transformation was cultured by spread plating dilution series from 10^{-1}-10^{-3} on LB Agar with appropriate antibiotics and grown O/N (18-24 h) at 37°C.

2.10.4.3 Cellular transfections for gene expression

HEK293 cells were seeded as required into multi-well tissue culture plates (Corning Inc, Corning, NY, USA) with cMEM + 10% FBS and allowed to grow O/N (18-24 h) at 37°C with 5% CO_2. Liposome:DNA complexes were formed using Lipofectamine® 2000 (Life Technologies Inc, Carlsbad, CA, USA) and plasmid DNA of choice, as per manufacturer's protocol at a ratio of 2 µl lipofectamine:0.8 µg DNA. In brief, complexes were formed in cMEM without FBS or antibiotics. Transfection of cells occurred in the same media for 4 h at 37°C with 5% CO_2, after which the media was removed and replaced with cMEM + 10% FBS for plasmid expression over 24 h.

2.10.5 *E. coli* clone selection

Clones were screened for successful DNA ligation and transformation by selecting individual colonies that were subsequently grown O/N and plasmid isolation performed. Plasmids were visualized for band shifts on 1% agarose gels as described, as well as the insert size verified by restriction enzyme digestion and DNA sequencing performed for final sequence confirmation. Alternatively, DNA screening was performed by colony PCR. Individual colonies were inoculated into single PCR tubes by a sterile toothpick and the reaction buffer (as described) containing T7 forward and T7 terminator primers added. Amplification was performed with the following standard conditions: initial denaturing at 95°C for 10 min followed by repeated cycles (36×) of denaturing at 95°C for 30 sec, annealing with primer-specific temperature 63°C for 30 sec, extension at 74°C at 1 kb min^{-1}, and maintained at 4°C until further processing. PCR products were visualized by electrophoresis and staining with EtBr as described.

2.11 Generation of protein expression vectors

Using standard molecular cloning techniques, protein expression clones in pET-41a were altered such that the enterokinase (EK) cleavage site (DDDDK↓X), was replaced with a Tobacco Etch Virus (TEV) protease cleavage site (ENLYFQ↓S) (368). To enable biotin labeling of proteins, a protease cleavable C-terminal biotin ligase recognition sequence (biotin tag) (GLNDIFEAQKIEWHE; AviTag™, Avidity LLC, Aurora, CO, USA)

containing a 5' gly-gly spacer was genetically engineered onto genetic constructs within the reverse cloning primers (**Table 13**). All constructs were transformed into both *E. coli* XL1 Blue for plasmid preservation and *E. coli* BL21 (DE3) or Origami B (DE3) for protein expression (**Table 11**).

2.12 Generation of SpeC protein expression clones and variants

Plasmid constructs containing $speC_{WT}$ (372), $speC_{Y15A}$ (368) and $speC_{D203A}$ (286) for expression within pET-41a were previously described. In this study, $speC_{Y15A/D203A}$ for protein expression was generated. The 627 bp gene was amplified by standard PCR with an annealing temperature of 55°C from a previously generated construct containing $speC_{Y15A/D203A}$ (373) using primers in **Table 13**. The resulting PCR product was cloned into pET-41a::TEV for protein expression using standard molecular cloning techniques as described and transformed into *E. coli* BL21 (DE3).

2.13 Generation of murine scFv5T4 and linked SpeC variants for protein expression

Expression pET-28a constructs containing murine *scFv5T4* alone (372) or genetically linked $speC_{D203A}$ or $speC_{Y15A/D203A}$ (373) were previously generated. In this study, the linked constructs were developed further to include a C-terminal biotin tag, as described, which was added by standard PCR amplification with an annealing temperature of 50°C. Primers used are listed in Table 13. The resulting 1443 bp product was initially generated within pBluescript II SK (+) as an intermediate step with blunt-end ligation and subsequently by standard cloning techniques, into pET-28a for protein expression. For further product development, the murine scFv5T4 alone was designed to contain a C-terminal biotin tag and codon optimized for expression in *E. coli.* The 798 bp gene was manufactured by GenScript Corp (Piscataway, NJ, USA) and cloned by restriction enzyme digestion and standard techniques into pET-28a as well as pET-32a, an expression vector containing N-terminal thioredoxin (TrxA) and His_6 tags. The synthesized scFv5T4 was genetically linked to previously constructed $speC_{D203A}$ or $speC_{Y15A/D203A}$ with existing biotin tags by standard cloning methods and transformed into either *E. coli* BL21 (DE3) or Origami B (DE3) for co-expression with pBirAcm.

2.14 Design and generation of humanized scFv5T4 construct for protein expression

The humanized scFv was designed in this study based on the predicted CDRs of the characterized murine scFv specific for the human 5T4 TAA (243). The cDNA sequence for a humanized *scFv5T4* was recoded for *E. coli* expression and manufactured by GenScript Inc (Piscataway, NJ, USA). Amino acid substitutions were made in the backbone sequence of scFv5T4 from the original murine sequence (243), determined by aligning with a human consensus sequence. The consensus sequence was generated from 10 previously sequenced human scFv fragments taken from NCBI Protein Database (www.ncbi.nlm.nih.gov/protein) and aligned using MacVector (MacVector Inc, Cary, NC, USA). The CDR loops specific for 5T4, and the immediate amino acids flanking the predicted loops were not altered to maintain antibody structure and specificity. Amino acids within the CDRs were determined based on predicted topological modeling using PyMol Software (Schrödinger, New York, NY, USA) of scFv5T4 with the structure modeled from human 80R scFv (PDB 2GHW22) (375) with 75.9 sequence identity by SWISS-MODEL (www.swissmodel.expasy.org). Lastly, the gene was also designed to include a TEV cleavable C-terminal biotin tag as well as restriction enzyme sites for strategic cloning purposes. The synthesized 819 bp gene was cloned by restriction enzyme digestion using standard techniques into pET-32a for protein expression. The final construct development was to arrange the protease cleavage sites so that the TEV recognition site was N-terminal for TrxA and His_6 removal and the EK recognition site was C-terminal for removal of the biotin tag. The construct was amplified by PCR, with an annealing temperature of 65°C. The primers used are listed in **Table 13**. The resulting product for scFv5T4 was cloned by standard molecular techniques into pET-32a for protein expression in either *E. coli* BL21 (DE3) or Origami B (DE3) for co-expression with pBirAcm.

2.15 Generation of humanized scFv5T4 linked mRFP1

mRFP1 was amplified by standard PCR with an annealing temperature of 58°C from previously generated shuttle vector pMSP3535::*mRFP1* (**Table 11**). The resulting 687 bp product, containing a GGP linker was translationally fused to humanized *scFv5T4* by

standard molecular cloning procedures within pET-32a vector. The final construct was transformed into *E. coli* BL21 (DE3) for protein expression. Primers are listed within **Table 13**.

2.16 Generation of humanized scFv5T4 linked SpeC variants

Humanized *scFv5T4* from the pUC57::*scFv5T4* construct was genetically linked with previously biotin-tagged $speC_{D203A}$ or $speC_{Y15A/D203A}$ by restriction enzyme digestion and standard molecular cloning techniques into pET-32a to generate protein expression constructs. The final constructs were amplified by PCR, with an annealing temperature of 65°C to arrange the protease cleavage sites so that the TEV recognition site was N-terminal for TrxA and His_6 removal and the EK recognition site was C-terminal for removal of the biotin tag. Primers used are listed in **Table 13**. The resulting 1443 bp products were cloned into pET-32a and were transformed for co-expression with pBirAcm in *E. coli* BL21 (DE3) or Origami B (DE3).

2.17 Generation of transfection plasmids for human cell lines

Transfection vectors pCMV6-XL5::*5t4* and pEGFP-N1 were purchased from Origene Technologies, Inc. (Rockville, MD, USA), and Clontech Laboratories, Inc. (Mountain View, CA, USA), respectively. pEGFP-N1::*5t4* engineered to genetically link *5t4* to *eGFP* was previously generated (372). In this study, control vehicle pCMV6-XL5 was generated by removal of *5t4* from pCMV6-XL5::*5t4* by restriction enzyme digestion and the remaining fragment purified from gel electrophoresis and ligated to complete the vector. Transfection control vector pCMV6-XL5::*eGFP* was generated by the replacement of *5t4* of pCMV6-XL5::*5t4* with *eGFP* from pEGFP-N1 (replicated in *E. coli* SCS110) by restriction enzyme digestion and standard molecular techniques. The resulting constructs (**Table 11**) were transformed into *E. coli* XL1 Blue.

2.18 Protein visualization

2.18.1 Sodium Dodecyl Sulfate Polyacrylamide Gel Electrophoresis (SDS-PAGE)

To visualize proteins, 1-D vertical gel electrophoresis was performed for 50 min at 200 V

(Mini-PROTEAN System, Bio-Rad Laboratories Inc, Hercules, CA, USA) using 12% polyacrylamide resolving gels with 5% stacking gels in Tris-Glycine Running Buffer. Prior to electrophoresis, samples were mixed 3:1 with 4× Laemmli buffer and boiled for 5 min. Gels were fixed and stained for 1 h with coomassie blue staining solution containing Coomassie Brilliant Blue R-250 (Bio-Rad Laboratories Inc, Hercules, CA, USA) followed by replacing destain solution several times until background of the gel was resolved. For size determination, experimental proteins were compared to Prestained Broad Range P7708S Protein Marker (New England BioLabs Inc, Ipswich, MA, USA). Buffer and reagent composition are listed in **Table 12**.

2.18.2 Western Blot

To probe specific proteins, samples were separated by gel electrophoresis by SDS-PAGE on 12% polyacrylamide resolving gels as described, without end-stage staining. To immobilize proteins for detection, the samples were transferred from the gel matrix to an Immobilon-FL polyvinylidene difluoride (PVDF) membrane (EMD Millipore, Billerica, MA, USA) by electroblotting (Mini Trans-Blot® Cell, Bio-Rad Laboratories Inc, Hercules, CA, USA) for 1 h at 100 V (or 25 V O/N). Prior to transfer, the membrane was immersed for 5 min in methanol (100%) and equilibrated in Western blot transfer buffer. After transfer, to reduce non-specific binding, the membrane was blocked for 0.5 h with 5% (w/v) non-fat dry milk in 1×PBS. For specific protein detection the biotinylated tag was probed for 1 h with conjugated streptavidin-IRDye800 (1:10 000 in 1×PBS with 1% [w/v] non-fat dry milk). The membrane was washed 3× 15 min with 1×PBST prior to viewing with LI-COR Odyssey® Infrared Imaging System (LI-COR, Lincoln, NE, USA). All incubations had slight agitation. Buffer and reagent composition are located in **Table 12**.

2.19 Protein expression and purification

Recombinant proteins were produced using an *E. coli* BL21 (DE3) or Origami B (DE3) expression system. For biotinylation of proteins, the *E. coli* was engineered by bacterial transformation to contain pBirAcm, an IPTG inducible plasmid containing the *birA* gene encoding biotin ligase. Cells were grown aerobically, with shaking, at 37°C in LB

medium with the appropriate antibiotics to OD_{600} = 0.5. For the final constructs, protein expression was induced O/N (18-24 h) at RT with 0.2 mM IPTG (Bio Basic Inc, Markham, ON, Canada) and biotinylated with the addition of 50 μM D-biotin (Bio Basic Inc, Markham, ON, Canada). Cells were pelleted at 4°C, 7000 × *g* for 5 min and resuspended in cold 20 mM Tris-HCl, pH 7.4, 200 mM NaCl (or 1×HEPES Buffer for SAg alone) containing 0.25 mg mL^{-1} lysozyme (Sigma-Aldrich, St. Louis, MO, USA) and 0.02 mg mL^{-1} DNaseI (Sigma-Aldrich, St. Louis, MO, USA). Cells were incubated on ice for 1 h prior to lysis with a continuous head flow cell disruptor (Constant Systems Ltd, Daventry, United Kingdom) at 25 psi, followed by sonication with output 4, using 1 pulse per mL of sample. Cellular debris was pelleted at 4°C, 10 000 × *g* for 10 min. Supernatants were applied to a charged (100 mM $NiSO_4$) Ni-NTA affinity column (Novagen, EMD Millipore, Billerica, MA, USA), washed with buffer and eluted with increasing concentration of imidazole (5 mL each of 15 mM, 30 mM, 60 mM, and 200 mM imidazole in 20 mM Tris-HCl, pH 7.4, 200 mM NaCl or 1×HEPES Buffer). Purified fractions were dialyzed 3× against the respective buffer and the N-terminal tags cleaved by autoinactivation-resistant His_7::TEV (376) as previously described (377) with O/N (18-24 h) incubation at RT. Cleaved proteins were applied and eluted as described from a second Ni-NTA affinity column to remove TEV protease and obtain a pure protein. Proteins were dialyzed 3× against the respective buffer or 0.9% NaCl (saline), assessed for homogeneity and purity by SDS-PAGE, and quantified with Pierce™ BCA Protein Assay Kit (Thermo Fisher Scientific Inc, Waltham, MA, USA) using manufacturer's instructions. In brief, protein aliquots were mixed with the kit formulation, based on bicinchoninic acid (BCA), for colorimetric detection of protein complexes at absorbance 562 nm (Bio-Rad Microplate Reader 680, Bio-Rad Laboratories Inc, Hercules, CA, USA). The protein quantification was reported with reference to a common protein standard, BSA.

2.20 Binding detection of humanized scFv5T4 to 5T4 antigen

HT-29 (1.0×10^6) or transfected HEK293 cells (1.0×10^6) containing either pCMV6-XL5 or pCMV6-XL5::5T4, were incubated for 1 h at RT with either anti-human mAb5T4 (1:200; ab88091, Abcam, Cambridge, United Kingdom) or scFv5T4-biotin (1:100; 2 mg

mL^{-1}), washed with 1×PBS followed by incubation with fluorescein isothiocyanate (FITC) anti-mouse IgG (1:1000; eBioscience, San Diego, CA, USA) or streptavidin-FITC (1:1000; Rockland Immunochemiclas Inc, Pottstown, PA, USA), respectively, for 1 h at 4°C. Cells were washed and either assessed with fluorescence-activated cell sorting (FACS) (BD FACSCanto II, BD Biosciences, Franklin Lakes, NJ, USA) or viewed with fluorescence microscopy (Olympus IX71 Inverted Micropscope, Olympus Canada Inc, Richmond Hill, ON, Canada). For FACS analysis, mouse IgG2bκ isotype control was also included (1:200, eBioscience, San Diego, CA, USA). Alternatively, transfected HEK293 cells were incubated with anti-human mAb5T4 (1:200, Clone EPR5529; Abcam, Cambridge, United Kingdom) in conjunction with scFv5T4-biotin (1:100; 2 mg mL^{-1}), for 1 h at RT, followed by tetramethylrhodamine (TRITC) anti-rabbit IgG (1:1000; Jackson ImmunoResearch Labs, West Grove, PA, USA) and streptavidin-FITC (1:1000; Rockland Immunochemiclas Inc, Pottstown, PA, USA), for 1 h at 4°C, washed and viewed for co-staining by fluorescence microscopy (Olympus IX71 Inverted Microscope, Olympus Canada Inc, Richmond Hill, ON, Canada). Lastly, HEK293 cells, transfected for expression of either pEGFP-N1::5T4 or vehicle pEGFP-N1, were incubated with scFv5T4::mRFP1 (1:100; 2 mg mL^{-1}) for 1 h at RT and subsequently washed and viewed with fluorescence microscopy (Olympus IX71 Inverted Microscope, Olympus Canada Inc, Richmond Hill, ON, Canada). All microscopy images were taken using ImagePro Plus Software (MediaCybernetics, Rockville, MD, USA) and FACS analysis was completed using FlowJo Software (FlowJo, LLC, Ashland, OR, USA). Buffer reagent composition is in **Table 12** and antibodies and dyes are in **Table 14**.

2.21 SpeC-mediated PBMC proliferation

2.21.1 Radioactive proliferation assay

Human PBMCs were isolated and prepared as described. PBMCs (2×10^5) were cultured in cRPMI + 10% FBS containing 2 μg mL^{-1} Polymyxin B (MP Biomedicals, Santa Ana, CA, USA) with titrating SpeC variants (10^{-4}-10^0 μg mL^{-1}), including $SpeC_{WT}$, $SpeC_{Y15A/D203A}$, $SpeC_{D203A}$, or titrating SpeC variants in addition to scFv5T4, scFv5T4::$SpeC_{Y15A/D203A}$ or scFv5T4::$SpeC_{D203A}$ (2×10^{-2} - 2×10^2 nM) in U-bottom

Table 14. Antibodies and dyes used within the study

Antibody or Dye	Clone or Catalog No.	Dilution	Application	Source
7-AAD	A1310	2 µl	FACS	Molecular Probes, Life Technologies
Alexa Fluor® 488 goat anti-rabbit IgG (H+L)	A-11008	1:400-1:1000	IHC	Life Technologies
AlexaFluor700 anti-human CD8	RPA-T8	1:200	FACS	BD Pharmingen
APC anti-human CD3	UCHT1	1:200	FACS	BD Pharmingen
CFSE	C34554	10 µM	FACS	Molecular Probes, Life Technologies
DAPI nuclear stain	B2261	1:1000	IHC	Sigma-Aldrich
FITC rat anti-mouse IgG	11-4011-85	1:1000	FACS/microscopy	eBioscience
mouse anti-human 5T4	ab88091	1:200	FACS/microscopy	Abcam
mouse IgG2bκ Isotype Control	eBMG2b/14-4732-85	1:200	FACS	eBioscience
PE anti-human CD4	RPA-T4	1:200	FACS	BD Pharmingen
rabbit anti-CD3	SP7	1:50	IHC	Abcam
rabbit anti-human 5T4	EPR5529	1:200	FACS/microscopy	Abcam
rabbit anti-Ki67	NB500-170	1:20	IHC	Novus Biologicals
rabbit anti-vWF	A0082	1:400	IHC	Dako
Rhodamine (TRITC) goat anti-rabbit IgG (H+L)	111-025-003	1:1000	FACS/microscopy	Jackson ImmunoResearch Labs
streptavidin-FITC	S000-02	1:1000	FACS/microscopy	Rockland Immunochemicals
streptavidin-IRDye800	S000-32	1:10 000	Western Blot	Rockland Immunochemicals
TACS® 2 TdT In situ FITC Apoptosis Detection Kit	4812-30-K	As per kit	IHC	Trevigen

96-well microplates (BD Biosciences, Franklin Lakes, NJ, USA). Cells were incubated for 72 h and subsequently labeled with ^{3}H-thymidine (PerkinElmer, Waltham, MA, USA) incorporation for 18 h at 37°C with 5% CO_2. Cells were harvested to glass-fiber filters and DNA-incorporated ^{3}H-thymidine was measured in a beta scintillation counter (Wallac 1450 MicroBeta Counter, PerkinElmer, Wallac Oy, Turku, Finland).

2.21.2 CFSE proliferation assay

Human PBMCs were isolated and prepared as described and labeled with CellTrace™ carboxyfluorescein succinimidyl ester (CFSE) Cell Proliferation Kit (carboxyfluorescein diacetate; Molecular Probes®, Life Technologies Inc, Carlsbad, CA, USA) as per manufacturer's instructions. In brief, cells (10×10^6 mL^{-1}) were suspended in pre-warmed RPMI-1640 and labeled with 10 μM CFSE for 10 min in a 37°C water bath, protected from light. To stop the reaction, cold cRPMI + 10% FBS was added to the cells and incubated on ice for 5 min. Cells were pelleted and resuspended for assay. Cells (0.8×10^6-1.0×10^6) were cultured in cRPMI + 10% FBS containing 2 μg mL^{-1} Polymyxin B (MP Biomedicals, Santa Ana, CA, USA) and treated with either $SpeC_{WT}$ or variants $SpeC_{Y15A}$, $SpeC_{D203A}$ or $SpeC_{Y15A/D203A}$ (1 μg mL^{-1}) and incubated for 5 days at 37°C with 5% CO_2 in 5 mL round-bottom polystyrene tubes (BD Falcon™, BD Biosciences, Franklin Lakes, NJ, USA). Cells were then washed with FACS buffer by centrifugation and stained in the dark with anti-human CD3 (1:200), anti-human CD4 (1:200) and anti-human CD8 (1:200) antibodies for 30 min on ice. Cells were washed in FACS buffer, labeling with 7-aminoactinomycin D (7-AAD; 2 μl sample^{-1}) and analyzed by FACS (BD FACSCanto II, BD Biosciences, Franklin Lakes, NJ, USA). FACS analysis was completed using FlowJo Software (FlowJo, LLC, Ashland, OR, USA). Buffer and reagent composition are listed in **Table 12** and antibodies and dyes are listed in **Table 14.**

2.22 SpeC-mediated PBMC cytotoxicity assays

2.22.1 JAM-assay

Cytotoxicity *in vitro* was evaluated using the just another method (JAM)-assay (378) by labeling WiDr cells (2.5×10^4) grown O/N (18-24 h) with ^{3}H-thymidine (PerkinElmer,

Waltham, MA, USA) for 18 h in flat bottom 96-well microplates (BD Biosciences, Franklin Lakes, NJ, USA) at 37°C with 5% CO_2 and incubating with isolated human PBMCs (as described) at an effector:target cell ratio of 10:1 with titrating SAgs (10^0-10^3 ng mL^{-1}) including $SpeC_{WT}$, $SpeC_{Y15A}$, and $SpeC_{D203A}$. Incubation periods in cRPMI + 10% FBS containing 2 µg mL^{-1} Polymyxin B (MP Biomedicals, Santa Ana, CA, USA) were 24, 48, 72, 96 and 168 h to determine time-response. At each time point, supernatants were aspirated, removing PBMCs and any non-adherent (dead) WiDr cells. Remaining live cells were washed with 1×PBS and incubated with 0.05% trypsin-EDTA (Gibco®, Life Technologies Inc, Carlsbad, CA, USA) for 20 min at 37°C with 5% CO_2 and subsequently harvested to glass-fiber filters. Live cells containing DNA-incorporated ^{3}H-thymidine were measured in a beta scintillation counter (Wallac 1450 MicroBeta Counter, PerkinElmer, Wallac Oy, Turku, Finland). The specific apoptosis was calculated according to the formula with counts per minute (CPM) (spontaneous) condition equivalent to WiDr incubated with PBMCs alone:

$$\%\ \text{specific apoptosis} = \frac{\text{CPM(spontaneous)} - \text{CPM(experimental)}}{\text{CPM(spontaneous)}} \times 100\%$$

2.22.2 Flow cytometry

Human PBMCs were co-cultured with either WiDr or HT-29 cells previously grown (24-48 h) on flat well microplates (BD Biosciences, Franklin Lakes, NJ, USA) at a ratio of 10:1 and titrated SpeC variants for 48 h at 37°C with 5% CO_2 in cRPMI + 10% FBS containing 2 µg mL^{-1} Polymyxin B (MP Biomedicals, Santa Ana, CA, USA). Cells were harvested and labeled with 7-AAD following the manufacturer's protocol and analyzed by FACS (BD FACSCanto II, BD Biosciences, Franklin Lakes, NJ, USA). Using FlowJo software, the WiDr or HT-29 populations were gated upon by comparison of human PBMC alone samples and subsequently assessed for presence or absence of 7-AAD. Additional experimentation was repeated as above to further include the cytotoxic potential of scFv5T4::$SpeC_{D203A}$, and controls scFv5T4 and scFv5T4::$SpeC_{Y15A/D203A}$.

2.22.3 ^{51}Cr-release assay

Human PBMCs were treated with SAg, scFv5T4, or fusion proteins as in the FACS assay

for 48 h in U-bottom 96-well microplates (BD Biosciences, Franklin Lakes, NJ, USA) at 37°C with 5% CO_2 in cRPMI + 10% FBS containing 2 μg mL^{-1} Polymyxin B (MP Biomedicals, Santa Ana, CA, USA). Target HT-29 cells were labeled with $(Na)_2{}^{51}CrO_4$ (PerkinElmer, Waltham, MA, USA) in cRPMI + 10% FBS. PBMCs were added at effector:target cell ratios of either 1:1, 5:1 or 10:1 against HT-29. Cytotoxicity was determined after 4–6 h incubation at 37°C with 5% CO_2 in a standard chromium release assay measuring the ^{51}Cr content of culture supernatants using a gamma-counter (Wallac Wizard 1470 Automatic Counter, PerkinElmer, Wallac Oy, Turku, Finland). Total release control was obtained by exposing target cells to 1% SDS (EMD Millipore, Billerica, MA, USA). The specific lysis was calculated according to the formula:

$$\%\ \text{specific lysis} = \frac{\text{experimental release - spontaneous release}}{\text{total release-spontaneous release}} \times 100\%$$

2.23 Mouse housing and breeding

Immunodeficient NOD.Cg-*Prkdc*^{scid} *Il2rgt*^{m1Wjl}/SzJ (NSG) mice were bred and housed in an animal barrier facility (Western University, London, ON, Canada) under sterile conditions with food and water ad libitum.

2.24 TTS *in vivo* tumour-killing model

Twenty-eight NSG mice, male and female, aged 13 weeks were used throughout the experimental timeline. Based on a previously developed protocol (242, 335) mice were injected intraperitoneally (ip) with 3×10^6 HT-29 cells in 0.2 mL vehicle (1×PBS). Three weeks later, once tumours were palpable, the mice were injected ip with either vehicle alone (n=3) or 1×10^6 human PBMCs in 0.2 mL vehicle (1×PBS). Two hours after receiving PBMCs, 2 μM kg^{-1} of treatment, controls, or vehicle alone was injected intravenously (iv). Mice were grouped (n=4), ensuring weight- and sex-match distrubtion (**Appendix 6**), with a random number generator to receive either scFv5T4::$SpeC_{D203A}$, $SpeC_{D203A}$, scFv5T4, scFv5T4::$SpeC_{Y15A/D203A}$, or vehicle alone (saline), however ensuring an even distribution of male and female animals. Mice with no PBMCs received vehicle alone. Intravenous (iv) injections were given daily for 7 additional days. Animals

were monitored and weighed every second day until Day 25 of the experiment (injection of PBMCs), and then daily until end of experiment (Day 60). Primary tumours were measured daily by caliper (height and width) beginning on Day 28 (treatment Day 4) until end of experiment (Day 60). Blood was collected prior to treatment and subsequently drawn once per week after treatment through the saphenous vein. In brief, the animal fur was removed surrounding the vein and Vaseline applied prior to venous puncture, and subsequently collecting drops of whole blood (200 µL total) in a microfuge tube. Blood was processed by centrifugation for 5 min at 3000 × *g* and supernatant collected for serum and stored at -20°C. Four weeks after the final injection, the mice were electively euthanized under anesthetics by exsanguination through cardiac puncture for a terminal blood draw and serum was processed as above. The mice were examined visually for overall tumour burden and macro-metastases were scored accordingly based on the degree of regional spread distant from the primary tumour site. All tumours were excised, size- and weight-measured in a blinded fashion and the total tumour volume was calculated. Tumour-associated organs, along with all livers and spleens were also harvested and all tissues were processed for histological assessment as described. All reagents used are listed in **Table 12**.

2.25 Histology of *in vivo* TTS animal model

2.25.1 Histological tissue processing, embedding, and sectioning

Tissues were fixed in 10% neutralized formalin buffer (BDH, VWR, Radnor, PA, USA) for 48 h at RT, followed by 5× washes with 1×PBS every 12 h with a final wash in 70% ethanol. Tissues were dissected as follows: the primary tumours were dissected longitudinally, dividing the tumour in half, and embedded so that the internal surface was exposed for sectioning. The remaining tumours were dissected on an individual basis, with aim to section both tumour with surrounding normal tissue. Livers were dissected into respective lobes: median, right, left, and caudal, and embedded as separate tissues. Spleens were dissected longitudinally and embedded so that the internal surface was exposed for sectioning. Dissected tissues were placed in Fisherbrand™ TRUFLOW™ Tissue and Biopsy Cassettes (Fisher Scientific, Whitby, ON, Canada), processed using

the ‘brain and bone’ program for paraffin wax treatment in a Leica ASP300 (Leica Biosystems, Nussloch, Germany) at the Molecular Pathology Core Facility (Robarts Research Institute, Western University, London, ON, Canada) and were embedded with proper orientation in paraffin wax. Serial sections (5 μm) of the tissues were cut using MB35 Premier Blades (Thermo Scientific, Waltham, MA, USA) on a Leitz 1512 microtome (Leica Biosystems, Nussloch, Germany) and mounted on Fisherbrand™ Superfrost™ Plus microscope slides (Fisher Scientific, Whitby, ON, Canada). Slides were incubated at 37°C for 48 h and either stored or processed for histological staining. All reagents used are listed in **Table 12**.

2.25.2 Histological staining and immunohistochemistry

Prior to staining or immunohistochemistry (IHC) analysis, sections were deparaffinized and rehydrated using a Leica AutoStainer XL (Leica Biosystems, Concord, ON, Canada) at the Molecular Pathology Core Facility (Robarts Research Institute, Western University, London, ON, Canada). Sections were stained with hematoxylin and eosin (H&E) using a standard protocol within the Leica Autostainer XL (Leica Biosystems, Concord, ON, Canada) and sealed with a coverslip using low-viscosity Richard-Allan Scientific® Cytoseal™ 60 mounting medium (Thermo Scientific, Waltham, MA, USA). For apoptosis detection and IHC staining, all sections of the primary tumours from the TTS treatment group (scFv5T4::SpeC$_{D203A}$) and control group (scFv5T4::SpeC$_{Y15A/D203A}$) were used. Specifically, for apoptosis detection, sections were stained with TACS® 2 TdT *in situ* Fluorescein Apoptosis Detection Kit (Trevigen, Gaithersburg, MD, USA) as per the manufacturer’s protocol. In brief, slides were washed for 2× 10 min in 1×PBS, followed by a 30 min incubation in Cytonin™ permeabilization buffer and a 2× 2 min wash in deionized water. Sections were incubated with 1× terminal deoxynucleotidyl transferase (TdT) labeling buffer for 5 min prior to addition of labeling reaction consisting of TdT dNTP mix, cations (Mg^{2+}, Mn^{2+}, or Co^{2+}), TdT enzyme (TACS-Nuclease™) and TdT labeling buffer, incubated for 60 min at 37°C in a humidified chamber. The reaction was stopped by addition of 1×TdT stop buffer for 5 min. Slides were washed 2× 2 min in PBS followed by 20 min incubation in the dark with Strep-Fluorescein solution. Final washes were 3× 2 min in 1×PBS and slides were mounted with VECTASHIELD® Mounting

Medium with 4',6-diamidino-2-phenylindole (DAPI) (Vector Laboratories, Burlingame, CA, USA) and sealed with a coverslip. Reagent composition is listed in **Table 12**.

Prior to IHC staining, sections were pretreated with Target Retrieval Solution (Dako Canada Inc, Burlington, ON, Canada) for 30 min in pre-warmed solution at 95°C within a water bath. Slides were allowed to cool within the solution for 20 min prior to rinsing 3× with RT TBST buffer. Sections were blocked for 30 min at RT with 10% goat serum in TBST. The following primary antibodies were then incubated for 2 h at RT or O/N (18-20 h) at 4°C on separate sections and slides including, anti-Ki67 (1:20; NB500-170, Novus Biologicals, Littleton, CO, USA), anti-vWF (1:400; A0082 Dako Canada Inc, Burlington, ON, Canada) or anti-CD3 (1:50; Clone SP7, ab16669, Abcam , Cambridge, United Kingdom) in tris-buffered saline (TBS) with 1% goat serum. Each slide had at least one negative control where the primary antibody was omitted and instead incubated with TBS with 1% goat serum. Sections were washed 3× with TBST for 10 min followed by incubation with secondary antibody, Alexa Fluor® 488 goat anti-rabbit IgG (1:1000 in TBST with 1% goat serum; Molecular Probes® Life Technologies Inc, Carlsbad, CA, USA) for 1 h at RT with further washing 3× with TBST for 10 min. Sections were counterstained with DAPI nuclear stain (1:1000, Sigma-Aldrich, St. Louis, MO, USA) in TBST for 5 min at RT. Sections were washed prior to application of anti-fade fluorescence mounting medium (Dako Canada Inc, Burlington, ON, Canada) and sealed with a coverslip. Buffer composition is listed in **Table 12** and antibodies are summarized in **Table 14.**

2.25.3 Histological imaging and evaluation

H&E sections were imaged with an Aperio ScanScope™ (Leica Biosystems, Concord, ON, Canada) for full slide scanning and images taken with Aperio ImageScope Viewing Software (Leica Biosystems, Concord, ON, Canada). Images taken for quantification purposes were captured by random field of view selection in a blinded fashion of one serial section at 400× using an Olympus BX61 fluorescent microscope (Olympus Canada Inc, Richmond Hill, ON, Canada) and analyzed by Image-Pro Plus Software (MediaCybernetics, Rockville, MD, USA). Images for figure representative purposes

were taken using a Zeiss Axio Imager Z1 (Carl Zeiss Canada Ltd, Toronto, ON, Canada) and imaged using Zen 2012 Software (Carl Zeiss Canada Ltd, Toronto, ON, Canada). All images were taken in same field of view with the same exposure time for each fluorescence filter.

IHC and apoptosis stains were quantified in a blinded-fasion by manually counting the positive fluorescence signals on each of the captured 5 high-power field of view images (400×) from each animal per treatment group (n=20) and subsequently averaged or index calculated. More specifically, von Willebrand factor $(vWF)^+$ blood vessels were considered to be a single, countable microvessel when any endothelial cell or cell cluster demonstrated antibody staining and was clearly separated from an adjacent cluster. For the CD3 stain, any cell showing antibody staining was considered to be a single, countable $CD3^+$ cell. For Ki67 and TUNEL, the number of positively stained cells, in addition to the number of DAPI positive cells, per same fields of view, were counted. Indexes (proliferative index and apoptotic score) were defined by dividing the positive stain count by the total number of nuclei in one image and indexes were subsequently averaged from each animal.

2.26 Statistical analysis

Statistical comparisons were performed using an unpaired Student *t* test or by 2-way ANOVA with Bonferroni multiple comparison test (GraphPad Prism Software, La Jolla, CA, USA). Differences were considered significant when $p<0.05$.

CHAPTER 3: RESULTS

3.1 SpeC mutant generation, expression, and protein purification

Prior work indicated that Tyr^{15} was a critical residue for the SpeC SAg to engage the TCR (368), and Asp^{203} was necessary to coordinate a zinc-mediated high-affinity interface with the β-chain of MHC II (**Figure 6B**) (272, 286, 369). Indeed, the single Asp^{203} to Ala mutation in SpeC has been demonstrated to dramatically reduce toxicity in a lethal model of toxic shock syndrome (369).

To supplement the previously generated variants, a double mutant version of SpeC containing both alanine substitutions at Tyr^{15} and Asp^{203} was generated to create a SpeC variant that maintained overall protein structure but was anticipated to be non-functional in eliciting an immune response. *speC*$_{Y15A/D203A}$ was amplified by PCR from a previously generated construct containing *speC*$_{Y15A/D203A}$ (373) where the forward primer used to amplify *speC* lacked the coding region for the 27-amino acid signal peptide (362). The resulting PCR product was cloned into pET-41a::TEV to generate a N-terminal translational fusion with glutathione S-transferase (GST) and His_6 purification tags, cleavable by TEV protease. The resulting genetic product, pET-41a::TEV::*speC*$_{Y15A/D203A}$ followed suit with the other translational genetic constructs **(Figure 7A)** for SpeC protein expression.

To generate and purify SAg proteins, following induced bacterial expression of either wild-type SpeC ($SpeC_{WT}$), $SpeC_{Y15A}$, $SpeC_{D203A}$, or $SpeC_{Y15A/D203A}$, the cell lysate was applied to a nickel resin column and eluted with increasing concentration of imidazole with the desired protein verified at the anticipated molecular weight of 59 kDa (**Figure 7B**). The purification tags were removed with autoinactivation-resistent His_7::TEV as described (368) (**Figure 7C**) and purified SpeC was eluted in low imidazole concentrations. Protein containing fractions were confirmed with the expected 25 kDa size (**Figure 7D**) and after buffer exchange, resulted in purified SpeC protein (**Figure 7E**).

Figure 7. Overview of recombinant SpeC SAg protein expression and purification

A) Schematic representation of a *speC* genetic construct contained within pET-41a for SAg protein expression, including TEV protease cleavable N-terminal purification tags, GST and His_6. Representative protein electrophoresis of typical SpeC purification steps including **B)** separation from crude extract (flow) using Ni^{2+}-affinity gravity chromatography and elution by increasing imidazole concentrations (mM), **C)** tag removal with autoinactivation-resistent His_7::TEV cleavage (368), **D)** separation from TEV protease with Ni^{2+}-affinity gravity chromatography and **E)** final purified SpeC protein. Representative images of coomassie blue stained protein gel electrophoresis of the purification of $SpeC_{Y15A/D203A}$.

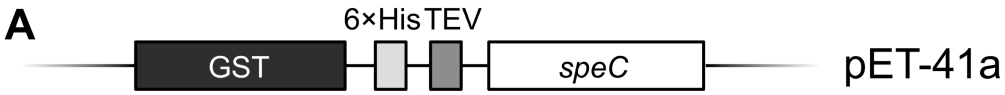
A
6×His TEV
GST
speC
pET-41a

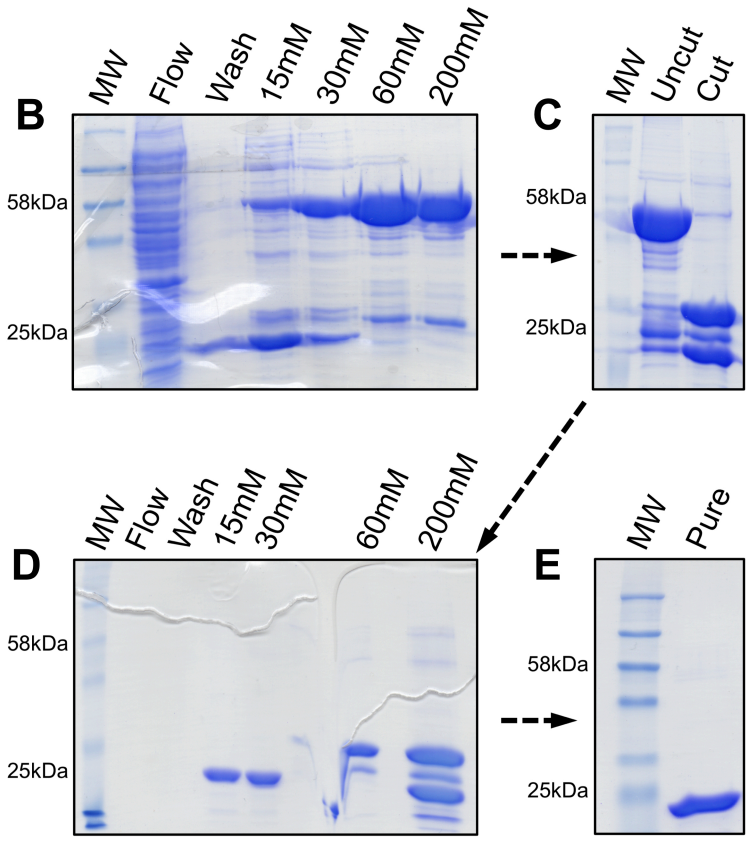
B
MW
Flow
Wash
15mM
30mM
60mM
200mM
58kDa
25kDa
C
MW
Uncut
Cut
58kDa
25kDa
D
MW
Flow
Wash
15mM
30mM
60mM
200mM
58kDa
25kDa
E
MW
Pure
58kDa
25kDa

3.2 SpeC-mediated T cell activation and cytotoxicity evaluation

3.2.1 PBMC proliferation and T cell activation

The ability of $SpeC_{WT}$, $SpeC_{Y15A}$, $SpeC_{D203A}$, and $SpeC_{Y15A/D203A}$ to activate human PBMCs was evaluated. Firstly, activation of human PBMCs was assessed by induction of proliferation by incubation with increasing concentration of SAg. Both $SpeC_{Y15A}$ and $SpeC_{D203A}$ were impaired for the ability to expand PBMCS by >100-fold compared with $SpeC_{WT}$, and the $SpeC_{Y15A/D203A}$ double mutant was unable to induce PBMC proliferation (**Figure 8A**).

Also evaluated was the ability of the recombinant proteins (at 1 μg mL^{-1}) to specifically induce proliferation by measuring generations of dividing cells of human $CD3^+CD4^+$ and $CD3^+CD8^+$ T cell populations using FACS. Based on the dilution of CFSE ($CFSE^{low}$), $SpeC_{WT}$ and each of the single mutants were able to induce proliferation of both T cell subsets, as shown by the increase percent of $CFSE^{low}$, while the double mutant failed to induce proliferation of either subset (**Figure 8B**). The total $CD3^+$ $CFSE^{low}$ population was 21.7% after incubation with $SpeC_{WT}$, 16.0% and 18.9% with $SpeC_{Y15A}$ and $SpeC_{D203A}$ respectively, and 1.0% with $SpeC_{Y15A/D203A}$, comparable to the unstimulated treatment group, with 1.4% $CFSE^{low}$ staining (**Figure 8C**).

3.2.2 PBMC-induced cytotoxicity

The ability of $SpeC_{WT}$ and mutant variants to mediate a cytotoxic PBMC-dependent killing response towards human colon cancer cell line, WiDr, was evaluated *in vitro* by two methods. Firstly, WiDr cells, radiolabeled with ^{3}H-thymidine, were incubated over a 7-day period with human PBMCs and increasing concentrations of SpeC variants WT, Y15A, or D203A. The degree of cytotoxicity against WiDr was measured with a standard JAM-assay (378) . Based on DNA fragmentation that occurs as of one of the hallmarks of apoptosis, in the JAM-assay first reported by Matzinger (378), the intact DNA of viable cells are trapped within the glass fiber filters during cell harvesting, while the DNA of apoptotic cells as fragments are easily washed through the filter. Therefore, detectable radioactivity reflects the amount of intact DNA and remaining viable cells and is

Figure 8. SpeC-mediated T cell activation

A) Proliferation of human PBMCs mediated by $SpeC_{WT}$ or proteins containing mutated residues Y15A (TCR-binding mutant), D203A (MHC II-binding mutant) or Y15A/D203A was determined by the uptake of ^{3}H-thymidine after 72 h post-stimulation (n=4 in triplicate; data representative of one individual). **B-C)** Proliferation of CFSE labeled-human PBMCs mediated by $SpeC_{WT}$ or proteins containing mutated residues was determined by FACS five days post-stimulation, specifically measuring total $CD3^{+}$ T cell population, $CD3^{+}CD4^{+}$ T cells and, $CD3^{+}CD8^{+}$ T cells. Data shown (mean ± SEM) is from four independent human donors (n=4; FACS data representative of one individual).

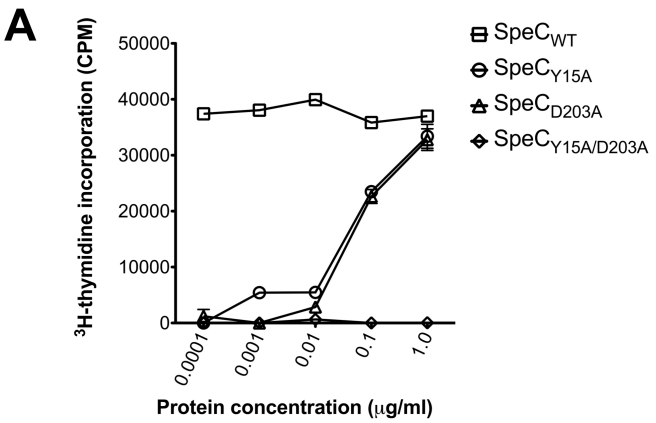
A
^{3}H-thymidine incorporation (CPM)
50000
40000
30000
20000
10000
0
0.0001
0.001
0.01
0.1
1.0
Protein concentration (μg/ml)
SpeC$_{WT}$
SpeC$_{Y15A}$
SpeC$_{D203A}$
SpeC$_{Y15A/D203A}$

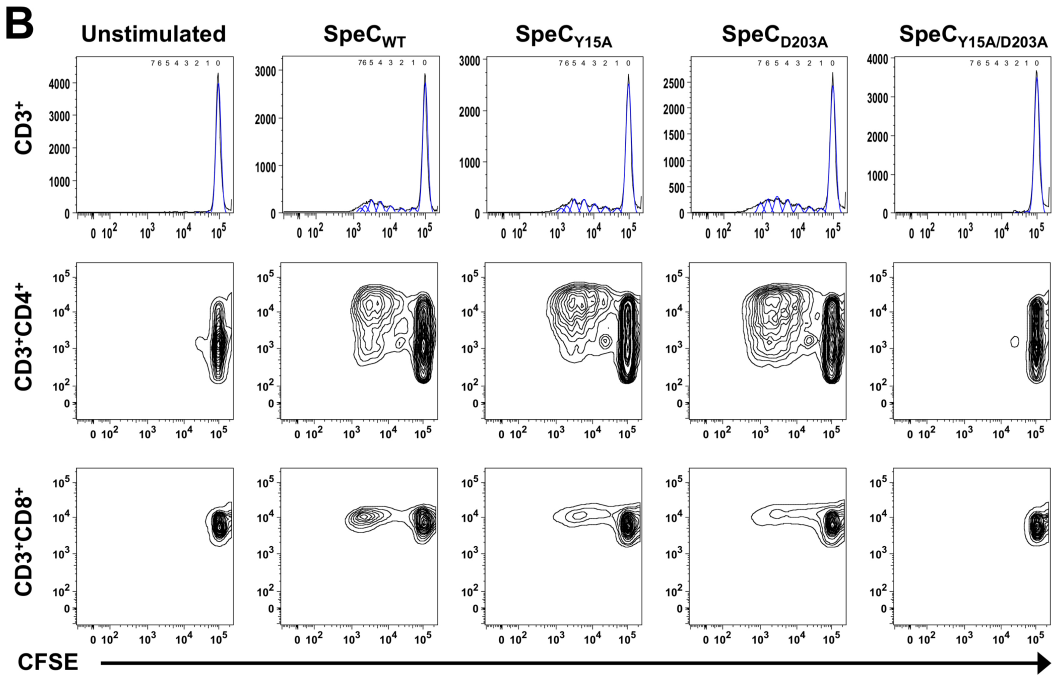
B
Unstimulated
SpeC$_{WT}$
SpeC$_{Y15A}$
SpeC$_{D203A}$
SpeC$_{Y15A/D203A}$
CD3$^+$
CD3$^+$CD4$^+$
CD3$^+$CD8$^+$
CFSE

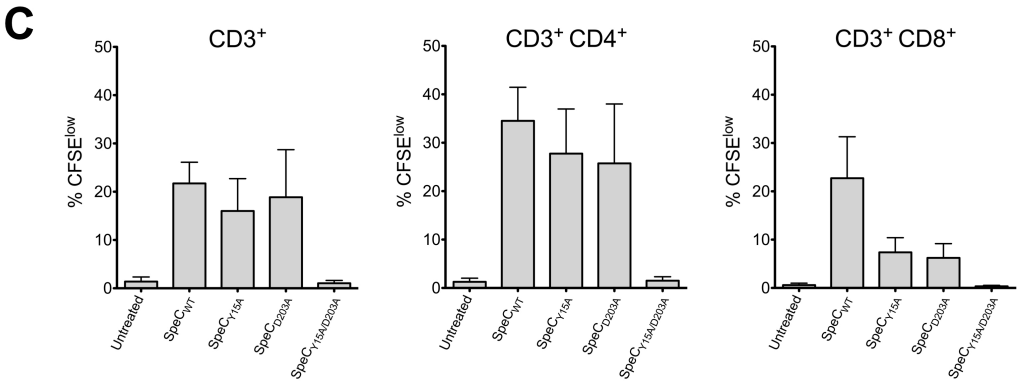
C
CD3$^+$
CD3$^+$ CD4$^+$
CD3$^+$ CD8$^+$
% CFSE^{low}
Untreated
SpeC$_{WT}$
SpeC$_{Y15A}$
SpeC$_{D203A}$
SpeC$_{Y15A/D203A}$

correlated to the degree of cellular death (percent apoptosis) (378, 379). Cellular death was demonstrated in both a time- and dose-dependent manner (**Figure 9A**). After 24 h incubation, there was an evident dose-dependent increase in percent apoptosis with treatment of $SpeC_{WT}$, however not with the either of the mutant variants. The cytotoxiceffect mediated by $SpeC_{WT}$ was more profound after 48 h and could also begin to be noted with the higher concentrations of $SpeC_{Y15A}$ and $SpeC_{D203A}$, although the cytotoxic response appeared dampened considerably compared to $SpeC_{WT}$. This trend was evident throughout the experimental time course and even 168 h (7 days) post-incubation, mutant versions were revealed to display hindered PBMC cytotoxic affects towards WiDr cells, with the exception at the highest used concentration. Based on the JAM-assay results, subsequent killing assays were performed with a 48 h period of PBMC stimulation.

Secondly, to assess the degree of cytotoxicity further, WiDr cancer cells were co-cultured with human PBMCs and increasing concentration of either SpeC variants WT, Y15A, D203A, or Y15A/D203A and analyzed by FACS (**Figure 9B**). After 48 h incubation, all cells were harvested and stained with 7-AAD, a dye that intercalates with DNA to form a fluorescent complex, however is generally excluded from the intact membrane of live cells in order to measure cell death. Within the WiDr cell population, $SpeC_{Y15A}$ caused a significant reduction in WiDr cytotoxicity compared with $SpeC_{WT}$, and both the $SpeC_{D203A}$ and $SpeC_{Y15A/D203A}$ mutants failed to induce WiDr cytotoxicity (**Figure 9B**).

These data, including proliferation and cytotoxicity, indicated that TCR and MHC II engagement are important for induction of immune cell-mediated killing by $SpeC_{WT}$, and that $SpeC_{D203A}$ may be a suitable mutant to reduce or prevent systemic immune cell activation while maintaining full engagement with the TCR.

3.3 Development of genetic constructs and expression of murine scFv5T4 proteins

In order to develop a specific targeting mechanism for $SpeC_{D203A}$, a single chain variable fragment (scFv) from the characterized mouse scFv (729 bp) specific for the human 5T4 TAA (243) was generated (scFv5T4) (372). This construct, as well as the genetically

Figure 9. Cytotoxicity potential of human PBMC mediated by $SpeC_{WT}$ and SpeC mutants

A) Dose- and time-dependent manner of cytotoxicity directed against human colon cancer cell line (WiDr) elicited by $SpeC_{WT}$ (black), $SpeC_{Y15A}$ (white), and $SpeC_{D203A}$ (grey). Incorporation of ^{3}H-thymidine was used to assess the specific apoptosis (%) of cancer cells in JAM-assay. Data representative of one human PBMC donor. **B)** Dose-dependent cytotoxicity of 7-AAD^{+} WiDr cells measured by FACS after 48 h incubation with human PBMCs and either $SpeC_{WT}$, $SpeC_{Y15A}$, $SpeC_{D203A}$, or $SpeC_{Y15A/D203A}$ (n=3–6 per group represented as mean ± SEM. *$p<0.05$, **$p<0.01$, ***$p<0.001$, compared to $SpeC_{WT}$).

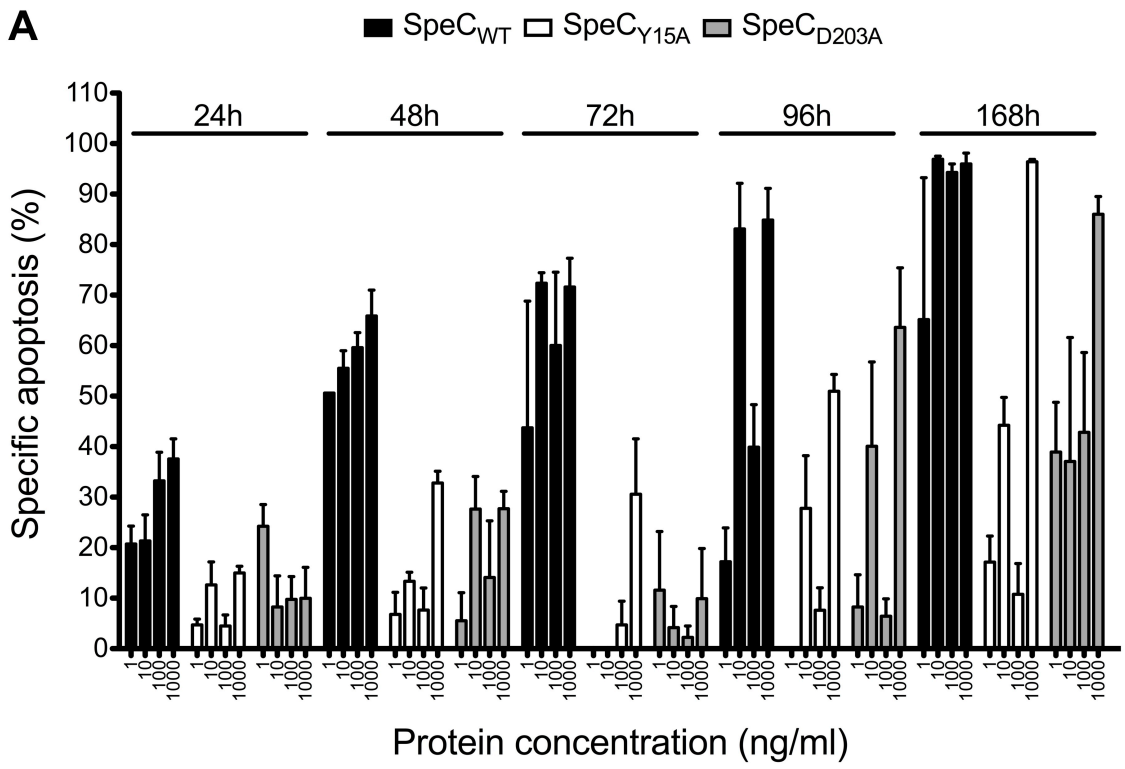
A
SpeC$_{WT}$
SpeC$_{Y15A}$
SpeC$_{D203A}$
24h
48h
72h
96h
168h
Specific apoptosis (%)
Protein concentration (ng/ml)

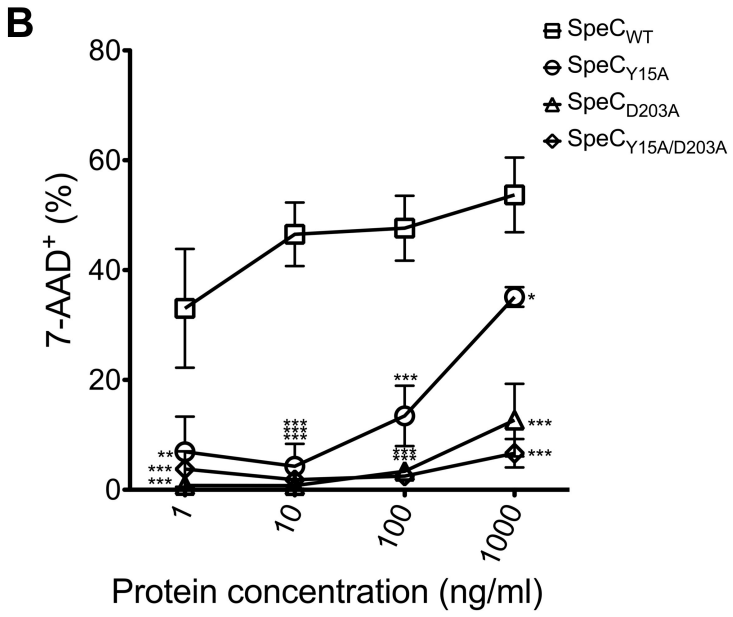
B
SpeC$_{WT}$
SpeC$_{Y15A}$
SpeC$_{D203A}$
SpeC$_{Y15A/D203A}$
7-AAD$^+$ (%)
Protein concentration (ng/ml)

linked (gly-gly-pro) *speC*$_{D203A}$ or *speC*$_{Y15A/D203A,}$ was cloned into pET-41a and pET-28a (373) **(Figure 10A)**. However, these proteins proved difficult for successful protein production within the *E. coli* BL21 (DE3) system. In this study, attempts were taken to improve on the overall protein yield. This involved the optimization of induction time and temperature throughout expression, concentration of the inducer (IPTG), and enhancements on the subsequent purification steps, including the analysis of a variety of diverse buffer compositions to increase solubility. Despite these efforts, the overall expression of soluble proteins containing scFv5T4 resulted in poor production with low protein yield. Efforts to increase purification yield from the soluble fraction, including use of various columns with high performance liquid chromatography (HPLC), although robust, did not result in an improved yield of protein product (data not shown).

To enhance the sensitivity and protein capture within the purification methods, the high affinity and specific interaction between biotin and (strept)avidin molecules was applied to the development of the construct. This peptide tag system has been well established and is commonly developed for the basis of molecular biology products for detection and purification of proteins (380-383). As such, this technology was applied to the pET-28a system with aims to increase protein yield by use of this strong interaction as a purification tag, as well as to develop a more rigorous protein detection method. For the *in vivo* enzymatic biotinylation of the protein, the genetic constructs were designed to include a unique 15 amino acid peptide sequence (AviTag™ Technology, Avidity) that is specifically recognized by the BirA enzyme for the addition of biotin onto the specified peptide sequence (biotin tag). For the addition of the biotin tag to existing genetic constructs, a reverse primer containing the specific sequence along with a TEV protease cleavage sequence site was used. The resulting PCR product was cloned intermediately into pBluescript II SK+ and subsequently into pET-28a, creating a TEV protease cleavable C-terminal translational fusion of the biotinylation peptide tag with *scFv5t4* genetically linked *speC* variants. Similar to the previous translational protein expression plasmids, the resulting constructs were pET-28a::*scFv5t4*::*speC*$_{Y15A/D203A}$::TEV::biotin, and pET-28a::*scFv5t4*::*speC*$_{D203A}$:TEV::biotin (**Figure 10B; Table 11**). The *E. coli* BL21 (DE3) clones were further engineered to co-express pBirA, an IPTG inducible plasmid

Figure 10. Genetic construct development for expression of soluble recombinant fusion protein

Schematic illustrations representing the stepwise development of constructs containing a murine scFv targeted toward human 5T4 (scFv5T4) (243) genetically fused to $SpeC_{D203A}$ via gly-gly-pro linker **A)** cloned within pET-28a protein expression vector containing N-terminal thrombin (Thr) cleavable 6×His purification tag and **B)** genetically altered to remove 6×His and addition of C-terminal TEV cleavable biotin tag for enzymatic biotinylation. Codon-optimized version of murine scFv5T4 (grey bar) cloned within **C)** pET-28a construct containing the C-terminal biotin tag and **D)** pET-32a expression vector for addition of N-terminal EK cleavable TrxA and 6×His tag.

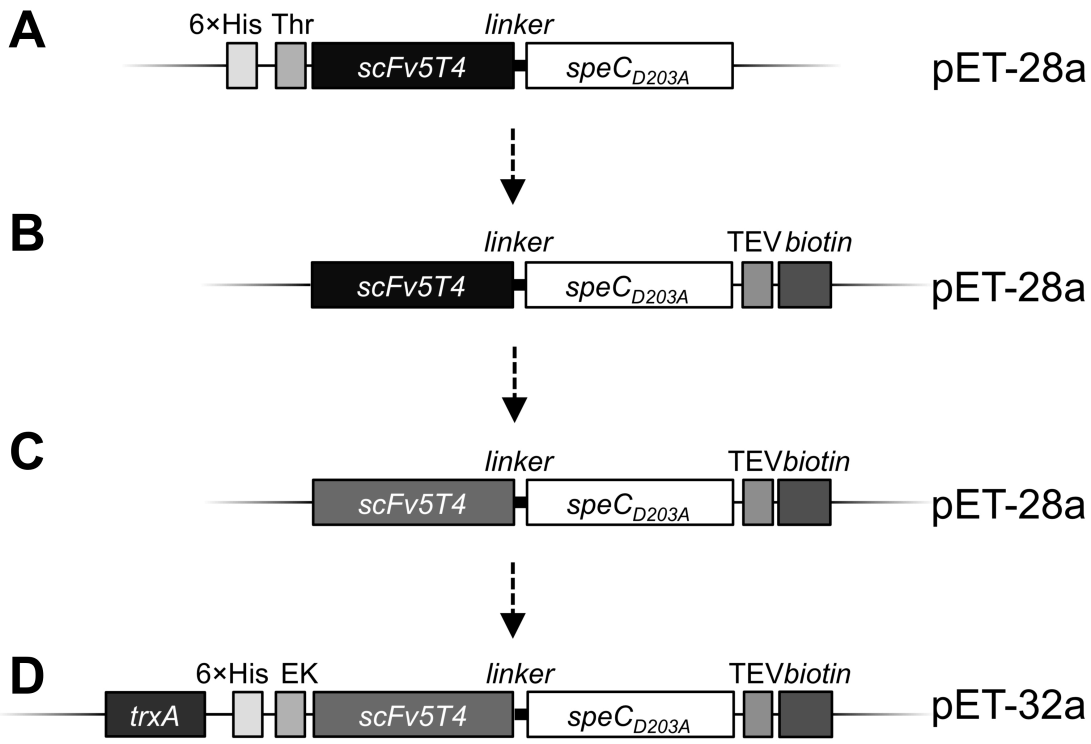
A
6×His Thr
linker
scFv5T4
speC D203A
pET-28a
B
linker
TEV biotin
scFv5T4
speC D203A
pET-28a
C
linker
TEV biotin
scFv5T4
speC D203A
pET-28a
D
6×His EK
linker
TEV biotin
trxA
scFv5T4
speC D203A
pET-32a

containing the BirA gene for protein biotinylation. Upon protein induction, similar to the original design, these constructs did not result in sufficient expression of soluble protein, however the *in vivo* biotinylation of the protein proved successful and aided in the detection sensitivity of the expressed constructs (data not shown). Conversely however, the attempted purification methods utilizing the biotinylated tag were not advantageous to the overall yield of the protein. From these results and after pellet solubilization in 8 M urea, it was determined with that upon targeted gene overexpression in *E. coli*, the proteins formed intracellular, insoluble protein within aggregates, termed inclusion bodies. While the particular optimization completed within this study for inclusion body isolation, purification, protein denaturation, and refolding proved successful from previous constructs mentioned, the concentration yield was low and the success rate for obtaining its native structure was particularly difficult to determine for regaining full biological activity. This method was overall inefficient to obtain adequate protein for proper therapeutic assessment.

For further development of the immunotherapeutic, it was perceived that occasionally in the recombinant protein *E. coli* expression system, low levels of soluble protein expression can occur, despite the use of strong transcriptional and translational signals. It has been noted that this may be due to the mRNA codon usage of the heterologous protein (384-386). Each organism has a preference for codons that are recognized (major codons) whereas those not preferentially used (rare codons) and forced high-level expression of proteins can deplete the pool of rare tRNAs. As a result, this can stall translation, decrease mRNA stability, and can potentially inhibit protein synthesis by generating genetic frame-shifts, deletions, misincorporations, and premature termination of transcription or translation. Within the murine sequence of scFv5T4, 16 rare codons of *E. coli* were noted (7%) (386). The scFv5T4 containing constructs were co-expressed with the genes encoding for a number of the rare codon tRNAs within BL21 (DE3) CodonPlus-RIL cells (Stratagene, La Jolla, California, USA) reducing the number of rare codons to 11 (5%), however no difference in protein expression level was noted (data not shown). Furthermore, the murine *scFv5t4* gene sequence was codon optimized for *E. coli* and synthesized, and subsequently cloned within the pET-28a system (**Figure 10C;**

Table 11). However, the expression of soluble protein remained low from the codon optimized *scFv5t4* gene (data not shown).

Efforts were subsequently focused on increasing protein solubility, with results monitored through protein biotinylation. Firstly, a common approach to address solubility issues is to fuse the target protein with a highly soluble carrier protein (380). TrxA has been widely used as such (380, 387-389), including scFv constructs (390, 391). Secondly, to encourage maintenance of overall protein structure for solubility, the disulfide bridges contained within scFv5T4 require a proper folding environment. To generate a construct conducive to these considerations, the codon optimized *scFv5t4* and genetically linked *speC* constructs were cloned into the pET-32a, a protein expression vector containing EK cleavable N-terminal TrxA and His_6 tags, and transformed into both *E. coli* BL21 (DE3) as well as *E. coli* Origami B (DE3), an *E. coli* designed to improve disulfide bond-dependent protein folding. The resulting genetic products were pET-32a::*scFv5t4*::TEV::biotin, pET-32a::*scFv5t4*::*speC*$_{Y15A/D203A}$:TEV::biotin, and pET-32a::*scFv5t4*::*speC*$_{D203A}$:TEV::biotin (**Figure 10D; Table 11**). The *E. coli* was also engineered to contain pBirAcm for *in vivo* biotinylation of each protein construct. All experimental attempts to optimize and increase soluble protein yield, such as those previously mentioned, were assessed. Through all of the efforts, it was clear that sufficient protein yield of the murine scFv5T4, as a soluble product, continued and still remains a challenge within this field.

3.4 Development and generation of humanized 5T4-targeting scFv

In this work, the generated murine scFv5T4 constructs proved to be a challenge for purification, therefore, with aims to advance the specific targeting mechanism for $SpeC_{D203A}$, a humanized scFv specifically targeted for human 5T4 was designed and generated. This construct should be beneficial as a therapeutic with a reduction in the overall HAMA immunological response. Based on the amino acid sequence of the backbone structure and from preliminary work conducted (data not shown), it was predicted that human recombinant scFv proteins would be readily produced in soluble form. The cDNA sequence was designed to incorporate a ‘humanized’ backbone

sequence, with the CDRs remaining specific for human 5T4. The CDRs were designed from the characterized mouse scFv specific for the human 5T4 TAA (243), formerly used within this study. Amino acid substitutions were determined by aligning the previously described mouse scFv5T4 with 10 human scFv sequences to generate a consensus sequence of the V_H and V_L regions of the antibody and subsequently linking the Fv with a general peptide linker (**Figure 11**). The CDR loops specific for 5T4, and the immediate amino acids flanking the predicted loops were not altered to maintain antibody structure and specificity, predicted from topological modeling. This cDNA sequence was codon optimized for *E. coli* (**Figure 12A**), synthesized, and was subsequently used for the generation of a number of recombinant proteins (**Table 11**). The final amino acid sequence for the translated protein is found in **Figure 12B**. All subsequent results were generated using the humanized scFv5T4. Based on former experience of the murine scFv5T4 protein expression, the humanized scFv5T4 was directly inserted into the pET-32a protein expression system for genetic fusion with TrxA to increase protein solubility. The resulting genetic product was pET-32a::*scFv5t4*::TEV::biotin (**Figure 13A**), containing N-terminal EK cleavable TrxA and His_6 tags and a C-terminal TEV cleavable biotin tag for *in vivo* enzymatic biotinylation. The humanized scFv5T4 construct was transformed and overexpressed as a soluble protein from BL21 (DE3) and Origami B (DE3), both engineered to express BirA. The final protein, cartoon depicted (**Figure 13B**), was purified with the His_6 tag, and subsequently cleaved for removal of the N-terminal tags then dialyzed, generating a pure, biotinylated humanized scFv5T4 protein of anticipated 27 kDa size. A cartoon ribbon diagram depicts the predicted location and structure of the generated 5T4-specific CDR loops of each of the Fv regions (**Figure 13C**). The humanized scFv5T4, when fused with TrxA within the *E. coli* recombinant expression system, was successfully producced and purified as a highly soluble protein.

3.5 Engineered human scFv5T4 specifically targets the 5T4 tumour-associated antigen

To examine the specificity of the humanized scFv5T4 for binding to human 5T4, the scFv5T4 was either engineered with a biotinylated C-terminal biotin tag, to be detected with streptavidin conjugated fluorescence reagents or genetically fused to monomeric red

Figure 11. Humanized scFv5T4 sequence generation

Multiple sequence alignment of human scFv proteins (n=10) compared to murine anti-human 5T4 scFv. Conserved amino acids (dark grey) generate a consensus human backbone sequence shown below the alignment. CDR loops and the linker are labeled above their predicted regions. All sequences were taken from NCBI Protein Database (www.ncbi.nlm.nih.gov/protein) and analyzed using MacVector. References to human scFv proteins are found in the **Appendix 8.**

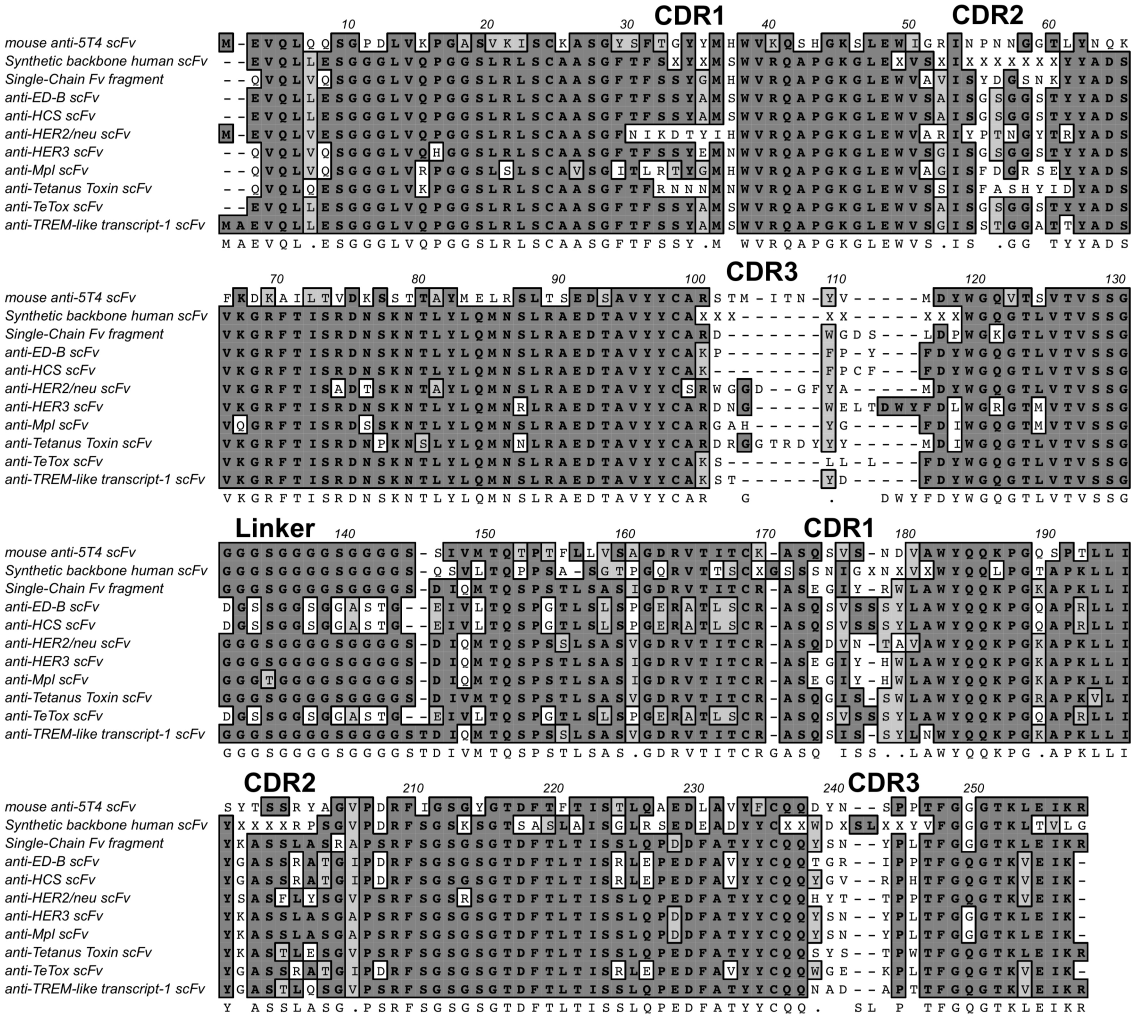
CDR1
CDR2
CDR3
Linker
CDR1
CDR2
CDR3
mouse anti-5T4 scFv
Synthetic backbone human scFv
Single-Chain Fv fragment
anti-ED-B scFv
anti-HCS scFv
anti-HER2/neu scFv
anti-HER3 scFv
anti-Mpl scFv
anti-Tetanus Toxin scFv
anti-TeTox scFv
anti-TREM-like transcript-1 scFv

Figure 12. cDNA and amino acid sequence of humanized scFv5T4

A) Generated DNA sequence of the consensus human scFv backbone with maintained human 5T4-targeting CDRs and **B)** translated amino acid sequence. scFv was constructed as V_H-linker-V_L with polylinker denoted in bold.

A

GAA GTG CAG CTG GTT GAA AGC GGC GGT GGC CTG GTG CAG CCG
GGT GGC TCT CTG CGT CTG AGT TGC GCG GCC AGC GGT TTT ACC
TTC ACG GGC TAT TAC ATG CAT TGG GTG CGT CAG GCA CCG GGT
AAA GGT CTG GAA TGG GTT GGT CGC ATT AAC CCG AAC AAT GGT
GGC ACC CTG TAT GCA GAT AGC GTT AAA GGC CGT TTT ACC ATC
TCT CGC GAT AAC AGT AAA AAT ACG CTG TAC CTG CAG ATG AAC
AGC CTG CGT GCA GAA GAT ACC GCG GTG TAT TAC TGC GCA CGC
TCT ACC ATG ATC ACG AAC TAC GTT ATG GAT TAC TGG GGC CAG
GGT ACC CTG GTG ACG GTT AGC TCT GGT GGC GGT GGC AGC GGT
GGC GGT GGC TCT GGT GGC GGT GGC TCT GAT ATT GTG ATG ACC
CAG AGC CCG TCT ACG CTG AGT GCA AGC GTG GGT GAT CGT GTT
ACC ATC ACG TGT CGC GCC TCT CAG AGT GTG AGC AAC GAT GTT
GCA TGG TAT CAG CAG AAA CCG GGT AAA GCG CCG AAA CTG CTG
ATT TAT TAC ACC AGT AGC CGT TAC GCG GGC GTT CCG AGC CGC
TTT TCT GGC AGT GGT AGC GGC ACC GAT TTC ACC CTG ACG ATC
TCT AGT CTG CAG CCG GAA GAT TTT GCC ACG TAT TAC TGT CAG
CAG GAT TAT AAT AGT CCG CCG ACC TTC GGT CAG GGC ACG AAA
CTG GAA ATC AAA

B

EVQLVESGGGLVQPGGSLRLSCAASGFTFTGYYMHWVRQAPGKGLEWVGRINPNNGG
TLYADSVKGRFTISRDNSKNTLYLQMNSLRAEDTAVYYCARSTMITNYVMDYWGQGT
LVTVSS**GGGGSGGGGSGGGG**SDIVMTQSPSTLSASVGDRVTITCRASQSVSNDVAWY
QQKPGKAPKLLIYYTSSRYAGVPSRFSGSGSGTDFTLTISSLQPEDFATYYCQQDYN
SPPTFGQGTKLEIK

Figure 13. Humanized 5T4-targeting scFv constructs and predicted structure

A) Schematic illustration of genetic construct for expression of humanized scFv5T4 within pET-32a, containing an N-terminal TEV cleavable TrxA and 6×His tags and C-terminal EK cleavable biotin tag for enzymatic biotinylation. **B)** Schematic representation of purified scFv5T4 protein (grey) containing biotinylated C-terminal tag (green) and **C)** cartoon representation of predicted humanized scFv5T4 structure (grey) containing V_H and V_L regions fused with a polylinker. Structure modeled from human 80R scFv (PDB 2GHW22) (375) with 75.9 sequence identity using SWISS-MODEL (www.swissmodel.expasy.org). 5T4-targeting CDR loops of each fragment are coloured as follows: CDR1, *red*; CDR2, *blue*; CDR3, *magenta.*

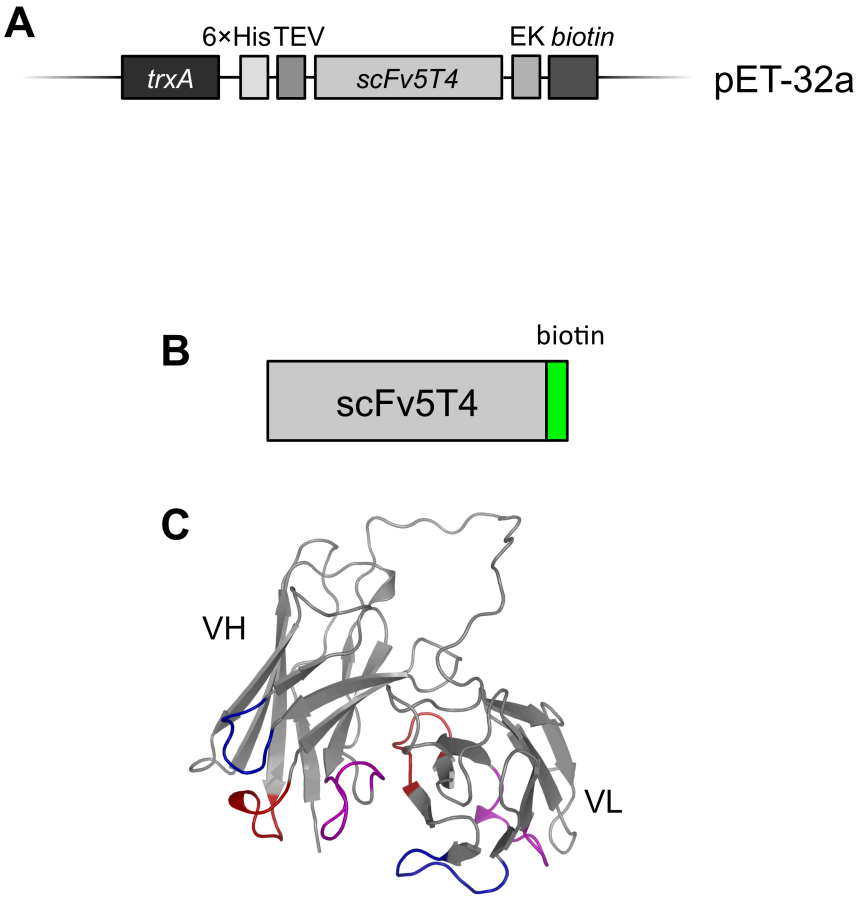
A
6×His TEV
EK biotin
trxA
scFv5T4
pET-32a
B
biotin
scFv5T4
C
VH
VL

fluorescent protein 1 (mRFP1) (392). Upon incubation with the human HT-29 colon cancer cells known to express 5T4 (**Appendix 7**) (194, 224), from which WiDr cells are also derived (393), scFv5T4 bound to the surface of these cells comparable to commercial anti-human 5T4 mAb (mAb5T4) (**Figure 14A**). Furthermore, both mAb5T4, as well as the scFv5T4 fragment, bound to HEK293 cells engineered to express the 5T4 antigen by transfection with pCMV6-XL5::*5t4* as shown by FACS and immunofluorescence microscopy, whereas control HEK293 cells that contain only the vector (pCMV6-XL5) did not stain with either antibody (**Figure 14B-C**).

The scFv5T4 targeting for 5T4 was also determined by co-incubation of scFv5T4 and mAb5T4 with HEK293 cells engineered to express 5T4 and resulted in the same cells binding both antibodies (**Figure 15A**). Lastly, specificity for 5T4 was verified with HEK293 cells transfected with pEGFP-N1::5T4, or control vector pEGFP-N1. Microscopic analysis of GFP::5T4-expressing HEK293 cells demonstrated that scFv5T4 bound only to those cells expressing the 5T4::GFP fusion, but not to control transfected cells (**Figure 15B**). Together, these data indicate that the humanized scFv5T4 can bind specifically to human 5T4.

3.6 Generation of scFv5T4::SpeC$_{D203A}$

In order to target SpeC to 5T4, SpeC was genetically fused with a small flexible linker (Gly-Gly-Pro) to the humanized scFv5T4 resulting in recombinant scFv5T4::SpeC$_{D203A}$. For soluble protein expression, similar to the scFv5T4 alone, the fusion scFv5T4::SpeC$_{D203A}$ construct was cloned into the pET-32a protein expression system creating an N-terminal translational fusion of TrxA and His$_6$ purification tags with a C-terminal translational biotin tag. For all of the final construct designs, including the scFv5T4 and non-functional fusion protein containing SpeC$_{Y15A/D203A}$, the pET-32a vector was altered as such that the EK cleavage site (DDDDK↓X), was replaced with a TEV protease cleavage site (ENLYFQ↓S) (368) and the C-terminal biotin tag (AviTag™, Avidity) containing a 5' gly-gly spacer was engineered to include an EK cleavage site (**Figure 16A-B**; **Table 11**). Constructs were transformed into either *E. coli* BL21 (DE3) or Origami B (DE3), both engineered to co-express pBirAcm for biotinylation. No

Figure 14. Human 5T4-targeting of scFv5T4

A-B) Histograms demonstrating surface binding of the indicated antibodies, either commercial mAb5T4 or scFv5T4 (empty curves) to **A)** colon cancer cell line HT-29 and **B)** HEK293 cells transfected with pCMV6-XL5 or pCMV6-XL5::5T4 measured by FACS. The shaded curves show the IgG2b isotype control (top panels) or streptavidin-FITC alone (bottom panels). Inlays represent dot plots of histogram. **C)** Visualization of commercial mAb5T4, or generated scFv5T4, targeting of HEK293 cells transfected with vehicle control (pCMV6-XL5) or pCMV6-XL5::5T4 by fluorescence microscopy. Representative images taken at 400× magnification.

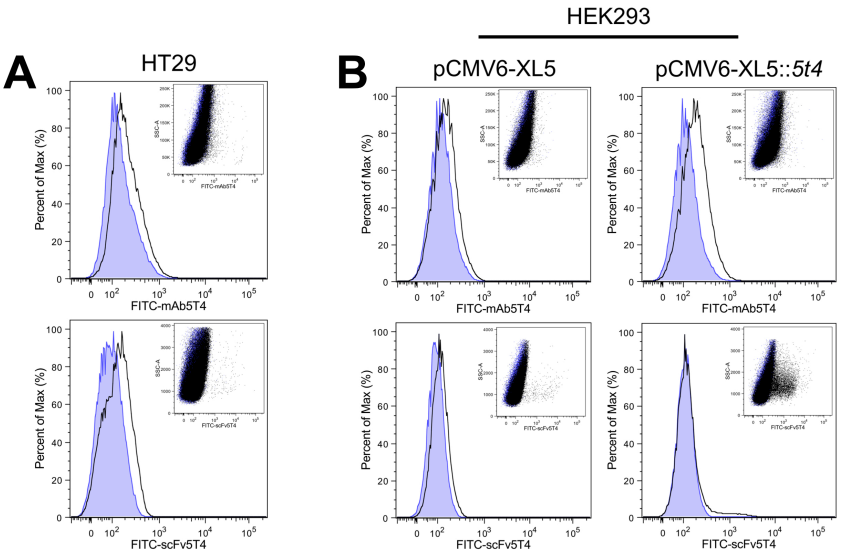
A
HT29
B
HEK293
pCMV6-XL5
pCMV6-XL5::5t4
Percent of Max (%)
FITC-mAb5T4
FITC-scFv5T4

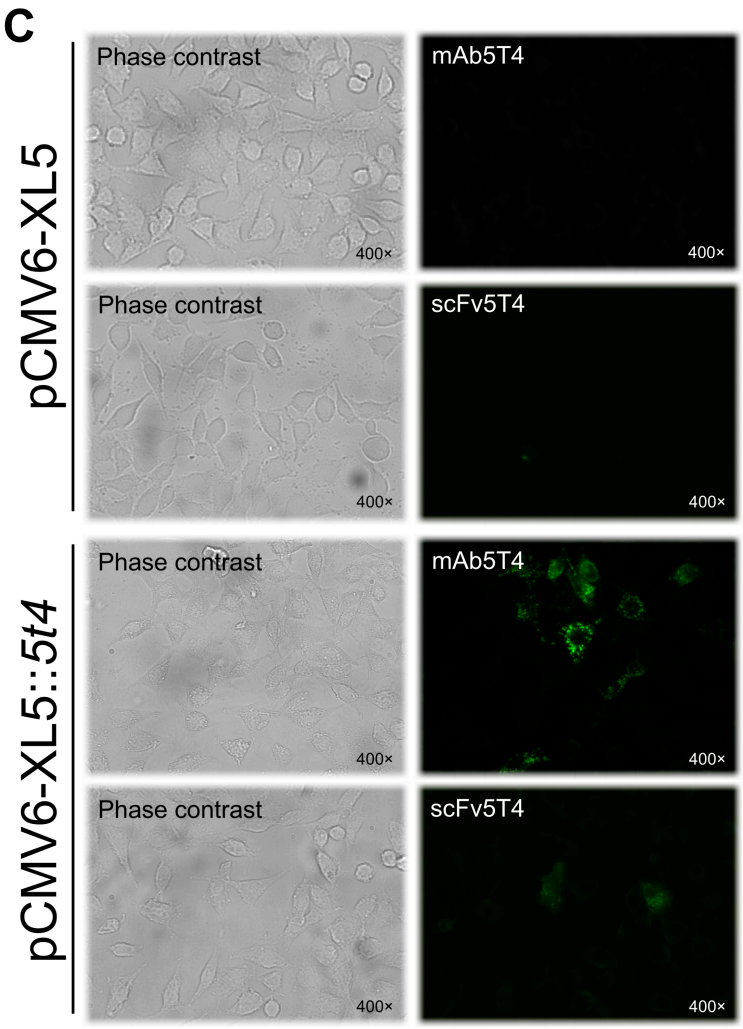
C
pCMV6-XL5
pCMV6-XL5::5t4
Phase contrast
mAb5T4
scFv5T4
400×

Figure 15. Specific human 5T4-targeting of scFv5T4

Visualization of HEK293 transfected with **A)** vehicle control (pCMV6-XL5) or pCMV6-XL5::5T4 co-stained with commercial mAb5T4 (red; TRITC) and scFv5T4 (green; FITC) and **B)** pEGFP-N1 or pEGFP-N1::5T4 and incubated with recombinant scFv5T4::mRFP1. Same field of view photographs were taken under phase contrast, and green and red fluorescent filters at 100× or 400× magnification.

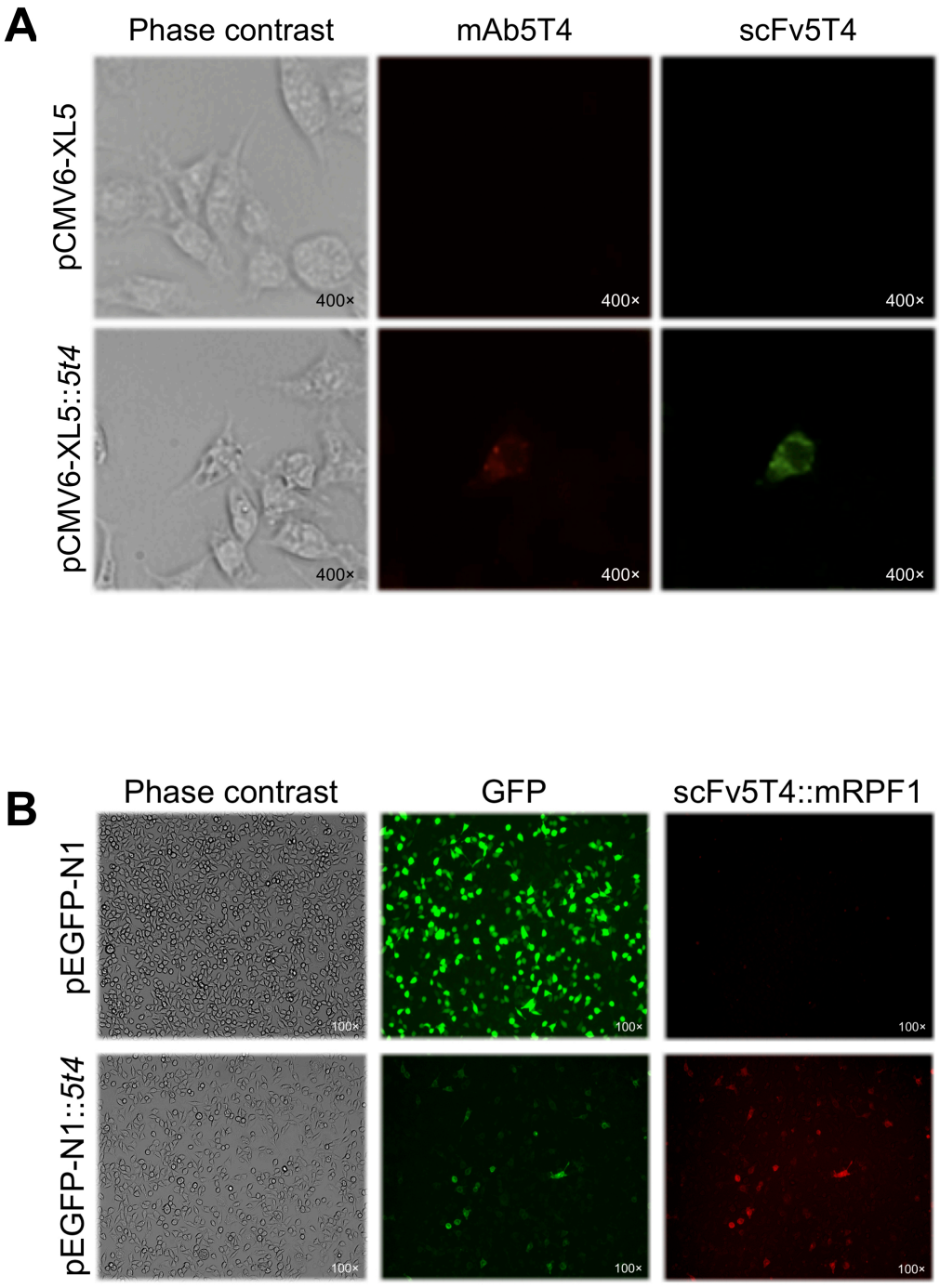
A
Phase contrast
mAb5T4
scFv5T4
pCMV6-XL5
pCMV6-XL5::5t4
400×
B
Phase contrast
GFP
scFv5T4::mRPF1
pEGFP-N1
pEGFP-N1::5t4
100×

Figure 16. Schematic illustration and predicted protein structure of scFv5T4::SpeC$_{D203A}$ fusion protein and control reagent

Schematic illustration representing the final genetic constructs for the expression of fusion proteins **A)** scFv5T4::SpeC$_{D203A}$ and **B)** control reagent, scFv5T4::SpeC$_{Y15A/D203A}$. The genetic constructs are generated within pET-32a containing N-terminal TEV cleavable TrxA and 6×His tags and C-terminal EK cleavable biotin tag for enzymatic biotinylation. Cartoon representation and illustrations of humanized scFv5T4 (grey), genetically fused by a gly-gly-pro linker to SpeC (blue) either containing **C)** an alanine substitution at residue D203 or **D)** an additional alanine substitution at residue Y15. **E-F)** Fusion structures modeled from human 80R scFv (375) (PDB 2GHW) with 75.9 sequence identity using SWISS-MODEL (swissmodel.expasy.org) and SpeC-TCR (285) (PDB code 1KTK). Residues are coloured orange and 5T4-targeting CDR loops of each V_H and V_L fragments are coloured red. All constructs were generated to contain a C-terminal biotin tag (green).

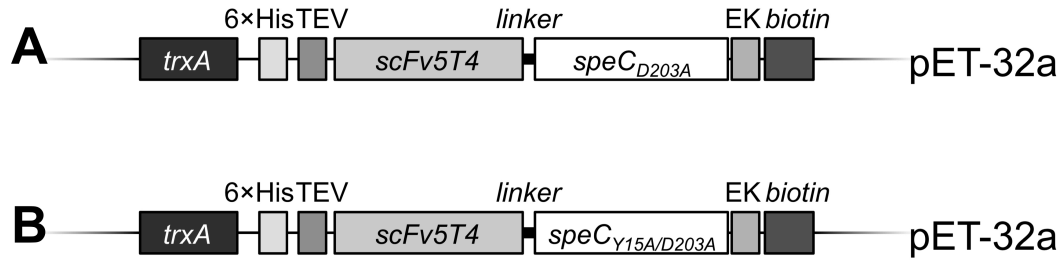
A
6×HisTEV
linker
EK biotin
trxA
scFv5T4
speC D203A
pET-32a
B
6×HisTEV
linker
EK biotin
trxA
scFv5T4
speC Y15A/D203A
pET-32a

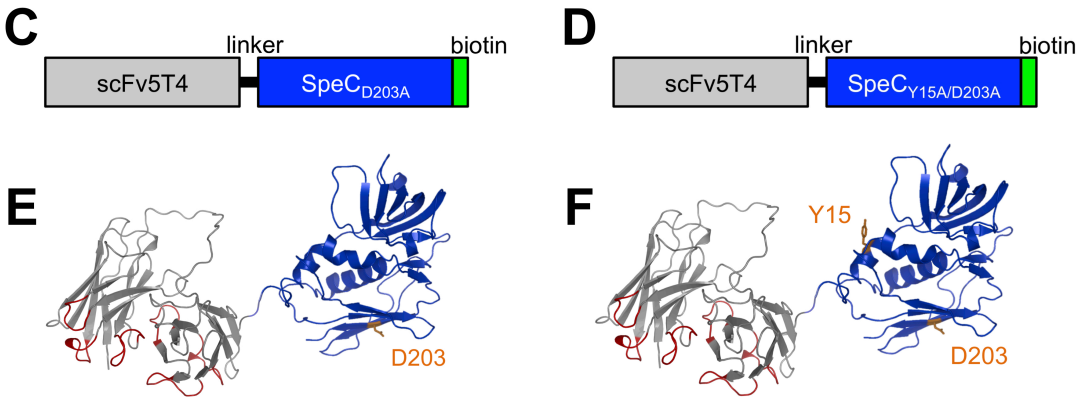
C
linker
biotin
scFv5T4
SpeC D203A
D
linker
biotin
scFv5T4
SpeC Y15A/D203A
E
D203
F
Y15
D203

difference with protein yield between strains was notable (data not shown). The final fusion protein design and predicted molecular structure, once expressed and purified, is highlighted as representative images in **Figure 16C-F**.

For protein expression and purification of the fusion construct scFv5T4::$SpeC_{D203A}$ and controls, following induced bacterial expression, the cell lysate was applied to a nickel resin column for purification with the His_6 tag and eluted with increasing concentration of imidazole. The expression of desired protein with TrxA was verified of the anticipated molecular weight of 64 kDa for fusion proteins and 39 kDa for scFv5T4 alone and purification tags were removed with autoinactivation-resistent His_7::TEV as described (368). The purified proteins were eluted in low imidazole concentrations and protein containing fractions were confirmed with expected 52 kDa and 27 kDa for fusion protein and scFv5T4 alone respectively and after buffer exchange, resulted each as soluble purified proteins (**Figure 17A**). The positive probed signal for biotin signified the successful *in vivo* biotinylation of each protein, including scFv5T4::$SpeC_{D203A}$ and control reagents scFv5T4 and scFv5T4::$SpeC_{Y15A/D203A}$ (**Figure 17B**). The genetic fusion of the humanized scFv5T4 and $SpeC_{D203A,}$ with use of the multi-tag system, resulted in successful expression and purification of the potential TTS.

3.7 scFv5T4::$SpeC_{D203A}$ and recombinant protein panel for therapeutic potential assessment

Purified recombinant proteins, including scFv5T4::$SpeC_{D203A}$, control reagents scFv5T4 and scFv5T4::$SpeC_{Y15A/D203A}$, as well as SAgs, $SpeC_{WT}$, $SpeC_{D203A}$ and $SpeC_{Y15A/D203A}$ were all biotinylated and diluted in saline (0.9%) to the same molar concentrations for comparative use *in vitro* and *in vivo* (**Figure 18**). All proteins were of predicted 25, 27, and 52 kDa size for SAgs, scFv5T4 and fusion constructs, respectively. The protein bands corresponded to relative concentrations of each dilution as well as represented the purity of the final product.

Figure 17. Purified recombinant scFv5T4::SpeC$_{D203A}$ fusion protein and control reagents

The purified recombinant proteins shown by **A)** SDS-PAGE stained with coomassie blue and **B)** detected by Western blot analysis by streptavidin-IRDye800.

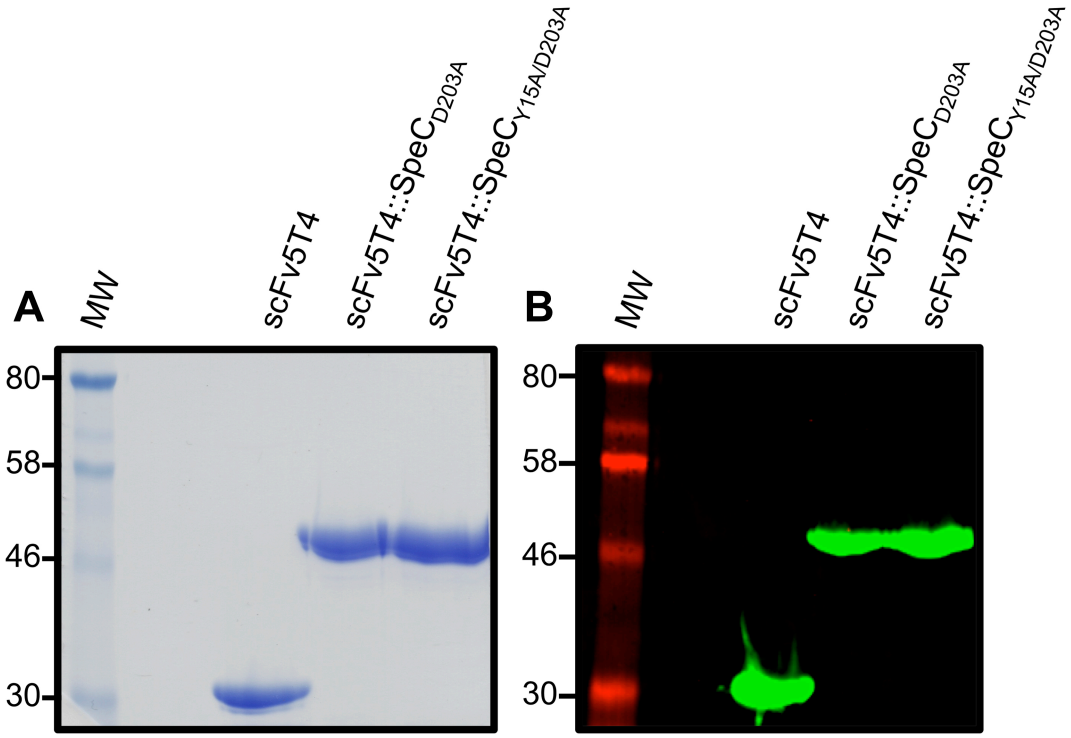
A
MW
scFv5T4
scFv5T4::SpeC$_{D203A}$
scFv5T4::SpeC$_{Y15A/D203A}$
80
58
46
30
B
MW
scFv5T4
scFv5T4::SpeC$_{D203A}$
scFv5T4::SpeC$_{Y15A/D203A}$
80
58
46
30

Figure 18. Recombinant protein panel for *in vitro* and *in vivo* therapeutic potential assessment

Purified recombinant proteins diluted in saline (0.9%) used *in vitro* and *in vivo* are shown by **A)** SDS-PAGE stained with coomassie blue and **B)** detected by Western blot analysis by streptavidin-IRDye800. Left and right lane represents 2000 nM and 200 nM dilutions, respectively.

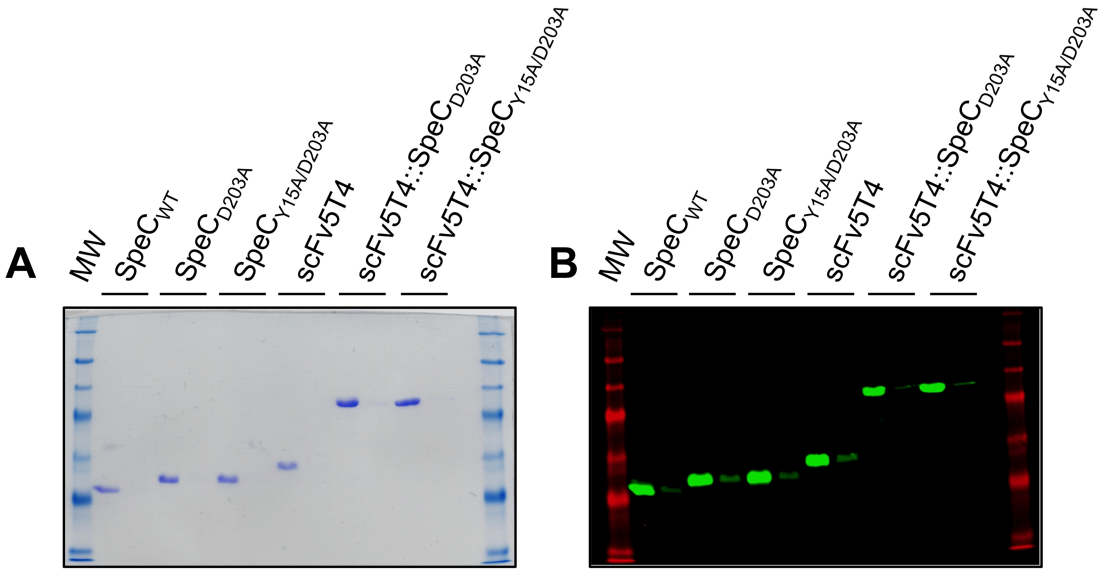
A
MW
SpeC$_{WT}$
SpeC$_{D203A}$
SpeC$_{Y15A/D203A}$
scFv5T4
scFv5T4::SpeC$_{D203A}$
scFv5T4::SpeC$_{Y15A/D203A}$
B
MW
SpeC$_{WT}$
SpeC$_{D203A}$
SpeC$_{Y15A/D203A}$
scFv5T4
scFv5T4::SpeC$_{D203A}$
scFv5T4::SpeC$_{Y15A/D203A}$

3.8 Human T-cell proliferation induced by scFv5T4::SpeC$_{D203A}$

Functionality of the SpeC$_{D203A}$ containing scFv5T4 TTS was assessed for the ability to induce proliferation of human PBMCs compared to control proteins. scFv5T4::SpeC$_{D203A}$ induced a dose-dependent proliferative response of human lymphocytes that was comparable to SpeC$_{D203A}$ (**Figure 19**). Notably however, the activation induced by scFv5T4::SpeC$_{D203A}$ remained significantly reduced compared to that of SpeC$_{WT}$. Furthermore, and importantly, the scFv5T4 antibody fragment alone and the double mutant fusion (scFv5T4::SpeC$_{Y15A/D203A}$) did not induce significant proliferative responses. This result indicated that the SpeC$_{D203A}$ portion of the fusion is responsible for inducing PBMC activation.

3.9 Human T-cell cytotoxicity of human CRC cells induced by scFv5T4::SpeC$_{D203A}$

Human SpeC-reactive PBMCs were used in two assays to evaluate the TTS immunotherapeutic agent for the ability to mediate tumour cell killing. First, the human colon cancer cell line WiDr was used as the target in a 7-AAD-based killing assay. Efficient cell killing was observed after human PBMCs were stimulated with 200 nM of the agent for 48 hours, compared to wild-type SpeC and unstimulated controls (**Figure 20A**). Second, HT-29 colon cancer cells labeled with ^{51}Cr were used as targets. Efficient cell killing was observed in a dose-dependent manner after human PBMCs were stimulated with the agent for 48 hours, and subsequently added to tumour cells with increasing effector to target (E:T) ratios (**Figure 20B**) Furthermore, the single mutant fusion (scFv5T4::SpeC$_{D203A}$) was more efficient than that of the similar double mutant fusion (scFv5T4::SpeC$_{Y15A/D203A}$) or antibody alone, but was reduced when compared with SpeC$_{WT}$. These data indicate that scFv5T4::SpeC$_{D203A}$ is functional for inducing immune cell-mediated cancer cell death and that SpeC$_{D203A}$, scFv5T4, and scFv5T4::SpeC$_{Y15A/D203A}$ proteins can function as precise controls to evaluate the requirement for targeting and SAg activity *in vivo*.

Figure 19. Functionality assay of recombinant protein panel for human PBMC proliferation *in vitro*

SpeC proteins were used to compare scFv5T4 alone, scFv5T4::$SpeC_{Y15A/D203A}$ and subsequently scFv5T4::$SpeC_{D203A}$ in the uptake of ^{3}H-thymidine as a measure of PBMC proliferation after 4 day incubation. Data shown is one representative human donor (mean ± SEM) of five independent human donors (n=5 in triplicate). *$p<0.05$, **$p<0.01$, ***$p<0.001$, compared to $SpeC_{WT}$.

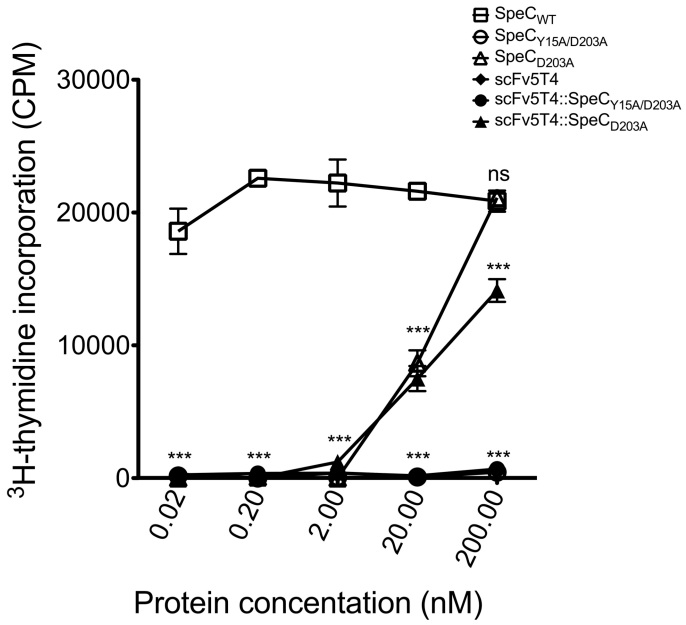
SpeC$_{WT}$
SpeC$_{Y15A/D203A}$
SpeC$_{D203A}$
scFv5T4
scFv5T4::SpeC$_{Y15A/D203A}$
scFv5T4::SpeC$_{D203A}$
^{3}H-thymidine incorporation (CPM)
30000
20000
10000
0
ns
***
0.02
0.20
2.00
20.00
200.00
Protein concentation (nM)

Figure 20. Cytotoxic potential of SpeC mutants and fusion proteins *in vitro*

Dose-dependent, SpeC-mediated PBMC cytotoxicity of scFv5T4::$SpeC_{D203A}$ compared with SpeC controls, scFv5T4 alone and scFv5T4::$SpeC_{Y15A/D203A}$. **A)** Percent cell death by 7-AAD exclusion staining of human colon cancer cell line WiDr after 48 h incubation with stimulated human PBMCs (n=3; mean ± SEM compared to $SpeC_{WT}$) and **B)** by ^{51}Cr-release from ^{51}Cr-labeled HT-29 human colon cancer cells with increasing effector:target ratios using human PBMCs stimulated for 48 h. Data shown (mean ± SEM compared to the inactive $SpeC_{Y15A/D203A}$ control protein) is from four independent human donors each completed in triplicate. ns = non-significant, *$p<0.05$, **$p<0.01$, ***$p<0.001$.

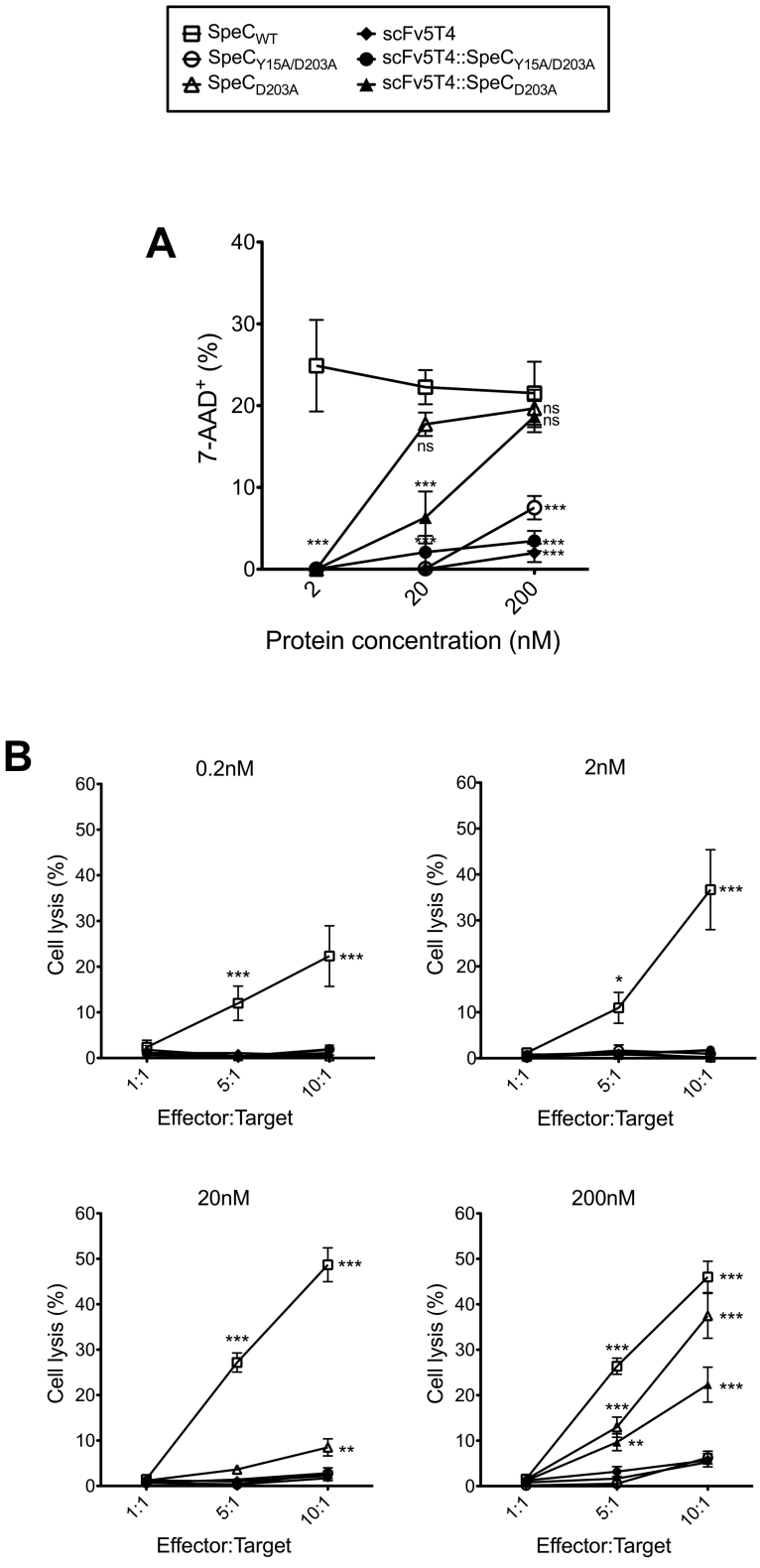
SpeC$_{WT}$
SpeC$_{Y15A/D203A}$
SpeC$_{D203A}$
scFv5T4
scFv5T4::SpeC$_{Y15A/D203A}$
scFv5T4::SpeC$_{D203A}$
A
7-AAD$^+$ (%)
Protein concentration (nM)
ns
***
B
0.2nM
2nM
20nM
200nM
Cell lysis (%)
Effector:Target
1:1
5:1
10:1
*
**

3.10 Immunotherapy of established colon cancer using scFv5T4::SpeC$_{D203A}$

SpeC is specific for human Vβ2^{+} T cells, but this SAg does not recognize mouse T cells (366). Thus, testing the SpeC-based TTS required a model utilizing human lymphocytes. Furthermore, the human 5T4 targeting scFv has minimal cross-reactivity with murine 5T4 (243). Therefore, human tumour cells expressing human 5T4 were necessary for the experiments. Based on a previously developed model (242, 335), an animal model using immunodeficient NSG mice was employed for the engraftment of 5T4^{+} human HT-29 colon cancer cells. NSG mice lack T, B, and NK cells (394) and represent an optimum mouse strain for human tumour engraftment (395, 396). Furthermore, these mice would permit the survival of transferred human immune cells (394, 397). HT-29 cells were injected ip into NSG mice and once solid tumours were palpable at 3 weeks post-injection (**Figure 21B**), treatments were initiated with iv injection (2 μM kg^{-1} per injection) of scFv5T4::SpeC$_{D203A}$, 2 hours post-ip injection of human PBMCs. Followed by 7 daily iv treatments, animals were electively euthanized 4 weeks post-treatment (**Figure 21A**). Control NSG mice did not receive PBMCs, or received PBMCs without additional treatments. Additional groups included the scFv5T4 alone, SpeC$_{D203A}$ alone, or inactive scFv5T4::SpeC$_{Y15A/D203A}$.

Three weeks post-injection of the HT-29 cancer cells, further internal assessment revealed a visual mass on the mouse peritoneum of an established tumour growth at the site of injection (**Figure 21C**). Histological evaluation by H&E stain of the tumour site showed distinct tissue morphology compared to the surrounding normal peritoneal tissue (**Figure 21D**).

Change in individual animal weight was monitored throughout the experiment and results suggested that weight fluctuation in the animals receiving the scFv5T4::SpeC$_{D203A}$ TTS was highly reduced compared to all other groups, and in general remained relatively close to original baselines, in particular near the termination of the time course (**Figure 22**). The tumour surface area was monitored using caliper measurement throughout the experiment and demonstrated little to no growth of the tumours in the

Figure 21. *In vivo* model of SpeC-based TTS therapy of established HT-29 colon cancer

A) Schematic illustration of the xenograft solid tumour model experimental timeline. NSG mice with established (3 week) ip human HT-29 tumours were injected once with human PBMC ip, followed by 8 daily intravenous injections of scFv5T4::$SpeC_{D203A}$, or individual controls (2 μM kg^{-1} per injection) and sacrificed 4 weeks post-treatment. HT-29 tumour growth after 3 weeks shows palpable and visual establishment at the site of injection **B)** externally (black circle), **C)** internally on the peritoneum (dashed circles), and **D)** histologically by H&E stain of tumour (T) and surrounding normal peritoneum tissue (P). Black bar represents 2 mm.

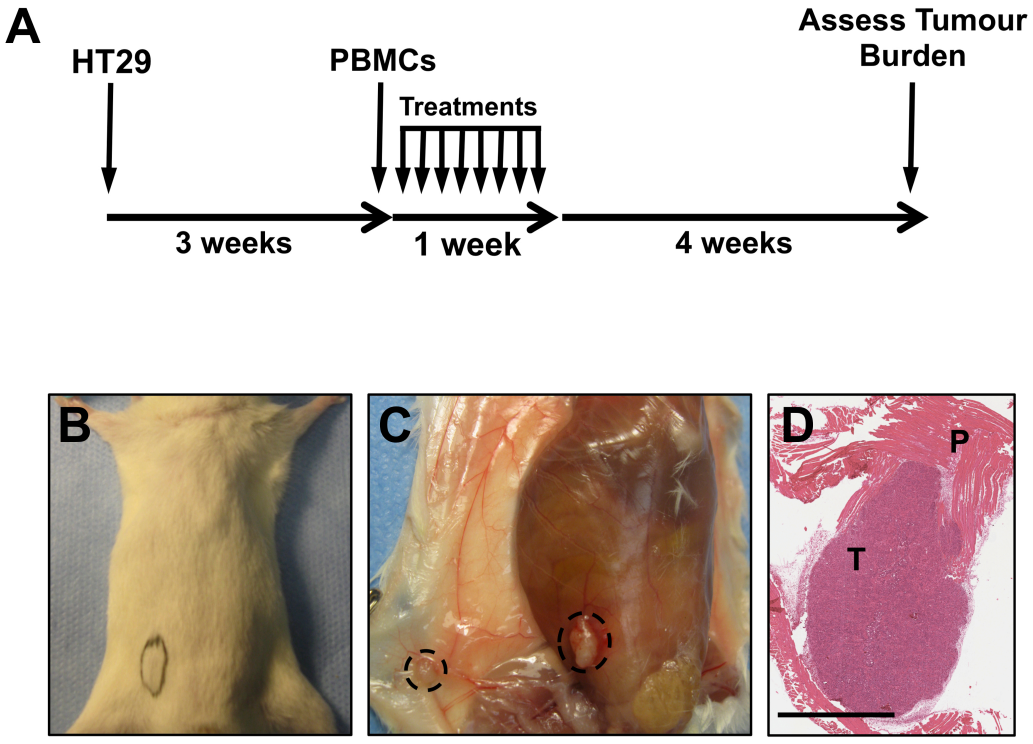
A
HT29
PBMCs
Treatments
Assess Tumour Burden
3 weeks
1 week
4 weeks
B
C
D
P
T

Figure 22. Weight change of NSG mice throughout tumour establishment and TTS therapy

Weight of animals was measured throughout the experimental timeline (total = 60 days) and fluctuation evaluated from initial baseline measurement taken Day 0 and represented as individual animals. All groups contained n=4, with exception of saline treated, no PBMC control group (n=3).

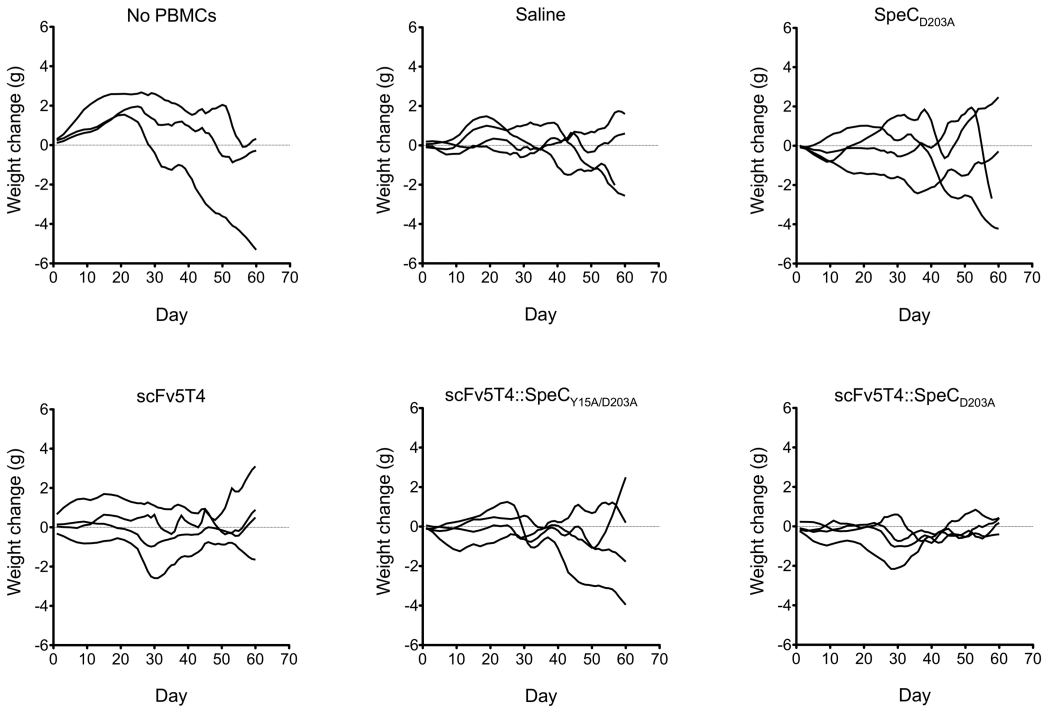
No PBMCs
Saline
SpeC$_{D203A}$
scFv5T4
scFv5T4::SpeC$_{Y15A/D203A}$
scFv5T4::SpeC$_{D203A}$
Weight change (g)
Day
6
4
2
0
-2
-4
-6
0 10 20 30 40 50 60 70

scFv5T4::SpeC$_{D203A}$ treatment group, while growth was observed in all other group (**Figure 23A**). The animals were electively euthanized at week 8 of the experiment and tumours were evaluated in a blinded fashion. Exterior overviews demonstrated evidence of the outgrowth size of the primary tumour at the injection site in all treatment groups, as well as visual metastatic sites on the upper right side of select control treated animals (**Figure 23B**). Upon internal exposure of the tumour injection site, it was evident that the human HT-29 cells established a primary solid tumour from the peritoneal cavity in all groups, which extended and attached to the inner skin surface. Gross pathology and H&E histological analysis suggested that the TTS treated animals had a reduced size in primary tumour, compared to all other treatment groups (**Figure 23C-D**), but that similar morphology and tissue composition of all primary tumours indicated that the tumours were of the same origin. Upon necropsy of the animals, tumours distant from the primary injection site at the time of sacrifice were evident within all treatment groups, however from a gross pathology overview of the peritoneal cavity, the metastatic burden was much reduced in the TTS treated animals (**Figure 24A**). Furthermore, the rate of liver metastasis was also diminished (**Figure 24B**). Of note however, the TTS treatment did not completely eliminate all metastasis as 2 out of 4 animals had evidence of at least 2 established metastases, albeit smaller comparable volume to control groups (**Table 15**). The degree of metastatic burden was visually characterized based on the location spread within the animal and also histologically analyzed by H&E stained sections to compare the composition of the metastases to the original solid tumour and to distinguish from existing healthy tissues. From this, 5 distinct locations distant from the primary tumour were defined (**Figure 24C-D**).

Of note, two animals did not reach the full experimental term of 60 days. Ethically, these animals were electively euthanized due to procedural requirements. Specifically, one male that had received the treatment of PBMCs alone followed by saline injections had a survival of 57 days. The total tumour volume of this particular animal was approximately 1615 mm^3 and had 3 tumours distant to the primary solid tumour (**Table 15**). The second animal was a female that received the treatment of SpeC$_{D203A}$, and had a survival day of 58. The total tumour volume for this particular animal was 539 mm^3 with 3 tumours

Figure 23. Size comparison of primary tumours from *in vivo* treatment groups

A) Primary tumour size was evaluated throughout the experimental timeline by external caliper measurements, individual animals represented by each graph line. Representative photographs of primary tumour at initial injection site at the time of sacrifice as **B)** overview of abdomen showing relative exterior size (dashed circles) and visible distant tumour (arrows), **C)** interior view (dashed outline) developed from peritoneal site and **D)** H&E stained histological sections (5 μm) of respective primary tumours. Black bars represent 5 mm. All groups contained n=4, with exception of saline treated, no PBMC control group (n=3).

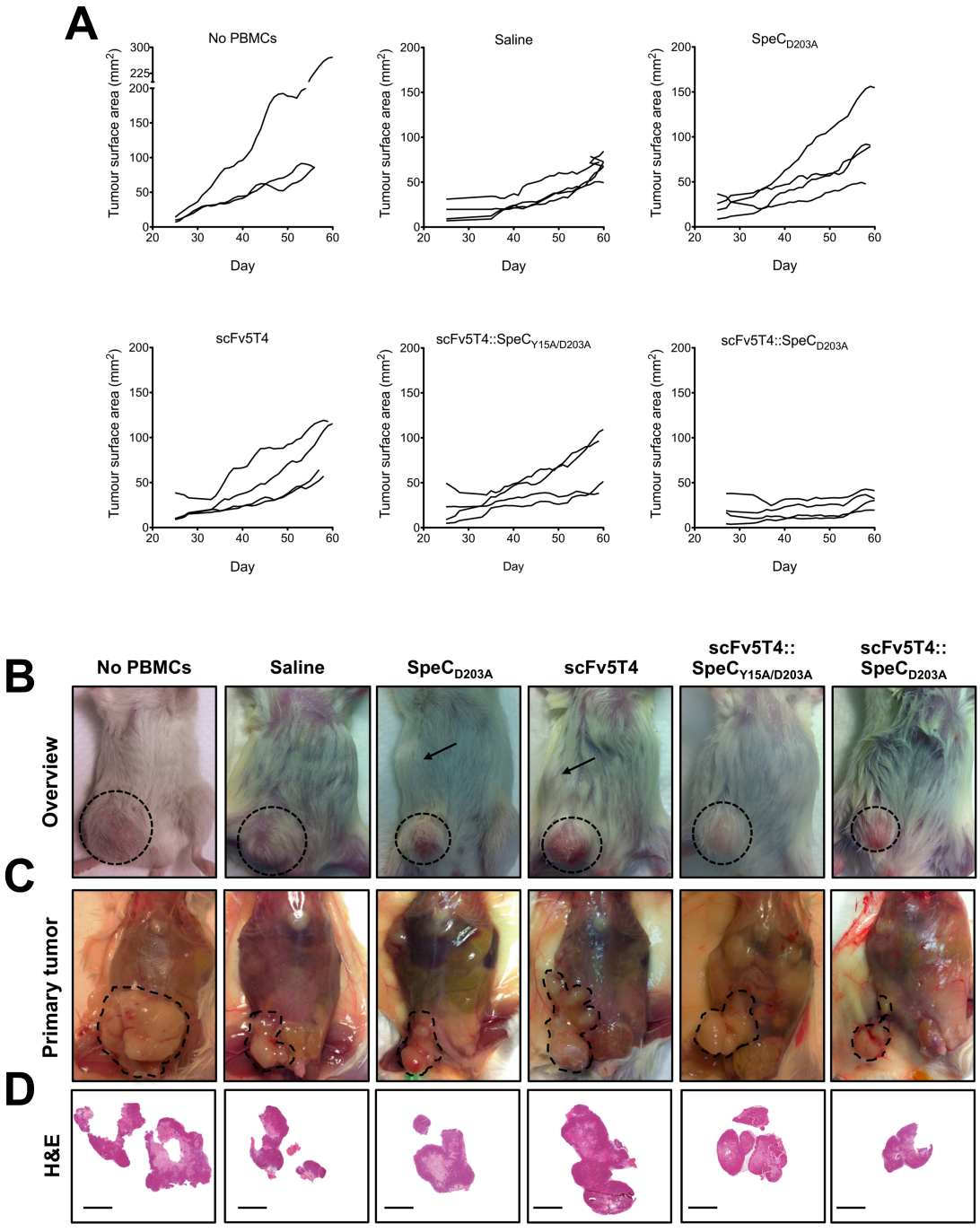
A
No PBMCs
Saline
SpeC$_{D203A}$
scFv5T4
scFv5T4::SpeC$_{Y15A/D203A}$
scFv5T4::SpeC$_{D203A}$
Tumour surface area (mm^2)
Day
B
C
D
Overview
Primary tumor
H&E
No PBMCs
Saline
SpeC$_{D203A}$
scFv5T4
scFv5T4:: SpeC$_{Y15A/D203A}$
scFv5T4:: SpeC$_{D203A}$

Figure 24. Tumour metastases from SpeC-based TTS therapy of established HT-29 colon cancer

Tumours distant from the primary injection site at the time of sacrifice shown as representative photographs of **A)** gross pathology overview of peritoneal cavity focused on tumours distant from primary site (black arrows) on the right side of animal and **B)** livers removed and analyzed for presence of tumour mass (white arrows). Primary tumour and metastases were characterized for metastatic scoring based on **C)** location within the animal (labeled i through vi), where (i) is the primary solid tumour and histologically analyzed by **D)** H&E staining sections (5 μm) of the locations to distinguish tissues. All H&E images taken from representative saline treated animal control group (n=4) (T, tumour; P, peritoneal wall; L, liver; D, diaphragm; K, kidney). Illustration (C) modified from The Anatomy of the Laboratory Mouse (http://www.informatics.jax.org/).

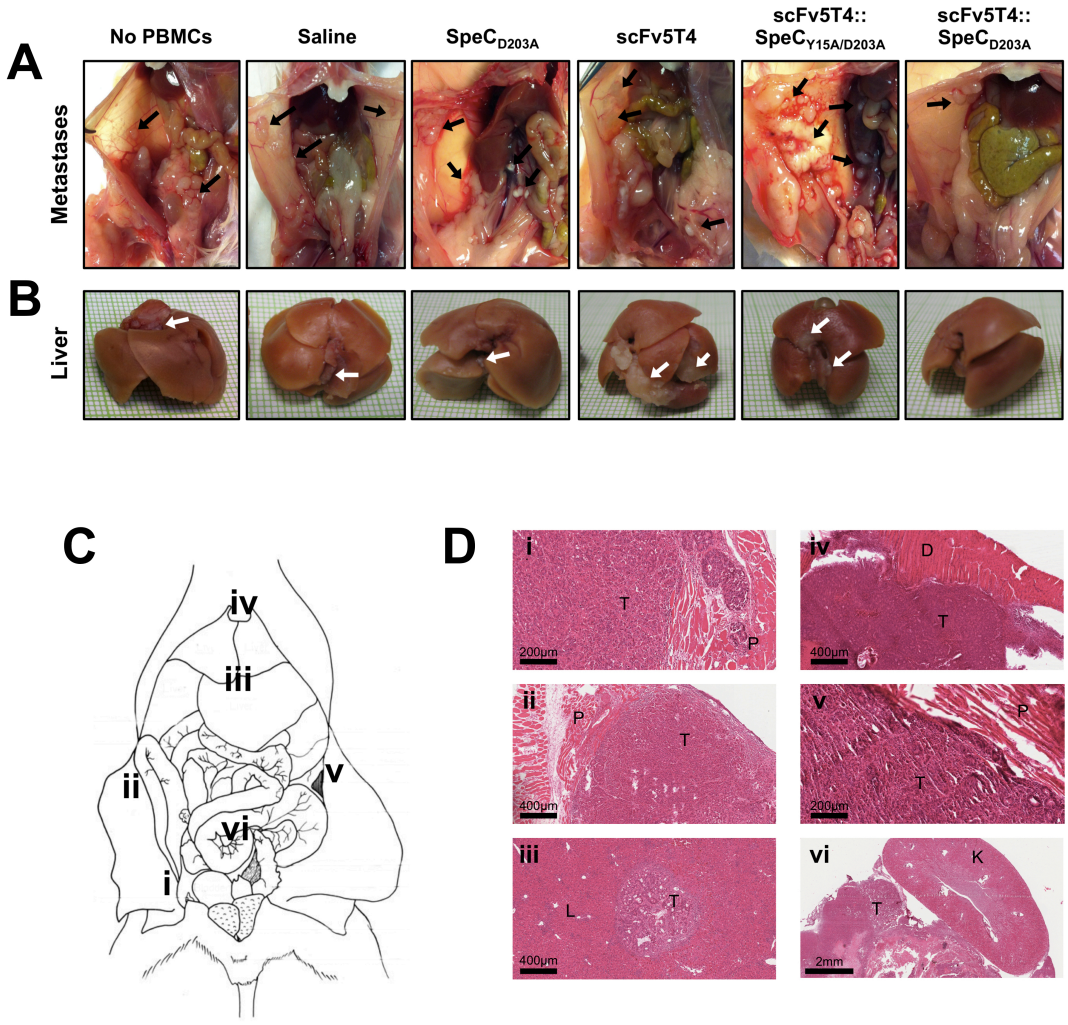
A
No PBMCs
Saline
SpeC$_{D203A}$
scFv5T4
scFv5T4::
SpeC$_{Y15A/D203A}$
scFv5T4::
SpeC$_{D203A}$
Metastases
B
Liver
C
iv
iii
ii
v
vi
i
D
i
T
P
200μm
iv
D
T
400μm
ii
P
T
400μm
v
P
T
200μm
iii
L
T
400μm
vi
K
T
2mm

Table 15. Animal characteristics and individual data generated from *in vivo* immunotherapy TTS model with human HT-29 cancer cells

After solid tumour establishment, mice were divided by sex and subsequently grouped (n=3-4) with a random number generator to receive either scFv5T4::$SpeC_{D203A}$ TTS, or control. Noted are: animal survival day, wet weight (g) of the primary solid tumour located at the site of initial injection site, total tumour volume (mm^3), and number of visually identified metastases.

Treatment Group	Sex	Survival day	Primary tumour weight (g)	Total tumour volume (mm^3)	Number of metastases
No PBMCs/Saline	M	60	1.17	1353.5	4
	M	60	0.71	1887.5	5
	M	60	2.50	2677.6	3
Saline	M	57	1.44	1615.8	3
	M	60	0.38	1932.9	2
	M	60	0.35	1052.0	4
	F	60	0.63	642.3	2
$SpeC_{D203A}$	M	60	1.17	2046.3	2
	M	60	1.02	4753.7	4
	F	58	0.30	539.2	3
	F	60	1.07	2058.6	3
scFv5T4	M	60	1.08	5893.3	2
	M	60	1.89	2011.8	3
	F	60	0.48	674.5	4
	F	60	0.42	673.7	3
scFv5T4::$SpeC_{Y15A/D203A}$	M	60	1.12	1951.9	4
	M	60	0.62	2020.1	2
	M	60	0.81	1332.2	2
	F	60	0.18	938.3	3
scFv5T4::$SpeC_{D203A}$	M	60	0.34	380.0	2
	M	60	1.07	900.8	2
	M	60	0.53	123.9	0
	F	60	0.49	400.6	1

distant to the primary solid tumour (**Table 15**). No other abnormalities were visually noted during the necropsy other than dehydration, and weight loss. Furthermore, one male that had received the TTS treatment, but not the full dose due to initial injection technique, had a notable larger total tumour volume as well as primary tumour size (**Table 15**). A potential sex bias was also noted within the model as the male animals responded better to overall tumour growth from human HT-29 cancer cells in comparison to the females within this strain of mice (**Table 15**).

Overall, this experiment demonstrated a dramatic reduction in the total tumour volume and metastastic burden after treatment with scFv5T4::SpeC$_{D203A}$ that was significantly different from mice that did not receive PBMCs, sham treated mice (saline), and mice treated SpeC$_{D203A}$ alone, or with control treatment scFv5T4::SpeC$_{Y15A/D203A}$ (**Figure 25A-B**). Importantly, there were no differences in tumour volumes or number of metastases between mice that received PBMCs alone and the different control reagents (**Figure 25A-B**).

Immunohistochemistry of the solid primary tumours was performed comparing the TTS treated animals to the non-immune inducing scFv5T4::SpeC$_{Y15A/D203A}$ treatment group. The rate of cellular proliferation, blood vessel formation, as well as cellular apoptosis showed no significant difference among the two treatment groups. Furthermore, there was no distinction between the numbers of $CD3^+$ cells within the solid tumours at this time point (**Figure 26A-B**).

Together, these data indicate that although there was no specific differences in the IHC of the solid primary tumours, the TTS treated group demonstrated an overall weight maintenance and dramatic reduction in the total tumour volume with a significant reduction in the total metastases score compared to control treatment groups.

Figure 25. Tumour burden from SpeC-based TTS therapy of established HT-29 colon cancer

Twenty-eight days post-final injection, **A)** final tumour volume was measured and **B)** metastatic score evaluated. All groups contained n=4, with exception of saline alone control (n=3). *$p<0.05$, **$p<0.005$.

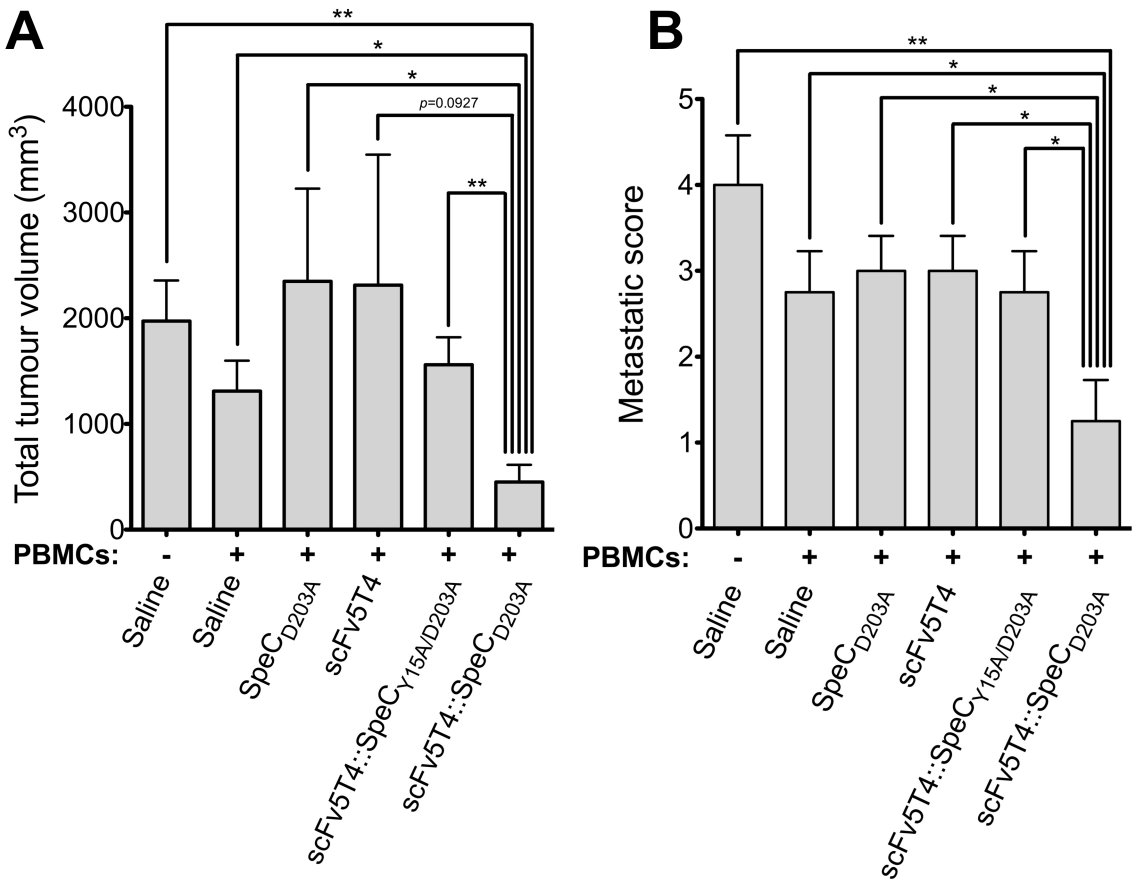
A
Total tumour volume (mm3)
4000
3000
2000
1000
0
**
*
*
p=0.0927
**
PBMCs: - + + + + +
Saline
Saline
SpeCD203A
scFv5T4
scFv5T4::SpeCY15A/D203A
scFv5T4::SpeCD203A
B
Metastatic score
5
4
3
2
1
0
**
*
*
*
*
PBMCs: - + + + + +
Saline
Saline
SpeCD203A
scFv5T4
scFv5T4::SpeCY15A/D203A
scFv5T4::SpeCD203A

Figure 26. Immunohistochemistry profiles of TTS treated primary HT-29 tumours
Twenty-eight days post-final injection, primary tumours were excised, sectioned (5 μm) and assessed by IHC. Similar histological profiles are shown as **A)** representative images of primary tumour sections and **B)** quantification of staining from animals receiving either TTS or control treatments and stained for proliferative marker Ki67, endothelial cell marker vWF, apoptosis by TUNEL, and T cell marker CD3. All sections were counterstained with nuclear stain DAPI and imaged with fluorescence microscopy. White bars represent 50 μm. Images are representative of 1 stained section from each animal (n=4). Quantification was generated with blinded counting of positive stains from 5 random high-power fields (hpf) per section per animal (n=20 per stain per treatment group; mean ± SEM).

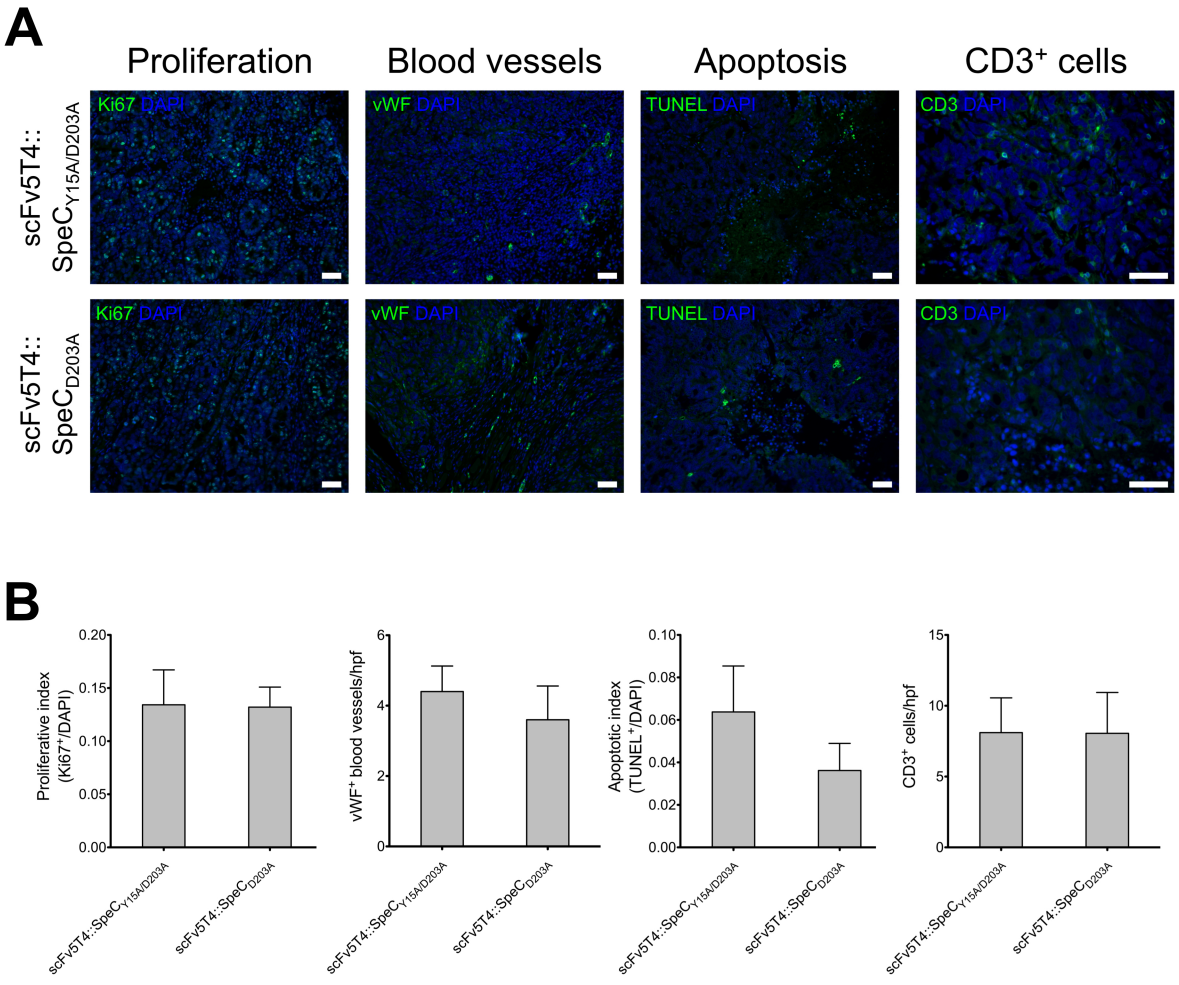
A
Proliferation
Blood vessels
Apoptosis
CD3+ cells
scFv5T4::SpeCY15A/D203A
scFv5T4::SpeCD203A
Ki67 DAPI
vWF DAPI
TUNEL DAPI
CD3 DAPI
B
Proliferative index (Ki67+/DAPI)
vWF+ blood vessels/hpf
Apoptotic index (TUNEL+/DAPI)
CD3+ cells/hpf
scFv5T4::SpeCY15A/D203A
scFv5T4::SpeCD203A

CHAPTER 4: DISCUSSION

T lymphocytes are recognized as one of the most important immune cells involved in tumour regression within the field of cancer immunotherapy, and bacterial SAgs are among the most potent naturally occurring specific activators of T cells. Thus, the appropriation of SAgs to target cancer cells (309) has received significant attention and has become very promising in the advancement of targeted immunotherapies. Of particular interest are those where mAbs are used (338, 342) and encouragingly, TTS therapeutics are now being evaluated in human clinical trials (323-325, 337, 338, 342, 348).

In Canada, cancer is the leading cause of death, responsible for nearly 30% of all deaths and in recent reports, it is expected that new cases will dramatically rise over the next 15 years due to the increasing aging population (3). In this work, the focus was on colorectal cancer, one of the four major contributors to new cancer diagnose. This cancer accounts for more than half of all cancers within Canada and is the second and third most common cause of cancer death for males and females, respectively (3). With few clinical symptoms evident until the onset of stage III or IV, this carcinoma is difficult to diagnose. As such, ~20% of diagnosed patients present with inoperable CRC and ~25% of operable patients will develop metastases due to recurrence, resulting in a relatively high overall mortality rate (~45%) for CRC (10, 15). It is clear that advances in treatment, diagnosis, and prevention strategies of this carcinoma are of considerable importance.

Successful treatments of an invasive cancer, in addition to addressing the primary site, must also direct targeted effects towards the distant metastases, therefore mAbs have been employed to direct targeted cytotoxic responses (398, 399). mAbs of murine origin and mouse/human chimeras have been used either alone or linked to a therapeutic agent with encouraging results, of which some have been FDA approved for use in the clinic (*e.g.* ibritumomab tiuxetan, rituximab, cetuximab) (400). However, concerns have arisen using whole murine and chimeric mAbs in humans. Firstly, the whole murine mAbs can induce HAMA responses (153) along with systemic toxicity due to the requirement for high doses for effective treatment (323, 337). Furthermore, it has been found that surface molecule specific whole mAbs do not efficiently penetrate solid tumours (401), are not uniform in final biodistribution, and can have high serum levels leading to toxicities

(183). Engineering smaller antibodies can minimize these issues associated with whole mAbs and this has led to the development of recombinant molecules such as Fab and scFv fragments. This results in much smaller, tumour-penetrating molecules in particular for scFv fragments, that retain the binding activity of the full IgG molecule (401, 402). However, scFv fragments have decreased stability and tumour retention (183), as well as a shorter half-life in serum and are cleared more rapidly compared to larger fragments (403). An ideal tumour-targeting reagent would be of intermediate size which could provide rapid tissue penetration, high target retention, and rapid blood clearance (183). For example, this sized reagent can be generated by incorporating the scFv into a complex molecule such as a fusion with an immune stimulatory molecule (402).

The tumour-associated antigen, 5T4, is of particular interest for advancement of targeted immunotherapeutics (226) as its expression is restricted on normal adult tissues, but it is upregulated on an array of carcinomas, including CRC (196). Although this antigen is expressed throughout cancer progression, it has been most frequently detected on malignant cells with no evidence of downregulation (198) and has been associated specifically with metastasis in CRC (199). Indeed, further investigation of this antigen demonstrated that upon expression it is involved in decreasing cellular adhesion, influencing cytoskeletal organization, and promoting cell motility and migration (223, 224). As a result, poor clinical outcome in some cancers is associated with these altered cell properties (223). 5T4 has been the target of a number of developing immunotherapies, including chimeric antigen receptors (404), antibody-drug conjugates (241), a vaccine undergoing clinical trials (405-407), as well as TTSs (338, 343), all demonstrating promising results.

An effective targeted immunotherapeutic will direct activated cytotoxic lymphocytes to the tumour for eradication. SAgs, microbial toxins produced primarily by staphylococcal and streptococcal species, are known for having some of the most potent immunostimulatory properties. Of the streptococcal SAgs presently studied, SpeC is the best characterized and has been extensively described in terms of both structure (272, 285, 365) and function (277, 286, 366-369) for engagement of host receptors. A complete binding map for specific interactions between SpeC and TCR Vβ2.1 (277, 368), as well

as the high-affinity zinc-dependent binding interface with MHC II β-chain (369) and low-affinity MHC II α-chain binding interface (286) of this SAg has been established. With this knowledge, strategic SAg mutations may be applied to modulate the T cell stimulatory capacity of this SAg, generating, to the best of our knowledge, the first streptococcal SAg to be employed in TTS immunotherapeutics, enabling expansion of the current TTS repertoire. Specifically, to prevent high-affinity and non-specific binding of MHC II molecules, Asp^{203}, a residue involved in the coordination of the zinc ion of the high affinity site (272) can be altered to Ala such that the potent immune stimulation, and therefore toxicity, of the SAg is reduced (286, 369). Indeed, this study provided further evidence that Asp^{203}, when altered to Ala, reduced a stimulated human immune response (**Figure 8**). Importantly however, it was also demonstrated that this reduced stimulation was still sufficient for the ability to induce immune-mediated cancer cell death (**Figure 9**). Similarly, the high-affinity MHC II binding site of the SAg SEA has been characterized (328) and a mutation of Asp^{227} to Ala has been shown to reduce systemic side effects (331, 335, 338). As a result, this mutational design has also been incorporated into TTSs currently undergoing human clinical trials. This suggested that this particular variant of SpeC would be beneficial in the overall development of TTSs while reducing off-target activation of the immune system. Further, within the SAg SpeC, Tyr^{15} has been reported to be a critical residue in the interaction with the TCR binding interface leading to T cell activation (368). As such, this residue when mutated to Ala, in combination with the altered Asp^{203}, can be used for the generation of precise control reagents that maintain structural integrity and targeting, but lack immune stimulation activity. The importance of Tyr^{15} for the engagement of the TCR was further supported by this work, both as a single and a double mutant SpeC variant, demonstrating reduced and absence of induced immune stimulation, respectively (**Figure 8, 9**).

As indicated, the concept for using a TTS as an immunotherapeutic is not novel (309), and has great potential for future cancer immunotherapy. Promising results from such TTSs have been demonstrated in both murine studies (322, 335, 341) as well as human clinical trials (323, 337, 338, 342, 348) where a murine Fab antibody portion, targeting a TAA is fused to SEA. The most developed of these TTSs specifically targets the TAA

5T4, and in preclinical studies, a reduction in the number of tumours present, as well as a reduction in overall tumour mass, with the absence of obvious systemic side effects was demonstrated (335). Modifications were engineered within the SAg portion of the TTS for use in human clinical trials to reduce systemic immune activation (338) as well as alterations designed to reduce host antibody recognition in the most current version, naptumomab estafenatox (ABR-217620; Fab5T4-SEA/E-120) (242, 339) for use in Phase I (342, 343) and subsequent Phase II/III trials (348). Although this treatment showed promise, aside from T cell activating properties, staphylococcal SAgs are also the agents of staphylococcal food-borne illness (261), a property not shared among the streptococcal SAgs (253, 262). This was noted from side effects seen in Phase I and II/III clinical trials that included nausea, vomiting, and diarrhea (337, 338, 342). To date, TTSs have been exclusively built using members of the SE class of SAg, all sharing emetic properties. Evidence also suggested that the murine Fab portion had led to high levels of HAMA after multiple cycles of treatment (337), and unexpectedly, in recent Phase II/III trials, patients had higher than anticipated baseline levels of anti-SEA/E-120 antibodies, which may have contributed to suboptimal therapy (209, 346, 348). Collectively, this information led to the design of a novel "next generation" TTS composed of a scFv antibody fragment directed against a TAA and a potent streptococcal T cell activating SAg. More specifically, within this study, a scFv directed against human 5T4 fused to the streptococcal SAg prototype, SpeC, was developed and preclinically tested *in vitro* and *in vivo*.

The earliest form of the TTS molecule consisted of a previously described murine scFv antibody specific for human 5T4 (243), genetically fused by a short peptide linker (Gly-Gly-Pro) to an altered SpeC containing an Asp^{203} to Ala mutation (scFv5T4::$SpeC_{D203A}$) (372, 373). In addition, the fusion protein was further constructed to contain an Ala mutation at residue 15, replacing the endogenous Tyr, to generate a precise non-immune stimulating control reagent (scFv5T4::$SpeC_{Y15A/D203A}$) (373). Expression of the recombinant fusion proteins from the *E. coli* bacterial system proved successful, however unlike the typical SAg portion alone (**Figure 7**), the proteins formed insoluble, misfolded aggregates termed inclusion bodies. Over-expression of heterologous proteins in *E. coli* is frequently hindered by the formation of inclusion bodies, and is incidentally common

amongst scFv proteins (408-411). As a result, isolating and refolding of proteins from inclusion bodies has become an essential requirement in the study of proteomics and this method has been quite useful as a means of recovering functional proteins (412). However, in protein expression studies, optimization of the host culture conditions, or the fusion to a large affinity tag can often prevent the necessity of isolating these misfolded aggregates (389). Within this study, the preparation and refolding methods used for inclusion bodies, although successful, were not ideal for the downstream processing requirements of large-scale therapeutic production; therefore, the optimization of protein expression continued to be the strategy to obtain a soluble, bioactive protein. Notably, alternative expression organisms may be also used to prevent inclusion bodies, such as yeast (*Saccharomyces cerevisiae*) (390) or eukaryotic cell lines (413, 414), however, would prove to be considerably laborious, and non-cost and -time effective when compared to the well-established, easily manipulated, and high biomass-to-cost ratio (389) that could be obtained from the *E. coli* platform.

Over the course of this study, several considerations and alterations were applied to the genetic construct containing the murine scFv5T4 fused to $SpeC_{D203A}$, as well as to the expression and purification methods for improved protein yield. Of these, a highlight included the addition of a C-terminal high-affinity unique peptide tag (biotin tag; AviTag™ Technology, Avidity) to use the strong interaction of biotin and avidin with aims to enhance the sensitivity of protein capture and increase protein detection. Although this tag was not advantageous to the overall purification of the product, this technology was extremely useful for enhanced detection sensitivity of the expressed constructs. Additionally, the solubility of a target protein can be enhanced by fusion with a highly soluble carrier protein such as maltose-binding protein (MBP) or a hydrophilic tag such as a transcription termination anti-termination factor (NusA), TrxA, or protein disulfide isomerase I (DsbA) (380). However, hydrophilic tags must be used in combination with a smaller affinity tag, for example His_6 or FLAG, within an expression system for purification (380). This multi-tag approach has become a common tactic to address solubility issues (380, 381) and since recognized, have become widely commercially available. Notably, TrxA has been widely used to increase protein solubility (387-389), including specifically for scFv constructs (390, 391) and therefore,

efforts focused on increasing protein solubility for scFv5T4::SpeC$_{D203A}$ generated an expression system in which TrxA was fused to the N-terminus of the genetic constructs, along with a His_6 tag for affinity purification. Through all experimental attempts and efforts to optimize and increase soluble protein expression, it was clear that sufficient yield of the murine scFv5T4, as a soluble product, remained a significant challenge.

Due to the limitations associated with generating the murine scFv5T4, an alternate approach was applied to generate a recombinant soluble molecule for large-scale production as well as to further develop the 5T4-specific streptococcal TTS by designing a 'humanized' scFv5T4 antibody fragment to also prevent HAMA responses. Indeed, the approach of genetically grafting the 5T4-specific CDR loops from the murine fragment onto a 'humanized' scFv backbone (**Figure 11, 12**) successfully generated and produced a highly soluble protein when fused with TrxA within the *E. coli* expression system.

Evaluations of the humanized scFv5T4 demonstrated specific 5T4-targeting ability *in vitro* (**Figure 14, 15**) and provided further preclinical evidence for 5T4 as a potential TAA for targeted immunotherapy. Although this work highlights the binding capabilities of the humanized scFv5T4 to its target 5T4, further evaluation to conclusively determine the specificity and binding affinity would be beneficial. For example, while the original 5T4-targeting mAb was evaluated for distribution on normal and neoplastic tissues (196, 243), verification that the humanized scFv5T4 retains the consistent non-specific binding to various cell and tissue types would be of value. Similarly, further verification of the high affinity binding measured for the murine scFv5T4 (K_d = ~10^{-9}) (243) of the altered humanized scFv5T4 would advance the application of these targeting therapeutics. Although there has not been any evidence to date of 5T4 downregulation throughout cancer progression, characterization of the downstream effects as a result of binding from this targeted scFv fragment would be of value for elucidating the cellular role and consequence of the potential TTSs.

Upon genetic fusion of the humanized scFv5T4 and SpeC$_{D203A}$, with the consistent design of the multi-tag approach, successful expression and purification of the potential TTS was generated (**Figure 17**). Furthermore, the precise control reagents scFv5T4 alone, as well

as the non-immune stimulating scFv5T4::SpeC$_{Y15A/D203A}$ were produced. Further *in vitro* work provided evidence that the Asp^{203} to Ala mutation contained with the TTS reduced SAg-induced activity (**Figure 19)** but was sufficient in the ability to induce immune-mediated colon cancer cell death (**Figure 20**). Importantly, immune stimulation was not demonstrated by the control reagents, scFv5T4 and scFv5T4::SpeC$_{Y15A/D203A}$, indicating that SAg activity was required for tumour cell killing. This was the first account, to our knowledge, of a streptococcal SAg-based TTS inducing *in vitro* cytotoxicity towards colon cancer.

As SpeC does not recognize murine T cells (366), and the human 5T4 targeting scFv has minimal cross-reactivity with murine 5T4 (243), limited value would come from the use of a syngeneic murine model. Therefore, based on a previously developed model (242, 335), a xenogeneic model consisting of the engraftment of 5T4^{+} human HT-29 colon cancer cells and the transfer of human immune cells were applied to immunodeficient NSG mice. NSG mice lack T, B, and NK cells (394) and represent an optimum mouse strain for human tumour engraftment (395, 396) and also permit the survival of human immune cells (394, 397). Herein, it was demonstrated that the soluble recombinant fusion protein scFv5T4::SpeC$_{D203A}$ was able to specifically target 5T4 to elicit a T cell response that substantially reduced tumour burden *in vivo*. Importantly, a model of established tumours was used in order to robustly test the SpeC-based TTS. Within this model however, for reasons undetermined, there was a disparity of overall tumour growth amongst the male and female animals and though the males supported a more robust establishment of HT-29 cancer cells, among the matched groups (**Appendix 6**), the trend of results nevertheless remained. Importantly, the TTS treatment group at this dose had no observable side effects on animal health (**Figure 22**), suggesting that the treatment may be safe for further downstream evaluations and continued applications.

In this model, while the primary tumours did not appear to regress, the data clearly demonstrated that scFv5T4::SpeC$_{D203A}$ TTS was able to prevent further tumour growth as well as the development of peritoneal metastases. Expectedly however, the PBMC sham treatment group, as well as the control reagents, also had a marked decrease in overall tumour burden when compared to the saline control group (**Figure 25**). This can be

attributed to an allograft response caused by the mismatch of HLA between the donor PBMCs and the HT-29 cancer cells.

In summary, as scFv5T4::$SpeC_{D203A}$ and $SpeC_{D203A}$ showed similar activity *in vitro* (**Figure 19**), the inability of $SpeC_{D203A}$ to impact tumour size or metastatic disease indicates that the scFv5T4 moiety of the fusion protein was required for *in vivo* targeting of $5T4^+$ HT-29 cells (**Figure 25**). Likewise, the inability of scFv5T4 alone, or the inactive scFv5T4::$SpeC_{Y15A/D203A}$ fusion to show any measurable impact (**Figure 25**) demonstrates that T cell-dependent SAg activity was also required for tumour cell killing. Importantly, though the incorportation of the altered SAg was designed to decrease systemic T cell activation by reducing MHC II binding by the TTS, in the 5T4Fab-SEA/E-120 TTS, the mouse Fab moiety has been shown to effectively replace the MHC II binding domain such that T cells are efficiently activated when artificially 'presented' by the tumour (340). It is suspected that the humanized scFv5T4 moiety here played a similar role contributing to the dramatic reduction in tumour volume and metastatic disease. Closer analysis suggested that although the primary tumours of TTS treated (scFv5T4::$SpeC_{D203A}$) and the non-immune stimulating control (scFv5T4::$SpeC_{Y15A/D203A}$) did not display any immunohistological distinctions (**Figure 26**), it is anticipated that differences may be noted among the metastatic sites within degree of apoptosis, immune infiltration, and tumour development. The reduction in overall metastases in TTS treated animals is presumed to be due to the enhanced immune activation at these localized areas, however further investigation is warranted beyond the ‘snapshot’ captured from the primary tumours.

While this xenograft model of established human HT-29 colon cancer cells and engrafted human PBMCs clearly demonstrated an overall reduction in tumour burden with TTS treatment, there are also a number of limitations for consideration. Firstly, as the immune system is artificially delivered by means of an intraperitoneal injection of isolated human PBMCs, this model lacks the ability to evaluate the TTS to cause immune cell recruitment and migration for a localized anti-tumour response. Future experimentation may include intravenous delivery of the PBMCs to evaluate this response and any systemic effects that may be elicited by the TTS. Furthermore, as PBMC preparations are

used, the polymorphonuclear cell (PMN) populations, in general, are absent and therefore the full immune effect of the TTS is unable to be fully evaluated within this model. Lastly, this model limits the extensive interactions between the developing tumours and immune system, lacking the effects of immunoediting and resulting gradual heterogeneity development along with the generated immunosuppressive microenvironment typical of the tumour. Recently, much work has been achieved to meet the challenging need of new therapeutic treatment evaluation in the development of humanized NSG mice for immuno-oncological studies (415). For some time, these animals have been known to be able to support the development and function of multiple aspects of human immunity, including both myeloid and lymphoid cells from engraftment of human hemopoietic stem cells (394). As well, further evidence demonstrates that these humanized mice also allow the co-engraftment of a wide range of heterologous, allograft human tumours, providing a number of options for animal models that can act as the preclinical bridge for current immuno-oncology therapies (415).

Although the specific mechanisms of TTS-induced anticancer immunotherapy have not been fully elucidated, it can be speculated from the *in vivo* model that is it is the combined efforts of both the SAg as well as the targeting moiety. From studies focused on elucidating the role of 5T4, it has been recently shown with mouse embryonic cells that CXCR4/CXCL12 chemotaxis, signaling important for cell mobilization, can be blocked with mAbs to 5T4 *in vitro* (227). Importantly, treatments to block 5T4 antigen *in vivo* was also able to prevent the spread of human $5T4^{+}$ B-ALL cells (227), demonstrating that the observed reduction may be related to 5T4 function in regulating chemokine or signaling pathways. Although this effect has not been specifically observed to date within preclinical studies of TTSs, this study inclusive, the ability to have comparative analysis with 5T4-targeting alone treatments (scFv5T4 or scFv5T4::$SpeC_{Y15A/D203A}$), was generated. Based on this early work, consideration of antibody targeting and downstream effects of blocking 5T4 signaling merits further investigation.

Secondly, the ability of bacterial SAgs to induce cytokines that maintain T-cell activity as well as those that are tumouricidal are important features (308, 309, 320). Key

inflammatory cytokines for these specific effects are IL-2 and IFN-γ, the hallmarks of T cell activation, of which SAgs in general, including SpeC (248), are known to induce. Indeed, in previous TTS experimental preclinical models, in addition to perforin-mediated cytotoxicity, release of IFN-γ as well as TNF-α has been shown to be particularly important for anticancer effects (320, 355). The initial release of these SAg-induced cytokines will lead to induced proliferation of $CD4^+$ and $CD8^+$ T cells (416), in particular CTLs and NK cells. Early SEA-based TTS work *in vivo* demonstrated a massive influx of both $CD4^+$ and $CD8^+$ T cells into the targeted tumour, suggestive of the induced release of T cell specific chemokines to encourage cellular trafficking at the tumour site and when T cells were depleted, a complete abrogation of therapeutic effect was observed (320). In recent clinical studies with Naptumomab estafenatox (ABR-217620) therapy, select patient sampling also included PBMCs and analysis of associated changes in lymphocyte subsets (348). Most notable was the consistent expansion of TTS specific CD4+ and CD8+ T cells in peripheral blood that coincided with pronounced IL-2 production (348). Furthermore, in additional clinical studies with the same treatment, responding patients demonstrated that T cells infiltrate tumours (342). These secondary events, in addition to an overall heighted immune response, are also thought to be important in killing subsets of neighboring cancer cells that may not express the specific TAA (335). Based on evidence from the SEA-based clinical trials, it may be speculated that TTSs act mainly by induction of T cell activation, proliferation and maturation into effector cells and secondly, by recruitment and T cell killing of the tumour. Although the specifics of cytotoxic mechanisms directed toward CRC have yet to be studied for streptococcal SAgs, based on the similar T cell activation profiles of staphylococcal and streptococcal SAgs, it is predicted that the mechanism of immune-mediated cancer cell death of SpeC will be comparable to SEA-based TTS. Future analysis of serum samples collected from animals within this study may shed light on the cytokine profile induced by the humanized scFv5T4::$SpeC_{D203A}$. To ultimately determine the types and quantities of cytokines released for future therapeutic development would be of importance, in particular, should tailoring the response be desired of streptococcal based-TTSs. Of note however, compared to native SAg, a higher dose may be required to accommodate for the reduced binding capabilities of $SpeC_{D203A}$ to MHC II within patients as demonstrated in

this work (**Figures 8, 9, 19, 20**) and in Phase I dose studies using comparable SEA_{D227A} (342). Nonetheless, even with the limited Vβ2 repertoire of SpeC (283, 366), the potent response of the induced cytotoxic T cells, in combination with the targeting moiety, still resulted in a dramatic reduction in tumour volume and metastatic disease within preclinical assessment (**Figure 25**).

There are some potential advantages, and disadvantages, in using TTSs for tumour immunotherapy that require further consideration. As described, the use of a mouse derived antibody as a targeting motif may result in HAMA responses since murine mAbs are highly immunogenic (153). This may limit the utility of subsequent treatments and thus the use of a humanized scFv containing TTS as developed in this work may provide clinical benefit. Second, bacterial SAgs are produced by bacteria that are often frequent colonizers in humans and thus many individuals will have pre-existing and neutralizing antibodies to many streptococcal and staphylococcal SAgs (417, 418). To overcome this issue, it is foreseen in future generations of 'combinatorial' TTSs with different SAgs, a panel could be generated such that individual patients could be screened for SAg neutralizing antibodies and then treated with an appropriate TTS. Early work in this area demonstrated that multiple SEs are capable of inducing T cell-mediated cytotoxicity against cancer cells (310); however, it is envisioned that the SAg panel would include members from the Group IV and Group V subclass of SAgs (248, 253, 377), as these subclasses contain only streptococcal SAgs and SEl SAgs, that collectively lack the emetic properties of the bona fide SEs (253, 262). Indeed, the SEl-M, SEl-N, and SEl-O SAgs from the *egc* have recently been demonstrated to induce T cell dependent killing of a broad panel of human tumour cells *in vitro* (419). Also, human serum levels of neutralizing antibodies against the *egc* SEs have been shown to be lower than those directed against the 'classic' SEs (264). In addition, each of the Group IV and V SAgs have a well-defined zinc-binding motif (248) involved in high-affinity MHC II binding (272, 273) that can be targeted for appropriate mutagenesis to prevent systemic immune activation as shown here and previously for SEA (328, 331). In anticipation of designing a panel of TTSs, the fusion construct was specifically designed within this study to include an additional restriction enzyme digestion site on the C-terminal end of the scFv5T4 fragment. This not only enables genetic replacement of SpeC with SAg

variations with the option to allow for 'fine-tuning' of the desired immune response, but it may also prove particularly beneficial in the future in the design of a TTS panel with a diversity of SAgs and/or targeting scFvs for a variety of TAAs. Indeed, an additional TTS has recently been designed, composed of a humanized scFv directed at the human TAA Her2/neu [designed from the Fab Herceptin (420)] and a Group VI SAg, SmeZ, with a high-affinity site mutation Asp^{204} to Ala for reduction in systemic immune cell activation in preclinical experimentation (McCormick laboratory, unpublished).

A third important limitation to TTS immunotherapy is that bacterial SAgs are well known to induce Vβ-specific T cell deletion or anergy (294), which includes $CD8^+$ T cells (296). Thus, repeated administration of the same TTS in humans may result in populations of non-responsive T cells. However, using the B16 model of melanoma, a sufficient resting period between treatments did restore immune responsiveness resulting in prolonged survival with repeated cycles of therapy (322). Nevertheless, this limitation could potentially be circumvented by the use of multiple SAgs with different Vβ profiles. From this work, $CD3^+$ T cells remained engrafted within the primary tumour after TTS treatment (**Figure 26**). Further investigation warrants the potential activation of this subset of T cells for full eradication of the cancer cells with either a repeated dose of SpeC-based TTS or an alternative Vβ-targeting SAg TTS. From the prospective of the TAA, similarly, a remaining and important issue with TTS immunotherapy is the targeting of a single TAA. An effective TTS would likely invoke a form of cancer immunoediting (71), and simple down regulation of the TAA may provide a means of escape. The TTS immunotherapy platform offers an approach for targeting a number of different TAAs, and it will be of future interest to engineer and combine TTSs that utilize SAgs with different Vβ profiles.

As with the majority of cancer therapeutics, it is anticipated that the TTS alone would not be sufficient to eradicate the entirety of the cancer. mAbs that target VEGF (*e.g.* Bevacizumab) and EGFR (*e.g.* Cetuximab or Panitumumab) have shown benefit in patients with mCRC (55, 56, 58), and a future area of interest would be to test TTS combination therapies with these treatments. Immunotherapies such as the CARs targeting CD19 have now demonstrated some extraordinary clinical outcomes in patients

with advanced B cell leukemia (119, 123, 421, 422). In addition, blocking immune system regulatory 'checkpoints' with antibodies (*e.g.* anti-CTLA-4 or anti-PD-1) is promising (423). In preclinical combinational therapies, SEA-based TTS directed at colon carcinoma antigen C215 has been shown to achieve synergistic antitumour effects, prolong long term survival and maintain compatibility with both immune modulators IL-2 (357) and IFN-α (344) and the well-established cytostatic drug docetaxel (341). Furthermore, this TTS in combination with antagonistic CTLA-4 mAb, demonstrated a favorable shift in the ratio between T effector and Treg cells in preclinical studies and that a CTL response was significantly prolonged, enhancing antitumour activity (361).

To conclude, within this work, a novel TTS treatment was designed and successfully generated as a soluble recombinant fusion protein in a bacterial protein expression system. The TTS fusion protein consisted of a humanized scFv targeting 5T4 and an altered SAg SpeC as a prototype to reduce systemic immune effects. Following *in vitro* evaluations, the scFv5T4 specifically targeted 5T4 and the TTS was shown to mediate PBMC activation and cytotoxicity of colon cancer cells. Lastly, the TTS demonstrated overall reduced total tumour volume and metastases burden in an established colon cancer *in vivo* model. This was, to our knowledge, the first streptococcal SAg to be employed in TTS immunotherapeutics, enabling the expansion of the current TTS repertoire. From this work, a platform of TTSs may be constructed, offering an additional approach for targeting a number of different TAAs, and combinations with alternate SAgs targeting various Vβ subsets of T cells. Additionally, this TTS may have prospective use in combinational therapies, overall increasing the selection of treatments to achieve synergistic and optimal anticancer effects. Evidence suggests that TTSs may represent a future 'off-the-shelf' therapy to harness Vβ-specific subsets of T cells without the requirement for manipulation of autologous T cells. This mode of action may be highly effective against tumours, in particular metastases, and those considered to be non-immunogenic. This work may help to guide the 'next generation' of TTSs for tailored cancer immunotherapy.

REFERENCES

1. 2014. World Cancer Factsheet. Cancer Research UK, London.

2. 2015. Cancer Fact sheet N°297. 297. World Health Organization.

3. **Canadian Cancer Society**. 2015. Canadian Cancer Society's Advisory Committee on Cancer Statistics. Canadian Cancer Statistics 1–151.

4. **Jemal A**, **Bray F**, **Center MM**, **Ferlay J**, **Ward E**, **Forman D**. 2011. Global cancer statistics. CA Cancer J Clin **61**:69–90.

5. 2015. SEER Cancer Statistics Review, 1975-2012. National Cancer Institute, Bethesda, MD.

6. **Benson AB**. 2007. Epidemiology, disease progression, and economic burden of colorectal cancer. J Manag Care Pharm **13**:S5–18.

7. **Kuriki K**, **Tajima K**. 2006. Increasing Incidence of Colorectal Cancer and the Preventive Strategy in Japan. Asian Pacific Journal of Cancer Prevention.

8. **Center MM**, **Jemal A**, **Ward E**. 2009. International Trends in Colorectal Cancer Incidence Rates. Cancer Epidemiology Biomarkers & Prevention **18**:1688–1694.

9. **Sobin LH**, **Gospodarowicz MK**, **Wittekind C**. 2011. TNM Classification of Malignant Tumours. John Wiley & Sons.

10. **Meyerhardt JA**, **Mayer RJ**. 2005. Systemic therapy for colorectal cancer. The New England Journal of Medicine **352**:476–487.

11. **O'Connell JB**, **Maggard MA**. 2004. Colon cancer survival rates with the new American Joint Committee on Cancer sixth edition staging. Journal of the National Cancer Institue.

12. **Haggar F**, **Boushey R**. 2009. Colorectal Cancer Epidemiology: Incidence, Mortality, Survival, and Risk Factors. Clinics in Colon and Rectal Surgery **22**:191–197.

13. **Giovannucci E**. 2002. Modifiable risk factors for colon cancer. - PubMed - NCBI. Gastroenterol Clin North Am **4**:925–943.

14. **Gonzalez-Pons M**, **Cruz-Correa M**. 2015. Colorectal Cancer Biomarkers: Where Are We Now? BioMed Research International **2015**:1–14.

15. **Schmoll HJ**, **Van Cutsem E**, **Stein A**, **Valentini V**, **Glimelius B**, **Haustermans K**, **Nordlinger B**, **van de Velde CJ**, **Balmana J**, **Regula J**, **Nagtegaal ID**, **Beets-Tan RG**, **Arnold D**, **Ciardiello F**, **Hoff P**, **Kerr D**, **Köhne CH**, **Labianca R**, **Price T**, **Scheithauer W**, **Sobrero A**, **Tabernero J**, **Aderka D**,

Barroso S, **Bodoky G**, **Douillard JY**, **Ghazaly El H**, **Gallardo J**, **Garin A**, **Glynne-Jones R**, **Jordan K**, **Meshcheryakov A**, **Papamichail D**, **Pfeiffer P**, **Souglakos I**, **Turhal S**, **Cervantes A**. 2012. ESMO Consensus Guidelines for management of patients with colon and rectal cancer. A personalized approach to clinical decision making. Annals of Oncology **23**:2479–2516.

16. **Fearon ER**, **Vogelstein B**. 1990. A genetic model for colorectal tumorigenesis. Cell **61**:759–767.

17. **Kheirelseid EAH**, **Miller N**, **Kerin MJ**. 2013. Molecular biology of colorectal cancer: Review of the literature. AJMB **03**:72–80.

18. **Markowitz SD**, **Bergtagnolli MM**. 2009. Molecular basis of colorectal cancer. The New England Journal of Medicine **361**:2449–2460.

19. **Lao VV**, **Grady WM**. 2011. Epigenetics and colorectal cancer. Nature Reviews Gastroenterology & Hepatology **8**:686–700.

20. **Kinzler KW**, **Vogelstein B**. 1996. Lessons from Hereditary Colorectal Cancer. Cell **87**:159–170.

21. **Arvelo F**, **Sojo F**, **Cotte C**. 2015. Biology of colorectal cancer. ecancermedicalscience **9**:DOI: 10.3332–ecancer.2015.520.

22. **Wood LD**, **Parsons DW**, **Jones S**, **Lin J**, **Sjoblom T**, **Leary RJ**, **Shen D**, **Boca SM**, **Barber T**, **Ptak J**, **Silliman N**, **Szabo S**, **Dezso Z**, **Ustyanksky V**, **Nikolskaya T**, **Nikolsky Y**, **Karchin R**, **Wilson PA**, **Kaminker JS**, **Zhang Z**, **Croshaw R**, **Willis J**, **Dawson D**, **Shipitsin M**, **Willson JKV**, **Sukumar S**, **Polyak K**, **Park BH**, **Pethiyagoda CL**, **Pant PVK**, **Ballinger DG**, **Sparks AB**, **Hartigan J**, **Smith DR**, **Suh E**, **Papadopoulos N**, **Buckhaults P**, **Markowitz SD**, **Parmigiani G**, **Kinzler KW**, **Velculescu VE**, **Vogelstein B**. 2007. The Genomic Landscapes of Human Breast and Colorectal Cancers. Science **318**:1108–1113.

23. **Vogelstein B**, **Kinzler KW**. 2002. The Genetic Basis of Human Cancer. McGraw Hill Professional 1–821.

24. **Herzig DO**, **Tsikitis VL**. 2014. Molecular markers for colon diagnosis, prognosis and targeted therapy. J Surg Oncol **111**:96–102.

25. **Pino MS**, **Chung DC**. 2010. The Chromosomal Instability Pathway in Colon Cancer. Gastroenterology **138**:2059–2072.

26. **Grady WM**. 2004. Genomic instability and colon cancer. Cancer Metastasis Rev **23**:11–27.

27. **Boland CR**, **Goel A**. 2010. Microsatellite Instability in Colorectal Cancer. Gastroenterology **138**:2073–2087.e3.

28. **Lynch HT**, **Smyrk T**, **Lynch JF**. 1998. Molecular Genetics and Clinical-Pathology Features of Hereditary Nonpolyposis Colorectal Carcinoma (Lynch Syndrome). Oncology **55**:103–108.

29. **Toyota M**, **Ahuja N**, **Ohe-Toyota M**, **Herman JG**, **Baylin SB**, **Issa JPJ**. 1999. CpG island methylator phenotype in colorectal cancer. Proceedings of the National Academy of Sciences **96**:8681–8686.

30. **Shen L**, **Toyota M**, **Kondo Y**, **Lin E**, **Zhang L**, **Guo Y**, **Hernandez NS**, **Chen X**, **Ahmed S**, **Konishi K**, **Hamilton SR**, **Issa JPJ**. 2007. Integrated genetic and epigenetic analysis identifies three different subclasses of colon cancer. Proc Natl Acad Sci **104**:18654–18659.

31. **Lynch HT**, **la Chapelle de A**. 2003. Hereditary colorectal cancer. The New England Journal of Medicine **348**:919–932.

32. **Jasperson KW**, **Tuohy TM**, **Neklason DW**, **Burt RW**. 2010. Hereditary and Familial Colon Cancer. Gastroenterology **138**:2044–2058.

33. **Cheadle JP**, **Sampson JR**. 2012. Exposing the MYtH about base excision repair and human inherited disease. Human Molecular Genetics **12**:R159–R165.

34. **Van Cutsem E**, **Nordlinger B**, **Adam R**, **Köhne C-H**, **Pozzo C**, **Poston G**, **Ychou M**, **Rougier P**. 2006. Towards a pan-European consensus on the treatment of patients with colorectal liver metastases. European Journal of Cancer **42**:2212–2221.

35. **Guyot F**, **Faivre J**, **Manfredi S**, **Meny B**, **Bonithon-Kopp C**, **Bouvier AM**. 2005. Time trends in the treatment and survival of recurrences from colorectal cancer. Annals of Oncology **16**:756–761.

36. **Pawlik TM**, **Choti MA**. 2007. Surgical Therapy for Colorectal Metastases to the Liver. J Gastrointest Surg **11**:1057–1077.

37. **Cassidy J**, **Tabernero J**, **Twelves C**, **Brunet R**, **Butts C**, **Conroy T**, **Debraud F**, **Figer A**, **Grossmann J**, **Sawada N**, **Schöffski P**, **Sobrero A**, **Van Cutsem E**, **Díaz-Rubio E**. 2004. XELOX (Capecitabine Plus Oxaliplatin): Active First-Line Therapy for Patients With Metastatic Colorectal Cancer. Journal of Clinical Oncology **22**:2084–2091.

38. **Pasetto LM**, **Jirillo A**, **G I**, **Rossi E**, **Paris MK**, **Monfardini S**. 2005. FOLFOX versus FOLFIRI: a comparison of regimens in the treatment of colorectal cancer metastases. Anticancer Research **25**:563–576.

39. **Tournigand C**, **André T**, **Achille E**, **Lledo G**, **Flesh M**, **Mery-Mignard D**, **Quinaux E**, **Couteau C**, **Buyse M**, **gan G**, **Landi B**, **Colin P**, **Louvet C**, **de Gramont A**. 2004. FOLFIRI Followed by FOLFOX6 or the Reverse Sequence in Advanced Colorectal Cancer: A Randomized GERCOR Study. Journal of

Clinical Oncology **22**:229–237.

40. **Marshall J**. 2005. The Role of Bevacizumab as First-line Therapy for Colon Cancer. Seminars in Oncology **32**:43–47.

41. **Grothey A**, **Flick ED**, **Cohn AL**, **Bekaii-Saab T**, **Bendell J**, **Kozloff M**, **Roach N**, **Mun Y**, **Fish S**, **Hurwitz H**. 2014. Bevacizumab exposure beyond first disease progression in patients with metastatic colorectal cancer: analyses of the ARIES observational cohort study. Pharmacoepidemiology and Drug Safety **23**:726–734.

42. **Van Cutsem E**, **Tabernero J**, **Lakomy R**, **Prenen H**, **Prausova J**, **Macarulla T**, **Ruff P**, **van Hazel GA**, **Moiseyenko V**, **Ferry D**, **McKendrick J**, **Polikoff J**, **Tellier A**, **Castan R**, **Allegra C**. 2012. Addition of Aflibercept to Fluorouracil, Leucovorin, and Irinotecan Improves Survival in a Phase III Randomized Trial in Patients With Metastatic Colorectal Cancer Previously Treated With an Oxaliplatin-Based Regimen. Journal of Clinical Oncology **30**:3499–3506.

43. **He K**, **Cui B**, **Li G**, **Wang H**, **Jin K**, **Teng L**. 2012. The effect of anti-VEGF drugs (bevacizumab and aflibercept) on the survival of patients with metastatic colorectal cancer (mCRC). OncoTargets and therapy **5**:59.

44. **Price TJ**, **Peeters M**, **Kim TW**, **Li J**, **Cascinu S**, **Ruff P**, **Suresh AS**, **Thomas A**, **Tjulandin S**, **Zhang K**, **Murugappan S**, **Sidhu R**. 2014. Panitumumab versus cetuximab in patients with chemotherapy-refractory wild-type KRAS exon 2 metastatic colorectal cancer (ASPECCT): a randomised, multicentre, open-label, non-inferiority phase 3 study. The Lancet **15**:569–579.

45. **Van Cutsem E**, **Köhne C-H**, **Láng I**, **Folprecht G**, **Nowacki MP**, **Cascinu S**, **Shchepotin I**, **Maurel J**, **Cunningham D**, **Tejpar S**, **Schlichting M**, **Zubel A**, **Celik I**, **Rougier P**, **Ciardiello F**. 2011. Cetuximab Plus Irinotecan, Fluorouracil, and Leucovorin As First-Line Treatment for Metastatic Colorectal Cancer: Updated Analysis of Overall Survival According to Tumor KRAS and BRAF Mutation Status. Journal of Clinical Oncology **29**:2011–2019.

46. **Nordlinger B**, **Van Cutsem E**, **Gruenberger T**, **Glimelius B**, **Poston G**, **Rougier P**, **Sobrero A**, **Ychou M**, **European Colorectal Metastases Treatment Group**, **Sixth International Colorectal Liver Metastases Workshop**. 2009. Combination of surgery and chemotherapy and the role of targeted agents in the treatment of patients with colorectal liver metastases: recommendations from an expert panel. Annals of Oncology **20**:985–992.

47. **Grothey A**, **Galanis E**. 2009. Targeting angiogenesis: progress with anti-VEGF treatment with large molecules. Nat Rev Clin Oncol **6**:507–518.

48. **Hurwitz HI**, **Yi J**, **Ince W**, **Novotny WF**, **Rosen O**. 2009. The clinical benefit of bevacizumab in metastatic colorectal cancer is independent of K-ras mutation status: analysis of a phase III study of bevacizumab with chemotherapy in

previously untreated metastatic colorectal cancer. The Oncologist **14**:22–28.

49. **Hurwitz HI**, **Tebbutt NC**, **Kabbinavar F**, **Giantonio BJ**, **Guan Z-Z**, **Mitchell L**, **Waterkamp D**, **Tabernero J**. 2013. Efficacy and Safety of Bevacizumab in Metastatic Colorectal Cancer: Pooled Analysis From Seven Randomized Controlled Trials. The Oncologist **18**:1004–1012.

50. **Feng Q-Y**. 2014. Anti-EGFR and anti-VEGF agents: Important targeted therapies of colorectal liver metastases. WJG **20**:4263.

51. **Bergers G**, **Hanahan D**. 2008. Modes of resistance to anti-angiogenic therapy. Nat Rev Cancer **8**:592–603.

52. **Golfinopoulos V**, **Salanti G**, **Pavlidis N**, **Ioannidis JP**. 2007. Survival and disease-progression benefits with treatment regimens for advanced colorectal cancer: a meta-analysis. The Lancet Oncology **8**:898–911.

53. **Cascinu S**. 2002. Raltitrexed plus oxaliplatin (TOMOX) as first-line chemotherapy for metastatic colorectal cancer. A phase II study of the Italian Group for the Study of Gastrointestinal Tract Carcinomas (GISCAD). Annals of Oncology **13**:716–720.

54. **Bennouna J**, **Sastre J**, **Arnold D**, **Österlund P**, **Greil R**, **Van Cutsem E**, **Moos von R**, **Viéitez JM**, **Bouché O**, **Borg C**, **Steffens C-C**, **Alonso-Orduña V**, **Schlichting C**, **Reyes-Rivera I**, **Bendahmane B**, **André T**, **Kubicka S**. 2013. Continuation of bevacizumab after first progression in metastatic colorectal cancer (ML18147): a randomised phase 3 trial. The Lancet Oncology **14**:29–37.

55. **Hurwitz H**, **Fehrenbacher L**, **Novotny W**. 2004. Bevacizumab plus irinotecan, fluorouracil, and leucovorin for metastatic colorectal cancer. The New England Journal of Medicine **350**:2335–2342.

56. **Van Cutsem E**, **Köhne CH**, **Hitre E**. 2009. Cetuximab and chemotherapy as initial treatment for metastatic colorectal cancer. The New England Journal of Medicine **360**:1408–1417.

57. **Heinemann V**, **Weikersthal von LF**, **Decker T**, **Kiani A**, **Vehling-Kaiser U**, **Al-Batran S-E**, **Heintges T**, **Lerchenmüller C**, **Kahl C**, **Seipelt G**, **Kullmann F**, **Stauch M**, **Scheithauer W**, **Hielscher J**, **Scholz M**, **Müller S**, **Link H**, **Niederle N**, **Rost A**, **Höffkes H-G**, **Moehler M**, **Lindig RU**, **Modest DP**, **Rossius L**, **Kirchner T**, **Jung A**, **Stintzing S**. 2014. FOLFIRI plus cetuximab versus FOLFIRI plus bevacizumab as first-line treatment for patients with metastatic colorectal cancer (FIRE-3): a randomised, open-label, phase 3 trial. The Lancet Oncology **15**:1065–1075.

58. **Karapetis CS**, **Khambata-Ford S**. 2008. K-ras mutations and benefit from cetuximab in advanced colorectal cancer. The New England Journal of Medicine **359**:1757–1765.

59. **Di Nicolantonio F**, **Martini M**, **Molinari F**, **Sartore-Bianchi A**, **Arena S**, **Saletti P**, **De Dosso S**, **Mazzucchelli L**, **Frattini M**, **Siena S**, **Bardelli A**. 2008. Wild-Type BRAF Is Required for Response to Panitumumab or Cetuximab in Metastatic Colorectal Cancer. Journal of Clinical Oncology **26**:5705–5712.

60. **Canada H**, **Sanofi-Aventis Canada Inc.** 2014. Product Monograph: ZALTRAP(TM): Aflibercept.

61. **Luo HY**, **Xu RH**. 2014. Predictive and prognostic biomarkers with therapeutic targets in advanced colorectal cancer. World journal of gastroenterology: WJG **20**:3858–3874.

62. **Ehlrich P**. 1909. Ueber den jetzigen Stand der Karzinomforschung . [Translate: About the current state of cancer research]. Ned Tijdschr Geneeskd **5**:273–290.

63. **Burnet FM**. 1970. The concept of immunological surveillance. Prog Exp Tumor Res **13**:1–27.

64. **Thomas L**. 1959. Delayed hypersensitivity in health and disease. Edited Lawrence. In: Cellular and Humoral Aspects of the Hypersensitive States 529–532.

65. **Klein G**. 1976. Immune surveillance--a powerful mechanism with a limited range. National Cancer Institute Monograph **44**:109–113.

66. **Mittal D**, **Gubin MM**, **Schreiber RD**, **Smyth MJ**. 2014. New insights into cancer immunoediting and its three component phases—elimination, equilibrium and escape. Current Opinion in Immunology **27**:16–25.

67. **Dunn GP**, **Bruce AT**, **Ikeda H**, **Old LJ**, **Schreiber RD**. 2002. Cancer immunoediting: from immunosurveillance to tumor escape. Nature Immunology **3**:991–998.

68. **Dunn GP**, **Old LJ**, **Schreiber RD**. 2004. The Immunobiology of Cancer Immunosurveillance and Immunoediting. Immunity **21**:137–148.

69. **O'Sullivan T**, **Saddawi-Konefka R**, **Vermi W**, **Koebel CM**, **Arthur C**, **White JM**, **Uppaluri R**, **Andrews DM**, **Ngiow SF**, **Teng MWL**, **Smyth MJ**, **Schreiber RD**, **Bui JD**. 2012. Cancer immunoediting by the innate immune system in the absence of adaptive immunity. Journal of Experimental Medicine **209**:1869–1882.

70. **Matsushita H**, **Vesely MD**, **Koboldt DC**, **Rickert CG**, **Uppaluri R**, **Magrini VJ**, **Arthur CD**, **White JM**, **Chen Y-S**, **Shea LK**, **Hundal J**, **Wendl MC**, **Demeter R**, **Wylie T**, **Allison JP**, **Smyth MJ**, **Old LJ**, **Mardis ER**, **Schreiber RD**. 2012. Cancer exome analysis reveals a T-cell-dependent mechanism of cancer immunoediting. Nature **482**:400–404.

71. **Vesely MD**, **Schreiber RD**. 2013. Cancer immunoediting: antigens, mechanisms, and implications to cancer immunotherapy. Annals of the New York Academy of Sciences **1284**:1–5.

72. **DuPage M**, **Mazumdar C**, **Schmidt LM**, **Cheung AF**, **Jacks T**. 2012. Expression of tumour-specific antigens underlies cancer immunoediting. Nature **482**:405–409.

73. **Boehmer von L**, **Mattle M**, **Bode P**, **Landshammer A**, **Schäfer C**, **Nuber N**, **Ritter G**, **Old L**, **Moch H**, **Schäfer N**, **Jäger E**, **Knuth A**, **van den Broek M**. 2013. NY-ESO-1–specific immunological pressure and escape in a patient with metastatic melanoma. Cancer Immunity … **13**:12.

74. **Nicholaou T**, **Chen W**, **Davis ID**, **Jackson HM**. 2011. Immunoediting and persistence of antigen-specific immunity in patients who have previously been vaccinated with NY-ESO-1 protein formulated in ISCOMATRIX™. Cancer Immunology Immunotherapy **60**:1625–1637.

75. **Dunn GP**, **Old LJ**, **Schreiber RD**. 2004. The Three Es of Cancer Immunoediting. Annu Rev Immunol **22**:329–360.

76. **Schreiber RD**, **Old LJ**, **Smyth MJ**. 2011. Cancer immunoediting: integrating immunity's roles in cancer suppression and promotion. Science **331**:1565–1570.

77. **Hanahan D**, **Weinberg RA**. 2011. Hallmarks of Cancer: The Next Generation. Cell **144**:646–674.

78. **Gajewski TF**, **Schreiber H**, **Fu Y-X**. 2013. Innate and adaptive immune cells in the tumor microenvironment. Nature Immunology **14**:1014–1022.

79. **Pancione M**, **Giordano G**, **Remo A**, **Febbraro A**, **Sabatino L**, **Manfrin E**, **Ceccarelli M**, **Colantuoni V**. 2014. Immune Escape Mechanisms in Colorectal Cancer Pathogenesis and Liver Metastasis. Journal of Immunology Research **2014**:1–11.

80. **Markman JL**, **Shiao SL**. 2015. Impact of the immune system and immunotherapy in colorectal cancer. Journal of gastrointestinal oncology **6**:208–223.

81. **Kloor M**, **Michel S**, **Knebel Doeberitz von M**. 2010. Immune evasion of microsatellite unstable colorectal cancers. International Journal of Cancer Journal international du cancer **127**:1001–1010.

82. **Grimm M**, **Gasser M**, **Bueter M**, **Strehl J**, **Wang J**, **Nichiporuk E**, **Meyer D**, **Germer CT**, **Waaga-Gasser AM**, **Thalheimer A**. 2010. Evaluation of immunological escape mechanisms in a mouse model of colorectal liver metastases. BMC Cancer **10**:82.

83. **Koch M**, **Beckhove P**, **op den Winkel J**, **Autenrieth D**, **Wagner P**, **Nummer D**, **Specht S**, **Antolovic D**, **Galindo L**, **Schmitz-Winnenthal FH**, **Schirrmacher V**, **B chler MW**, **Weitz JR**. 2006. Tumor Infiltrating T Lymphocytes in Colorectal Cancer. Annals of Surgery **244**:986–993.

84. **Halama N**, **Braun M**, **Kahlert C**, **Spille A**, **Quack C**, **Rahbari N**, **Koch M**, **Weitz J**, **Kloor M**, **Zoernig I**, **Schirmacher P**, **Brand K**, **Grabe N**, **Falk CS**. 2011. Natural Killer Cells are Scarce in Colorectal Carcinoma Tissue Despite High Levels of Chemokines and Cytokines. Clinical Cancer Research **17**:678–689.

85. **Bin Zhang**, **Wang Z**, **Wu L**, **Zhang M**, **Li W**, **Ding J**, **Zhu J**, **Wei H**, **Zhao K**. 2013. Circulating and Tumor-Infiltrating Myeloid-Derived Suppressor Cells in Patients with Colorectal Carcinoma. PLoS ONE **8**:e57114.

86. **Salama P**, **Phillips M**, **Grieu F**, **Morris M**, **Zeps N**, **Joseph D**, **Platell C**, **Iacopetta B**. 2009. Tumor-Infiltrating FOXP3+ T Regulatory Cells Show Strong Prognostic Significance in Colorectal Cancer. Journal of Clinical Oncology : official journal of the American Society of Clinical Oncology **27**:186–192.

87. **Fontenot JD**, **Gavin MA**, **Rudensky AY**. 2003. Foxp3 programs the development and function of CD4+CD25+ regulatory T cells. Nature Immunology **4**:330–336.

88. **Ladoire S**, **Martin F**, **Ghiringhelli F**. 2011. Prognostic role of FOXP3+ regulatory T cells infiltrating human carcinomas: the paradox of colorectal cancer. Cancer Immunology Immunotherapy **60**:909–918.

89. **Wu D**, **Wu P**, **Huang Q**, **Liu Y**, **Ye J**, **Huang J**. 2013. Interleukin-17: a promoter in colorectal cancer progression. Clinical and Developmental Immunology **2013**:1–7.

90. **Waldner MJ**, **Foersch S**, **Neurath MF**. 2012. Interleukin-6 - A Key Regulator of Colorectal Cancer Development. Int J Biol Sci **8**:1248–1253.

91. **Kloor M**. 2005. Immunoselective Pressure and Human Leukocyte Antigen Class I Antigen Machinery Defects in Microsatellite Unstable Colorectal Cancers. Cancer Res **65**:6418–6424.

92. **Droeser RA**, **Hirt C**, **Viehl CT**, **Frey DM**, **Nebiker C**, **Huber X**, **Zlobec I**, **Eppenberger-Castori S**, **Tzankov A**, **Rosso R**, **Zuber M**, **Muraro MG**, **Amicarella F**, **Cremonesi E**, **Heberer M**, **Iezzi G**, **Lugli A**, **Terracciano L**, **Sconocchia G**, **Oertli D**, **Spagnoli GC**, **Tornillo L**. 2013. Clinical impact of programmed cell death ligand 1 expression in colorectal cancer. European Journal of Cancer **49**:2233–2242.

93. **Rezaei N**. 2014. Cancer Immunology: Bench to Bedside Immunotherapy of Cancers. Springer Berlin Heidelberg, Berlin, Heidelberg.

94. **Mellman I**, **Coukos G**, **Dranoff G**. 2011. Cancer immunotherapy comes of age. Nature **480**:480–489.

95. **Bickels J**, **Kollender Y**, **Merinsky O**, **Meller I**. 2002. Coley's toxin: historical perspective. Isr Med Assoc J **4**:471–472.

96. **Coley WB**. 1910. The Treatment of Inoperable Sarcoma by Bacterial Toxins (the Mixed Toxins of the Streptococcus erysipelas and the Bacillus prodigiosus). Proceedings of the Royal Society of Medicine **3**:1.

97. **Coley WB**. 1893. The Treatment of Malignat Tumors by Repeated Inoculations of Erysipelas: With a Report of Ten Original Cases. The American Journal of the Medical Sciences **105**:487.

98. **Nauts HC**, **Swift WE**, **Coley BL**. 1946. The treatment of malignant tumors by bacterial toxins as developed by the late William B. Coley, MD, reviewed in the light of modern research. Cancer Res **6**:205–216.

99. **Kirkwood JM**, **Butterfield LH**, **Tarhini AA**, **Zarour HM**, **Kalinski P**, **Ferrone S**. 2012. Immunotherapy of cancer in 2012. CA Cancer J Clin **62**:309–335.

100. **Drake CG**, **Lipson EJ**, **Brahmer JR**. 2013. Breathing new life into immunotherapy: review of melanoma, lung and kidney cancer. Nat Rev Clin Oncol **11**:24–37.

101. **Pardoll D**, **Drake C**. 2012. Immunotherapy earns its spot in the ranks of cancer therapy. Journal of Experimental Medicine **209**:201–209.

102. **Gajewski T**. 2012. Cancer immunotherapy. Molecular Oncology **6**:242–250.

103. **Schiller JT**, **Lowy DR**. 2010. Vaccines to Prevent Infections by Oncoviruses *. Annu Rev Microbiol **64**:23–41.

104. **Hacohen N**, **Fritsch EF**, **Carter TA**, **Lando PA**, **Wu CJ**. 2013. Getting Personal with Neoantigen-Based Therapeutic Cancer Vaccines. Cancer Immunology Research **1**:11–15.

105. **Rosenberg SA**, **Yang JC**, **Restifo NP**. 2004. Cancer immunotherapy: moving beyond current vaccines. Nat Med **10**:909–915.

106. **Speiser DE**, **Miranda R**, **Zakarian A**, **Bachmann MF**, **McKall-Faienza K**, **Odermatt B**, **Hanahan D**, **Zinkernagel RM**, **Ohashi PS**. 1997. Self Antigens Expressed by Solid Tumors Do Not Efficiently Stimulate Naive or Activated T Cells: Implications for Immunotherapy. The Journal of Experimental Medicine **186**:645–653.

107. **Overwijk WW**, **Theoret MR**, **Finkelstein SE**, **Surman DR**, **de Jong LA**,

Vyth-Dreese FA, **Dellemijn TA**, **Antony PA**, **Spiess PJ**, **Palmer DC**, **Heimann DM**, **Klebanoff CA**, **Yu Z**, **Hwang LN**, **Feigenbaum L**, **Kruisbeek AM**, **Rosenberg SA**, **Restifo NP**. 2003. Tumor Regression and Autoimmunity after Reversal of a Functionally Tolerant State of Self-reactive CD8+ T Cells. The Journal of Experimental Medicine **198**:569–580.

108. **Clive KS**, **Tyler JA**, **Clifton GT**, **Holmes JP**, **Mittendorf EA**, **Ponniah S**, **Peoples GE**. 2010. Use of GM-CSF as an adjuvant with cancer vaccines: beneficial or detrimental? Expert Rev Vaccines **9**:519–525.

109. **Dranoff G**. 2004. Cytokines in cancer pathogenesis and cancer therapy. Nat Rev Cancer **4**:11–22.

110. **Schwartzentruber DJ**, **Lawson DH**, **Richards JM**, **Conry RM**, **Miller DM**, **Treisman J**, **Gailani F**, **Riley L**, **Conlon K**, **Pockaj B**, **Kendra KL**, **White RL**, **Gonzalez R**, **Kuzel TM**, **Curti B**, **Leming PD**, **Whitman ED**, **Balkissoon J**, **Reintgen DS**, **Kaufman HL**, **Marincola FM**, **Merino MJ**, **Rosenberg SA**, **Choyke P**, **Vena D**, **Hwu P**. 2011. gp100 peptide vaccine and interleukin-2 in patients with advanced melanoma. The New England Journal of Medicine **364**:2119–2127.

111. **Binder DC**, **Schreiber H**. 2014. Dual blockade of PD-1 and CTLA-4 combined with tumor vaccine effectively restores T-cell rejection function in tumors—letter. Cancer Res **74**:632.

112. **Rahma OE**, **Khleif SN**. 2011. Therapeutic vaccines for gastrointestinal cancers. Gastroenterology & hepatology **7**:517–527.

113. **Schulze T**, **Kemmner W**, **Weitz J**, **Wernecke KD**, **Schirrmacher V**, **Schlag PM**. 2008. Efficiency of adjuvant active specific immunization with Newcastle disease virus modified tumor cells in colorectal cancer patients following resection of liver metastases: results of a prospective randomized trial. Cancer Immunol Immunother **58**:61–69.

114. **Amin M**, **Lockhart AC**. 2015. The potential role of immunotherapy to treat colorectal cancer. Expert Opin Investig Drugs **24**:329–344.

115. **Rosenberg SA**, **Restifo NP**. 2015. Adoptive cell transfer as personalized immunotherapy for human cancer. Science **348**:62–68.

116. **June CH**. 2007. Principles of adoptive T cell cancer therapy. Journal of Clinical Investigation **117**:1204–1212.

117. **Dudley ME**, **Wunderlich JR**, **Robbins PF**, **Yang JC**. 2002. Cancer regression and autoimmunity in patients after clonal repopulation with antitumor lymphocytes. Science **298**:850–854.

118. **Barrett DM**, **Singh N**, **Porter DL**, **Grupp SA**, **June CH**. 2014. Chimeric

Antigen Receptor Therapy for Cancer. Annu Rev Med **65**:333–347.

119. **Kalos M**, **Levine BL**, **Porter DL**, **Katz S**, **Grupp SA**, **Bagg A**, **June CH**. 2011. T cells with chimeric antigen receptors have potent antitumor effects and can establish memory in patients with advanced leukemia. Science Translational Medicine **3**:95ra73.

120. **Robbins PF**, **Morgan RA**, **Feldman SA**, **Yang JC**, **Sherry RM**, **Dudley ME**, **Wunderlich JR**, **Nahvi AV**, **Helman LJ**, **Mackall CL**, **Kammula US**, **Hughes MS**, **Restifo NP**, **Raffeld M**, **Lee CCR**, **Levy CL**, **Li YF**, **El-Gamil M**, **Schwarz SL**, **Laurencot C**, **Rosenberg SA**. 2011. Tumor Regression in Patients With Metastatic Synovial Cell Sarcoma and Melanoma Using Genetically Engineered Lymphocytes Reactive With NY-ESO-1. Journal of Clinical Oncology **29**:917–924.

121. **Porter DL**, **Kalos M**, **Zheng Z**, **Levine BL**, **June CH**. 2011. Chimeric Antigen Receptor Therapy for B-cell Malignancies. Journal of Cancer **2**:331–332.

122. **Maude SL**, **Frey N**, **Shaw PA**, **Aplenc R**, **Barrett DM**, **Bunin NJ**, **Chew A**, **Gonzalez VE**, **Zheng Z**, **Lacey SF**, **Mahnke YD**, **Melenhorst JJ**, **Rheingold SR**, **Shen A**, **Teachey DT**, **Levine BL**, **June CH**, **Porter DL**, **Grupp SA**. 2014. Chimeric Antigen Receptor T Cells for Sustained Remissions in Leukemia. The New England Journal of Medicine **371**:1507–1517.

123. **Porter DL**, **Levine BL**, **Kalos M**, **Bagg A**. 2011. Chimeric antigen receptor–modified T cells in chronic lymphoid leukemia. The New England Journal of Medicine **365**:725–733.

124. **Maus MV**, **Grupp SA**, **Porter DL**, **June CH**. 2014. Antibody-modified T cells: CARs take the front seat for hematologic malignancies. Blood **123**:2625–2635.

125. **Gogas H**, **Ioannovich J**, **Dafni U**, **Stavropoulou-Giokas C**, **Frangia K**, **Tsoutsos D**, **Panagiotou P**, **Polyzos A**, **Papadopoulos O**, **Stratigos A**, **Markopoulos C**, **Bafaloukos D**, **Pectasides D**, **Fountzilas G**, **Kirkwood JM**. 2006. Prognostic Significance of Autoimmunity during Treatment of Melanoma with Interferon. The New England Journal of Medicine **354**:709–718.

126. **Fyfe G**, **Fisher RI**, **Rosenberg SA**, **Sznol M**, **Parkinson DR**, **Louie AC**. 1995. Results of treatment of 255 patients with metastatic renal cell carcinoma who received high-dose recombinant interleukin-2 therapy. Journal of Clinical Oncology **13**:688–696.

127. **Rosenberg SA**, **Lotze MT**, **Yang JC**, **Topalian SL**, **Chang AE**, **Schwartzentruber DJ**, **Aebersold P**, **Leitman S**, **Linehan WM**, **Seipp CA**, **White DE**, **Steinberg SM**. 1993. Prospective Randomized Trial of High-Dose Interleukin-2 Alone or in Conjunction With Lymphokine-Activated Killer Cells for the Treatment of Patients With Advanced Cancer. Journal of the National Cancer Institute **85**:622–632.

128. **Correale P**, **Tagliaferri P**, **Fioravanti A**, **Del Vecchio MT**, **Remondo C**, **Montagnani F**, **Rotundo MS**, **Ginanneschi C**, **Martellucci I**, **Francini E**, **Cusi MG**, **Tassone P**, **Francini G**. 2008. Immunity Feedback and Clinical Outcome in Colon Cancer Patients Undergoing Chemoimmunotherapy with Gemcitabine + FOLFOX followed by Subcutaneous Granulocyte Macrophage Colony-Stimulating Factor and Aldesleukin (GOLFIG-1 Trial). Clinical Cancer Research **14**:4192–4199.

129. **Correale P**, **Botta C**, **Rotundo MS**, **Guglielmo A**, **Conca R**, **Licchetta A**, **Pastina P**, **Bestoso E**, **Ciliberto D**, **Cusi MG**, **Fioravanti A**, **Guidelli GM**, **Bianco MT**, **Misso G**, **Martino E**, **Caraglia M**, **Tassone P**, **Mini E**, **Mantovani G**, **Ridolfi R**, **Pirtoli L**, **Tagliaferri P**. 2014. Gemcitabine, Oxaliplatin, Levofolinate, 5-Fluorouracil, Granulocyte-Macrophage Colony-Stimulating Factor, and Interleukin-2 (GOLFIG) Versus FOLFOX Chemotherapy in Metastatic Colorectal Cancer Patients. Journal of Immunotherapy **37**:26–35.

130. **Parry RV**, **Chemnitz JM**, **Frauwirth KA**, **Lanfranco AR**, **Braunstein I**, **Kobayashi SV**, **Linsley PS**, **Thompson CB**, **Riley JL**. 2005. CTLA-4 and PD-1 Receptors Inhibit T-Cell Activation by Distinct Mechanisms. Molecular and Cellular Biology **25**:9543–9553.

131. **Wing K**, **Onishi Y**, **Prieto-Martin P**, **Yamaguchi T**, **Miyara M**, **Fehervari Z**, **Nomura T**, **Sakaguchi S**. 2008. CTLA-4 Control over Foxp3+ Regulatory T Cell Function. Science **322**:271–275.

132. **Chambers CA**, **Kuhns MS**, **Egen JG**, **Allison JP**. 2001. CTLA-4-Mediated Inhibition in Regulation of T Cell Responses: Mechanisms and Manipulation in Tumor Immunotherapy. Annu Rev Immunol **19**:565–594.

133. **Prieto PA**, **Yang JC**, **Sherry RM**, **Hughes MS**, **Kammula US**, **White DE**, **Levy CL**, **Rosenberg SA**, **Phan GQ**. 2012. CTLA-4 blockade with ipilimumab: long-term follow-up of 177 patients with metastatic melanoma. Clinical Cancer Research **18**:2039–2047.

134. **Graziani G**, **Tentori L**, **Navarra P**. 2012. Ipilimumab: a novel immunostimulatory monoclonal antibody for the treatment of cancer. Pharmacological Research **65**:9–22.

135. **Leach DR**, **Krummel MF**, **Allison JP**. 1996. Enhancement of Antitumor Immunity by CTLA-4 Blockade. Science **271**:1734–1736.

136. **Hodi FS**, **O'Day SJ**, **McDermott DF**, **Weber RW**, **Sosman JA**, **Haanen JB**, **Gonzalez R**, **Robert C**, **Schadendorf D**, **Hassel JC**, **Arkerley W**, **van den Eertwegh AJM**, **Lutzky J**, **Lorigan P**, **Vaubel JM**, **Linette GP**, **Hogg D**, **Ottensmeier CH**, **Lebbe C**, **Peschel C**, **Quirt I**, **Clark JI**, **Wolchok JD**, **Weber JS**, **Tian J**, **Yellin MJ**, **Nichol GM**, **Hoos A**, **Urba WJ**. 2010. Improved survival with ipilimumab in patients with metastatic melanoma. The New England Journal of Medicine **363**:711–723.

137. **Lipson EJ**, **Drake CG**. 2011. Ipilimumab: An Anti-CTLA-4 Antibody for Metastatic Melanoma. Clinical Cancer Research **17**:6958–6962.

138. **Graziani G**, **Tentori L**, **Navarra P**. 2014. Monoclonal Antibodies to CTLA-4 with Focus on Ipilimumab. Springer-Verlag Wien 233–258.

139. **Y Ishida YAKSTH**. 1992. Induced expression of PD-1, a novel member of the immunoglobulin gene superfamily, upon programmed cell death. The EMBO Journal **11**:3887.

140. **Keir ME**, **Butte MJ**, **Freeman GJ**, **Sharpe AH**. 2008. PD-1 and Its Ligands in Tolerance and Immunity. Annu Rev Immunol **26**:677–704.

141. **Gao Q**, **Wang XY**, **Qiu SJ**, **Yamato I**, **Sho M**, **Nakajima Y**, **Zhou J**, **Li BZ**, **Shi YH**, **Xiao YS**, **Xu Y**, **Fan J**. 2009. Overexpression of PD-L1 Significantly Associates with Tumor Aggressiveness and Postoperative Recurrence in Human Hepatocellular Carcinoma. Clinical Cancer Research **15**:971–979.

142. **Gadiot J**, **Hooijkaas AI**, **Kaiser A**, **van Tinteren H**, **van Boven H**, **Blank C**. 2011. Overall survival and PD-L1 expression in metastasized malignant melanoma. Cancer **117**:2192–2201.

143. **Ohaegbulam KC**, **Assal A**, **Lazar-Molnar E**, **Yao Y**, **Zang X**. 2015. Human cancer immunotherapy with antibodies to the PD-1 and PD-L1 pathway. Trends in Molecular Medicine **21**:24–33.

144. **Herbst RS**, **Soria J-C**, **Kowanetz M**, **Fine GD**, **Hamid O**, **Gordon MS**, **Sosman JA**, **McDermott DF**, **Powderly JD**, **Gettinger SN**, **Kohrt HEK**, **Horn L**, **Lawrence DP**, **Rost S**, **Leabman M**, **Xiao Y**, **Mokatrin A**, **Koeppen H**, **Hegde PS**, **Mellman I**, **Chen DS**, **Hodi FS**. 2014. Predictive correlates of response to the anti-PD-L1 antibody MPDL3280A in cancer patients. Nature **515**:563–567.

145. **Scott AM**, **Wolchok JD**, **Old LJ**. 2012. Antibody therapy of cancer. Nat Rev Cancer **12**:278–287.

146. **Strebhardt K**, **Ullrich A**. 2008. Paul Ehrlich's magic bullet concept: 100 years of progress. Nat Rev Cancer **8**:473–480.

147. **Köhler G**, **Milstein C**. 1975. Continuous cultures of fused cells secreting antibody of predefined specificity. Nature **256**:495–497.

148. **Weiner LM**, **Surana R**, **Wang S**. 2010. Monoclonal antibodies: versatile platforms for cancer immunotherapy. Nat Rev Immunol **10**:317–327.

149. **Hughes B**. 2010. Antibody–drug conjugates for cancer: poised to deliver? Nat Rev Drug Discov **9**:665–667.

150. **Scott AM**, **Allison JP**, **Wolchok JD**. 2012. Monoclonal antibodies in cancer therapy. Cancer Immunity … **12**:14–22.

151. **Carter PJ**. 2006. Potent antibody therapeutics by design. Nat Rev Immunol **6**:343–357.

152. **Epenetos AA**, **Snook D**, **Durbin H**, **Johnson PM**, **Taylor-Papadimitriou J**. 1986. Limitations of radiolabeled monoclonal antibodies for localization of human neoplasms. Cancer Res **46**:3183–3191.

153. **Swann PG**, **Tolnay M**, **Muthukkumar S**, **Shapiro MA**, **Rellahan BL**, **Clouse KA**. 2008. Considerations for the development of therapeutic monoclonal antibodies. Current Opinion in Immunology **20**:493–499.

154. **Oldham RK**, **Dillman RO**. 2008. Monoclonal Antibodies in Cancer Therapy: 25 Years of Progress. Journal of Clinical Oncology **26**:1774–1777.

155. **Courtenay-Luck NS**, **Epenetos AA**, **Moore R**, **Larche M**, **Pectasides D**, **Dhokia B**, **Ritter MA**. 1986. Development of primary and secondary immune responses to mouse monoclonal antibodies used in the diagnosis and therapy of malignant neoplasms. Cancer Res **46**:6489–6493.

156. **Shawler DL**, **Bartholomew RM**, **Smith LM**, **Dillman RO**. 1985. Human immune response to multiple injections of murine monoclonal IgG. Journal of Immunology (Baltimore, Md : 1950) **135**:1530–1535.

157. **Clark M**. 2000. Antibody humanization: a case of the “Emperor”s new clothes’? Immunology Today **21**:397–402.

158. **Hwang WYK**, **Foote J**. 2005. Immunogenicity of engineered antibodies. Methods **36**:3–10.

159. **Shapiro MA**, **Swann PG**, **Ricci MS**. 2014. Regulatory Considerations in the Development of Monoclonal Antibodies for Diagnosis and Therapy, pp. 1231–1262. *In* Dübel, S, Reichert, JM (eds.), Handbook of Therapeutic Antibodies. Wiley-VCH Verlag GmbH & Co. KGaA, Weinheim, Germany.

160. **Glennie MJ**, **Johnson PWM**. 2000. Clinical trials of antibody therapy. Immunology Today **21**:403–410.

161. **Morrison SL**, **Johnson MJ**, **Herzenberg LA**, **Oi VT**. 1984. Chimeric human antibody molecules: mouse antigen-binding domains with human constant region domains. Proc Natl Acad Sci USA **81**:6851–6855.

162. **Boulianne GL**, **Hozumi N**, **Shulman MJ**. 1984. Production of functional chimaeric mouse/human antibody. Nature **312**:643–646.

163. **Riechmann L**, **Clark M**, **Waldmann H**, **Winter G**. 1988. Reshaping human

antibodies for therapy. Nature **332**:323–329.

164. **Jones PT**, **Dear PH**, **Foote J**, **Neuberger MS**, **Winter G**. 1986. Replacing the complementarity-determining regions in a human antibody with those from a mouse. Nature **321**:522–525.

165. **Gonzales NR**, **De Pascalis R**, **Schlom J**, **Kashmiri SVS**. 2005. Minimizing the Immunogenicity of Antibodies for Clinical Application. Tumor Biol **26**:31–43.

166. **Hoogenboom HR**. 2005. Selecting and screening recombinant antibody libraries. Nature Biotechnology **23**:1105–1116.

167. **de Haard HJ**, **van Neer N**, **Reurs A**, **Hufton SE**, **Roovers RC**, **Henderikx P**, **de Bruine AP**, **Arends JW**, **Hoogenboom HR**. 1999. A Large Non-immunized Human Fab Fragment Phage Library That Permits Rapid Isolation and Kinetic Analysis of High Affinity Antibodies. Journal of Biological Chemistry **274**:18218–18230.

168. **Griffiths AD**, **Mamqvist M**, **Marks JD**, **Bye JM**, **Embleton MJ**, **McCafferty J**, **Baier M**, **Holligner KP**, **Gorick BD**, **Hughes-Jones NC**, **Hoogenboom HR**, **Winter G**. 1993. Human anti-self antibodies with high specificity from phage display libraries. The EMBO Journal **12**:725–734.

169. **Fishwild DM**, **O'Donnell SL**, **Bengoechea T**, **Hudson DV**, **Harding F**, **Bernhard SL**, **Jones D**, **Kay RM**, **Higgins KM**, **Schramm SR**, **Lonberg N**. 1996. High-avidity human IgGκ monoclonal antibodies from a novel strain of minilocus transgenic mice. Nature Biotechnology **14**:845–851.

170. **Nicholson IC**, **Zou X**, **Popov AV**, **Cook GP**, **Corps EM**, **Humphries S**, **Ayling C**, **Goyenechea B**, **Xian J**, **Taussig MJ**, **Neuberger MS**, **Brüggemann M**. 1999. Antibody Repertoires of Four- and Five-Feature Translocus Mice Carrying Human Immunoglobulin Heavy Chain and κ and λ Light Chain Yeast Artificial Chromosomes. The Journal of Immunology **163**:6898–6906.

171. **Mendez MJ**, **Green LL**, **Corvalan JRF**, **Jia X-C**, **Maynard-Currie CE**, **Yang X-D**, **Gallo ML**, **Louie DM**, **Lee DV**, **Erickson KL**, **Luna J**, **Roy CMN**, **Abderrahim H**, **Kirschenbaum F**, **Noguchi M**, **Smith DH**, **Fukushima A**, **Hales JF**, **Finer MH**, **Davis CG**, **Zsebo KM**, **Jakobovits A**. 1997. Functional transplant of megabase human immunoglobulin loci recapitulates human antibody response in mice. Nat Genet **15**:146–156.

172. **Lonberg N**. 2005. Human antibodies from transgenic animals. Nature Biotechnology **23**:1117–1125.

173. **Thurber GM**, **Zajic SC**, **Wittrup KD**. 2007. Theoretic Criteria for Antibody Penetration into Solid Tumors and Micrometastases. Journal of Nuclear Medicine **48**:995–999.

174. **Jain RK**, **Baxter LT**. 1988. Mechanisms of heterogeneous distribution of monoclonal antibodies and other macromolecules in tumors: significance of elevated interstitial pressure. Cancer Res **48**:7022–7032.

175. **Jain RK**. 1990. Physiological barriers to delivery of monoclonal antibodies and other macromolecules in tumors. Cancer Res **50**:814s–819s.

176. **Foltz IN**, **Karow M**, **Wasserman SM**. 2013. Evolution and Emergence of Therapeutic Monoclonal Antibodies: What Cardiologists Need to Know. Circulation **127**:2222–2230.

177. **Rudnick SI**, **Adams GP**. 2009. Affinity and avidity in antibody-based tumor targeting. Cancer biotherapy and radiopharmaceuticals **24**:155–161.

178. **Fujimori K**, **Covell DG**, **Fletcher JE**, **Weinstein JN**. 1989. Modeling analysis of the global and microscopic distribution of immunoglobulin G, F(ab′)2, and Fab in tumors. Cancer Res **49**:5656–5663.

179. **Carter P**. 2001. Improving the efficacy of antibody-based cancer therapies. Nat Rev Cancer **1**:118–129.

180. **Shields RL**, **Namenuk AK**, **Hong K**, **Meng YG**, **Rae J**, **Briggs J**, **Xie D**, **Lai J**, **Stadlen A**, **Li B**, **Fox JA**, **Presta LG**. 2000. High Resolution Mapping of the Binding Site on Human IgG1 for Fcgamma RI, Fcgamma RII, Fcgamma RIII, and FcRn and Design of IgG1 Variants with Improved Binding to the Fcgamma R. Journal of Biological Chemistry **276**:6591–6604.

181. **Vaccaro C**, **Zhou J**, **Ober RJ**, **Ward ES**. 2005. Engineering the Fc region of immunoglobulin G to modulate in vivo antibody levels. Nature Biotechnology **23**:1283–1288.

182. **Salfeld JG**. 2007. Isotype selection in antibody engineering. Nature Biotechnology **25**:1369–1372.

183. **Holliger P**, **Hudson PJ**. 2005. Engineered antibody fragments and the rise of single domains. Nature Biotechnology **23**:1126–1136.

184. **Baeuerle PA**, **Kufer P**, **Lutterbüse R**. 2003. Bispecific antibodies for polyclonal T-cell engagement. Current Opinion in Molecular Therapeutics **5**:413–419.

185. **Grothey A**. 2010. EGFR Antibodies in Colorectal Cancer: Where Do They Belong? Journal of Clinical Oncology **28**:4668–4670.

186. **Broadbridge VT**, **Karapetis CS**, **Price TJ**. 2012. Cetuximab in metastatic colorectal cancer. Expert Rev Anticancer Ther **12**:555–565.

187. **Amado RG**, **Wolf M**, **Peeters M**, **Van Cutsem E**, **Siena S**, **Freeman DJ**, **Juan**

T, **Sikorski R**, **Suggs S**, **Radinsky R**, **Patterson SD**, **Chang DD**. 2008. Wild-Type KRAS Is Required for Panitumumab Efficacy in Patients With Metastatic Colorectal Cancer. Journal of Clinical Oncology **26**:1626–1634.

188. **Boon T**, **Van den Eynde B**. 2003. Tumour immunology. Current Opinion in Immunology **15**:129–130.

189. **Stern PL**. 2014. Immunotherapies Targeting a Tumor-Associated Antigen, 5T4 Oncofetal Glycoprotein, pp. 409–425. *In* Rezaei, N (ed.), Cancer Immunology: Bench to Bedside Immunotherapy of Cancers. Springer Berlin Heidelberg, Berlin, Heidelberg.

190. **Gires O**, **Seliger B**. 2009. Tumor-Associated Antigens. John Wiley & Sons.

191. **Zarour HM**, **DeLeo A**, **Finn OJ**, **Storkus WJ**. 2003. Categories of Tumor Antigens, 6 ed. Holland-Frei Cancer Medicine, BC Decker.

192. **Minenkova O**, **Pucci A**, **Pavoni E**, **De Tomassi A**, **Fortugno P**, **Gargano N**, **Cianfriglia M**, **Barca S**, **De Placido S**, **Martignetti A**, **Felici F**, **Cortese R**, **Monaci P**. 2003. Identification of tumor-associated antigens by screening phage-displayed human cDNA libraries with sera from tumor patients. International Journal of Cancer Journal international du cancer **106**:534–544.

193. **Durrant LG**, **McDowell KM**, **Holmes RA**, **Liu DT**. 1994. Screening of monoclonal antibodies recognizing oncofetal antigens for isolation of trophoblasts from maternal blood for prenatal diagnosis. Prenatal Diagnosis **14**:131–140.

194. **N Hole PLS**. 1988. A 72 kD trophoblast glycoprotein defined by a monoclonal antibody. Br J Cancer **57**:239.

195. **Viatte S**, **Alves PM**, **Romero P**. 2006. Reverse immunology approach for the identification of CD8 T-cell-defined antigens: Advantages and hurdles. Immunology and Cell Biology **84**:318–330.

196. **Southall PJ**, **Boxer GM**, **Bagshawe KD**, **Hole N**, **Bromley M**, **Stern PL**. 1990. Immunohistological distribution of 5T4 antigen in normal and malignant tissues. Br J Cancer **61**:89.

197. **Connor ME**, **Stern PL**. 1990. Loss of MHC class-I expression in cervical carcinomas. International Journal of Cancer Journal international du cancer **46**:1029–1034.

198. **Starzynska T**, **Rahi V**, **Stern PL**. 1992. The expression of 5T4 antigen in colorectal and gastric carcinoma. Br J Cancer **66**:867.

199. **Starzynska T**, **Marsh PJ**, **Schofield PF**, **Roberts SA**, **Myers KA**, **Stern PL**. 1994. Prognostic significance of 5T4 oncofetal antigen expression in colorectal

carcinoma. Br J Cancer **69**:899.

200. **Mulder WM**, **Stern PL**, **Stukart MJ**, **de Windt E**, **Butzelaar RM**, **Meijer S**, **Adér HJ**, **Claessen AM**, **Vermorken JB**, **Meijer CJ**, **Wagstaff J**, **Scheper RJ**, **Bloemena E**. 1997. Low intercellular adhesion molecule 1 and high 5T4 expression on tumor cells correlate with reduced disease-free survival in colorectal carcinoma patients. Clinical Cancer Research **3**:1923–1930.

201. **Naganuma H**, **Kono K**, **Mori Y**, **Takayoshi S**, **Stern PL**, **Tasaka K**, **Matsumoto Y**. 2002. Oncofetal antigen 5T4 expression as a prognostic factor in patients with gastric cancer. Anticancer Research **22**:1033–1038.

202. **Starzynska T**, **Wiechowska-Kozlowska A**, **Mariiez K**, **Bromley M**, **Roberts SA**, **Lawniczak M**, **Kolodziej B**, **Zyluk A**, **Stern PL**. 1998. 5T4 oncofetal antigen in gastric carcinoma and its clinical significance. European Journal of Gastroenterology & Hepatology **10**:479.

203. **Damelin M**, **Geles KG**, **Follettie MT**, **Yuan P**, **Baxter M**, **Golas J**, **DiJoseph JF**, **Karnoub M**, **Huang S**, **Diesl V**, **Behrens C**, **Choe SE**, **Rios C**, **Gruzas J**, **Sridharan L**, **Dougher M**, **Kunz A**, **Hamann PR**, **Evans D**, **Armellino D**, **Khandke K**, **Marquette K**, **Tchistiakova L**, **Boghaert ER**, **Abraham RT**, **Wistuba II**, **Zhou BBS**. 2011. Delineation of a Cellular Hierarchy in Lung Cancer Reveals an Oncofetal Antigen Expressed on Tumor-Initiating Cells. Cancer Res **71**:4236–4246.

204. **McGinn OJ**, **Marinov G**, **Sawan S**, **Stern PL**. 2012. CXCL12 receptor preference, signal transduction, biological response and the expression of 5T4 oncofoetal glycoprotein. Journal of Cell Science **125**:5467–5478.

205. **Ali A**, **Langdon J**, **Stern P**, **Partridge M**. 2001. The pattern of expression of the 5T4 oncofoetal antigen on normal, dysplastic and malignant oral mucosa. Oral Oncol **37**:57–64.

206. **Wrigley E**, **McGown AT**, **Rennison J**, **Swindell R**, **Crowther D**, **Starzynska T**, **Stern PL**. 1995. 5T4 oncofetal antigen expression in ovarian carcinoma. Int J Gynecol Cancer **5**:269–274.

207. **Abern M**, **Kaufman H**, **Latchamsetty K**. 2011. An update on TroVax(R) for the treatment of progressive castration-resistant prostate cancer. OncoTargets and therapy **4**:33.

208. **Griffiths RW**, **Gilham DE**, **Dangoor A**, **Ramani V**, **Clarke NW**, **Stern PL**, **Hawkins RE**. 2005. Expression of the 5T4 oncofoetal antigen in renal cell carcinoma: a potential target for T-cell-based immunotherapy. Br J Cancer **93**:670–677.

209. **Eisen T**, **Hedlund G**, **Forsberg G**, **Hawkins R**. 2014. Naptumomab Estafenatox: Targeted Immunotherapy with a Novel Immunotoxin. Curr Oncol

Rep **16**:370–6.

210. **Myers KA**, **Rahi-Saund V**, **Davison M**, **Young JA**, **Cheater AJ**, **Stern PL**. 1994. Isolation of a cDNA encoding 5T4 oncofetal trophoblast glycoprotein. An antigen associated with metastasis contains leucine-rich repeats. The Journal of Biological Chemistry **269**:9319–9324.

211. **Zhao Y**, **Malinauskas T**, **Harlos K**, **Jones EY**. 2014. Structural Insights into the Inhibition of Wnt Signaling by Cancer Antigen 5T4/Wnt-Activated Inhibitory Factor 1. Structure **22**:1–9.

212. **King KW**, **Sheppard FC**, **Westwater C**, **Stern PL**, **Myers KA**. 1999. Organisation of the mouse and human 5T4 oncofoetal leucine-rich glycoprotein genes and expression in foetal and adult murine tissues. Biochim Biophys Acta **1445**:257–270.

213. **Shaw DM**, **Woods AM**, **Myers KA**, **Westwater C**, **Rahi-Saund V**, **Davies MJ**, **Renouf DV**, **Hounsell EF**, **Stern PL**. 2002. Glycosylation and epitope mapping of the 5T4 glycoprotein oncofoetal antigen. Biochem J **363**:137–145.

214. **Kobe B**. 2001. The leucine-rich repeat as a protein recognition motif. Current Opinion in Structural Biology **11**:725–732.

215. **Awan A**, **Lucic MR**, **Shaw DM**, **Sheppard F**, **Westwater C**, **Lyons SA**, **Stern PL**. 2002. 5T4 interacts with TIP-2/GIPC, a PDZ protein, with implications for metastasis. Biochem Biophys Res Commun **290**:1030–1036.

216. **De Vries L**, **Lou X**, **Zhao G**, **Zheng B**, **Farquhar MG**. 1998. GIPC, a PDZ domain containing protein, interacts specifically with the C terminus of RGS-GAIP. Proceedings of the National Academy of Sciences **95**:12340–12345.

217. **Ward CM**, **Eastham AM**, **Stern PL**. 2006. Cell surface 5T4 antigen is transiently upregulated during early human embryonic stem cell differentiation: effect of 5T4 phenotype on neural lineage formation. Exp Cell Res **312**:1713–1726.

218. **Ward CM**, **Barrow K**, **Woods AM**, **Stern PL**. 2003. The 5T4 oncofoetal antigen is an early differentiation marker of mouse ES cells and its absence is a useful means to assess pluripotency. Journal of Cell Science **116**:4533–4542.

219. **Eastham AM**, **Spencer H**, **Soncin F**, **Ritson S**, **Merry CLR**, **Stern PL**, **Ward CM**. 2007. Epithelial-mesenchymal transition events during human embryonic stem cell differentiation. Cancer Res **67**:11254–11262.

220. **Spencer HL**, **Eastham AM**, **Merry CLR**, **Southgate TD**, **Perez-Campo F**, **Soncin F**, **Ritson S**, **Kemler R**, **Stern PL**, **Ward CM**. 2007. E-cadherin inhibits cell surface localization of the pro-migratory 5T4 oncofetal antigen in mouse embryonic stem cells. Mol Biol Cell **18**:2838–2851.

221. **Nieto MA**, **Cano A**. 2012. The epithelial–mesenchymal transition under control: Global programs to regulate epithelial plasticity. Seminars in Cancer Biology **22**:361–368.

222. **Thiery JP**, **Acloque H**, **Huang R**, **Nieto MA**. 2009. Epithelial-mesenchymal transitions in development and disease. Cell **139**:871–890.

223. **Southgate TD**, **McGinn OJ**, **Castro FV**, **Rutkowski AJ**, **Al-Muftah M**, **Marinov G**, **Smethurst GJ**, **Shaw D**, **Ward CM**, **Miller CJ**, **Stern PL**. 2010. CXCR4 Mediated Chemotaxis Is Regulated by 5T4 Oncofetal Glycoprotein in Mouse Embryonic Cells. PLoS ONE **5**:e9982.

224. **Carsberg CJ**, **Myers KA**, **Evans GS**, **Allen TD**, **Stern PL**. 1995. Metastasis-associated 5T4 oncofoetal antigen is concentrated at microvillus projections of the plasma membrane. Journal of Cell Science **108**:2905–2916.

225. **Carsberg CJ**, **Myers KA**, **Stern PL**. 1996. Metastasis‐associated 5T4 antigen disrupts cell‐cell contacts and induces cellular motility in epithelial cells. International Journal of Cancer **68**:84–92.

226. **Woods AM**, **Wang WW**, **Shaw DM**, **Ward CM**, **Carroll MW**, **Rees BR**, **Stern PL**. 2002. Characterization of the murine 5T4 oncofoetal antigen: a target for immunotherapy in cancer. Biochem J **366**:353–365.

227. **Castro FV**, **McGinn OJ**, **Krishnan S**, **Marinov G**, **Li J**, **Rutkowski AJ**, **Elkord E**, **Burt DJ**, **Holland M**, **Vaghjiani R**, **Gallego A**, **Saha V**, **Stern PL**. 2012. 5T4 oncofetal antigen is expressed in high risk of relapse childhood pre-B acute lymphoblastic leukemia and is associated with a more invasive and chemotactic phenotype. Leukemia **26**:1487–1498.

228. **Balkwill F**. 2004. The significance of cancer cell expression of the chemokine receptor CXCR4. Seminars in Cancer Biology **14**:171–179.

229. **Burger JA**, **Kipps TJ**. 2006. CXCR4: a key receptor in the crosstalk between tumor cells and their microenvironment. Blood **107**:1761–1767.

230. **Vandercappellen J**, **Van Damme J**, **Struyf S**. 2008. The role of CXC chemokines and their receptors in cancer. Cancer Lett **267**:226–244.

231. **Kagermeier-Schenk B**, **Wehner D**, **Özhan-Kizil G**, **Yamamoto H**, **Li J**, **Kirchner K**, **Hoffmann C**, **Stern P**, **Kikuchi A**, **Schambony A**, **Weidinger G**. 2011. Waif1/5T4 Inhibits Wnt/β-Catenin Signaling and Activates Noncanonical Wnt Pathways by Modifying LRP6 Subcellular Localization. Developmental Cell **21**:1129–1143.

232. **MacDonald BT**, **Tamai K**, **He X**. 2009. Wnt/β-catenin signaling: components, mechanisms, and diseases. Developmental Cell **17**:9–26.

233. **Polakis P**. 2012. Drugging Wnt signalling in cancer. The EMBO Journal **31**:2737–2746.

234. **Logan CY**, **Nusse R**. 2004. The Wnt Signaling Pathway In Development And Disease. Annu Rev Cell Dev Biol **20**:781–810.

235. **Nusse R**. 2005. Wnt signaling in disease and in development. Cell Res **15**:28–32.

236. **Mani SA**, **Guo W**, **Liao MJ**, **Eaton EN**, **Ayyanan A**, **Zhou AY**, **Brooks M**, **Reinhard F**, **Zhang CC**, **Shipitsin M**, **Campbell LL**, **Polyak K**, **Brisken C**, **Yang J**, **Weinberg RA**. 2008. The epithelial-mesenchymal transition generates cells with properties of stem cells. Cell **133**:704–715.

237. **Stern PL**, **Brazzatti J**, **Sawan S**, **McGinn OJ**. 2014. Understanding and exploiting 5T4 oncofoetal glycoprotein expression. Seminars in Cancer Biology **29**:13–20.

238. **Mulryan K**, **Ryan MG**, **Myers KA**, **Shaw D**, **Kingsman SM**, **Stern PL**, **Carroll MW**. 2002. Attenuated recombinant vaccinia virus expressing oncofetal antigen (tumor-associated antigen) 5T4 induces active therapy of established tumors. Mol Cancer Ther **1**:1129.

239. **Harrop R**, **Ryan MG**, **Myers KA**, **Redchenko I**, **Kingsman SM**, **Carroll MW**. 2006. Active treatment of murine tumors with a highly attenuated vaccinia virus expressing the tumor associated antigen 5T4 (TroVax) is CD4+ T cell dependent and antibody mediated. Cancer Immunology, Immunotherapy **55**:1081–1090.

240. **Boghaert ER**, **Sridharan L**, **Khandke KM**, **Armellino D**, **Ryan MG**, **Myers K**, **Harrop R**, **Kunz A**, **Hamann PR**, **Marquette K**. 2008. The oncofetal protein, 5T4, is a suitable target for antibody-guided anti-cancer chemotherapy with calicheamicin. International Journal of Oncology **32**:221–234.

241. **Sapra P**, **Damelin M**, **DiJoseph J**, **Marquette K**, **Geles KG**, **Golas J**, **Dougher M**, **Narayanan B**, **Giannakou A**, **Khandke K**, **Dushin R**, **Ernstoff E**, **Lucas J**, **Leal M**, **Hu G**, **O'Donnell CJ**, **Tchistiakova L**, **Abraham RT**, **Gerber HP**. 2013. Long-term Tumor Regression Induced by an Antibody-Drug Conjugate That Targets 5T4, an Oncofetal Antigen Expressed on Tumor-Initiating Cells. Mol Cancer Ther **12**:38–47.

242. **Forsberg G**, **Skartved N-J**, **Wallén-Ohman M**, **Nyhlén HC**, **Behm K**, **Hedlund G**, **Nederman T**. 2010. Naptumomab Estafenatox, an Engineered Antibody-superantigen Fusion Protein With Low Toxicity and Reduced Antigenicity. Journal of Immunotherapy **33**:492–499.

243. **Shaw DM**, **Embleton MJ**, **Westwater C**, **Ryan MG**, **Myers KA**, **Kingsman SM**, **Carroll MW**, **Stern PL**. 2000. Isolation of a high affinity scFv from a monoclonal antibody recognising the oncofoetal antigen 5T4. Biochim Biophys Acta **1524**:238–246.

244. **BioMedica O**. 2014. Press Release: Combined LentiVector(R) and 5T4 platforms - Initiating CAR-T 5T4 Programme. Website: oxfordbiomedicacouk.

245. **Guest R**, **Hawkins R**, **Kirillova N**, **Cheadle E**, **Arnold J**, **O'Neill A**, **Irlam J**, **Chester K**, **Kemshead J**, **Shaw D**, **Embleton M**, **Stern P**, **Gilham D**. 2005. The role of extracellular spacer regions in the optimal design of chimeric immune receptors - Evaluation of four different scFvs and antigens. J Immunother **28**:203–211.

246. **Al-Muftah MA**. 2011. The Generation of a Novel Chimeric Antigen Receptor for Cancer Immunotherapy. Qatar Foundation Annual Research Forum Proceedings BMOS1.

247. **Marrack P**, **Kappler J**. 1990. The staphylococcal enterotoxins and their relatives. Science **248**:705–711.

248. **McCormick JK**, **Yarwood JM**, **Schlievert PM**. 2001. Toxic shock syndrome and bacterial superantigens: an update. Annu Rev Microbiol **55**:77–104.

249. **Proft T**, **Fraser JD**. 2003. Bacterial superantigens. Clinical & Experimental Immunology **133**:299–306.

250. **Fraser J**, **Arcus V**, **Kong P**, **Baker E**, **Proft T**. 2000. Superantigens – powerful modifiers of the immune system. Molecular Medicine Today **6**:125–132.

251. **Llewelyn M**, **Cohen J**. 2002. Superantigens: microbial agents that corrupt immunity. The Lancet Infectious Diseases **2**:156–162.

252. **Janeway CA**, **Yagi J**, **Conrad PJ**, **Katz ME**, **Jones B**, **Vroegop S**, **Buxser S**. 1989. T-Cell Responses to Mls and to Bacterial Proteins that Mimic its Behavior#. Immunological Reviews **107**:61–88.

253. **Xu SX**, **McCormick JK**. 2012. Staphylococcal superantigens in colonization and disease. Frontiers in Cellular and Infection Microbiology **2**:1–11.

254. **Spaulding AR**, **Salgado-Pabon W**, **Kohler PL**, **Horswill AR**, **Leung DYM**, **Schlievert PM**. 2013. Staphylococcal and Streptococcal Superantigen Exotoxins. Clinical Microbiology Reviews **26**:422–447.

255. **Cone LA**, **Woodard DR**, **Schlievert PM**, **Tomory GS**. 1987. Clinical and Bacteriologic Observations of a Toxic Shock–like Syndrome Due to Streptococcus pyogenes. The New England Journal of Medicine **317**:146–149.

256. **Stevens DL**, **Tanner MH**, **Winship J**, **Swarts R**, **Ries KM**, **Schlievert PM**, **Kaplan E**. 1989. Severe Group A Streptococcal Infections Associated with a Toxic Shock-like Syndrome and Scarlet Fever Toxin A. The New England Journal of Medicine **321**:1–7.

257. **Commons RJ**, **Smeesters PR**, **Proft T**, **Fraser JD**, **Robins-Browne R**, **Curtis N**. 2014. Streptococcal superantigens: categorization and clinical associations. Trends in Molecular Medicine **20**:48–62.

258. **Lowy FD**. 1998. Staphylococcus aureus Infections. The New England Journal of Medicine **339**:520–532.

259. **Lina G**, **Bohach GA**, **Nair SP**, **Hiramatsu K**, **Jouvin-Marche E**, **Mariuzza R**. 2004. Standard nomenclature for the superantigens expressed by Staphylococcus. The Journal of Infectious Diseases **189**:2334–2336.

260. **McCormick JK**, **Bohach GA**, **Schlievert PM**. 2003. Pyrogenic, lethal, and emetic properties of superantigens in rabbits and primates, pp. 245–253. *In* Krakauer, T (ed.), Superantigen Protocols. Methods in Molecular Biology.

261. **Dinges MM**, **Orwin PM**, **Schlievert PM**. 2000. Exotoxins of Staphylococcus aureus. Clinical Microbiology Reviews **13**:16–34.

262. **Schlievert PM**, **Jablonski LM**, **Roggiani M**, **Sadler I**, **Callantine S**, **Mitchell DT**, **Ohlendorf DH**, **Bohach GA**. 2000. Pyrogenic toxin superantigen site specificity in toxic shock syndrome and food poisoning in animals. Infection and Immunity **68**:3630–3634.

263. **Jarraud S**, **Peyrat MA**, **Lim A**, **Tristan A**, **Bes M**, **Mougel C**, **Etienne J**, **Vandenesch F**, **Bonneville M**, **Lina G**. 2001. egc, A Highly Prevalent Operon of Enterotoxin Gene, Forms a Putative Nursery of Superantigens in Staphylococcus aureus. Journal of Immunology (Baltimore, Md : 1950) **166**:669–677.

264. **Holtfreter S**, **Bauer K**, **Thomas D**, **Feig C**, **Lorenz V**, **Roschack K**, **Friebe E**, **Selleng K**, **Lovenich S**, **Greve T**, **Greinacher A**, **Panzig B**, **Engelmann S**, **Lina G**, **Broker BM**. 2004. egc-Encoded Superantigens from Staphylococcus aureus Are Neutralized by Human Sera Much Less Efficiently than Are Classical Staphylococcal Enterotoxins or Toxic Shock Syndrome Toxin. Infection and Immunity **72**:4061–4071.

265. **Walker MJ**, **Barnett TC**, **McArthur JD**, **Cole JN**, **Gillen CM**, **Henningham A**, **Sriprakash KS**, **Sanderson-Smith ML**, **Nizet V**. 2014. Disease Manifestations and Pathogenic Mechanisms of Group A Streptococcus. Clinical Microbiology Reviews **27**:264–301.

266. **Bohach GA**, **Fast DJ**, **Nelson RD**, **Schlievert PM**. 1990. Staphylococcal and Streptococcal Pyrogenic Toxins Involved in Toxic Shock Syndrome and Related Illnesses. Critical Reviews in Microbiology **17**:251–272.

267. **Kasper KJ**, **Zeppa JJ**, **Wakabayashi AT**, **Xu SX**, **Mazzuca DM**, **Welch I**, **Baroja ML**, **Kotb M**, **Cairns E**, **Cleary PP**, **Haeryfar SMM**, **McCormick JK**. 2014. Bacterial Superantigens Promote Acute Nasopharyngeal Infection by

Streptococcus pyogenes in a Human MHC Class II-Dependent Manner. PLoS Pathog **10**:e1004155.

268. **Fraser JD**, **Proft T**. 2008. The bacterial superantigen and superantigen‐like proteins. Immunological Reviews **225**:226–243.

269. **Mitchell DT**, **Levitt DG**, **Schlievert PM**, **Ohlendorf DH**. 2000. Structural Evidence for the Evolution of Pyrogenic Toxin Superantigens. J Mol Evol **51**:520–531.

270. **Jardetzky TS**, **Brown JH**, **Gorga JC**, **Stern LJ**, **Urban RG**, **Chi Y**, **Stauffacher CV**, **Strominger J**, **Wiley D**. 1994. Three-dimensional structure of a human class II histocompatibility molecule complexed with superantigen. Nature **368**:711–718.

271. **Kim J**, **Urban R**, **Strominger J**, **Wiley D**. 1994. Toxic shock syndrome toxin-1 complexed with a class II major histocompatibility molecule HLA-DR1. Science **266**:1870–1874.

272. **Li Y**, **Li H**, **Dimasi N**, **McCormick JK**, **Martin R**, **Schuck P**, **Schlievert PM**, **Mariuzza RA**. 2001. Crystal structure of a superantigen bound to the high-affinity, zinc-dependent site on MHC class II. Immunity **14**:93–104.

273. **Petersson K**, **Håkansson M**, **Nilsson H**. 2001. Crystal structure of a superantigen bound to MHC class II displays zinc and peptide dependence. The EMBO Journal **20**:3306–3312.

274. **Fields BA**, **Malchiodi EL**, **Li H**, **Ysern X**, **Stauffacher CV**, **Schlievert PM**, **Karjalainen K**, **Mariuzza RA**. 1996. Crystal structure of a T-cell receptor beta-chain complexed with a superantigen. Nature **384**:188–192.

275. **Li H**, **Llera A**, **Tsuchiya D**, **Leder L**, **Ysern X**, **Schlievert PM**, **Karjalainen K**, **Mariuzza RA**. 1998. Three-dimensional structure of the complex between a T cell receptor β chain and the superantigen staphylococcal enterotoxin B. Immunity **9**:807–816.

276. **Andersen PS**, **Schuck P**, **Sundberg EJ**, **Geisler C**, **Karjalainen K**, **Mariuzza RA**. 2002. Quantifying the energetics of cooperativity in a ternary protein complex. Biochemistry **41**:5177–5184.

277. **Rahman AKMN-U**, **Bonsor DA**, **Herfst CA**, **Pollard F**, **Peirce M**, **Wyatt AW**, **Kasper KJ**, **Madrenas J**, **Sundberg EJ**, **McCormick JK**. 2011. The T Cell Receptor β-Chain Second Complementarity Determining Region Loop (CDR2β) Governs T Cell Activation and Vβ Specificity by Bacterial Superantigens. Journal of Biological Chemistry **286**:4871–4881.

278. **Sundberg EJ**, **Deng L**, **Mariuzza RA**. 2007. TCR recognition of peptide/MHC class II complexes and superantigens. Seminars in Immunology **19**:262–271.

279. **Papageorgiou AC**, **Acharya KR**. 1997. Superantigens as immunomodulators: recent structural insights. Structure **5**:991–996.

280. **Li H**, **Llera A**, **Malchiodi EL**, **Mariuzza RA**. 1999. The Structural Basis of Cell Activation by Superantigens. Annu Rev Immunol **17**:435–466.

281. **Arden B**, **Clark SP**, **Kabelitz D**, **Mak TW**. 1995. Human T-cell receptor variable gene segment families. Immunogenetics **42**:455–500.

282. **Wei S**, **Charmley P**, **Robinson MA**, **Concannon P**. 1994. The extent of the human germline T-cell receptor V beta gene segment repertoire. Immunogenetics **40**:27–36.

283. **Fleischer B**, **Necker A**, **Leget C**, **Malissen B**, **Romagne F**. 1996. Reactivity of mouse T-cell hybridomas expressing human Vbeta gene segments with staphylococcal and streptococcal superantigens. Infection and Immunity **64**:987–994.

284. **Hennecke J**. 2000. Structure of a covalently stabilized complex of a human alphabeta T-cell receptor, influenza HA peptide and MHC class II molecule, HLA-DR1. The EMBO Journal **19**:5611–5624.

285. **Sundberg EJ**, **Li H**, **Llera AS**, **McCormick JK**, **Tormo J**, **Schlievert PM**, **Karjalainen K**, **Mariuzza RA**. 2002. Structures of two streptococcal superantigens bound to TCR β chains reveal diversity in the architecture of T cell signaling complexes. Structure **10**:687–699.

286. **Kasper KJ**, **Xi W**, **Rahman AN-U**, **Nooh MM**, **Kotb M**, **Sundberg EJ**, **Madrenas J**, **McCormick JK**. 2008. Molecular Requirements for MHC Class II α-Chain Engagement and Allelic Discrimination by the Bacterial Superantigen Streptococcal Pyrogenic Exotoxin C. Journal of Immunology (Baltimore, Md : 1950) **181**:3384–3392.

287. **Sundberg EJ**, **Andersen PS**, **Schlievert PM**, **Karjalainen K**, **Mariuzza RA**. 2003. Structural, energetic, and functional analysis of a protein-protein interface at distinct stages of affinity maturation. Structure **11**:1151–1161.

288. **Herrmann T**, **Baschieri S**, **Lees RK**, **MacDonald HR**. 1992. In vivo responses of CD4+ and CD8+ cells to bacterial superantigens. European Journal of Immunology **22**:1935–1938.

289. **Hayworth JL**, **Mazzuca DM**, **Vareki SM**, **Welch I**, **McCormick JK**, **Haeryfar SMM**. 2011. CD1d-independent activation of mouse and human iNKT cells by bacterial superantigens. Immunology and Cell Biology **7**:699–709.

290. **Morita CT**, **Li H**, **Lamphear JG**, **Rich RR**, **Fraser JD**, **Mariuzza RA**, **Lee HK**. 2001. Superantigen recognition by γδ T cells: SEA recognition site for human Vγ2 T cell receptors. Immunity **14**:331–344.

291. **Ami K**, **Ohkawa T**, **Koike Y**, **Sato K**, **Habu Y**, **Iwai T**, **Seki S**, **Hiraide H**. 2002. Activation of human T cells with NK cell markers by staphylococcal enterotoxin A via IL-12 but not via IL-18. Clinical & Experimental Immunology **128**:453–459.

292. **Taylor AL**, **Cross ELA**, **Llewelyn MJ**. 2012. Induction of contact-dependent CD8+ regulatory T cells through stimulation with staphylococcal and streptococcal superantigens*. Immunology **135**:158–167.

293. **Taylor AL**, **Llewelyn MJ**. 2010. Superantigen-induced proliferation of human CD4+ CD25− T cells is followed by a switch to a functional regulatory phenotype. Journal of Immunology **185**:6591–6598.

294. **Kawabe Y**, **Ochi A**. 1990. Selective anergy of V beta 8+, CD4+ T cells in Staphylococcus enterotoxin B-primed mice. The Journal of Experimental Medicine **172**:1065–1070.

295. **Rellahan BL**, **Jones LA**, **Kruisbeek AM**, **Fry AM**, **Matis LA**. 1990. In vivo induction of anergy in peripheral V beta 8+ T cells by staphylococcal enterotoxin B. The Journal of Experimental Medicine **172**:1091–1100.

296. **Sundstedt A**, **Höidén I**, **Hansson J**, **Hedlund G**, **Kalland T**, **Dohlsten M**. 1995. Superantigen-induced anergy in cytotoxic CD8+ T cells. The Journal of Immunology **154**:6306–6313.

297. **Lussow AR**, **MacDonald HR**. 1994. Differential effects of superantigen-induced “anergy” on priming and effector stages of a T cell-dependent antibody response. European Journal of Immunology **24**:445–449.

298. **Schlievert PM**, **Shands KN**, **Dan BB**, **Schmid GP**, **Nishimura RD**. 1981. Identification and Characterization of an Exotoxin from Staphylococcus aureus Associated with Toxic-Shock Syndrome. Journal of Infectious Diseases **143**:509–516.

299. **Bergdoll M**, **Crass BA**, **Reiser RF**, **Robbins RN**, **Lee ACM**, **Chesney PJ**, **Davis JP**, **Vergeront JM**, **Wand PJ**. 1982. An Enterotoxin-Like Protein in Staphylococcus aureus Strains from Patients with Toxic Shock Syndrome. Ann Intern Med **96**:969–971.

300. **Schlievert PM**. 1986. Staphylococcal enterotoxin B and toxic-shock syndrome toxin-1 are significantly associated with non-menstrual TSS. Lancet **1**:1149–1150.

301. **Argudín MÁ**, **Mendoza MC**, **Rodicio MR**. 2010. Food Poisoning and Staphylococcus aureus Enterotoxins. Toxins **2**:1751–1773.

302. **Hovde CJ**, **Marr JC**, **Hoffmann ML**, **Hackett SP**, **Chi Y-I**, **Crum KK**, **Stevens DL**, **Stauffacher CV**, **Bohach GA**. 1994. Investigation of the role of the

disulphide bond in the activity and structure of staphylococcal enterotoxin C1. Molecular Microbiology **13**:897–909.

303. **Petersson K**, **Thunnissen M**, **Forsberg G**, **Walse B**. 2002. Crystal Structure of a SEA Variant in Complex with MHC Class II Reveals the Ability of SEA to Crosslink MHC Molecules. Structure **10**:1619–1626.

304. **Swietnicki W**, **Barnie AM**, **Dyas BK**, **Ulrich RG**. 2003. Zinc binding and dimerization of Streptococcus pyogenes pyrogenic exotoxin C are not essential for T-cell stimulation. The Journal of Biological Chemistry **278**:9885–9895.

305. **Fernández MM**, **De Marzi MC**, **Berguer P**, **Burzyn D**, **Langley RJ**, **Piazzon I**, **Mariuzza RA**, **Malchiodi EL**. 2006. Binding of natural variants of staphylococcal superantigens SEG and SEI to TCR and MHC class II molecule. Molecular Immunology **43**:927–938.

306. **Munson SH**, **Tremaine MT**, **Betley MJ**, **Welch RA**. 1998. Identification and characterization of staphylococcal enterotoxin types G and I fromStaphylococcus aureus. Infection and Immunity **66**:3337–3348.

307. **Günther S**, **Varma AK**, **Moza B**, **Kasper KJ**, **Wyatt AW**, **Zhu P**, **Rahman AKMN-U**, **Li Y**, **Mariuzza RA**, **McCormick JK**, **Sundberg EJ**. 2007. A Novel Loop Domain in Superantigens Extends their T Cell Receptor Recognition Site. J Mol Biol **371**:210–221.

308. **Dohlsten M**, **Hedlund G**, **Akerblom E**, **A LP**, **Kalland T**. 1991. Monoclonal antibody-targeted superantigens: a different class of anti-tumor agents. Proc Natl Acad Sci USA **88**:9287.

309. **Dohlsten M**, **Abrahmsén L**, **Björk P**, **A LP**, **Hedlund G**, **Forsberg G**, **Brodin T**, **Gascoigne N**, **Förberg C**, **Lind P**. 1994. Monoclonal antibody-superantigen fusion proteins: tumor-specific agents for T-cell-based tumor therapy. Proc Natl Acad Sci USA **91**:8945.

310. **Dohlsten M**, **PA L**, **Hedlund G**, **Trowsdale K**, **Kalland T**. 1990. Targeting of human cytotoxic T lymphocytes to MHC class II-expressing cells by staphylococcal enterotoxins. Immunology **71**:96.

311. **Hedlund G**, **Dohlsten M**, **A LP**, **Kalland T**. 1990. Staphylococcal enterotoxins direct and trigger CTL killing of autologous HLA-DR+ mononuclear leukocytes and freshly prepared leukemia cells. Cellular Immunology **129**:426–434.

312. **Hedlund G**, **Dohlsten M**, **Petersson C**, **Kalland T**. 1993. Superantigen-based tumor therapy: in vivo activation of cytotoxic T cells. Cancer Immunology, Immunotherapy **36**:89–93.

313. **Kalland T**, **Hedlund G**, **Dohlsten M**, **A LP**. 1991. Staphylococcal Enterotoxin-Dependent Cell-Mediated Cytotoxicity, pp. 81–92. *In* Superantigens. Current

Topics in Microbiology and Immunology, Berlin, Heidelberg.

314. **Kalland T**, **Dohlsten M**, **Lind P**, **Sundstedt A**, **Abrahmsén L**, **Hedlund G**, **Björk P**, **Lando P**, **Björklund M**. 1993. Monoclonal antibodies and superantigens: a novel therapeutic approach. Medical oncology & Tumor Pharmacotherapy **10**:37–47.

315. **Björk P**, **Jönsson U**, **Svedberg H**, **Larsson K**, **Lind P**, **Dillner J**, **Hedlund G**, **Dohlsten M**, **Kalland T**. 1993. Isolation, partial characterization, and molecular cloning of a human colon adenocarcinoma cell-surface glycoprotein recognized by the C215 mouse monoclonal antibody. The Journal of Biological Chemistry **268**:24232–24241.

316. **Johansson C**, **Nilsson O**, **Baeckstr ouml m D**, **Jansson E-L**, **Lindholm L**. 1991. Novel Epitopes on the CA50-Carrying Antigen: Chemical and Immunochemical Studies. Tumor Biol **12**:159–170.

317. **Haglund C**, **Lundin J**, **Kuusela P**, **Roberts PJ**. 1994. CA 242, a new tumour marker for pancreatic cancer: a comparison with CA 19-9, CA 50 and CEA. Br J Cancer **70**:487–492.

318. **Dohlsten M**, **Lando PA**, **Bj rk P**, **Abrahms n L**, **Ohlsson L**, **Lind P**, **Kalland T**. 1995. Immunotherapy of human colon cancer by antibody-targeted superantigens. Cancer Immunol Immunother **41**:162–168.

319. **Lando PA**, **Dohlsten M**, **Ohlsson L**, **Kalland T**. 1995. Tumor-reactive superantigens suppress tumor growth in humanized scid mice. International Journal of Cancer Journal international du cancer **62**:466–471.

320. **Dohlsten M**, **Hansson J**, **Ohlsson L**, **Litton M**, **Kalland T**. 1995. Antibody-targeted superantigens are potent inducers of tumor-infiltrating T lymphocytes in vivo. Proc Natl Acad Sci USA **92**:9791–9795.

321. **Rosendahl A**, **Hansson J**, **Sundstedt A**, **Kalland T**, **Dohlsten M**. 1996. Immune response during tumor therapy with antibody-superantigen fusion proteins. International Journal of Cancer **68**:109–113.

322. **Rosendahl A**, **Kristensson K**, **Hansson J**, **Ohlsson L**, **Kalland T**, **Dohlsten M**. 1998. Repeated treatment with antibody-targeted superantigens strongly inhibits tumor growth. International Journal of Cancer Journal international du cancer **76**:274–283.

323. **Nielsen SE**, **Zeuthen J**, **Lund B**, **Persson B**, **Alenfall J**, **Hansen HH**. 2000. Phase I study of single, escalating doses of a superantigen-antibody fusion protein (PNU-214565) in patients with advanced colorectal or pancreatic carcinoma. Journal of Immunotherapy **23**:146–153.

324. **Giantonio BJ**, **Alpaugh RK**, **Schultz J**, **McAleer C**, **Newton DW**, **Shannon B**,

Guedez Y, **Kotb M**, **Vitek L**, **Persson R**, **Gunnarsson PO**, **Kalland T**, **Dohlsten M**, **Persson B**, **Weiner LM**. 1997. Superantigen-based immunotherapy: a phase I trial of PNU-214565, a monoclonal antibody-staphylococcal enterotoxin A recombinant fusion protein, in advanced pancreatic and colorectal cancer. Journal of Clinical Oncology **15**:1994–2007.

325. **Alpaugh RK**, **Schultz J**, **McAleer C**, **Giantonio BJ**, **Persson R**, **Burnite M**, **Nielsen SE**, **Vitek L**, **Persson B**, **Weiner LM**. 1998. Superantigen-targeted therapy: phase I escalating repeat dose trial of the fusion protein PNU-214565 in patients with advanced gastrointestinal malignancies. Clinical Cancer Research **4**:1903–1914.

326. **Hansson J**, **Ohlsson L**, **Persson R**, **Andersson G**, **Ilbäck N-G**, **Litton MJ**, **Kalland T**, **Dohlsten M**. 1997. Genetically engineered superantigens as tolerable antitumor agents. Proc Natl Acad Sci USA **94**:2489–2494.

327. **Miethke T**, **Wahl C**, **Regele D**, **Gaus H**, **Heeg K**, **Wagner H**. 1993. Superantigen Mediated Shock: A Cytokine Release Syndrome. Immunobiology **189**:270–284.

328. **Abrahmsen L**, **Dohlsten M**, **Segren S**, **Björk P**, **Jonsson E**, **Kalland T**. 1995. Characterization of two distinct MHC class II binding sites in the superantigen staphylococcal enterotoxin A. The EMBO Journal **14**:2978.

329. **Hudson KR**, **Tiedemann RE**, **Urban RG**, **Lowe SC**, **Strominger J**, **Fraser JD**. 1995. Staphylococcal enterotoxin A has two cooperative binding sites on major histocompatibility complex class II. Journal of Experimental Medicine **182**:711–720.

330. **Schad EM**, **Zaitseva I**, **Zaitsev VN**, **Dohlsten M**, **Kalland T**, **Schlievert PM**, **Ohlendorf DH**, **Svensson LA**. 1995. Crystal structure of the superantigen staphylococcal enterotoxin type A. The EMBO Journal **14**:3292–3301.

331. **Holzer U**, **Orlikowsky T**, **Zehrer C**, **Bethge W**, **Dohlsten M**, **Kalland T**, **Niethammer D**, **Dannecker GE**. 1997. T-cell stimulation and cytokine release induced by staphylococcal enterotoxin A (SEA) and the SEAD227A mutant. Immunology **90**:74–80.

332. **Dohlsten M**, **Björklund M**, **Sundstedt A**, **Hedlund G**, **Samson D**, **Kalland T**. 1993. Immunopharmacology of the superantigen staphylococcal enterotoxin A in T-cell receptor V beta 3 transgenic mice. Immunology **79**:520–527.

333. **Callahan JE**, **Herman A**, **Kappler JW**, **Marrack P**. 1990. Stimulation of B10. BR T cells with superantigenic staphylococcal toxins. The Journal of Immunology **144**:2473–2479.

334. **Gidlöf C**, **Dohlsten M**, **Lando P**, **Kalland T**, **Sundström C**, **Tötterman TH**. 1997. A Superantigen-Antibody Fusion Protein for T-Cell Immunotherapy of

Human B-Lineage Malignancies. Blood **89**:2089–2097.

335. **Forsberg G**, **Ohlsson L**, **Brodin T**, **Björk P**, **A LP**, **Shaw D**, **Stern PL**, **Dohlsten M**. 2001. Therapy of human non-small-cell lung carcinoma using antibody targeting of a modified superantigen. Br J Cancer **85**:129–136.

336. **Forsberg G**, **Forsgren M**, **Jaki M**, **Norin M**, **Sterky C**, **Enhörning A**, **Larsson K**, **Ericsson M**, **Björk P**. 1997. Identification of framework residues in a secreted recombinant antibody fragment that control production level and localization in Escherichia coli. The Journal of Biological Chemistry **272**:12430–12436.

337. **Cheng JD**, **Babb JS**, **Langer C**, **Aamdal S**, **Robert F**, **Engelhardt LR**, **Fernberg O**, **Schiller J**, **Forsberg G**, **Alpaugh RK**, **Weiner LM**, **Rogatko A**. 2004. Individualized Patient Dosing in Phase I Clinical Trials: The Role of Escalation With Overdose Control in PNU-214936. Journal of Clinical Oncology **22**:602–609.

338. **Shaw DM**, **Connolly NB**, **Patel PM**, **Kilany S**, **Hedlund G**, **O N**, **Forsberg G**, **Zweit J**, **Stern PL**, **Hawkins RE**. 2007. A phase II study of a 5T4 oncofoetal antigen tumour-targeted superantigen (ABR-214936) therapy in patients with advanced renal cell carcinoma. Br J Cancer **96**:567–574.

339. **Erlandsson E**, **Andersson K**, **Cavallin A**, **Nilsson A**, **Larsson-Lorek U**, **Niss U**, **Sjöberg A**, **Wallén-Öhman M**, **Antonsson P**, **Walse B**. 2003. Identification of the antigenic epitopes in staphylococcal enterotoxins A and E and design of a superantigen for human cancer therapy. J Mol Biol **333**:893–905.

340. **Hedlund G**, **Eriksson H**, **Sundstedt A**, **Forsberg G**, **Jakobsen BK**, **Pumphrey N**, **Rödström K**, **Lindkvist-Petersson K**, **Björk P**. 2013. The Tumor Targeted Superantigen ABR-217620 Selectively Engages TRBV7-9 and Exploits TCR-pMHC Affinity Mimicry in Mediating T Cell Cytotoxicity. PLoS ONE **8**:e79082.

341. **Sundstedt A**, **Celander M**, **Öhman MW**, **Forsberg G**, **Hedlund G**. 2009. Immunotherapy with tumor-targeted superantigens (TTS) in combination with docetaxel results in synergistic anti-tumor effects. International immunopharmacology **9**:1063–1070.

342. **Borghaei H**, **Alpaugh K**, **Hedlund G**, **Forsberg G**, **Langer C**, **Rogatko A**, **Hawkins R**, **Dueland S**, **Lassen U**, **Cohen RB**. 2009. Phase I dose escalation, pharmacokinetic and pharmacodynamic study of naptumomab estafenatox alone in patients with advanced cancer and with docetaxel in patients with advanced non-small-cell lung cancer. Journal of Clinical Oncology : official journal of the American Society of Clinical Oncology **27**:4116–4123.

343. **Robinson MK**, **Alpaugh RK**, **Borghaei H**. 2010. Naptumomab estafenatox: a new immunoconjugate. Expert Opin Biol Ther **10**:273–279.

344. **Sundstedt A**, **Celander M**, **Hedlund G**. 2008. Combining tumor-targeted superantigens with interferon-alpha results in synergistic anti-tumor effects. International immunopharmacology **8**:442–452.

345. **Eisen T**, **Hedlund G**, **Forsberg G**, **Nordle O**, **Hawkins R**. 2013. Baseline biomarker trend analysis of a randomized phase 2/3 study of naptumomab estafenatox plus IFN-α vs IFN-α in advanced renal cell carcinoma. Abstract ID: 2710. European Cancer Congress (ECCO).

346. **Hawkins R**, **Gore M**, **Shparyk Y**, **Bondar V**, **Gladkov O**, **Harza M**, **Polenkov S**, **Bondarenko I**, **Karlov P**, **Karyakin O**, **Khasanov R**, **Hedlund G**, **Forsberg G**, **Nordle O**, **Eisen T**. 2013. A randomized phase 2/3 study of naptumomab estafenatox plus IFN-α vs IFN-α in advanced renal cell carcinoma. Abstract ID: 3073. ASCO Annual Meeting.

347. **Yu H**, **Pardoll D**, **Jove R**. 2009. STATs in cancer inflammation and immunity: a leading role for STAT3. Nat Rev Cancer **9**:798–809.

348. **Elkord E**, **Burt DJ**, **Sundstedt A**, **O N**, **Hedlund G**, **Hawkins R**. 2015. Immunological response and overall survival in a subset of advanced renal cell carcinoma patients from a randomized phase 2/3 study of naptumomab estafenatox plus IFN-alpha versus IFN-alpha. Oncotarget **6**:4428–4439.

349. **Lando PA**, **Hedlund G**, **Dohlsten M**, **Kalland T**. 1991. Bacterial superantigens as anti-tumour agents: induction of tumour cytotoxicity in human lymphocytes by staphylococcal enterotoxin A. Cancer Immunol Immunother **33**:231–237.

350. **Litton MJ**, **Dohlsten M**, **Hansson J**, **Rosendahl A**, **Ohlsson L**, **Kalland T**, **Andersson J**, **Andersson U**. 1997. Tumor therapy with an antibody-targeted superantigen generates a dichotomy between local and systemic immune responses. The American journal of pathology **150**:1607.

351. **Lando PA**, **Dohlsten M**, **Kalland T**, **Sjogren HO**, **Carlsson R**. 1990. The TcR-CD3 Complex is Required for Activation of Human Lymphocytes with Staphylococcal Enterotoxin A. Scandinavian Journal of Immunology **31**:133–138.

352. **Fischer H**, **Dohlsten M**, **Andersson U**, **Hedlund G**, **Ericsson P**, **Hansson J**, **Sjogren HO**. 1990. Production of TNF-alpha and TNF-beta by staphylococcal enterotoxin A activated human T cells. The Journal of Immunology **144**:4663–4669.

353. **Litton MJ**, **Dohlsten M**, **Lando PA**, **Kalland T**, **Ohlsson L**, **Andersson J**, **Andersson U**. 1996. Antibody-targeted superantigen therapy induces tumor-infiltrating lymphocytes, excessive cytokine production, and apoptosis in human colon carcinoma. European Journal of Immunology **26**:1–9.

354. **Litton MJ**, **Dohlsten M**, **Rosendahl A**, **Ohlsson L**, **Søgaard M**, **Andersson J**, **Andersson U**. 1999. The distinct role of CD4+ and CD8+ T-cells during the

anti-tumour effects of targeted superantigens. Br J Cancer **81**:359–366.

355. **Rosendahl A**, **Kristensson K**, **Hansson J**, **Riesbeck K**, **Kalland T**, **Dohlsten M**. 1998. Perforin and IFN-γ are involved in the antitumor effects of antibody-targeted superantigens. Journal of Immunology (Baltimore, Md : 1950) **160**:5309–5313.

356. **Dohlsten M**, **Sundstedt A**, **Björklund M**, **Hedlund G**, **Kalland T**. 1993. Superantigen-induced cytokines suppress growth of human colon-carcinoma cells. International Journal of Cancer Journal international du cancer **54**:482–488.

357. **Søgaard M**, **Ohlsson L**, **Kristensson K**, **Rosendahl A**, **Sjöberg A**, **Forsberg G**, **Kalland T**, **Dohlsten M**. 1999. Treatment with tumor-reactive Fab-IL-2 and Fab-staphylococcal enterotoxin A fusion proteins leads to sustained T cell activation, and long-term survival of mice with established tumors. International Journal of Oncology **15**:873–955.

358. **Belfrage H**, **Dohlsten M**, **Hedlund G**, **Kalland T**. 1997. Prevention of superantigen-induced tolerance in vivo by interleukin-2 treatment. Cancer Immunol Immunother **44**:77–82.

359. **Rosendahl A**, **Kristensson K**, **Carlsson M**, **Skartved N-J**, **Riesbeck K**, **Søgaard M**, **Dohlsten M**. 1999. Long-term survival and complete cures of B16 melanoma–carrying animals after therapy with tumor-targeted IL-2 and SEA. International Journal of Cancer **81**:156–163.

360. **Zhou G**, **Drake CG**, **Levitsky HI**. 2006. Amplification of tumor-specific regulatory T cells following therapeutic cancer vaccines. Blood **107**:628–636.

361. **Sundstedt A**, **Celander M**, **Eriksson H**, **Törngren M**, **Hedlund G**. 2012. Monotherapeutically Nonactive CTLA-4 Blockade Results in Greatly Enhanced Antitumor Effects When Combined With Tumor-targeted Superantigens in a B16 Melanoma Model. Journal of Immunotherapy **35**:344–353.

362. **Goshorn SC**, **Schlievert PM**. 1988. Nucleotide sequence of streptococcal pyrogenic exotoxin type C. Infection and Immunity **56**:2518–2520.

363. **Schlievert PM**, **Bettin KM**, **Watson DW**. 1977. Purification and characterization of group A streptococcal pyrogenic exotoxin type C. Infection and Immunity **16**:673–679.

364. **Silva-Costa C**, **Carriço JA**, **Ramirez M**, **Melo-Cristino J**. 2014. Scarlet Fever Is Caused By a Limited Number of Streptococcus pyogenes Lineages and Is Associated with the Exotoxin Genes ssa, speA and speC. The Pediatric Infectious Disease Journal **33**:306–310.

365. **Roussel A**, **Anderson BF**, **Baker HM**, **Fraser JD**, **Baker EN**. 1997. Crystal structure of the streptococcal superantigen SPE-C: dimerization and zinc binding

suggest a novel mode of interaction with MHC class II molecules. Nature Structural & Molecular Biology **4**:635–643.

366. **Li PL**, **Tiedemann RE**, **Moffat SL**, **Fraser JD**. 1997. The superantigen streptococcal pyrogenic exotoxin C (SPE-C) exhibits a novel mode of action. Journal of Experimental Medicine **186**:375–383.

367. **McCormick JK**, **Tripp TJ**, **Olmsted SB**, **Matsuka YV**, **Gahr PJ**, **Ohlendorf DH**, **Schlievert PM**. 2000. Development of streptococcal pyrogenic exotoxin C vaccine toxoids that are protective in the rabbit model of toxic shock syndrome. Journal of Immunology **165**:2306–2312.

368. **Rahman AN-U**, **Herfst CA**, **Moza B**, **Shames SR**, **Chau LA**, **Bueno C**, **Madrenas J**, **Sundberg EJ**, **McCormick JK**. 2006. Molecular basis of TCR selectivity, cross-reactivity, and allelic discrimination by a bacterial superantigen: integrative functional and energetic mapping of the SpeC-Vβ2. 1 molecular interface. Journal of Immunology **177**:8595–8603.

369. **Tripp TJ**, **McCormick JK**, **Webb JM**, **Schlievert PM**. 2003. The zinc-dependent major histocompatibility complex class II binding site of streptococcal pyrogenic exotoxin C is critical for maximal superantigen function and toxic activity. Infection and Immunity **71**:1548–1550.

370. **Yamaoka J**, **Nakamura E**, **Takeda Y**, **Imamura S**, **Minato N**. 1998. Mutational analysis of superantigen activity responsible for the induction of skin erythema by streptococcal pyrogenic exotoxin C. Infection and Immunity **66**:5020–5026.

371. **Hu DL**, **Zhu G**, **Mori F**, **Omoe K**, **Okada M**, **Wakabayashi K**, **Kaneko S**, **Shinagawa K**, **Nakane A**. 2007. Staphylococcal enterotoxin induces emesis through increasing serotonin release in intestine and it is downregulated by cannabinoid receptor 1. Cellular Microbiology **9**:2267–2277.

372. **Dixon JL**. 2006. Development of a novel tumour-targeting immunotoxin by fusion of a superantigen with a single-chain variable fragment specific for the oncofetal antigen 5T4: MSc Thesis. University of Western Ontario, London, Ontario.

373. **Bastedo PS**. 2007. Development and testing of novel tumor-targeting streptococcal superantigens: Honors Thesis. University of Western Ontario, London, Ontario.

374. **Untergasser A**, **Cutcutache I**, **Koressaar T**, **Ye J**, **Faircloth BC**, **Remm M**, **Rozen SG**. 2012. Primer3—new capabilities and interfaces. Nucleic Acids Research **40**:e115.

375. **Hwang WC**, **Lin Y**, **Santelli E**, **Sui J**, **Jaroszewski L**, **Stec B**, **Farzan M**, **Marasco WA**, **Liddington RC**. 2006. Structural Basis of Neutralization by a

Human Anti-severe Acute Respiratory Syndrome Spike Protein Antibody, 80R. Journal of Biological Chemistry **281**:34610–34616.

376. **Kapust RB**, **Tozser J**, **Fox JD**, **Anderson DE**, **Cherry S**, **Copeland TD**, **Waugh DS**. 2001. Tobacco etch virus protease: mechanism of autolysis and rational design of stable mutants with wild-type catalytic proficiency. Protein Engineering Design and Selection **14**:993–1000.

377. **Brouillard J-NP**, **Günther S**, **Varma AK**, **Gryski I**, **Herfst CA**, **Rahman AKMN**, **Leung DYM**, **Schlievert PM**, **Madrenas J**, **Sundberg EJ**, **McCormick JK**. 2007. Crystal structure of the streptococcal superantigen SpeI and functional role of a novel loop domain in T cell activation by group V superantigens. J Mol Biol **367**:925–934.

378. **Matzinger P**. 1991. The JAM test A simple assay for DNA fragmentation and cell death. J Immunol Methods **145**:185–192.

379. **Hoves S**, **Krause SW**, **Schölmerich J**, **Fleck M**. 2003. The JAM-assay: optimized conditions to determine death-receptor-mediated apoptosis. Methods **31**:127–134.

380. **Terpe K**. 2003. Overview of tag protein fusions: from molecular and biochemical fundamentals to commercial systems. Appl Microbiol Biotechnol **60**:523–533.

381. **Ashraf SS**, **Benson RE**, **Payne ES**, **Halbleib CM**, **Grøn H**. 2004. A novel multi-affinity tag system to produce high levels of soluble and biotinylated proteins in Escherichia coli. Protein expression and purification **33**:238–245.

382. **Beckett D**, **Kovaleva E**, **Schatz PJ**. 1999. A minimal peptide substrate in biotin holoenzyme synthetase-catalyzed biotinylation. Protein Science **8**:921–929.

383. **Diamandis EP**, **Christopoulos TK**. 1991. The biotin-(strept) avidin system: principles and applications in biotechnology. Clinical chemistry **37**:625–636.

384. **Kane JF**. 1995. Effects of rare codon clusters on high-level expression of heterologous proteins in Escherichia coli. Current Opinion in Biotechnology **6**:494–500.

385. **Gustafsson C**, **Govindarajan S**, **Minshull J**. 2004. Codon bias and heterologous protein expression. Trends in Biotechnology **22**:346–353.

386. **Novy R**, **Drott D**, **Yaeger K**, **Mierendorf R**. 2001. Overcoming the codon bias of E. coli for enhanced protein expression. inNovations NewsLetter Advanced Products and Protocols for Molecular Biology 1–3.

387. **Esposito D**, **Chatterjee DK**. 2006. Enhancement of soluble protein expression through the use of fusion tags. Current Opinion in Biotechnology **17**:353–358.

388. **LaVallie ER**, **DiBlasio-Smith EA**, **Collins-Racie LA**, **Lu Z**, **McCoy JM**. 2002. Thioredoxin and Related Proteins as Multifunctional Fusion Tags for Soluble Expression in E. coli, pp. 119–140. *In* Vaillancourt, PE (ed.), E. coli Gene Expression Protocols. Methods in Molecular Biology, New Jersey.

389. **Walls D**, **Loughran ST**. 2010. Tagging recombinant proteins to enhance solubility and aid purification, pp. 151–175. *In* Walls, D, Loughran, ST (eds.), Protein Chromatography. Methods in Molecular Biology, Totowa, NJ.

390. **Miller KD**, **Weaver-Feldhaus J**, **Gray SA**, **Siegel RW**, **Feldhaus MJ**. 2005. Production, purification, and characterization of human scFv antibodies expressed in Saccharomyces cerevisiae, Pichia pastoris, and Escherichia coli. Protein expression and purification **42**:255–267.

391. **Jurado P**, **de Lorenzo V**, **Fernández LA**. 2006. Thioredoxin fusions increase folding of single chain Fv antibodies in the cytoplasm of Escherichia coli: evidence that chaperone activity is the prime effect of thioredoxin. J Mol Biol **357**:49–61.

392. **Campbell RE**, **Tour O**, **Palmer AE**, **Steinbach PA**, **Baird GS**, **Zacharias DA**, **Tsien RY**. 2002. A monomeric red fluorescent protein. PNAS **99**:7877–7882.

393. **Chen TR**, **Drabkowski D**, **Hay RJ**, **Macy M**, **Peterson W**. 1987. WiDr is a derivative of another colon adenocarcinoma cell line, HT-29. Cancer genetics and cytogenetics **27**:125–134.

394. **Shultz LD**, **Lyons BL**, **Burzenski LM**, **Gott B**, **Chen X**, **Chaleff S**, **Kotb M**, **Gillies SD**, **King M**, **Mangada J**, **Greiner DL**, **Handgretinger R**. 2005. Human lymphoid and myeloid cell development in NOD/LtSz-scid IL2Rγnull mice engrafted with mobilized human hemopoietic stem cells. Journal of Immunology **174**:6477–6489.

395. **Zhou Q**, **Facciponte J**, **Jin M**, **Shen Q**, **Lin Q**. 2014. Humanized NOD-SCID IL2rg–/– mice as a preclinical model for cancer research and its potential use for individualized cancer therapies. Cancer Lett **344**:13–19.

396. **Carreno BM**, **Garbow JR**, **Kolar GR**, **Jackson EN**, **Engelbach JA**, **Becker-Hapak M**, **Carayannopoulos LN**, **Piwnica-Worms D**, **Linette GP**. 2009. Immunodeficient mouse strains display marked variability in growth of human melanoma lung metastases. Clinical Cancer Research **15**:3277–3286.

397. **Ishikawa F**. 2005. Development of functional human blood and immune systems in NOD/SCID/IL2 receptor chainnull mice. Blood **106**:1565–1573.

398. **Caspi RR**. 2008. Immunotherapy of autoimmunity and cancer: the penalty for success. Nat Rev Immunol **8**:970–976.

399. **Adams GP**, **Weiner LM**. 2005. Monoclonal antibody therapy of cancer. Nature

Biotechnology **23**:1147–1157.

400. **Reichert JM**. 2011. Antibody-based therapeutics to watch in 2011. mAbs **3**:76.

401. **Yokota T**, **Milenic DE**, **Whitlow M**, **Schlom J**. 1992. Rapid tumor penetration of a single-chain Fv and comparison with other immunoglobulin forms. Cancer Res **52**:3402–3408.

402. **Myers KA**, **Ryan MG**, **Stern PL**, **Shaw DM**, **Embleton MJ**, **Kingsman SM**, **Carroll MW**. 2002. Targeting immune effector molecules to human tumor cells through genetic delivery of 5T4-specific scFv fusion proteins. Cancer Gene Ther **9**:884–896.

403. **Bird RE**, **Hardman KD**, **Jacobson JW**, **Johnson S**, **Kaufman BM**, **Lee S-M**. 1988. Single-chain antigen-binding proteins. Science **242**:423.

404. **Jiang HR**, **Gilham DE**, **Mulryan K**, **Kirillova N**, **Hawkins RE**, **Stern PL**. 2006. Combination of Vaccination and Chimeric Receptor Expressing T Cells Provides Improved Active Therapy of Tumors. Journal of Immunology **177**:4288–4298.

405. **Harrop R**, **Chu F**, **Gabrail N**, **Srinivas S**, **Blount D**, **Ferrari A**. 2013. Vaccination of castration-resistant prostate cancer patients with TroVax (MVA–5T4) in combination with docetaxel: a randomized phase II trial. Cancer Immunol Immunother **62**:1511–1520.

406. **Amato RJ**, **Hawkins RE**, **Kaufman HL**, **Thompson JA**, **Tomczak P**, **Szczylik C**, **McDonald M**, **Eastty S**, **Shingler WH**, **de Belin J**, **Goonewardena M**, **Naylor S**, **Harrop R**. 2010. Vaccination of Metastatic Renal Cancer Patients with MVA-5T4: A Randomized, Double-Blind, Placebo-Controlled Phase III Study. Clinical Cancer Research **16**:5539–5547.

407. **Harrop R**, **Connolly N**, **Redchenko I**, **Valle J**, **Saunders M**, **Ryan MG**, **Myers KA**, **Drury N**, **Kingsman SM**, **Hawkins RE**, **Carroll MW**. 2006. Vaccination of Colorectal Cancer Patients with Modified Vaccinia Ankara Delivering the Tumor Antigen 5T4 (TroVax) Induces Immune Responses which Correlate with Disease Control: A Phase I/II Trial. Clinical Cancer Research **12**:3416–3424.

408. **Sinacola JR**, **Robinson AS**. 2002. Rapid refolding and polishing of single-chain antibodies from Escherichia coli inclusion bodies. Protein expression and purification **26**:301–308.

409. **Tsumoto K**, **Shinoki K**, **Kondo H**, **Uchikawa M**, **Juji T**, **Kumagai I**. 1998. Highly efficient recovery of functional single-chain Fv fragments from inclusion bodies overexpressed in Escherichia coli by controlled introduction of oxidizing reagent—application to a human single-chain Fv fragment. J Immunol Methods **219**:119–129.

410. **Kou G**, **Shi S**, **Wang H**, **Tan M**, **Xue J**, **Zhang D**, **Hou S**, **Qian W**, **Wang S**, **Dai J**, **Li B**, **Guo Y**. 2007. Preparation and characterization of recombinant protein ScFv (CD11c)-TRP2 for tumor therapy from inclusion bodies in Escherichia coli. Protein expression and purification **52**:131–138.

411. **Tsumoto K**, **Umetsu M**, **Yamada H**, **Ito T**, **Misawa S**, **Kumagai I**. 2003. Immobilized oxidoreductase as an additive for refolding inclusion bodies: application to antibody fragments. Protein Engineering Design and Selection **16**:535–541.

412. **Qoronfleh MW**, **Hesterberg LK**, **Seefeldt MB**. 2007. Confronting high-throughput protein refolding using high pressure and solution screens. Protein expression and purification **55**:209–224.

413. **Geisse S**, **Gram H**, **Kleuser B**, **Kocher HP**. 1996. Eukaryotic expression systems: a comparison. Protein expression and purification **8**:271–282.

414. **Dalton AC**, **Barton WA**. 2014. Over-expression of secreted proteins from mammalian cell lines. Protein Science **23**:517–525.

415. **JAX Mice, Clinical and Research Services**. 2015. Humanized NSG Mice for Immuno-Oncology. The Jackson Laboratory 1–28.

416. **Kotb M**. 1995. Bacterial pyrogenic exotoxins as superantigens. Clinical Microbiology Reviews **8**:411–426.

417. **Basma H**, **Norrby-Teglund A**, **Guedez Y**, **McGeer A**, **Low DE**, **El-Ahmedy O**, **Schwartz B**, **Kotb M**. 1999. Risk factors in the pathogenesis of invasive group A Streptococcal infections: role of protective humoral immunity. Infection and Immunity **67**:1871–1877.

418. **Holtfreter S**, **Roschack K**, **Eichler P**, **Eske K**, **Holtfreter B**, **Kohler C**, **Engelmann S**, **Hecker M**, **Greinacher A**, **Bröker BM**. 2006. Staphylococcus aureus carriers neutralize superantigens by antibodies specific for their colonizing strain: a potential explanation for their improved prognosis in severe sepsis. Journal of Infectious Diseases **193**:1275–1278.

419. **Terman DS**, **Serier A**, **Dauwalder O**, **Badiou C**, **Dutour A**, **Thomas D**, **Brun V**, **Bienvenu J**, **Etienne J**, **Vandenesch F**, **Lina G**. 2013. Staphylococcal entertotoxins of the enterotoxin gene cluster (egcSEs) induce nitric oxide- and cytokine dependent tumor cell apoptosis in a broad panel of human tumor cells. Frontiers in Cellular and Infection Microbiology **3**:1–10.

420. **Cho H-S**, **Mason K**, **Ramyar KX**, **Stanley AM**, **Gabelli SB**, **Denney DW**, **Leahy DJ**. 2003. Structure of the extracellular region of HER2 alone and in complex with the Herceptin Fab. Nature **421**:756–760.

421. **Kochenderfer JN**, **Wilson WH**, **Janik JE**, **Dudley ME**, **Stetler-Stevenson M**,

Feldman SA, **Maric I**, **Raffeld M**, **Nathan DAN**, **Lanier BJ**, **Morgan RA**, **Rosenberg SA**. 2010. Eradication of B-lineage cells and regression of lymphoma in a patient treated with autologous T cells genetically engineered to recognize CD19. Blood **116**:4099–4102.

422. **Kochenderfer JN**, **Dudley ME**, **Feldman SA**, **Wilson WH**, **Spaner DE**, **Maric I**, **Stetler-Stevenson M**, **Phan GQ**, **Hughes MS**, **Sherry RM**, **Yang JC**, **Kammula US**, **Devillier L**, **Carpenter R**, **Nathan DAN**, **Morgan RA**, **Laurencot C**, **Rosenberg SA**. 2012. B-cell depletion and remissions of malignancy along with cytokine-associated toxicity in a clinical trial of anti-CD19 chimeric-antigen-receptor-transduced T cells. Blood **119**:2709–2720.

423. **Pardoll DM**. 2012. The blockade of immune checkpoints in cancer immunotherapy. Nat Rev Cancer **12**:252–264.

424. **Patterson KG**, **Pittaro JLD**, **Bastedo PS**, **Hess DA**, **Haeryfar SMM**, **McCormick JK**. 2014. Control of established colon cancer xenografts using a novel humanized single chain antibody-streptococcal superantigen fusion protein targeting the 5T4 oncofetal antigen. PLoS ONE **9**:e95200.

APPENDICES

Appendix 1. Human ethics approval certification

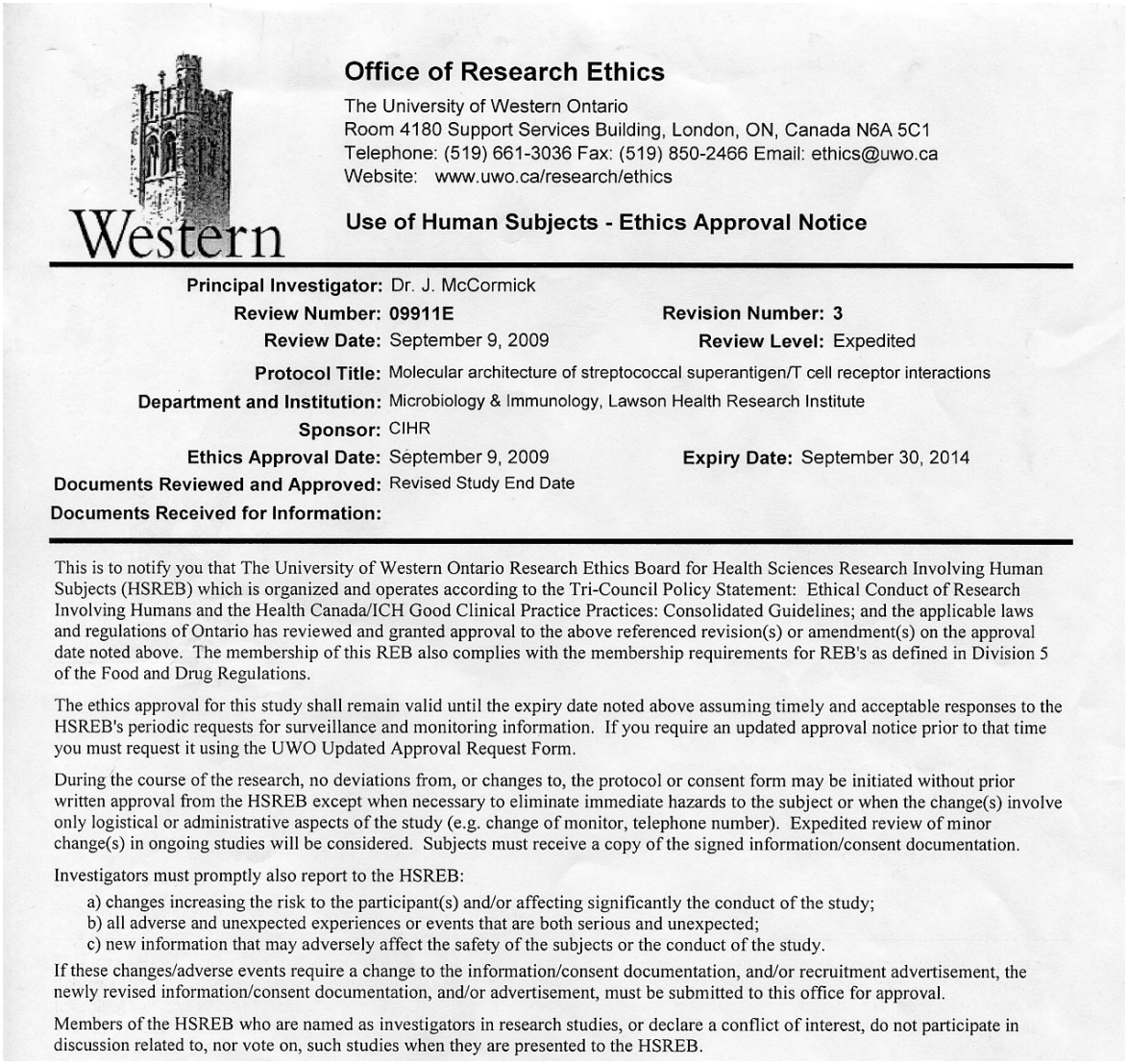

Western

Office of Research Ethics

The University of Western Ontario
Room 4180 Support Services Building, London, ON, Canada N6A 5C1
Telephone: (519) 661-3036 Fax: (519) 850-2466 Email: ethics@uwo.ca
Website: www.uwo.ca/research/ethics

Use of Human Subjects - Ethics Approval Notice

Principal Investigator: Dr. J. McCormick
Review Number: 09911E **Revision Number:** 3
Review Date: September 9, 2009 **Review Level:** Expedited
Protocol Title: Molecular architecture of streptococcal superantigen/T cell receptor interactions
Department and Institution: Microbiology & Immunology, Lawson Health Research Institute
Sponsor: CIHR
Ethics Approval Date: September 9, 2009 **Expiry Date:** September 30, 2014
Documents Reviewed and Approved: Revised Study End Date
Documents Received for Information:

This is to notify you that The University of Western Ontario Research Ethics Board for Health Sciences Research Involving Human Subjects (HSREB) which is organized and operates according to the Tri-Council Policy Statement: Ethical Conduct of Research Involving Humans and the Health Canada/ICH Good Clinical Practice Practices: Consolidated Guidelines; and the applicable laws and regulations of Ontario has reviewed and granted approval to the above referenced revision(s) or amendment(s) on the approval date noted above. The membership of this REB also complies with the membership requirements for REB's as defined in Division 5 of the Food and Drug Regulations.

The ethics approval for this study shall remain valid until the expiry date noted above assuming timely and acceptable responses to the HSREB's periodic requests for surveillance and monitoring information. If you require an updated approval notice prior to that time you must request it using the UWO Updated Approval Request Form.

During the course of the research, no deviations from, or changes to, the protocol or consent form may be initiated without prior written approval from the HSREB except when necessary to eliminate immediate hazards to the subject or when the change(s) involve only logistical or administrative aspects of the study (e.g. change of monitor, telephone number). Expedited review of minor change(s) in ongoing studies will be considered. Subjects must receive a copy of the signed information/consent documentation.

Investigators must promptly also report to the HSREB:

a) changes increasing the risk to the participant(s) and/or affecting significantly the conduct of the study;
b) all adverse and unexpected experiences or events that are both serious and unexpected;
c) new information that may adversely affect the safety of the subjects or the conduct of the study.

If these changes/adverse events require a change to the information/consent documentation, and/or recruitment advertisement, the newly revised information/consent documentation, and/or advertisement, must be submitted to this office for approval.

Members of the HSREB who are named as investigators in research studies, or declare a conflict of interest, do not participate in discussion related to, nor vote on, such studies when they are presented to the HSREB.

Appendix 2. Animal ethics approval certification

Western

AUP Number: 2012-026
PI Name: Mccormick, John
AUP Title: Next Generation Superantigen-based Immunotoxins For Cancer Therapy
Approval Date: 09/28/2012

Official Notice of Animal Use Subcommittee (AUS) Approval: Your new Animal Use Protocol (AUP) entitled "Next Generation Superantigen-based Immunotoxins For Cancer Therapy" has been APPROVED by the Animal Use Subcommittee of the University Council on Animal Care. This approval, although valid for four years, and is subject to annual Protocol Renewal.2012-026::1

1. This AUP number must be indicated when ordering animals for this project.
2. Animals for other projects may not be ordered under this AUP number.
3. Purchases of animals other than through this system must be cleared through the ACVS office. Health certificates will be required.

The holder of this Animal Use Protocol is responsible to ensure that all associated safety components (biosafety, radiation safety, general laboratory safety) comply with institutional safety standards and have received all necessary approvals. Please consult directly with your institutional safety officers.

Submitted by: Copeman, Laura
on behalf of the Animal Use Subcommittee
University Council on Animal Care

The University *of* Western Ontario
Animal Use Subcommittee / University Council on Animal Care

Appendix 3. Clinical trial outcome definitions

Acronym	Outcome	Definition[a]
AE	Adverse event	An unexpected medical problem that happens during treatment with a drug or other therapy. Adverse events do not have to be caused by the drug or therapy, and they may be mild, moderate, or severe
CR	Complete response	The disappearance of all signs of cancer in response to treatment. This does not always mean the cancer has been cured; also called complete remission
DFS	Disease-free survival	The length of time after primary treatment for a cancer ends that the patient survives without any signs or symptoms of that cancer
DLT	Dose-limiting toxicity	Describes side effects of a drug or other treatment that are serious enough to prevent an increase in dose or level of that treatment
DRR	Durable response rate	The length of time (usually displayed in months), that a partial or complete response is observed, as a result of treatment
MTD	Maximum tolerated dose	The highest dose of a drug or treatment that does not cause unacceptable side effects
OS	Overall survival	The length of time from either the date of diagnosis or the start of treatment, that patients diagnosed with the disease are still alive
OSR	Overall survival rate	The percentage of people in a study or treatment group who are still alive for a certain period of time after they were diagnosed with or started treatment. The overall survival rate is often stated as a five-year survival rate
PFS	Progression-free survival	The length of time during and after the treatment that a patient lives with the disease but it does not get worse
QoL	Quality of life	The overall enjoyment of life. Many clinical trials assess the effects of cancer and its treatment on the quality of life. These studies measure aspects of an individual's sense of well-being and ability to carry out various activities
PR	Partial response	A decrease in the size of a tumour, or in the extent of cancer in the body, in response to treatment
PK	Pharmacokinetics	The activity of drugs in the body over a period of time, including the processes by which drugs are absorbed, distributed in the body, localized in the tissues, and excreted

[a]Modified from National Cancer Institute Dictionary of Cancer Terms (http://www.cancer.gov/)

Appendix 4. Clinical trial phase definitions

Phase	Definition[a]
0	Exploratory study involving very limited human exposure to the drug, with no therapeutic or diagnostic goals (for example, screening studies, microdose studies)
I	Studies that are usually conducted with healthy volunteers and that emphasize safety. The goal is to find out what the drug's most frequent and serious adverse events are and, often, how the drug is metabolized and excreted
II	Studies that gather preliminary data on effectiveness (whether the drug works in people who have a certain disease or condition). For example, participants receiving the drug may be compared with similar participants receiving a different treatment, usually an inactive substance (called a placebo) or a different drug. Safety continues to be evaluated, and short-term adverse events are studied.
III	Studies that gather more information about safety and effectiveness by studying different populations and different dosages and by using the drug in combination with other drugs
IV	Studies occurring after FDA has approved a drug for marketing. These including postmarket requirement and commitment studies that are required of or agreed to by the sponsor. These studies gather additional information about a drug's safety, efficacy, or optimal use

[a]Modified from ClinicalTrials.gov Protocol Data Element Definitions

Appendix 5. TTS developmental timeline citations

Number	Author	Title	Year	Citation
1	Dohlsten *et al*.	Targeting of human cytotoxic T lymphocytes to MHC class II-expressing cells by staphylococcal enterotoxins	1990	(310)
2	Dohlsten *et al*.	Monoclonal antibody-targeted superantigens: a different class of anti-tumour agents	1991	(308)
3	Dohlsten *et al*.	Monoclonal antibody-superantigen fusion proteins: tumour-specific agents for T-cell-based tumour therapy	1994	(309)
4	Lando *et al*.	Tumour‐reactive superantigens suppress tumour growth in humanized scid mice	1995	(319)
5	Hansson *et al*.	Genetically engineered superantigens as tolerable antitumour agents	1997	(326)
6	Forsberg *et al.*	Identification of framework residues in a secreted recombinant antibody fragment that control production level and localization in *Escherichia coli*	1997	(336)
7	Giantonio *et al*.	Superantigen-based immunotherapy: a phase I trial of PNU-214565, a monoclonal antibody-staphylococcal enterotoxin A recombinant fusion protein, in advanced pancreatic and colorectal cancer	1997	(324)
8	Alpaugh *et al*.	Superantigen-targeted therapy: phase I escalating repeat dose trial of the fusion protein PNU-214565 in patients with advanced gastrointestinal malignancies.	1998	(325)
9	Søgaard *et al*.	Treatment with tumour-reactive Fab-IL-2 and Fab-staphylococcal enterotoxin A fusion proteins leads to sustained T cell activation, and long-term survival of mice with established tumours	1999	(357)
10	Nielsen *et al*.	Phase I study of single, escalating doses of a superantigen-antibody fusion protein (PNU-214565) in patients with advanced colorectal or pancreatic carcinoma	2000	(323)
11	Forsberg *et al*.	Therapy of human non-small-cell lung carcinoma using antibody targeting of a modified superantigen	2001	(335)
12	Erlandsson *et al*.	Identification of the antigenic epitopes in staphylococcal enterotoxins A and E and design of a superantigen for human cancer therapy	2003	(339)

13	Cheng *et al.*	Individualized Patient Dosing in Phase I Clinical Trials: The Role of Escalation With Overdose Control in PNU-214936	2004	(337)
14	Shaw *et al.*	A phase II study of a 5T4 oncofoetal antigen tumour-targeted superantigen (ABR-214936) therapy in patients with advanced renal cell carcinoma	2007	(338)
15	Sundstedt *et al*.	Combining tumour-targeted superantigens with interferon-alpha results in synergistic anti-tumour effects	2008	(344)
16	Sundstedt *et al*.	Immunotherapy with tumour-targeted superantigens (TTS) in combination with docetaxel results in synergistic anti-tumour effects	2009	(341)
17	Borghaei *et al*.	Phase I dose escalation, pharmacokinetic and pharmacodynamic study of naptumomab estafenatox alone in patients with advanced cancer and with docetaxel in patients with advanced non-small-cell lung cancer	2009	(342)
18	Forsberg *et al*.	Naptumomab Estafenatox, an Engineered Antibody-superantigen Fusion Protein With Low Toxicity and Reduced Antigenicity	2010	(242)
19	Sundstedt *et al*.	Monotherapeutically Nonactive CTLA-4 Blockade Results in Greatly Enhanced Antitumour Effects When Combined With Tumour-targeted Superantigens in a B16 Melanoma Model	2012	(361)
20	Patterson *et al*.	Control of Established Colon Cancer Xenografts Using a Novel Humanized Single Chain Antibody-Streptococcal Superantigen Fusion Protein Targeting the 5T4 Oncofetal Antigen	2014	(424)
21	Elkord *et al*.	Immunological response and overall survival in a subset of advanced renal cell carcinoma patients from a randomized phase 2/3 study of naptumomab estafenatox plus IFN-alpha versus IFN-alpha	2015	(348)

Appendix 6. Animal group pre-treatment characteristics

Treatment Group	ID	Cohort	Sex	Weight pre-tumour (g)	Weight pre-treatment (g)	Primary tumour palpable pre-treatment	Primary tumour size pre-treatment (mm^2)
No PBMCs/Saline	K9-NC	3	M	29.0	30.4	Yes	n/a
	K9-1R	3	M	28.0	30.0	Yes	n/a
	K9-1L	3	M	28.0	30.5	Yes	7.83
Saline	K4-1R	1	M	27.1	27.7	Yes	18.63
	K8-NC	2	M	28.6	29.6	Yes	7.44
	K8-1L	2	M	26.2	27.2	Yes	7.75
	K6-1R/1L	2	F	20.9	20.8	Yes	n/a
$SpeC_{D203A}$	K2-1R	1	M	31.1	32.0	Yes	12.90
	K5-1L	2	M	28.3	29.4	Yes	18.83
	K1 NC	1	F	24.9	23.7	Yes	n/a
	K7-NC	2	F	22.3	22.0	Yes	9.22
scFv5T4	K3-NC	1	M	30.3	30.0	Yes	23.4
	K8-1R	2	M	27.1	28.5	Yes	9.00
	K6-IR	2	F	22.5	23.1	Yes	5.16
	K7-1R	2	F	22.4	20.7	Yes	n/a
scFv5T4::$SpeC_{Y15A/D203A}$	K3-1L	1	M	30.3	30.7	Yes	19.00
	K4-2R	1	M	29.0	29.3	Yes	15.49
	K5-1R	2	M	30.8	32.1	Yes	7.70
	K6-1L	2	F	20.4	20.4	Yes	6.75
scFv5T4::$SpeC_{D203A}$	K2-NC	1	M	32.3	32.3	Yes	12.90
	K4-1L	1	M	29.0	29.0	Yes	n/a
	K5-NC	2	M	28.2	28.5	Yes	21.80
	K7-1L	2	F	24.8	23.7	Yes	3.57

ID = animal identification number (cage-ear punch code);
Abbreviations: M, male; F, female; g, gram; n/a, not applicable (tumour unable to be conclusively measured)

Appendix 7. *5t4* expression of human cell lines used within this study

Relative expression of *5t4* compared to housekeeping gene, GAPDH, of HEK293 cells compared to human colon cancer cell lines, HT-29 and WiDr determined by qPCR analysis (n=3 represented as mean ± SEM. *p<0.05, **p<0.005, compared to HEK293)

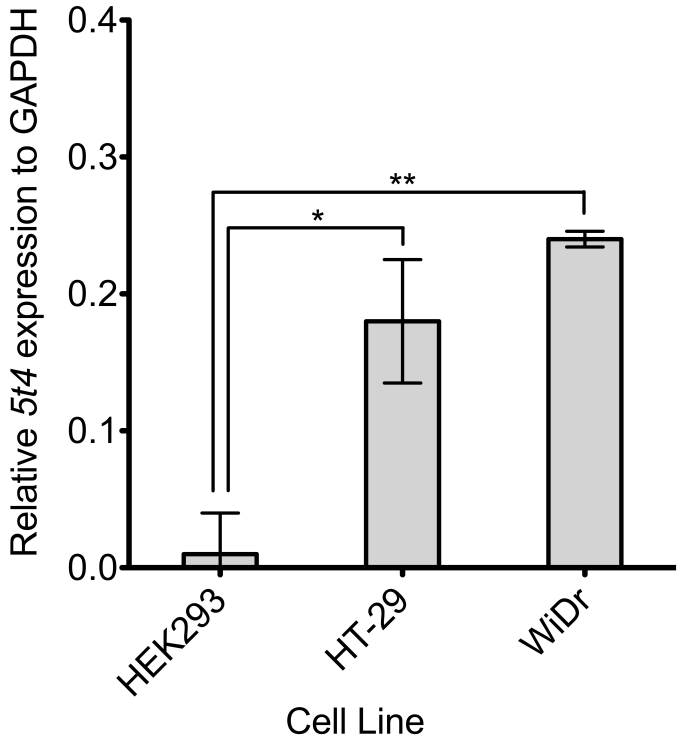

Appendix 8. Citations used for multiple sequence alignment of human scFv proteins

Definition	Reference
anti-5T4 murine scFv	Shaw, D.M., Embleton, M.J., Westwater, C., Ryan, M.G., Myers, K.A., Kingsman, S.M., Carroll, M.W. and Stern, P.L. 2000. Isolation of a high affinity scFv from a monoclonal antibody recognizing the oncofoetal antigen 5T4. *Biochimica et biophysica acta*. 1524, 2-3 (Dec. 2000), 238–246.
Synthetic backbone human scFv	Yang HY, *et al*. Construction of a large synthetic human scFv library with six diversified CDRs and high functional diversity. Mol Cells. 2009; 27(2):225-35
single-chain Fv fragment [Homo sapiens]	Kontermann RE, *et al*. Complement recruitment using bispecific diabodies. Nat Biotechnol. 1997; 15(7):629-31.
anti-(ED-B) scFV [Homo sapiens]	Pini A, *et al*. Design and use of a phage display library. Human antibodies with subnanomolar affinity against a marker of angiogenesis eluted from a two-dimensional gel. J Biol Chem. 1998; 273(34):21769-76.
anti-HCS scFv [Homo sapiens]	Pini A, *et al*. Design and use of a phage display library. Human antibodies with subnanomolar affinity against a marker of angiogenesis eluted from a two-dimensional gel. J Biol Chem. 1998; 273(34):21769-76.
anti-HER2/neu scFv [Homo sapiens]	Derived sequence from: Cho HS, *et al.* Structure of the extracellular region of HER2 alone and in complex with the Herceptin Fab. Nature. 2003; 421(6924):756-60.
anti-HER3 scFv [Homo sapiens]	Merchant AM, *et al*. An efficient route to human bispecific IgG. Nat Biotechnol. 1998; 16(7):677-81.
anti-Mpl scFv [Homo sapiens]	Merchant AM, *et al*. An efficient route to human bispecific IgG. Nat Biotechnol. 1998; 16(7):677-81.
anti-tetanus toxin scFv [synthetic construct]	Scott N, *et al.* Single-chain Fv phage display propensity exhibits strong positive correlation with overall expression levels. BMC Biotechnol. 2008; 8:97.
anti-TeTox scFv [Homo sapiens]	Pini A, *et al*. Design and use of a phage display library. Human antibodies with subnanomolar affinity against a marker of angiogenesis eluted from a two-dimensional gel. J Biol Chem. 1998; 273(34):21769-76.
anti-TREM-like transcript-1 antibody [synthetic construct]	Giomarelli B, *et al*. Inhibition of platelet aggregation using human single chain Fv antibodies specific for TREM-like transcript-1. Thromb Haemost. 2007; 97(6):955-63.

CURRICULUM VITAE

Kelcey G. Patterson, BScH

EDUCATION

2009-present Doctor of Philosophy candidate (PhD)
Department of Microbiology and Immunology, Schulich School of Medicine and Dentistry, University of Western Ontario, London, ON

2007-2009 Master's of Science candidate (MSc)
Department of Microbiology and Immunology, Schulich School of Medicine and Dentistry, University of Western Ontario, London, ON; transferred to Ph.D. program

2003-2007 Bachelor of Science Degree with Honours (BScH)
Department of Biology, Acadia University, Wolfville, NS

RESEARCH EXPERIENCE

2013-present **Research Scientist**, Sernova Corp, London, ON

2009-present **Ph.D. Candidate**, Department of Microbiology and Immunology, University of Western Ontario, London ON

Thesis: *Development of a novel humanized single chain antibody-streptococcal superantigen-derived immunotherapy targeting the 5T4 oncofetal antigen*

2007-2009 **M.Sc. Candidate**, Department of Microbiology and Immunology, University of Western Ontario, London, ON

Thesis: *Development of Novel Streptococcal Superantigen-Derived Tumour-Targeted Immunotherapy*
Transferred into PhD program to continue research

2006-2007 **Laboratory Quality Technician**, Michelin North America Corporation Inc., Waterville, NS

2005-2007 **B.Sc.H. Honours Thesis Candidate**, Biology Department, Acadia University, Wolfville, NS

Thesis: *Determining the potential of isolated bacterial colonies from soil contaminated with gasoline and diesel surrounding Alnus rugosa and Salix sp. in the role of hydrocarbon degradation in phytoremediation*

RELATED EXPERIENCE

Teaching Experience

2012-2013 Undergraduate Mentor
Supervised an undergraduate 4th year thesis project: Arya Afsahi
McCormick Lab, Department of Microbiology and Immunology,
University of Western Ontario, London, ON

2011-2013 Undergraduate Tutor
Tutoring 2 undergraduate nursing students in the field of Microbiology and Immunology, University of Western Ontario, London, ON

2010-2012 Teaching Assistant: MicroImm 3600G Laboratory Techniques in Microbiology and Immunology
Department of Microbiology and Immunology, University of Western Ontario, London, ON

2009-2010 Undergraduate Mentor
Supervised an undergraduate 4th year thesis project: Mathias Scinocca
McCormick Lab, Department of Microbiology and Immunology,
University of Western Ontario, London, ON

2007-2010 Teaching Assistant: MicroImm 2100A Biology of Prokaryotes
Department of Microbiology and Immunology, University of Western Ontario, London, ON

2005-2007 Teaching Assistant: Biol2053 Microbial Biodiversity, Biol2073 Animal Biodiversity, Chem2513 Organic Chemistry 1
Departments of Biology and Chemistry, Acadia University, Wolfville, NS

Leadership Experience

2010-2012 Graduate Student Representative for Microbiology and Immunology
Department of Microbiology and Immunology, University of Western Ontario, London, ON

2010-2011 Chair of Infection and Immunity Research Forum Organizing Committee
Department of Microbiology and Immunology, University of Western Ontario, London, ON

2006-2007 Acadia University Biology Society President
Department of Biology, Acadia University, Wolfville, NS

2006-2007 Co-Chair of Finances
Canadian Cancer Society Relay for Life, Acadia University, Wolfville, NS

HONOURS AND AWARDS

2009-2012	Western Graduate Research Scholarship, University of Western Ontario ($2835 per year)
2011	Danone Science Award (Best Student Seminar), University of Western Ontario ($500)
2011	Top Graduate Poster Presentation, Infection and Immunity Research Forum, University of Western Ontario ($100)
2011	Microbiology and Immunology Graduate Travel Award, University of Western Ontario ($1000)
2009	Microbiology and Immunology Graduate Travel Award, University of Western Ontario ($1000
2008	Top Graduate Poster Presentation, Canadian Society of Microbiology, Calgary, Alberta ($100)
2007-2008	Western Graduate Research Scholarship, Microbiology, University of Western Ontario ($2732)
2007-2008	Schulich Graduate Scholarship, University of Western Ontario ($784)
2007-2008	Schulich Scholarship for Medical Research, University of Western Ontario ($804)
2007	Acadia University Student Leadership Award
2004-2007	Clarke K. McLeod Pre-Medical Scholarships, Acadia University (Total: $6000)
2003-2007	University Scholar, Academic Honours Acadia University
2003-2006	Dr. Lalia B. Chase Scholarship, Acadia University Bursary (Total: $3900)
2003-2006	The Class of 1923 Scholarship, Acadia University Bursary (Total: $2100)
2003	Acadia University Entrance Bursary ($4000)
2003	Nova Scotia Teacher's Union Award ($250)
2003	Annapolis West Education Centre Alumni Bursary ($100)

PUBLICATIONS and PRESENTATIONS

Publications

2014 K.G.Patterson, J.L.Dixon Pittaro, P.S.Bastedo, D.A.Hess, S.M.M. Haeryfar, J.K.McCormick. 2014. Control of established colon cancer xenografts using a novel humanized single chain antibody-streptococcal superantigen fusion protein targeting the 5T4 oncofetal antigen. PLOS ONE 15; 9(4)

2013 R.V.Anantha, K.J.Kasper, K.G.Patterson, J.J.Zeppa, J.Delport, J.K.McCormick. 2013. Fournier's gangrene of the penis caused by *Streptococcus dysgalactiae* subspecies equisimilis: case report and incidence study in a tertiary-care hospital. BMC Infectious Diseases 3:381

Presentations

2011 K.G.Patterson, J.L.Dixon, P.S.Bastedo. H.C.Broughton, S.M.M. Haeryfar, D.A.Hess, J.K.McCormick. Development of streptococcal superantigen-derived anti-cancer immunotherapeutics. Poster presentation, Infection and Immunity Research Forum. London, Ontario
Top Graduate Poster Presentation was awarded for this poster.

2011 K.G.Patterson, J.L.Dixon, P.S.Bastedo. S.S.Gupta, J.K.McCormick. Development of superantigen-derived anti-cancer immunotherapeutics. Poster presentation, Canadian Cancer Immunotherapy Consortium. Lake Louise, Alberta

2011 K.G.Patterson, J.L.Dixon, P.S.Bastedo. S.S.Gupta, J.K.McCormick. Development of superantigen-derived anti-cancer immunotherapeutics. Poster presentation, Canadian Society for Immunology. Lake Louise, Alberta

2009 K.G.Patterson, J.L.Dixon, P.S.Bastedo. S.S.Gupta, J.K.McCormick. Development of superantigen-derived anti-cancer immunotherapeutics. Poster presentation, International Society for Biological Therapy of Cancer. National Harbor, Maryland

2009 K.G.Patterson, J.L.Dixon, P.S.Bastedo. S.S.Gupta, K.J.Kasper, J.K.McCormick. Development of superantigen-derived anti-cancer immunotherapeutics. Poster presentation, Infection and Immunity Research Forum. London, Ontario

2008 K.G.Patterson, J.L.Dixon, P.S.Bastedo. S.S.Gupta, K.J.Kasper, J.K.McCormick. Development of superantigen-derived anti-cancer immunotherapeutics. Poster presentation, Canadian Society of Microbiology Conference. Calgary, Alberta
Top Graduate Poster Presentation was awarded for this poster.

2008 K.G.Patterson, J.L.Dixon, P.S.Bastedo. S.S.Gupta, K.J.Kasper, J.K.McCormick. Development of superantigen-derived anti-cancer immunotherapeutics. Poster presentation, Infection and Immunity Research Forum. London, Ontario

2005 K. Moore, K. Patterson. E.Reekie, R.Evans, R. Newell, C.Stanley, P.Romkey and C. Bell. The role of bacterial communities of hydrocarbon spill sites in Atlantic Canada. Poster presentation, Canadian Society of Microbiology Conference. Halifax, Nova Scotia

SELECT VOLUNTEER EXPERIENCE

2010-2012 Scientific Judge, London District Science & Technology Fair
2008-2012 Infection and Immunity Research Forum Organizing Committee Member
2007-2010 Microbiology and Immunology Social Committee
2005-2007 Member of Volunteer Acadia
2004-2007 Wolfville Animal Hospital and Shelter
2003-2007 Relay for Life Committee, Canadian Cancer Society